Explorative nonlinear pushover analyses for historical unreinforced masonry churches

A Case Study in Zandeweer, Groningen

Madina Karim

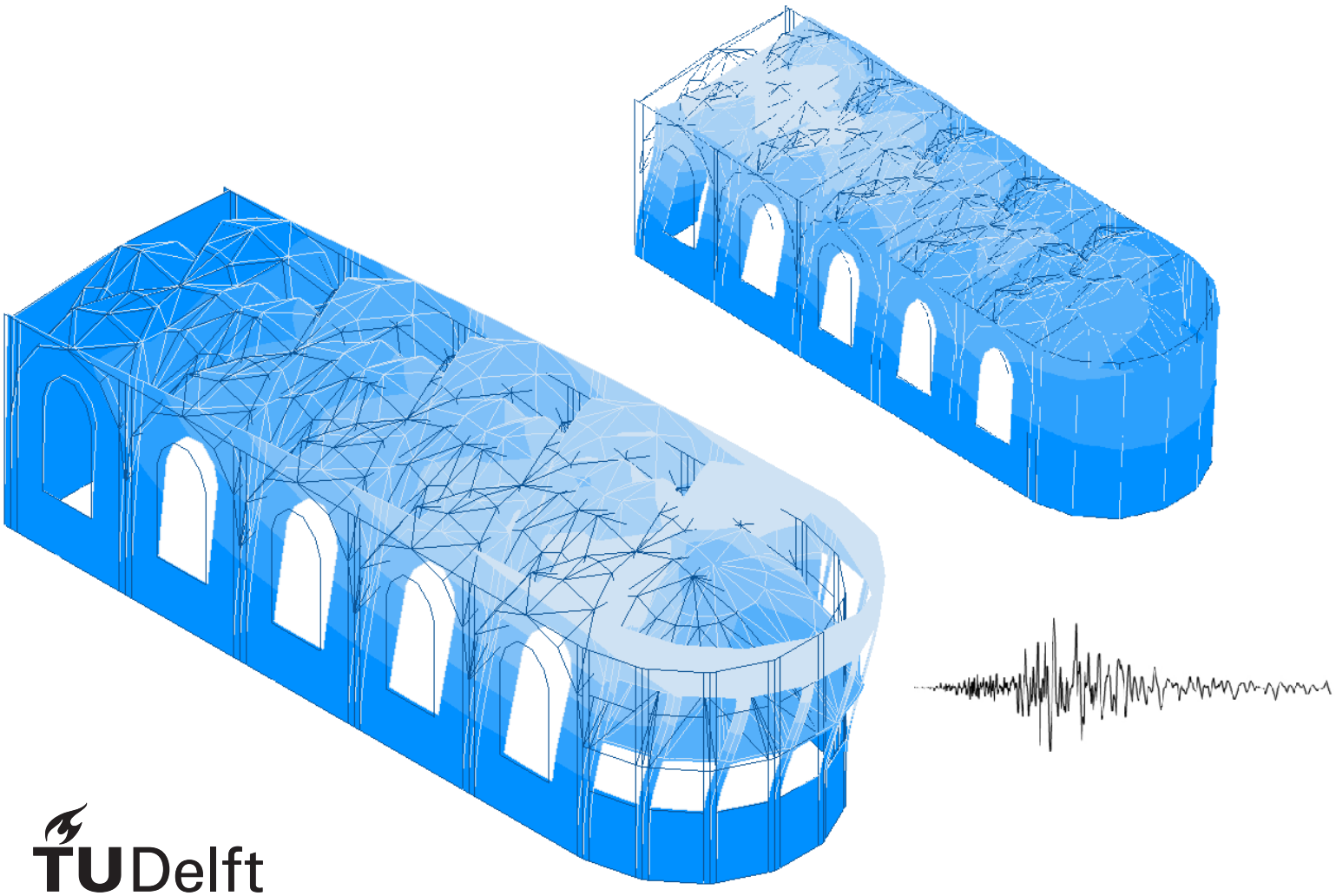

TU Delft

Explorative nonlinear pushover analyses for historical unreinforced masonry churches

A Case Study in Zandeweer, Groningen

by

Madina Karim

To obtain the degree of

Master of Science

in Structural Engineering at the Delft University of Technology,
to be defended publicly on Wednesday, November 13th, 2019.

Thesis committee:	Prof. dr. ir. J. G. Rots,	TU Delft, Chairman
	Msc. M. Longo,	TU Delft, Daily Supervisor
	Dr. Ir. R. Esposito,	TU Delft
	Dr. Ir. G. J. P. Ravenshorst,	TU Delft

An electronic version of this thesis is available at `http://repository.tudelft.nl/`.

TU Delft

Acknowledgements

This report summarized the results of my graduation project. The project cover the seismic analysis and assessment of the historical church in Zandeweer built in 1230 in Groningen, in the Netherlands and researches its change in global structural behaviour post structural modifications in 1932. This report is my last step towards the fulfillment of the requirements needed to obtain the title Master of Structural Engineering at the faculty of Civil Engineering and Geosciences at Delft University of Technology. The research was conducted and finalized under guidance and supervision of my graduation committee at Delft University of Technology. This thesis would not have been possible without the time and support of my committee members and important people in my life. I would like, therefore, to express my gratitude here for their support and guidance through my time at Delft University of Technology.

I would like start off with acknowledging the chair of my committee, Jan Rots, for introducing me to the field of Earthquake Engineering and providing me the opportunity to work on such an interesting topic. Also I would like to thank Jan for providing me interesting suggestions and valuable feedback during my committee meetings.

Michele Longo, my mentor and daily supervisor, thank you for your availability, scientific view and for providing such positive and constructive feedback on my work. I highly appreciated your flexibility, commitment to meet more frequently whenever needed, your patience and endless enthusiasm during the duration of this project. Your guidance has provided me valuable support during the challenges I faced throughout my thesis.

Rita Esposito, for her meticulous proofreading of my work, for her helpful suggestions and valuable feedback during the duration of this project.

Geert Ravenshorst, for providing interesting suggestions and invaluable feedback during my committee meetings.

Rijksmonumentendienst, for generously providing the technical drawing for the case study presented in this thesis. Without, this we couldn't have kicked off this project.

My dear family and friends for their endless support and encouragement in all situations. In particular, I would like to thank Ali for his unconditional support and valuable suggestions for my report as a whole.

Madina Karim
Delft, November 2019

Summary

In the past decades, gas productions in the province of Groningen in The Netherlands have caused a significant amount of shallow human-induced earthquakes. Its building stock that primarily is constructed by unreinforced masonry (URM) has shown to be highly vulnerable to these unexpected events. Among various building typologies, the province of Groningen is home to 11.3% of the Dutch historical churches. Up to July 2019, damage has been reported for approximately 12.9% of these churches. From the perspective of conservation and prevention of loss of our historical and cultural heritage, the assessment of churches is of importance. As a result of the observed damage, a significant amount of the existing URM stock have shown to require strengthening. However, a majority of historical structures have undergone restoration works, that can be favorable for their seismic performance. Therefore, it is worth noticing that for historical structures strengthening may not be necessary. Consequently, the question arises whether structural modifications during the lifespan of historical URM churches positively influences their seismic performance.

The assessment of the seismic performance of historical buildings is yet a very challenging task. As historical buildings by definition are unique buildings with many uncertainties and their complex design and technological constructive complexity often cannot be simplified to any standard structural scheme for which a detailed analysis methods would be available. Their complex design is often governed by macroelement behaviour and the inseparable construction of non-structural (e.g. ornaments) and structural elements. In addition the highly nonlinear behaviour of URM and the dynamic nature of the seismic loading add to this complexity. Therefore, for a reliable earthquake resistant assessment, appropriate (numerical) modelling of the structure and suitable analyses procedures are a prerequisite. This thesis researches the influence on the seismic performance of the Zandeweer church in Groningen, due to structural modifications during its lifespan. The scope of this thesis is limited to this particular case study only. The aim is to evaluate the seismic performance of the church by investigating the global nonlinear response and the structural elemental behaviour and by indicating uncertainties and damage. The first objective of this thesis is, to evaluate the global seismic behaviour of the church prior and post structural modifications by means of a Simplified Lateral Mechanism Analysis method (SLaMA) and a Nonlinear Pushover Analysis method (NLPO). With limited research and no experimental results available to support the applicability of these analyses methods for this building typology, the second objective is to investigate to which extend the analyses methods can provide insight in the global behaviour of this historical Dutch URM church. The applicability of the analyses method is discussed by comparison of the results of the two methods and their limitations.

The church in Zandeweer, Groningen was built by the Moncks of Abdij van Aduard in the year 1230 and underwent major renovation works in 1931. Its structure is composed of masonry walls, masonry ribbed cross vaults and a timber roof with timber cladding. The technical drawings provided by the Rijksmonumentdienst show that the 930mm thick walls are composed of two outer masonry brick layers and one inner rubble layer. During the restoration works in 1931, several modifications were added. The masonry walls and vaults were restored with new masonry and concrete infill, the timber roof was replaced entirely, steel columns were integrated in the piers of one of the façade in the longitudinal direction, window openings in the curved façade were closed and concrete beams were added on top of the main walls. In 1972, the church obtained a monumental status by Rijksmonumentendienst.

In the prediction studies conducted in this thesis, the seismic performance of the church model representation as built in 1230 is compared with the church model post structural modifications in 1931. The church model representations are modelled with regular curved shell elements and curved beam elements, based on the Mindlin-Reissner theorem. In all models both material as geometric nonlinearities are included. The numerical models are set-up using the commercial software package DIANA FEA 10.3. For the church model as built in 1230, a representation is chosen for which the masonry walls, ribbed masonry cross vaults and window openings in the curved façade are considered. For the church model post structural modifications in 1931 the influence of the following modifications to the church as built in 1230 are considered: the addition of the steel columns and shortening of the masonry piers at one facade in the longitudinal direction, the addition of the concrete beams on top of the main walls and closing the window opening at the curved façade. Note, that as the global response of the church structure is the main focus of this thesis that the gable and roof structure are not considered in model representations. The consequently introduced limitations to

the models have been accounted for by a post-analysis verification using the nonlinear kinematic analysis (NLKA) for the gable and by the addition of a line load on the main walls for the roof structure. All other earlier mentioned modifications to the church structure are not considered in order to reduce the complexity of the study. A representation of the church model as built in 1230 and the church model post structural modifications in 1931 as studied in this thesis are presented in Figure 1.

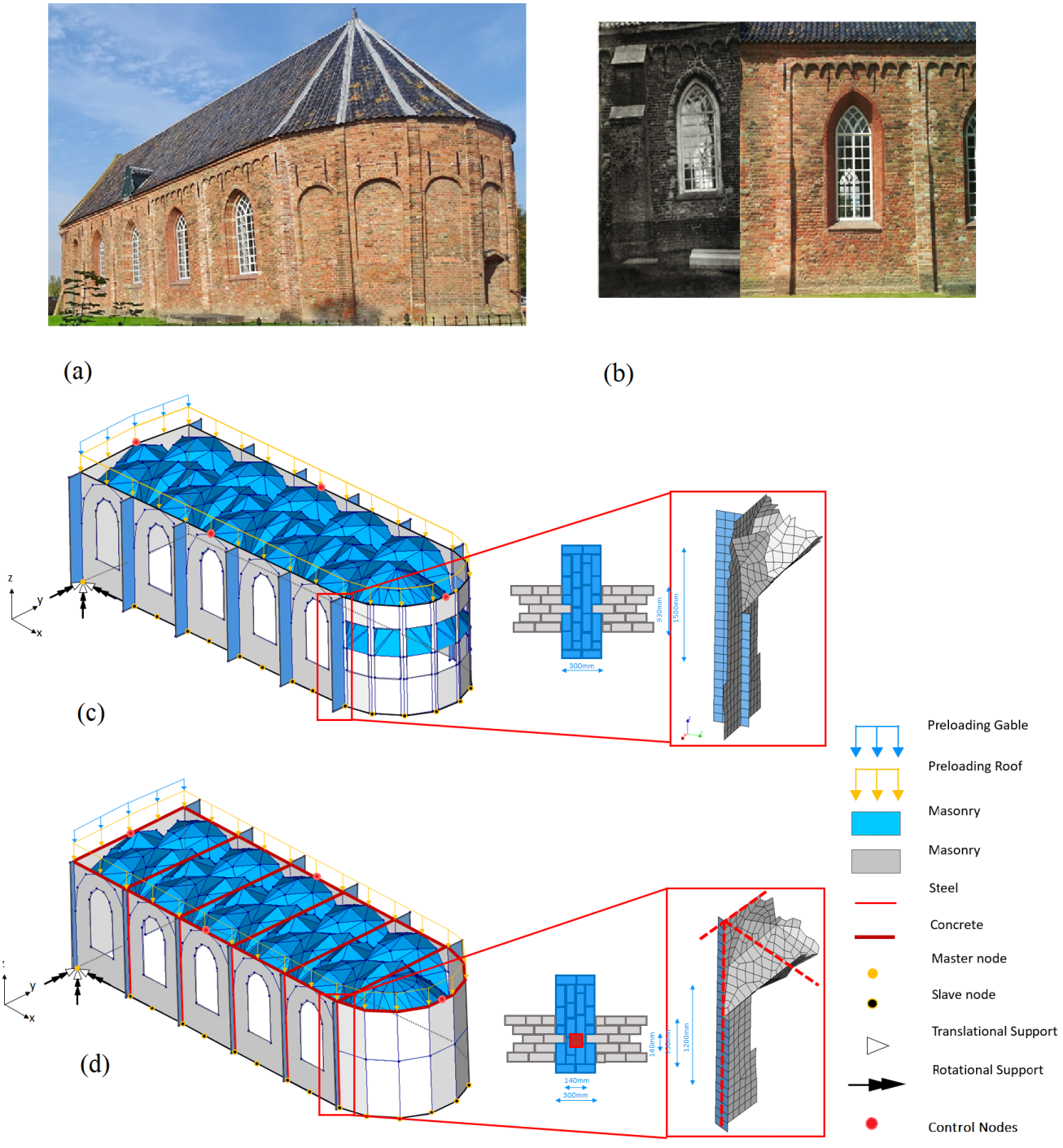

Figure 1: (a) Church Zandeweer Groningen, (b) Piers prior and post modifications and Numerical model representation for (c) Church as built in 1230 and, (d) Church post structural modifications in 1931

Prior to the study of the global seismic response by means SLaMA and NLPO analyses an eigenvalue analysis has been conducted for the church prior and post structural modifications. Results acquired in these analyses are the modal shapes, eigen periods and mass participation factors, which provides an initial insight in the influence of the modifications to the church structure. The eigenvalue analysis indicated that the structural modifications do have an influence on the global response in both global directions. In the longitudinal direction (X-direction in Figure 1) the out-of-plane mode for the transverse facade is governing for the prior and post structural modifications church model. With the addition of the structural modifications an increase in global stiffness, a reduction in deformations and a change in the mass participation factor from 43.9% to 61% is observed in this direction. For the transverse direction (Y-direction in Figure 1) a torsional mode is governing prior to the structural modifications and an out-of-plane mode for the longitudinal facades is governing post structural modifications as a consequence of change in global stiffness. The mass participation factor in this direction shifts from 49.8% to 65.8%. In both the prior and the post structural modifications stage a higher mass participation factor is activated in the transverse direction, which indicated a possible susceptibility to failure. However, within the time limit of this study it was chosen to study the global structural behaviour in the longitudinal direction. The governing modal shapes in the longitudinal directions are consequently used as input for the NLPO analyses, by performing a modal proportional analysis.

The Simplified Lateral Mechanism Analysis method (SLaMA) was used as a preliminary analysis to predict the seismic response of the church models in the positive longitudinal direction (X-direction in Figure 1). Followed by the Nonlinear Pushover Analysis method (NLPO) to predict the same global structural response. SLaMA is a mechanism based analysis method in which the seismic loading is applied as a lateral loading. For the analyses the roof structure, the vaults, the gable and the concrete beams were considered as overburden on the main walls. The results obtained by SLaMA show, for the church prior and post structural modifications, a displacement capacity of 100mm, an increase of base shear capacity of about 10% and an increase in softening behaviour of about 25%. In these analyses failure as a consequence of rocking in the piers of the main walls were observed. In the NLPO analyses the seismic loading for the models are applied in the governing modal shape in the longitudinal direction, which are gradually increased until collapse. For these analyses the roof structure and gable are not considered in the models. The capacity curves for the numerical models are determined by appropriate selection of control nodes. In this study four control nodes along the perimeter of the main walls were chosen (see Figure 1). By comparison of the results of the NLPO analysis for the church prior and post structural modifications with each other an increase of 100% in base shear capacity, a decrease of 50% in displacement capacity and an increase of 50% in initial stiffness was observed. For the numerical models no softening was observed as the post-peak stage was not captured. Severe damage was found in both church models in the vaults and slight to moderate damage was observed in the main walls. For both church models similar damage at similar locations were observed, but with a difference in value and spread. Cracking in the walls as a consequence of rocking was found in the church model prior and post modifications. In general the structural modifications had a positive influence on the deformation behaviour of the main walls, yet a counteractive effect on the behaviour of the vault structure. Damage in the vaults were increase significantly up to a severe state as a consequence of the modifications and led mostly likely to an early collapse of the vaults and the end of the analyses. When comparing the observed results for the NLPO with SLaMA in the longitudinal direction for the church model as built in 1230 show a 5 times higher base shear capacity and a 1.25 higher global stiffness. Results for the church model post structural modifications show a 6.5 times higher base shear capacity and a 1.25 higher global stiffness in comparison to the results of SLaMA. This difference can be explained by the modelling and loading approach in the two analysis methods. For the NLPO analyses a three-dimensional representation of the church is considered, whereas for the SLaMA a two-dimensional representation is used. Consequently, the influence of the vaults to the global behaviour is not considered in the response. Additionally, for SLaMA the sequence of inelastic failure, the redistribution of the forces and torsional effect are neither considered.

Limitations introduced by not modelling the gable in the SLaMA and NLPO analysis are accounted for with an NLKA-analysis as a posterior check in the assessment of the church. Based on the NLKA analysis of the gable, it was found that the collapse of the gable occurs very early on at a displacement of 0.8mm. The calculations are, however, on a conservative side as the for the analysis a one-dimensional representation of the gable was considered for which out-of-plane supports of the roof rafters could not be considered in this analysis. In case the gable would not be disregarded in the numerical models, one could avoid an early collapse by taking retrofitting measures and modelling the roof-rafters for an out-of-plane support.

The reliability of the numerical model results for the NLPO analyses were checked by means of the accuracy and convergence behaviour of the models. In the studies in this thesis, towards the end of the numerical

analyses, poor convergence and an early divergence were observed. The poor convergence was quantified in terms of exeedance of the out-of-balance forces in the norms adopted in this thesis. In this report, only fully converged results are presented. Main reasons for the observed non-convergence and divergence problems can be due to the occurrence of instability in either the physical models or the numerical models. Instability with a consequence of collapse in the physical model are most likely caused by extreme deformations in the curved façade in the church model prior to the modifications and in the vaults of the church model prior and post structural modifications. Instabilities in the numerical models are the consequence of a highly distorted mesh, which consequently introduce zero pivots in the global stiffness matrix of the numerical model. In the church models in this thesis a highly distorted mesh was observed for the vaults. As the instability problems are mainly found in the vaults, a sensitivity study is conducted in which the church model is considered with linear elastic vaults. This modelling choice allowed to reach convergence for a higher load level, however the improvement was not significant. In this case, the influence of the nonlinear material properties were excluded, however, the influence of the geometric nonlinearities are still considered in the model. This means that geometric nonlinear effects play an important role on the behaviour of the vaults and the convergence of the analyses. Additionally, several attempts were made by changing the numerical solvers in the analyses to find the root cause of the early divergence problems. Only with the aid of the Quasi-Secant method, it was possible to capture a ten times higher displacement capacity, but no post-peak behaviour. However, please note that this method is significantly less accurate than the Regular Newton-Raphson Method and that the results are merrily an approximation. The use of the arc-length method was not successful either and resulted in a poor convergence behaviour.

The capacity curves for the numerical models which were determined by the adoption of one-directional conventional pushover with a modal loading scheme, were subsequently compared against the seismic demand of a “weak” and a “strong” earthquake at the location of the case study in Zandeweer, Groningen. The so-called “weak” and “strong” earthquakes are defined as earthquakes with return periods of 95 and 2475 years, respectively. The assessment analysis in this thesis were done for the positive longitudinal direction only. As the gable is presumed to fail at 0.8mm, all values beyond this point cannot be considered. However, in case retrofitting measures are considered to ensure that the gable would not fail early onwards and the roof structure does not fail then in that case only the church post structural modifications based on the NLPO analyses, does not meet the demand of an weak earthquake in Zandeweer, Groningen. The capacity curve for the SLaMA analysis reach values up to 0.006g and a displacement of 100mm for both the church model prior and post structural modifications. The capacity curves obtained with the NLPO analyses for the church prior modifications reaches values up to 0.026g and a displacement of 8.18mm. For the church models post structural modifications values up to 0.039g and a displacement of 1.98mm are reached. Following the SLaMA approach the church prior and post structural modifications could meet the seismic demand at 6.18mm and 0.006g. Following the NLPO analysis, the church as built in 1230 could meets the seismic demand at 6.63mm at 0.026g, while the church post modification was not verified. For the damage, in general flexural crack patterns were observed, at the corners of window openings and the door opening in particular. The cracks appearing in the main walls were classified as very slight to moderate cracks depending on their location, whereas cracks appearing in the vaults were classified as very severe. The cracks pattern for the church model as built in 1230 for the location where the capacity curve could possibly meets the demand curve, in case failure of the gable was prevented, is presented in figure 2. Lastly, the drift limits for the main walls of both church models for both the severe damage stage and the near collapse stage the limits were not exceeded. This is not a surprising conclusion, as very slight to moderate damage was found for the walls.

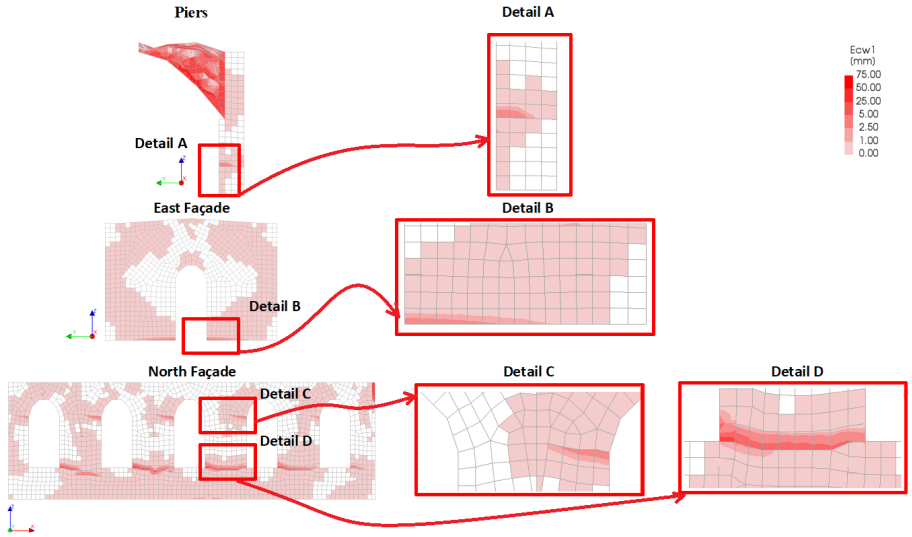

Figure 2: Crack Pattern Details for the church as built in 1230

Regardless of the provided information in the technical drawing and documentations, information regarding the structural connections and material properties are missing for this case study. Consequently, a sensitivity study on the influence of the modelling choices was made for the case of the connection between the piers and the walls for the church as built in 1230. To analyse the connection four models were chosen based on the assumptions of the interlocking of masonry units of the piers with the ones of the main walls. These four models are presented in Figure 3. In this study it was not possible to observe the influence of the local behaviour of the piers with the walls on the global behaviour of the church models. Therefore, a detailed modelling procedure is proposed to study this particular local behaviour in more detail.

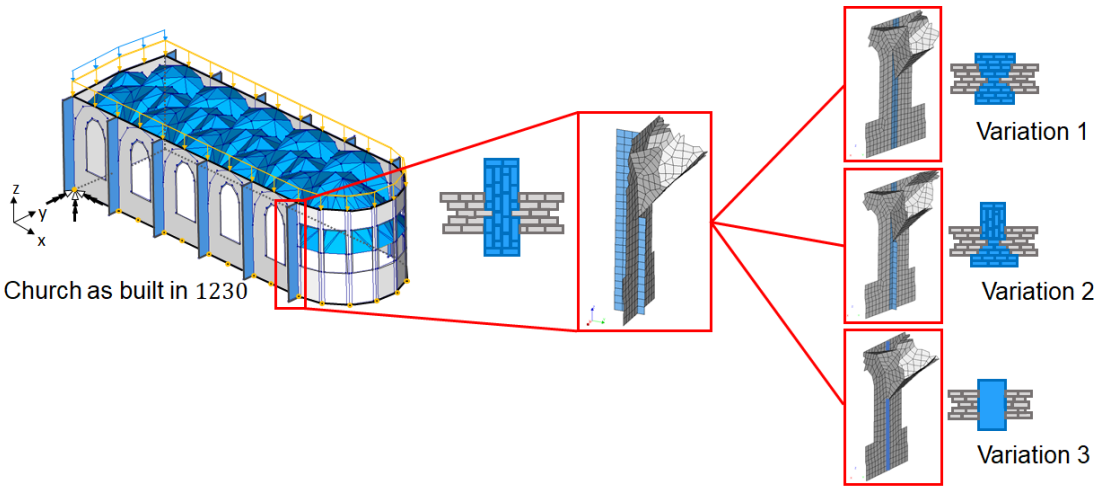

Figure 3: Numerical model representation for Church as built in 1230 and proposed variations on the pier-to-wall connections

Additionally, as the material properties are missing it was aimed for understanding the influence of the effect of (poor) masonry quality on the global behaviour of the structure. For the sensitivity of the global behaviour for poor masonry material properties it was concluded that the behaviour resemblance that of the standard masonry material properties. However, a reduced force capacity and initial stiffness was observed in the capacity curves. The analysis was conducted to present the influence on the global behaviour of the structure when a different assumption was made regarding the masonry material properties. In case one is interested in studying the influence of masonry material degradation, this single analysis is not sufficient to provide insight in the influence of poor material properties on the global behaviour and additional extensive studies need to be conducted on separate masonry material properties and their parameters. Lastly, with an additional sensitivity study the effect of the use of the Total Strain Crack model (TSCM) instead of the

Engineering Masonry Model (EMM) on the behaviour of the church was studied. The results for the TSCM showed a lower force capacity and initial stiffness in comparison to the EMM. Also in this case no post-peak was captured. As for the displacement pattern, for the TSCM a higher displacement was captured than with the EMM. For the crack pattern no difference was observed in the location and type of cracks occurring in the structure.

In this thesis a nonlinear pushover method and the SLaMA method were employed to capture the influence on the seismic response of a case study church prior and post structural modifications. Although, the presented results for the church models show an insight in the influence of the structural modifications for this particular case study it can be concluded that the results are highly conservative. The presented results do not provide an insight in the ductility behaviour of the structure as a consequence of the modifications and with respect to the base shear capacity it can be assumed that it is merely an estimation based on the simplifications and assumptions made in the presented models. From the results of the eigenvalue analysis in the longitudinal direction of the church, it could be concluded that adopted single-mode analysis methods (SLaMA and NLPO) are not suitable, as the structural response of the church is governed by multi-modes. Additionally, with the highly unpredictable behaviour of the vaults in the structure the presented results are greatly influence by physical and numerical instabilities. Therefore, additional studies need to be conducted with regards to the vaults and subsequently changes need to be made in the modelling and analysis procedure of the church in order to capture a better insight in the influence of the structural modifications on the seismic performance of the church models. Lastly, it should be noted that within the scope of this thesis a full assessment of the church models were not done. Additional analyses are required to complete the assessment, especially focusing on the local failure mechanisms. In this thesis a one-directional assessment was conducted without considering torsional effect, eccentricities and one load condition for the pushover was considered.

For future studies is recommended to dedicate a detailed study to the numerical modelling and analysis of masonry ribbed cross vault structures. In which either a single and a group of cross-vaults are studied. The study of masonry vaults is an interesting stand-alone topic with many research motivations for which their structural response can be explored. Examples for the study of these vaults could be the influence modelling of the shape, choice of finite element discretization, mesh discretization, influence of ribs, boundary conditions and dynamic or static load conditions. Parallel to the study of the vaults a detailed study on the church walls is suggested to employ, with flat lateral structural elements for which subsequently various analysis methods can be employed. For which additionally, the influence of orthotropy of walls on the global response, local failure for the walls and degradation of material properties can be studied. For the modelling approach, solid finite elements for the walls in combination with curved shell elements for the vaults can be used and the influence of the integration scheme can be studied. Compatibility of the finite elements can be ensured by appropriate use of tying. Moreover, a study in the orthotropy of multi-leaf walls is suggested for historical structures in particular as it reflect better the physical model. Layered curved shell elements can be used with appropriate material properties for the layers to study the effect of orthotropic walls for a three-dimensional case. The analysis method can be changed by the use of the Nonlinear Pushover Analysis (NLPO) method in combination with the Modal Response Spectrum Analysis (MRS) method or the Nonlinear Time History Analysis (NLTH) method. The methods provide a solution for considering multi-modes simultaneously and the use of dynamic analysis methods is known for its less numerical instability problems than for static analysis methods. Furthermore, a cyclic nonlinear analysis method is recommended for the study of the church structure and the study of the vaults in order to observe the degradation and propagation of the damage. To capture the post-peak behaviour, other solution methods, as the Sequential Linear analysis method are recommended in combination with a mesh refinement study. Additionally, to gain a better insight in the global seismic response of the church when using single-mode analysis methods such as in this thesis it is essential to study global behaviour of the church in both global direction. In this regard, an assessment of the global behaviour of the church in the transverse direction is highly recommended. It is recommended to do the assessment for both global directions considering the weakest direction including eccentricities and accounting for two load conditions. Lastly the scope of this thesis was limited to this particular case study, however, future studies can be conducted for other church typologies, such that a conclusion can be extrapolate based for several cases on the influence of structural modification to the seismic response of historical church structures in Groningen.

Keywords: Seismic Vulnerability, Nonlinear finite element Analyses, Curved shell finite elements, Historical Masonry Churches, Groningen

List of symbols

Symbol	Definition	Unit
E_x	Young's modulus parallel to bed-joints	N/mm^2
E_y	Young's modulus perpendicular to bed-joints	N/mm^2
G_{xy}	shear modulus	N/mm^2
f_t	tensile strength	N/mm^2
G_f	fracture energy in tension	N/m
f_c	compressive strength	N/mm^2
G_c	fracture energy in compression	N/m
c	cohesion	N/mm^2
Φ	friction angle	rad
G_s	fracture energy in shear	N/m

Acronyms

Abbreviation	**Definition**
PGA	Peak ground acceleration
URM	Unreinforced masonry
NC	Near collapse
SD	Significant damage
DL	damage limitation
LE	Linear elastic
NLE	Non-linear elastic
T_r	Return period
EEM	Engineering Masonry Model
TSCM	Total Strain Crack Model

Contents

1

Introduction

1.1. General context & Research motivation

In the past decades a significant amount of shallow human-induced earthquakes were experienced in Groningen, a region in the North of The Netherlands. Up until today, ever since the first earthquake in 1991 was measured, the total number of earthquakes in this region exceeds a 1,000. Figure 1.1 presents an overview of these events. As can be noted a majority of these earthquakes have a local magnitude M_L around and below 1.5 and can be therefore classified as relatively 'mild' earthquakes. Nevertheless, post-earthquake investigations conclude a considerable amount of light to severe damage to structures in the Groningen region due to these seismic activities. Moreover, with the occurrence of higher magnitude earthquakes in the recent years ($3.6M_L$ in 2012 in Huizinge, $3.4M_L$ in 2018 in Zeerijp, $3.4M_L$ in 2018 in Westerwijtwerd) a greater amount of severe damage and collapse of structures are reported ever since. Additionally, seismic hazard and risk prediction models show magnitudes of 5.0 with a 10% probability of exceeding in 50 years [1].

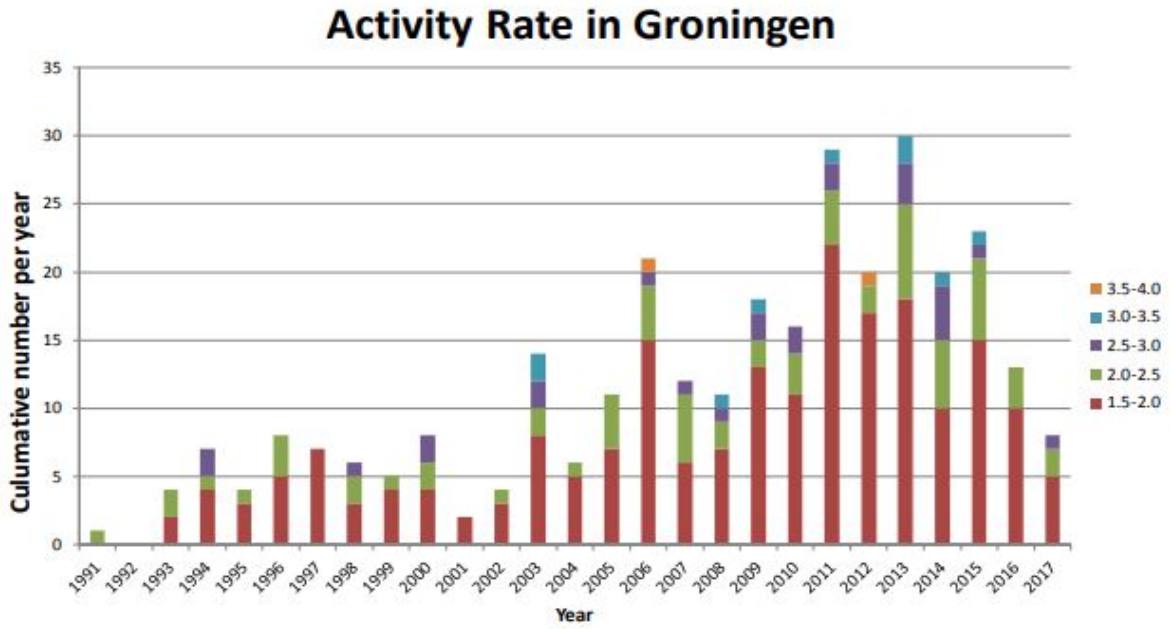

Figure 1.1: Number of events per year, categorized by local magnitude [1]

1.1.1. Seismic activity in Groningen

An earthquake is defined a phenomenon of the sudden release of extreme energy stored in the earth. The release of such energy, that is a resultant of stress changes in the earth, is triggered by a variety of root causes. The earthquakes in Groningen are caused by the subsidence of soil layers. Which is the antecedent of the gas extractions by the Nederlandse Aardolie Maatschappij (NAM) ever since the 1960's. The Groningen gas field is the largest gas field in Europe, and the tenth largest in the world.

Gas that is extracted from a permeable stone layer at a depth of about three kilometres results in a decrease in gas pressure within this layer. The non-permeable layer covering this layer is subsiding as a consequence of the decreasing gas pressure in the permeable layer. The subsidence either happens slowly or instantaneously [2].

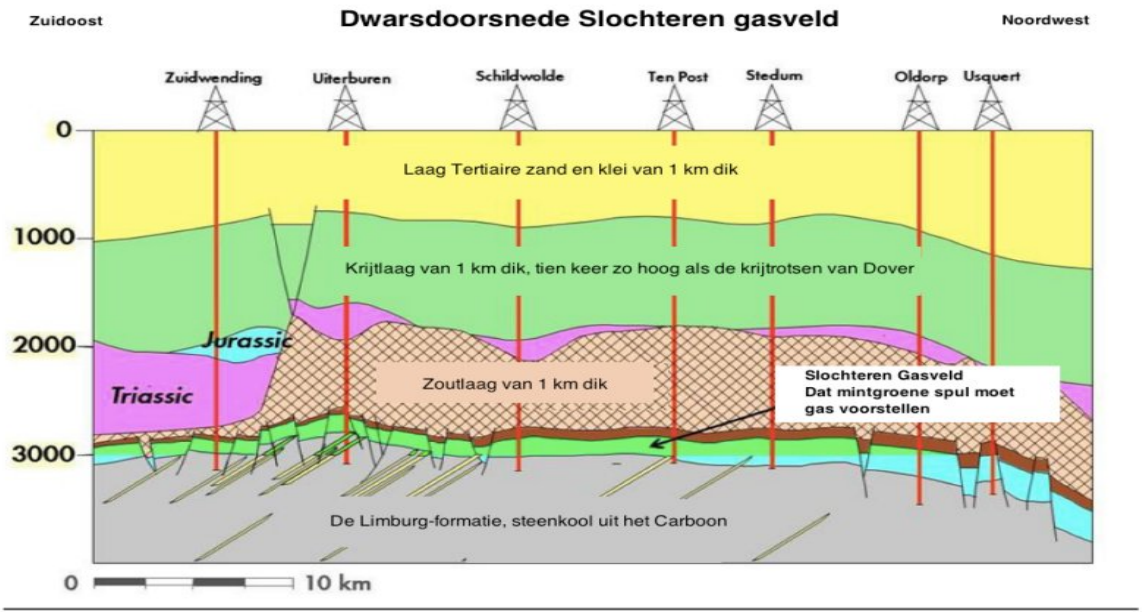

Figure 1.2: Cross-section underground layers gas field Groningen [2]

1.1.2. Monuments in Groningen

Since July 2019, 61.889 structures with a monumental status are recognized in the Netherlands. About 7.1% of these structures are monumental and historical churches. A big part of these churches, nearly 11.3%, is located in the province Groningen (see Figure 1.3 and 1.4).

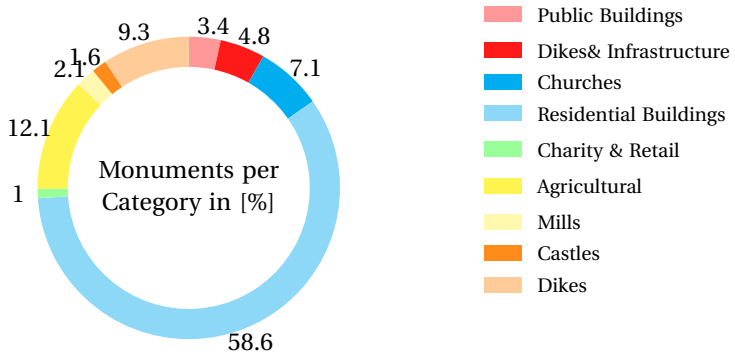

Figure 1.3: Monuments in the Netherlands per category. Total Dutch Heritage reported: 61.889 in July 2019 base on [3].

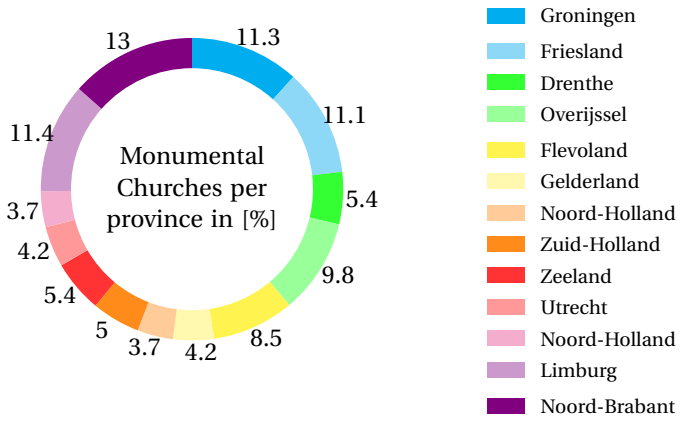

Figure 1.4: Monumental churches per province in the Netherlands [3]

So far, nearly 12.9% of the total stock of churches is reported to be damaged. This is relatively small in comparison with the damage reported to the stock of residential buildings in the province Groningen, which amounts 55.8%. Figure 1.5 presents reported damage per category monument structures in the province Groningen.

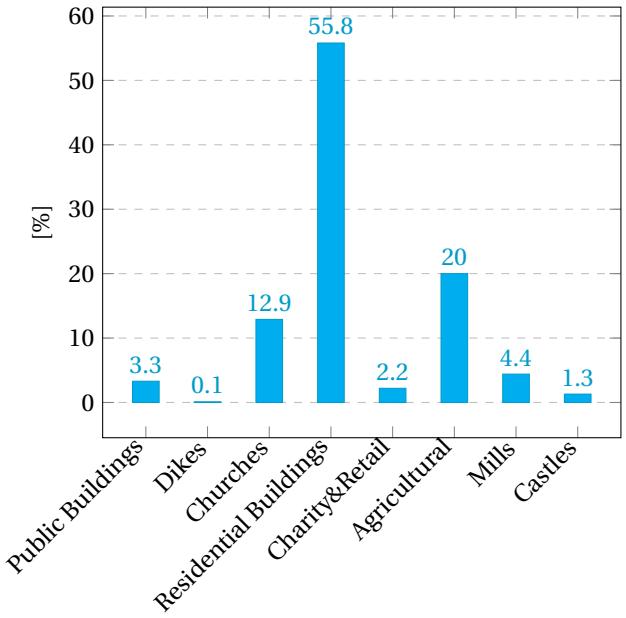

Figure 1.5: Damage reported to Monuments in Groningen, per category base on [3]

Among the buildings in Groningen, about 77% is constructed of unreinforced masonry (URM) for which no seismic guidelines are followed. From the perspective of conservation and prevention, their assessment becomes a necessity today. Within this URM building stock 2186 buildings are classified as monuments. Of which 28% are reported damaged by post-earthquake investigations up until 2017. During a *post-earthquake investigations* data on existing damage, either due to seismic activity or due to other causes, are collected. The collected data should provide us better insight in the risk for humans based on the type damage found. Depending on the damage level certain measures need to be taken. Figure 1.6 shows the locations of the monuments in the region Groningen, the importance of the archaeological heritage and the intensity of the earthquakes occurring. Most monuments are located in the municipality of Groningen, Mid-Groningen and Eemsmond. Most reported damaged are from the municipality of Groningen, Loppersum and Mid-Groningen [4]. The assessment of historical and monumental buildings should not be forgotten, as this will mean loss of our cultural and historical heritage.

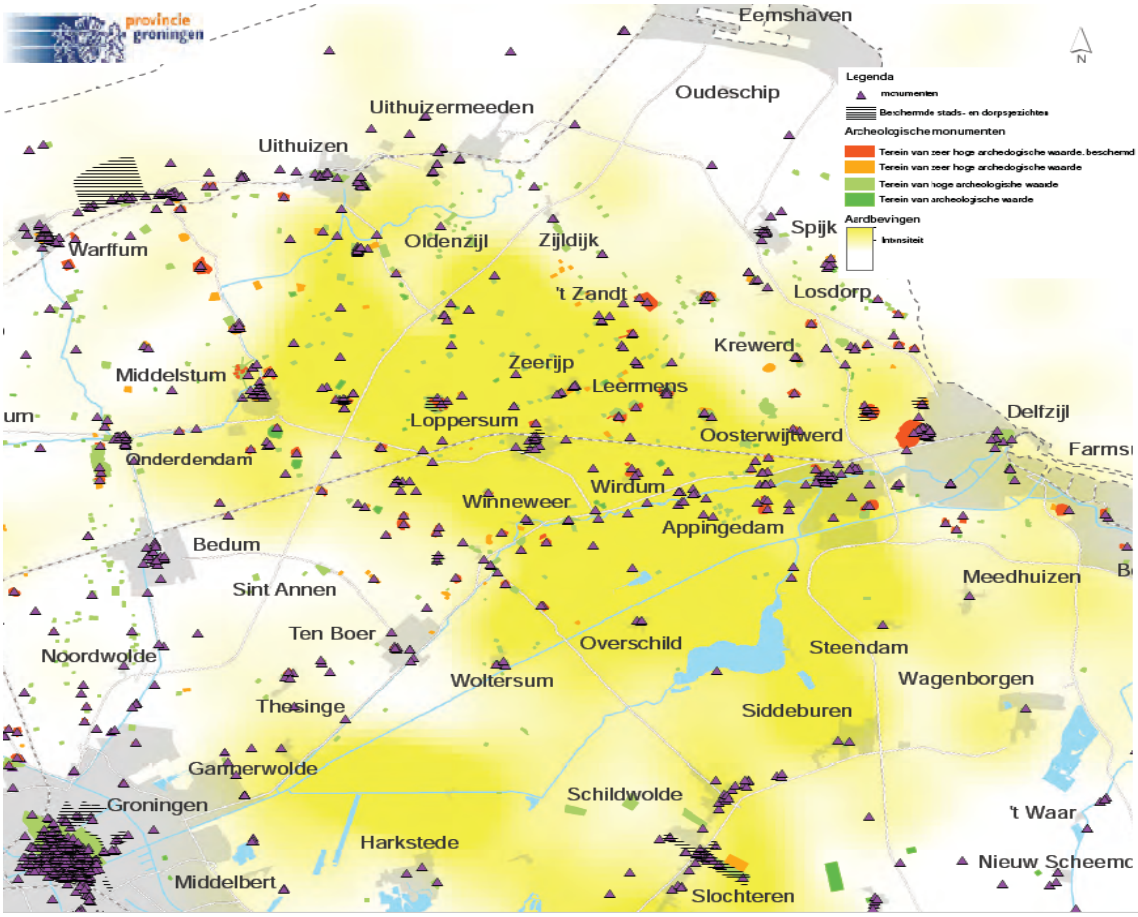

Figure 1.6: Monuments in Groningen [4]

1.1.3. Structural modelling, analyses & assessment

The *structural safety historical structures* can be assessed based on analytical and numerical prediction models to gain better insight in their structural response and behaviour. However, evaluating the seismic reliability of historical buildings is a very challenging task. Regardless of many uncertainties that are common for historical buildings their unique structural scheme often cannot be reduced to any standard scheme. As a majority of the historical buildings are very difficult to model due to their technological constructive complexity. Second, due to the nonlinear behaviour of URM and the dynamic nature of a seismic load it is a very challenging task for researchers and practitioners to evaluate their seismic reliability. For a reliable earthquake resistant design or assessment, appropriate numerical modelling of the structure and suitable analyses procedures are a prerequisite.

For this reason, recent studies [5–13] focus on these particular buildings. Up to this point, however, there is limited research conducted or available on the assessment of historical buildings in Groningen in comparison to a significant amount of research that has been conducted for residential URM buildings in the past decades. In particular, very limited research is available on the global behaviour and assessment of such complex structures. This is also reflected by the available regulations and codes. Such as, Eurocode 8 (EC8) and NPR9998 in which there is no a particular section devoted to the assessment of historical (URM) structures [14].

1.2. Objectives

As mentioned in the previous sections, a majority of historical unreinforced masonry structures have undergone restoration works, that can be favorable for their seismic performance. The main research question for this thesis is then formulated accordingly, as follows.

Main research question:

"How do the structural modifications during the lifespan of Dutch historical URM churches influence their seismic performance?"

The seismic performance will be investigating by evaluating the nonlinear global seismic response and the structural elemental behaviour and by indicating uncertainties and damage. The methodology used focuses on a global approach with the objective to assess the global capacity of the structure. The scope will be to considered primarily in capacities and secondary in displacements. Among various seismic analysis procedures two methods are chosen, namely the Simplified Lateral Mechanism Analysis method and the modal proportional Nonlinear Pushover Analysis method (NLPO). Two main objectives for this thesis can then be describe by the following research questions:

Sub research questions:

- *To which extend can the global behaviour of a Dutch historical URM structural church be predicted by means of a Simplified Lateral Mechanism Method (SLaMA)?*
- *To which extend can the global behaviour of a Dutch historical URM church be predicted by means of a Nonlinear Pushover method (NLPO)?*

The scope of this thesis is limited to the Zandeweer church in Groningen. For which, the seismic performance of the church as built in 1230 will be compared with the church after the structural modifications in 1931. Lastly, additional sub research questions are added to cover for uncertainties in the modelling approach and to consider the anisotropic properties of masonry by using the Engineering Masonry Material model.

Additional sub research questions

- *What is the influence on the global seismic behaviour of the church when using different numerical model representations for the pier-to-wall connection of the Church?*
- *Does the Engineering Masonry Constitutive Model in combination with Regular curved shell elements result in realist structural response for the URM structure?*

1.3. Synopsis

The research starts by providing the reader in Chapter 2, 3 and 4 the theoretical framework of this thesis. In this literature review, the features of church structures that may have a significant influence on the global seismic response are discussed (Chapter 2), analysis procedures and assessment methods for unreinforced masonry (URM) structures are reviewed (Chapter 3) and the structural behaviour and numerical modelling techniques for URM structures are presented (Chapter 4). In particular the Simplified Lateral Analysis method (SLAMA) and Nonlinear Pushover method (NLPO) are elaborated on in detail.

Then, the case study Church in Zandeweer, Groningen including its features, a prediction of the global seismic response of the case study church by SLaMA and the numerical models for the church prior and post structural modifications are discussed (Chapter 5). Followed by a presentation of the performed nonlinear pushover analysis for the global seismic response and the local response of the pier-to-wall connections for the church prior structural modifications (Chapter 6).

To understand what the influence of the numerical modelling approach for the pier-to-wall connection of the church models is on the global structural response, three variation of this connection are studied and analysed with the NLPO method (Chapter 7).

Additionaly, a set of sensitivity studies are conducted for the numerical solvers in order to catch the post-peak stage during the analysis, a study is done on the influence of the use of the Engineering Masonry Model and material properties on the global response of the structure (Chapter 8).

Thereafter, a comparison between the results of the NLPO analysis for the church prior and post structural modifications (Chapter 9) and the seismic performance of the church models including uncertainties are presented (Chapter 10).

Lastly, conclusions are drawn and recommendations for future research are proposed (Chapter 11).

1.4. Scope & limitations research

This thesis aims to analysis the influence on the seismic performance of the Zandeweer church in Groningen, due to structural modifications in 1931. The numerical and analytical representation of the unreinforced masonry church structure only include the stability elements and the following structural components are not considered explicitly:

- *Timber roof structure*
- *Masonry gable*
- *Foundation structural elements*
- *Mortar and brick/stone modelling. A smeared continuum orthotropic composite modelling approach is adopted (macro-modelling) for the numerical models.*

Additionally, the following aspects are disregarded in the analysis and assessment of the church structure:

- *The vertical load component of the seismic loading*
- *A pushover loading in the transverse direction for the analysis and assessment in that direction.*
- *Soil structure interaction is neglected by assuming a fully fixed base connection*
- *Strength degradation as a monotonic approach is used instead of a cyclic loading scheme*
- *One pushover loading scheme, namely a mode proportional loading. Within the time limits of this thesis a second loading scheme is not considered*

Lastly, note that a variation on the building typology, material properties, seismic activity, strengthening methods, etc is not done in this thesis.

2

Historical masonry structures

This chapter provides the reader a concise overview of the available literature on features of churches that are governing for their structural assessment and highlights a set of uncertainties regarding historical structures that makes their assessment a challenging task.

2.1. Uncertainties & features churches

Historical structures, churches in particular, which are often composed of an assemblage of structures are built in different periods in time, with a great variety in construction phases, construction techniques by workers and material usage. For most of these historical structures often limited information is available on their history regarding restoration, reconstruction work or other changes that may have an influence on their physical model. Their structural components vary widely in their typologies. Figure 2.1 and 2.2 show an overview of examples of possible peculiarities of churches. Chapter 4 of this thesis will provide the reader, a thorough explanation regards the physical and mechanical properties and failure mechanisms of these structural components.

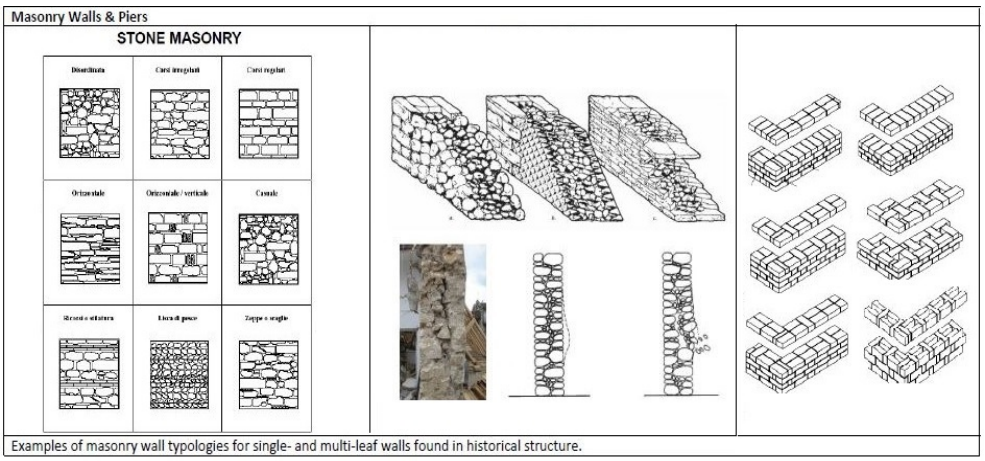

Figure 2.1: Masonry Wall Typologies found in Historical Structures [15]

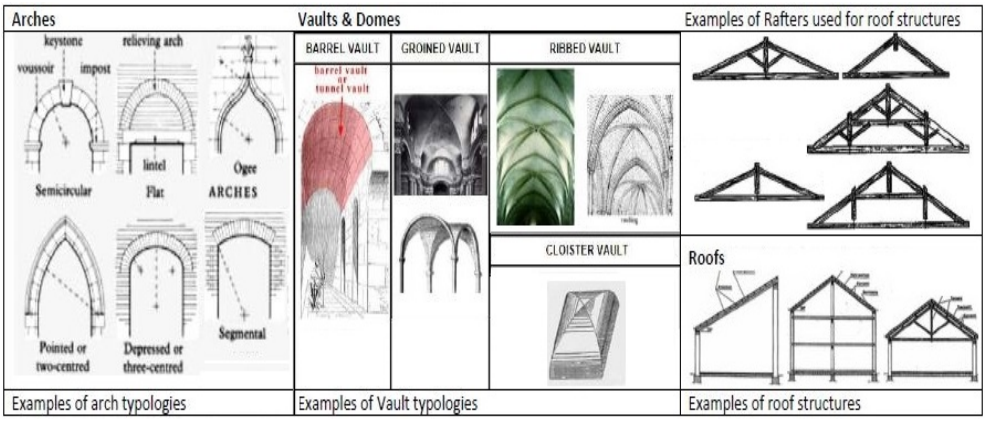

Figure 2.2: Structural Component Typologies found in Historical Structures [15]

2.2. Macro elements for churches

The assessment of the seismic reliability of historical structures remains a challenging task as these structural organisms cannot be easily reduced to any standard scheme. To overcome this problem, a macroelement approach can be used to analysis the structural response of such structures: the structural organism is then considered as the assemblage of few components whose behaviour is analogous to macroelements in buildings, whose possible collapse mechanisms can be identified. Lagomarsino [16] distinguishes 28 macroelements and their collapse mechanisms, these are all based on the collected data from more than 1000 post-earthquake investigations of churches in Umbria and Marches in Italy. Sixteen macroelements with possible damage mechanisms are presented in Figure 2.3. Subdivision of these structures in macroelements allows the development of precise vulnerability assessment methods. Among the methods that are developed today, Augusti et al. [5], describe the use of the macroelement approach in combination with a probabilistic approach can give a greater insight in an assessment procedure for the seismic reliability of monumental buildings. It provides a tool to predict the probability of failure of macroelements and the order of failure.

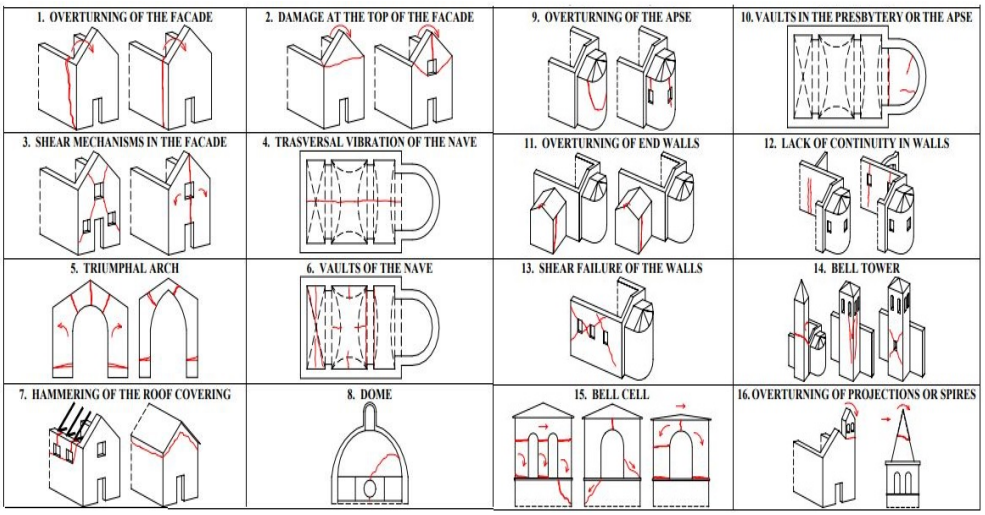

Figure 2.3: Damage mechanisms in macroelements of a church [16]

Lastly, the method is also very useful in combination with numerical simulations of churches under seismic load conditions. In this case macroelements can be identified based on the geometric data, prior to the simulation as a hypothesis for the results of a simulation. Or macroelements can be identified from the results after a simulation. In both cases, the method provides a better insight in possible seismic behaviour of the structure by predicting failure modes of the structure. This can be useful in case one is interested in local failure modes. Especially in cases where local failure modes trigger global failure modes of parts or the entire structure this can be a very fast method for the analysis of a church.

3

Seismic analyses & Assessment methods

3.1. Evaluating the seismic performance

The seismic performance of a structure can be evaluated based on a seismic demand, according to a performance based design approach. The demand depend on factors such as structural characteristics, geographic characteristics and type of seismic event and its characteristics. The seismic performance of structure can then be evaluated based on its seismic capacity that is dependent on its force & displacement capacity. Additionally, dependent on the limit state that will be assessed other characteristics of a structure may be also relevant for the seismic assessment. For example, damage due to cracking, the formation of local failure mechanisms or drift limits may be relevant factors.

3.2. Seismic Analysis Methods

A range of analyses methods are available to capture the structural response of a structure under seismic loading. The methods are categorized by two assumptions. First, whether the loading conditions are considered as static or dynamic. Second, whether linear or nonlinear material properties are considered. In this treatise an unreinforced masonry structure is considered. Unreinforced masonry structures are composed of structural elements that exist of masonry units and mortar. These materials are characterized by relatively low tensile strength and a quasi-brittle nature. This means that cracking of the units occurs at a relatively low lateral loading. Although,linear elastic analysis methods are relatively fast methods, results obtain via these methods are very conservative as these methods are not able to capture the nonlinear nature of masonry. Consequently, nonlinear dynamic analyses methods are the most suitable methods. As the seismic loading has a dynamic nature, the Nonlinear Time History Analysis (NLTH) would be the most suitable among the methods presented here. However, the NLTH analysis is computationally demanding and requires for reliable results multiple analyses with different ground acceleration motions. Therefore, nonlinear static analysis methods, for which the loading is considered in a quasi-static fashion, are computationally more efficient and result in less conservative results as these methods are able to capture the non-linearity of Masonry. Examples of these methods are the Nonlinear Pushover Method (NLPO) and the Simplified Lateral Assessment method (SLaMA). Figure 3.1 provides an overview of these analyses methods.

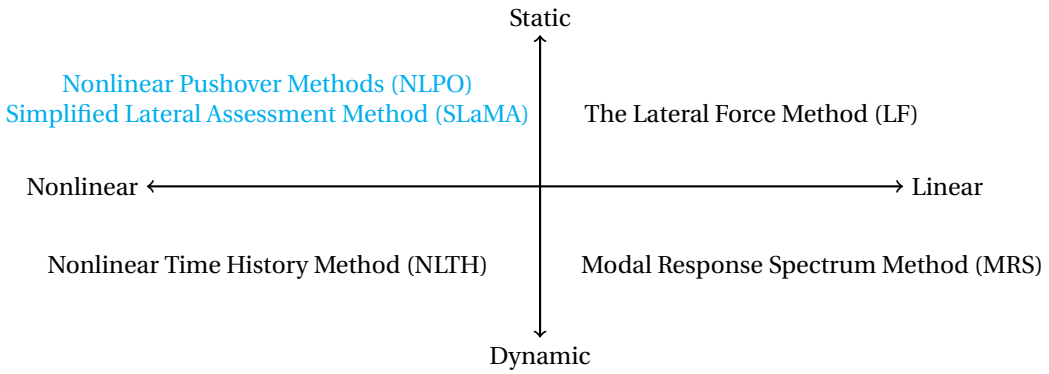

Figure 3.1: Analyses methods for the calculation of the seismic response of structures.

3.2.1. The Simple Lateral Mechanism Analysis (SLaMA)

The Simple Lateral Mechanism Analysis (SLaMA) method, is an analytical mechanism based method that is used in engineering practise as a starting point to determine the global nonlinear response of a structure. Priestley, Park and Calvi (1991-1996) initially developed this method extensively for reinforced concrete structures. The global response is captured by means of the summation of simple representations of the capacities of the individual structural components. This simplified technique makes it possible to predict the probable inelastic deformation mechanisms and their lateral strength and displacement capacity by examining load paths, the hierarchy of strength along this critical path, the available ductility/displacement capacity of the identified mechanisms and the manner in which various mechanisms might work together. With the emphasis on mechanism-based method based on a displacement-based approach this method is recommended as a first step for any assessment. With the objective to not count on sophisticated techniques without first developing an understanding of how the structure may resists seismic loads and identifying the various critical load paths and insight in the interaction of sub structures. The degree of simplification and assumptions regarding the structural response and capacity can be summarized by the following:

- *Initial modes of response are dominant and higher mode amplification can be therefore disregarded.*
- *The hierarchy of strength of connected elements can be analysed by comparison of comparable "internal action". For example, the relative capacity in flexure and shear for beams can be checked. However, the sequence of development of inelastic action between various structural elements may not be identified. For structures with low member ductility capacity there may be a high likelihood of overestimation of the load distribution and thus also the global strength and displacement capacity*
- *The governing mechanism at local element level is extrapolated to global structural level, with the assumption of that either load redistribution is likely (ductile response) or not (brittle global response).*

3.2.2. The Nonlinear Pushover Analysis Method (NLPO)

The pushover analysis method makes us of a lateral load application, which is equivalent to the lateral load that is excites in a structure during an earthquake. The load is either monotonically or cyclically applied until failure is reached [17]. The lateral load is applied in a predefined load pattern. The analysis provides information about the peak response in terms of floor displacements and storey drift. From which the relation between the displacements in the control point versus the base shear can be plotted. This is referred to as the so-called capacity curve.

Capacity Curve

The determination of the capacity curve is an essential part of the NLPO method. It defines the relationship between the base shear and the displacement of a control node. The relationship describes the capacity of the structure in terms of peak force and deformation and its deformation capacity. Figure 3.2 shows an example of a capacity curve. This method is recommended to be used where the buildings response is not significantly affected by contributions from modes of vibration higher than the fundamental mode.

Load patterns

The assumed load distribution on the structure represents the inertia forces which the structure would be experiencing during an earthquake. A conventional pushover analysis a lateral load is applied of which only

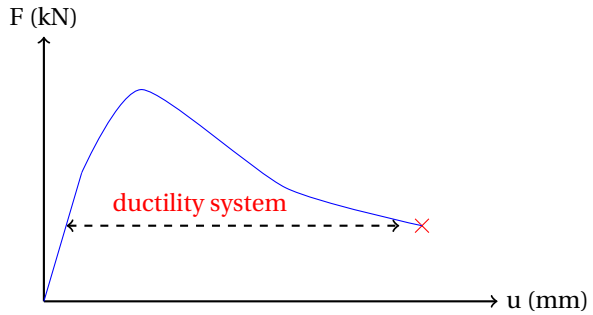

Figure 3.2: An example of a capacity curve

the magnitude is increasing and the shape distribution remains constant. The inertia forces are then an approximation. More accurate results are obtained for load patterns that vary during the analysis. The different load patterns are presented in Figure 3.3. It is worth noticed that for structures where the multi modes are governing, the conventional NLPO method gives conservative results and it is recommended to use an adaptive pushover method. Gupta et al. [18] and Shakeri et al. [19] studied in more detail the use of an adaptive pushover method.

The capacity of the structure will be reflecting the the deformation pattern of the structure at the end of each load step. Eurocode 8 and NPR9998 [14] prescribe the use of a constant load pattern. However, since this distribution method is incapable of capturing the variations in the response of the structure during the application of the seismic load, at least 2 different load patterns are required. In this treatise the following two load application methods will be adopted:

- *A* uniform distribution pattern that is mass proportional
- *A* modal distribution pattern that represents a dominant modal shape of the structure

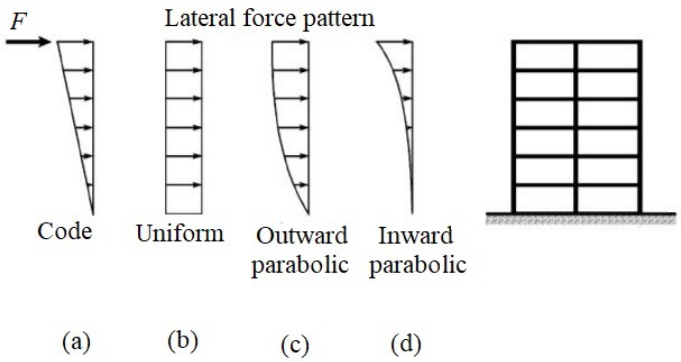

Figure 3.3: Lateral Force Distribution monotonic NLPO [20]: (a) code, (b) uniform, (c) outward parabolic and (d) inward parabolic

The Control Node

For the load-displacement relation of the structure the displacement of a node is extracted for every load step. The choice of the control node will influence the magnitude an shape of the capacity curve. For the analyses conducted in this report the control node is chosen, as the node with a maximum lateral displacement during a linear static analysis at the top elevation of the structure.

3.3. Seismic Assessment Methods

Capacity curves obtained by a pushover analysis are an significant element in the assessment of the seismic performance of structure. Seismic demand according to a performance-based design need to be calculated. Various methods, considering structures with rigid diaphragms, are available to calculate the seismic demand. The seismic demand is expressed in terms of target displacement. The target displacement is the

displacement till which the structure is pushed with a certain load pattern during a monotonic or cyclic analysis. Depending which performance level is studied the target displacement can be determined accordingly. Methods presented by different guidelines include:(1) The capacity Spectrum Method (ATC-40 / NPR9998), (2) The N2-Method (Eurocode 8) and (3) The Coefficient Method (ASCE/SEI41-13). For greater insight in these methods the readers is referred to the relevant codes. For the scope of this treatise the Capacity spectrum method and the N2-method are studied. As these are most commonly used in the Dutch industry.

3.3.1. The Capacity Spectrum Method according to NPR9998

The capacity spectrum method is presented as a relation between the acceleration-displacement response spectrum (ADRS). This relation provides the force demand and a deformation demand. The capacity spectrum method, which was initially proposed by Freeman and Tyrell [21], considers an inelastic behaviour by means of reducing the demand based on an equivalent damping level. This equivalent damping level is composed of the inherent damping of the structural system, the hysteric damping and the soil conditions.

Figure 3.4 provides an overview of obtaining the displacement demand with the Capacity Spectrum method. The displacement demand is then expressed as the intersection of capacity spectrum versus the response spectrum of the structure. The method consist of the following steps:

- *Step 1: Construct the Pushover Curve*
- *Step 2: Convert the Pushover Curve to the Capacity diagram*
- *Step 3: Convert the Elastic Response Spectrum to the Acceleration-Displacement diagram*
- *Step 4: From the intersection point of the capacity and demand spectrum curve find the target displacement*

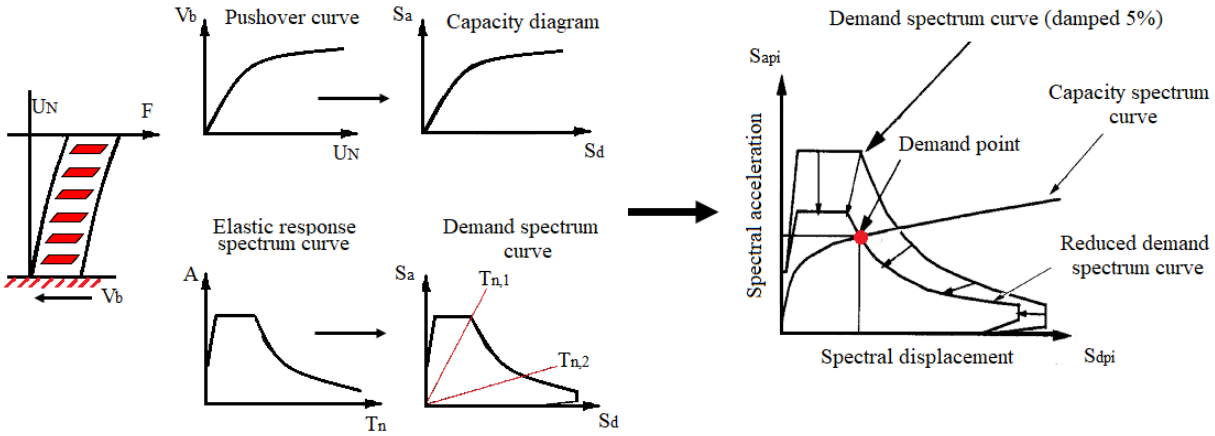

Figure 3.4: Capacity Spectrum Method as described by[17]

3.3.2. The N2-Method according to Eurocode 8

The N2-Method described by Eurocode 8 is characterized by determining the target displacement based on a short, medium or long-period response for an idealized single degree of freedom (SDOF) System. The N2-method, initially proposed by Fajfar [22], compares the natural period of an equivalent idealised SDOF system with the corner period of the demand. The non-linearity of the material is taken into account by a q-factor greater than 1. The method consist of the following steps:

- *Step 1: Determine the horizontal elastic response spectrum based on the equivalent damping of the system and the soil conditions depending on the location of the structure.*
  The equivalent damping of the system includes the inherent damping of the structural system, viscous damping and hysteric damping. Such a response spectrum is typically shown in terms of the spectral acceleration versus natural periods for a constant viscous damping. In addition, for the assessment, it is necessary to transform this graph into an acceleration versus displacement domain. The following

relation applies for this transformation:

$$S_d = \frac{T^2}{2\pi} S_a \tag{3.1}$$

where S_d, S_a and T are the target displacement, maximum peak acceleration and natural period, respectively. The conversion of the elastic response spectrum curve to the demand spectrum curve is depicted in Figure 3.5 and 3.6.

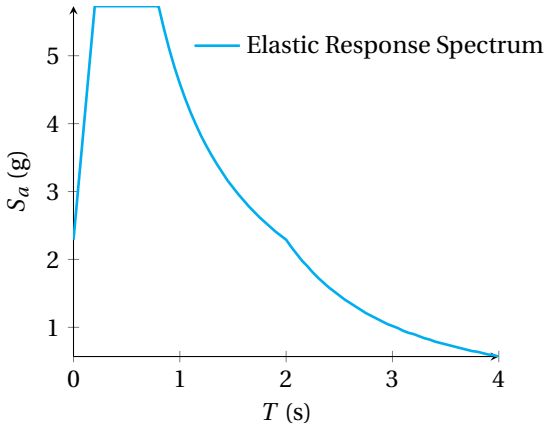

Figure 3.5: Traditional format

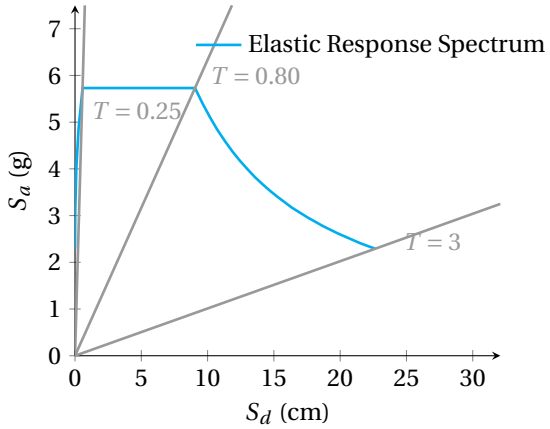

Figure 3.6: Acceleration-displacement format

- *Step 2: Transform the Multi-Degree of Freedom (MDOF) system into an equivalent SDOF system. By transforming the capacity curve from a force-displacement to a force-modal displacement graph:*

$$F_y^* = \frac{F_b}{\Gamma}, \quad d_y^* = \frac{d_n}{\Gamma}, \quad \Gamma = \Sigma F_i \, \Sigma(\frac{F_i^2}{m_i}) \tag{3.2}$$

where F_y^*, F_b and Γ are yield force, base shear force and transformation factor respectively. The yield displacement and peak displacement are denoted with d_y^* and d_n, respectively.
- *Step 3: Determine the Yield force, the yield displacement.*
The d_y^* can be formulated by:

$$d_y^* = 2\,(d_m^* - \frac{E_m^*}{F_y^*}) \tag{3.3}$$

where d_m^* and E_m^* are the ultimate displacement and elastic modulus of the system, respectively. This relationship is illustrated in Figure 3.7.

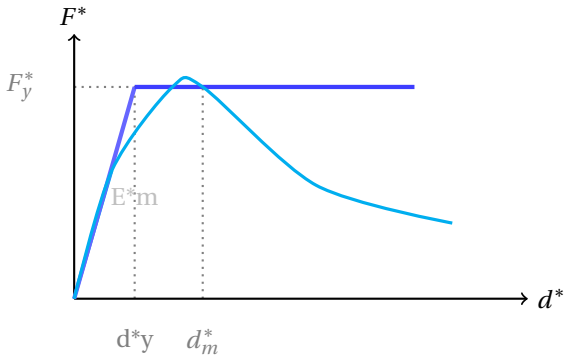

Figure 3.7: Stiffness relation of equivalent SDOF system based on [23]

- *Step 4: Transform the target displacement of the SDOF system into the target displacement of the MDOF system.*

$$d_t^* = S_d(T^*), \quad T^* = 2\pi\sqrt{\frac{m_{eff}d_y^*}{F_y^*}}, \quad m_{eff} = \Sigma m_i \phi_i \tag{3.4}$$

where m_{eff}, m_i, T^* and ϕ_i denote the effective and mass of the i-th story, elastic period and the normalized eigenvector, respectively.

Nonlinear material behaviour can be considered in case the response of the SDOF system is nonlinear. The response can be considered nonlinear in case the acceleration of the yield point of the SDOF is smaller than the spectral acceleration at period T^*. The q-factor is the ratio between the inelastic and infinitely elastic behaviour of the structure.

3.3.3. Limit states

Three limit states can be differentiated within Earthquake engineering dependent on the damage level one want to assess. Fundamental requirements regarding the state of damage are described in Eurocode 8 (see Table 3.1) [23, 24].

	Near Collapse[NC]	**Significant Damage[SD]**	**Damage Limitation[DL]**
Type of Damage to the Structure	heavily damaged	Significant damaged	light damaged
State structural components	Low residual lateral strength stiffness. Vertical elements can sustain vertical load.	Some residual lateral strength and stiffness. Vertical elements can sustain vertical loads	Structural elements prevented from yielding retaining their strength and stiffness properties.
State non-structural components	Most components collapsed	Damaged, but participation and in-fills and no out-of-plane failure	participation and infills may show distributed cracking, but the damage will be economic to repair.
Drifts	Large permanent drifts present.	Moderate permanent drifts present	Permanent drifts negligible.
General	Structure would most likely not be able to endure another earthquake with a moderate intensity.	Structure can sustain after-shocks of earthquakes with moderate intensity. However, damage is economically not feasible to repair.	Structure does not need to be repaired.

Table 3.1: Limit states based on [23]

Damage, in this study refers to cracking of masonry, is detrimental to a structure and could lead to partial or full collapse of a structure. Cracks are an indication of permanent loss of cohesion, permanent deformations without the loss of cohesion and permanent translations or rotations due to settlements or tilting of a structural component. As can be seen from table 3.1 on page 14 the description by Eurocode 8 [23] regarding damage in a structure is on qualitative basis. To be able to assess the damage in a quantitative manner various damage classification methods are proposed by for example, Korswagen et al. [25] and Giardina et al. [26]. A quantative approach allows to observe the progression and accumulation of damage in a structure. Korswagen et al.[25] discusses the quantification of light damage in structures and consider the damage limitation (DL) state. Whereas, Giardina et al. [26] considers the quantification of damage in the limit state classes of Near collapse (NC) and Significant Damage(SD). For this treatise the Limit states NC and SD are considered for the assessment of the structure. Therefore, the damage quantification system by Giardina et al. [26] is adopted (see Table 3.2).

3.3.4. Representation Seismic Load

Analysis techniques discussed in this chapter are the SLaMA and the NLPO method. It is recommended to start with SLaMA as the first step of any assessment to determine the global inelastic mechanisms. A SLaMA is considered an essential initial stage for any nonlinear modelling to help identify which areas may require more focus and which are unlikely to undergo any inelastic deformation. A SLaMA will also help to provide an

Damage Level	**Tensile Strain[%]**	**Crack width[mm]**	**Damage Class**
1	0 - 0.050	0.1	Negligible
2	0.050 - 0.075	1.0	Very Slight
3	0.075 - 0.150	5.0	Slight
4	0.150 - 0.300	5.0 - 15	Moderate
5	> 0.300	15 - 25	Severe
6	> 0.300	>25	Very Severe

Table 3.2: Damage classification for URM according to [26]

appreciation of how the various elements of the building are likely to interact. Nonlinear analysis techniques are appropriate for buildings which contain irregularities and when high levels of nonlinear behaviour are anticipated. If nonlinear pushover analyses are used, appropriate allowances in cyclic strength and stiffness degradation needs to be anticipated.

For both procedures it is assumed that torsional stiffness irregularities are not present and if torsional irregularity is present then an additional inelastic torsional check needs to be carried out. Higher mode effects are considered not critical. Linear dynamic analysis must be used parallel if higher modes effects are influential. In case of the NLPO, if a higher mode is critical (e.g. mass participation in the first translation modes are less than 60%), then two or more load/deformed shape vectors should be used for the pushover analysis.

4

Structural behaviour of URM structures

Traditional construction materials used in monumental or vernacular buildings are predominately materials as stone, earth or wood. In this treatise are the focus is on unreinforced masonry walls and timber diaphragm floors and roof systems. Hereafter, material model representations for the numerical model is further discussed.

4.1. Mechanical behaviour of masonry

Masonry, most used building material around the globe, resists gravity loading very well, is relatively cheap and easy to work with. The masonry general terminology is illustrated in Figure 4.1. However, it lacks resistance when loaded in lateral direction, for instance due to earthquake loading. Also in comparison to any other structural material available today, e.g. reinforced concrete, steel and timber, masonry is relatively weak in resisting lateral loading. Masonry, has a relatively low tensile strength and a brittle behaviour by nature. Due to its geometry, orthotropic behaviour and its material properties it has a complex behaviour. When URM walls or structures are loaded in cyclic manner complex failure mechanisms can develop and lead to damage or collapse of the entire structure. With this type of loading, unloading and reloading paths with recovery stiffness occur which makes modelling of materials such as masonry complex and a challenging task. This section will review and highlight some of the relevant and important material properties of masonry.

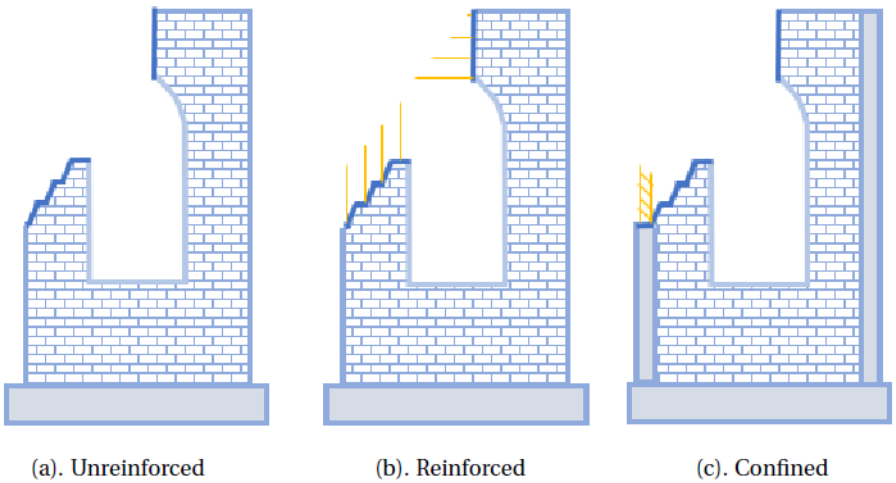

Figure 4.1: Masonry General Terminology: (a) unreinforced, (b) reinforced and (c) confined

4.1.1. Orthotropy

Masonry in the application of structures, is a composite material. That is composed of bricks and mortar. The manner in which the bricks and mortar are assembled together results a certain pattern for the final structural element/ assemblage. How the final assemblage will look depends on how the bricks are stacked together. The elements of an assemblage do not behave isotropic and the final assemblage itself has a orthotopic behaviour. This means that the properties of an assemblage differ in thickness, height and width direction. Figure 4.2 and 4.3 depict different masonry assemblage patterns.

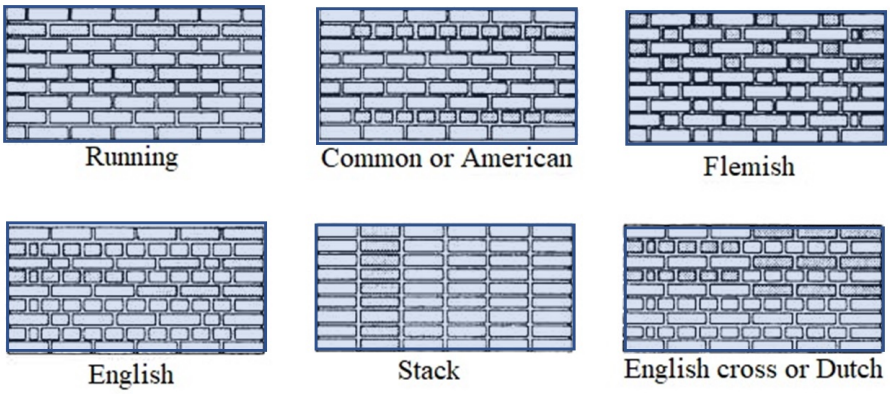

Figure 4.2: Masonry assemblages with various patterns

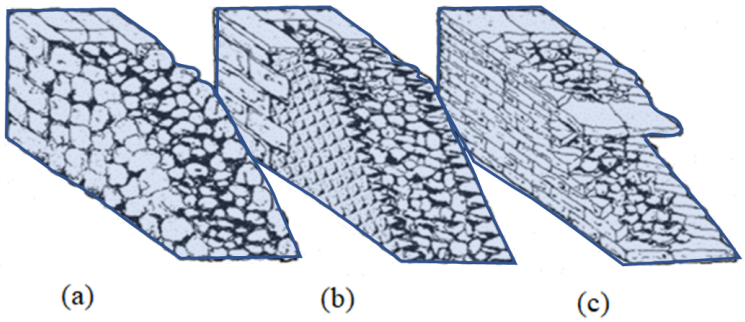

Figure 4.3: Different masonry assemblages in thickness

4.1.2. Properties of the composite

The interaction between the masonry units and mortar and the properties of the individual masonry constituents are not sufficient to represent the composite behavior. The mechanical properties of a composite material need to be considered. With the aid of uniaxial and biaxial tests the mechanical properties of such a masonry composite can be captured.

Uniaxial tensile behaviour

The weakest link in a composite material are its interfaces. Failure in a masonry component may occur perpendicular to the bed-joints and perpendicular to the head-joints. Failure will occur in the bed-joints if an element is loaded perpendicular to the bed-joints and the tensile strength normal to the bed-joints is approximately equal to the tensile bond strength parallel to the bed-joints. (Lourenco, 1996). However, failure may also occur in the units rather than in the interfaces in case of the application of certain weak masonry unit applications.In case an element is loaded in tension perpendicular to the head-joints, two different failure modes are often found; vertical crack through the head-joints and units or staircase cracks through the head- and bed-joints.

Uniaxial compression behaviour

The RILEM test can be performed to obtain the compressive strength of masonry perpendicular to the bed-joints. It is shown that the masonry under compression has a quasi-brittle behaviour [27]. The compressive behaviour of masonry perpendicular to the head-joints may have an effect on the capacity of the overall behaviour of a structural element and thus on the behaviour of a structure.

Biaxial behaviour

Dhanasekar et al. [28] have investigated the biaxial behaviour of masonry. They performed several studies in order to have a better understanding of masonry component under different load combinations. Additionally, they conducted several analyses to study the influence of principal stress rotation with respect to the axis parallel to the bed-joints and principal stress ratio on the failure process.

4.2. Mechanical behaviour URM components

Churches have some peculiar characteristics, compared to buildings, namely:

- *very slender walls, typically the slenderness reaches h / l = 10-12*
- *presence of pushing elements, such as arcs or vaults*
- *absence of intermediate horizontal structural elements. Such as floors.*
- *particular architectural elements (stuccos, ornaments)*

As for the vulnerability, churches damage can be detected even for low intensity. Greater damage is detected for churches compared to ordinary buildings under the same conditions. Concluded from the inspections done in Italy after the Earthquake Emilia in 2012. Ancient churches are sometimes build or an assemblage of structures built in a period that could be decades or even several centuries. These different construction phases corresponds also to change of workers, material and even techniques. In general most churches have a common aspect, that is, these churches have a single nave or three naves irrelevant of the geometric dimensions. Irrelevant of a wide variety in geometric shape, material type, construction methods, these churches do not have entirely a global response to seismic loading. Failure mechanisms can be described rather by distinct macro elements. These macro elements generally have an independent response from each other. For which the in-plane, out-of-plane and combined failure mechanism are possible.

4.2.1. In-plane failure mechanisms general - Walls

From the observations of the results of experimental tests on masonry walls under in-plane loading three typical failure modes were found: rocking failure due to flexure, sliding failure due to shear and diagonal cracking due to shear. Figure 4.4 depicts different masonry in-plane failure patterns.

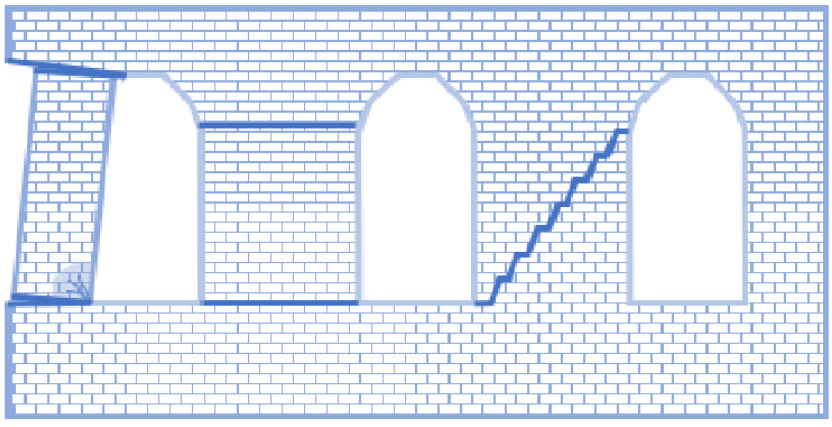

(a) Flexural cracking (rocking) including Toe crushing (b) Horizontal Sliding (c) Diagonal cracking

Figure 4.4: In-plane failure mechanisms

Rocking Failure
In this failure mode the lateral load causes tensile cracking at the toe of the pier. The entire pier start to behave as a rigid body rotating around the toe [29]. Around the other toe the wall is loaded in compression. If the compressive stress due to this loading is relatively high compared to the masonry strength, sub-cracks will occur around this toe. The failure of the masonry is then governed by toe crushing.

Sliding shear failure
Horizontal sliding along the bed-joint triggers this failure mode. Horizontal cracks are initially formed at the interface between the bed-joint and units as the lateral load is applied. When the friction coefficient of the interface is small and the compressive load on the pier is low this failure mode will occur.

Diagonal Cracking
In case diagonal cracking is governing, a diagonal crack pattern is to be observed in the pier. Which is formed at the centre and goes towards the corners of the pier. Depending on the properties of the masonry constituents, cracks are formed in a step-wise pattern over the bed- and head-joints, or through the masonry units [29].

4.2.2. Out-of-plane failure mechanisms general–Walls
Masonry structures under seismic events are often subject to in-plane and out-of-plane loads simultaneously. Regarding the out-of-plane response of URM walls various studies have been done so far. In particular, Griffith et al. [30] conducted tests on masonry panels loaded cyclic out-of-plane. Results from these tests showed a remarkable displacement for the out-of-plan direction, with values well above those adopted as limit in previous tests (equal to 2% of the wall height). Other publications investigated the influence of boundary conditions on the out-of-plane collapse of masonry walls [31–35]. Such as a research done by Tondelli et al. [36], who examined a four-storey building (scale 1 : 2) with simple masonry panels and reinforced concrete floors. From observations of these tests, it can be concluded that a rigid connection between wall and floor elements results in a good restraint of the horizontal action, caused by out-of-plane loading.

Brincker [37] conducted various tests on URM walls under load combinations of out-of-plane lateral loading and in-plane pressures. Results from these tests show that masonry has ductile behaviour properties. Which means that the yield line theory is applicable for laterally loaded masonry wall as a design method. D'Ayala et al. [38] studied the development of out-of-plane mechanisms. A direct relationship was found between the quality and strength of the connections and the connected structural elements. For URM walls with poor connections overturning failure modes were found, while for URM walls with strong connections relative to the connected structural elements the arch effect was a governing failure mode. Meisl et al. [39] performed four full-scale tests on a shaking table for URM walls. Sensitivity of out-of-plane response to the type of ground motion and the quality of the wall connection was investigated during these tests. Results however did not show a high correlation between these parameters and the peak response of the walls. Yet, for high amplitudes of the ground motion, a negative slope was observed in the force-displacement cure of the wall without the occurrence of instability in the structure.

4.3. Numerical modelling strategies

The Finite Element Method (FEM) is a powerful tool to study stresses and displacement in solids. A mathematical description of the material behaviour, which yields the relation between the stress and strain tensors in a material point of the structural element, is necessary for this purpose. Numerical modelling is then an useful tool to validate experimental results to understand complex nonlinear behaviour of structures. In this section the main numerical approaches available and used today are described. And further details on the two material models used in DIANA FEA 10.3 are discussed.

Various numerical modeling approaches and methods have been applied for masonry. All methods can be mainly categorized under Discrete Element Method (DEM) or the Finite Element Method (FEM). Depending on the problem at hand, different modeling techniques are adopted. Such as, the equivalent frame models, in which a structure is represented by beam elements with calibrated properties. Or such as, the plane-stress/shell representation in which a structure is either represented in 2D-space or 3D-space geometrically and its properties are calibrated along the 2D-plane [40]. Or such as the solid element representation, in which a structure is represented in 3D space with its geometry and properties. In this section the implemented FEM approaches in this research are further discussed in detail.

In general, the FEM modeling approaches can be subdivided into micro-, messo-, macro-scale for individual structural elements (e.g. beams/columns/plates/e.t.c.) or components (e.g. units/mortar/interface). The choice for a modeling method depends upon requirements such as accuracy and efficiency of the simulation. In Figure 4.5 different modeling strategies for masonry structural component are shown [41].

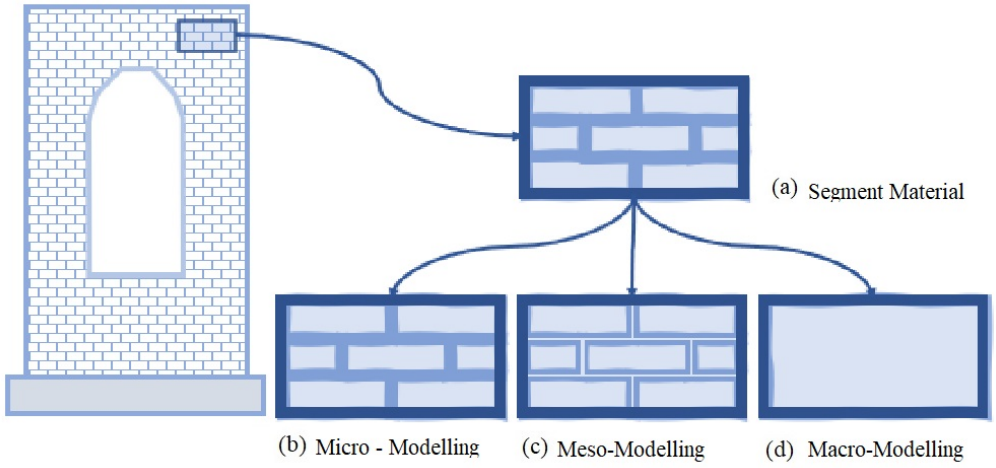

Figure 4.5: Modeling strategies described by Lourenco, 1996 [41]

Continuum elements are used to model units and mortar, while the interface is model with discontinuous elements. The continuum elements are suitable for the application of both elastic and inelastic material properties. And the discontinuous elements are used to represent potential crack/slip planes. Meso-modeling or also referred to as simplified micro-modeling is a modeling approach in which the mortar and interface elements are modelled as a joint and for which discontinuous elements are used. With this approach potential cracks and slip are modelled along joints between the units. The macro-modeling approach on the other hand considers the units, mortar and interfaces as a homogeneous material and therefore does not distinguish between all separate masonry components. Properties of all components are smeared out on continuum elements [41].

A micro-modeling technique is suitable for studying structural behaviour of single components, interaction between these components or local effects for a structural element in general. Applying the meso-modeling approach for these studies could result in a less computational expensive approach.Where as, applying the macro-modeling approach is a more suitable approach for simulating the global behaviour of a structure or structural elements. This method is for the mentioned purpose less demanding computationally and easily applicable in practise. This method is therefor also applied for the purpose of this research. The properties of the model are essentially the result of the assumptions made in the early phase of the construction of the numerical model. Assumptions are based on: literature, experimental tests and eigenvalue analyses.

5

Case study church Zandeweer & modelling assumptions

The aim of this chapter is to provide the reader an overview of the characteristics of the case study Zandeweer in Groningen, to provide an initial insight in the structural response of the church by means of a preliminary analysis and to present the characteristics of the numerical representation of this church.

5.1. Characteristics of the church in Zandeweer

The Reformed Church in Zandeweer is a historical monumental church built in 1230 in Groningen. The church is presented in Figure 5.1. Since 1972, the church and its tower obtained a monumental status by Rijksmonumentendienst. This indicates its importance to our cultural heritage and the necessity for conservation and preservation of the structure. Throughout, the past centuries both structures were expanded and renovated. Figure 5.2 shows an overview presented in a timeline of these modifications and events. Technical drawings and additional information provided by Rijksmonumentendienst can be found in appendix A. As for this particular church the tower is structurally detached from the church; The present study, hereafter, will be focused on the structure of the church only.

Figure 5.1: Church Zandeweer, Groningen

5.1.1. Characteristics church as built in 1230

The church can be described by 'box' shape and has some peculiarities that are described hereafter in more detail. The geometry of the West wall is a gable and the East wall has a curved shape, existing of 7 segments. The dimensions of the outer bays are significantly different than that of the inner bays. The dimensions of the inner bays do differ too, however, the difference is not more than 250mm and therefore these bays can be regarded as equivalent. All walls contain openings, which have a curved but rather slightly pitched circumference on the upper part. Note that the openings in the curved wall, the East Facade are closed during the construction work in 1932. The roof structure is composed of timber rafters and timber cladding. Moreover, cross vaults appear on top of the walls under the roof structure. Lastly, all walls are embedded 1m in the soil layer beneath the building. This part can be regarded as the foundation of structure. Figure 5.3, to 5.7 present an overview of the overall geometry of the church. Technical drawings and additional information provided by Rijksmonumentendienst can be found in appendix A.

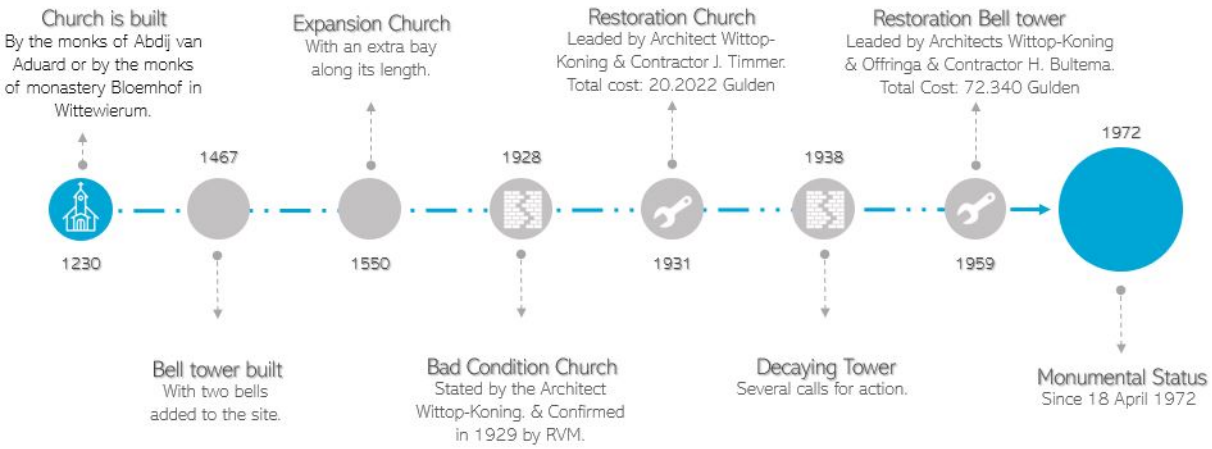

Figure 5.2: Timeline history of the church Zandeweer, Groningen

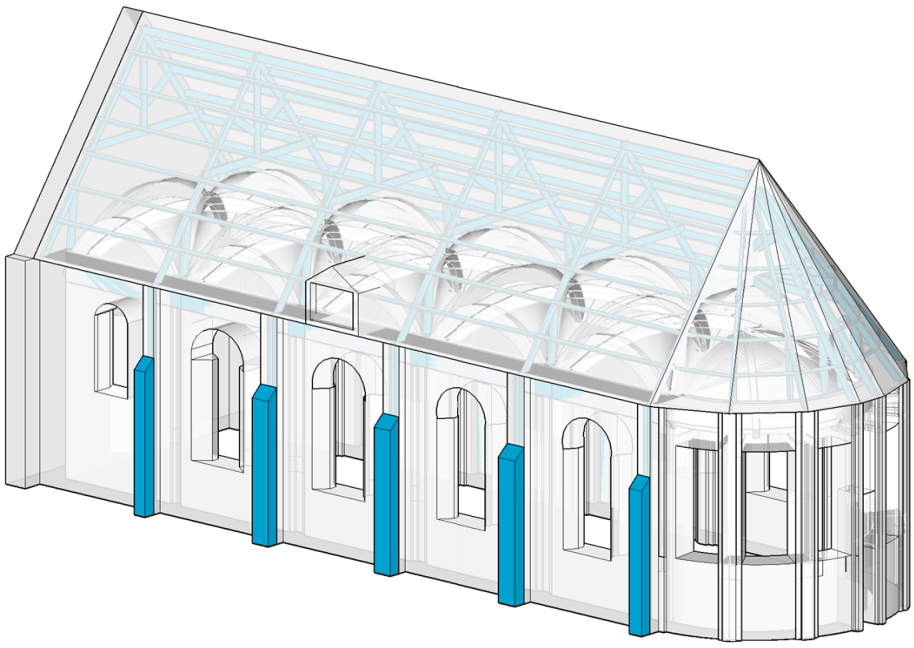

Figure 5.3: Iso-Parametric view of the church

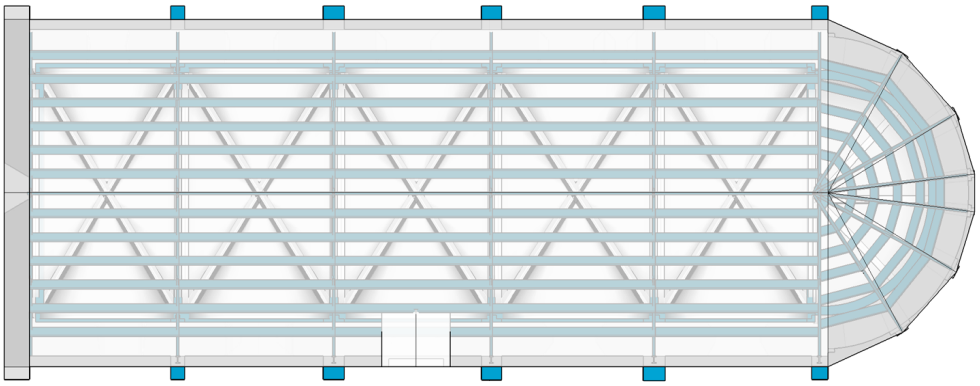

Figure 5.4: Top view of the church

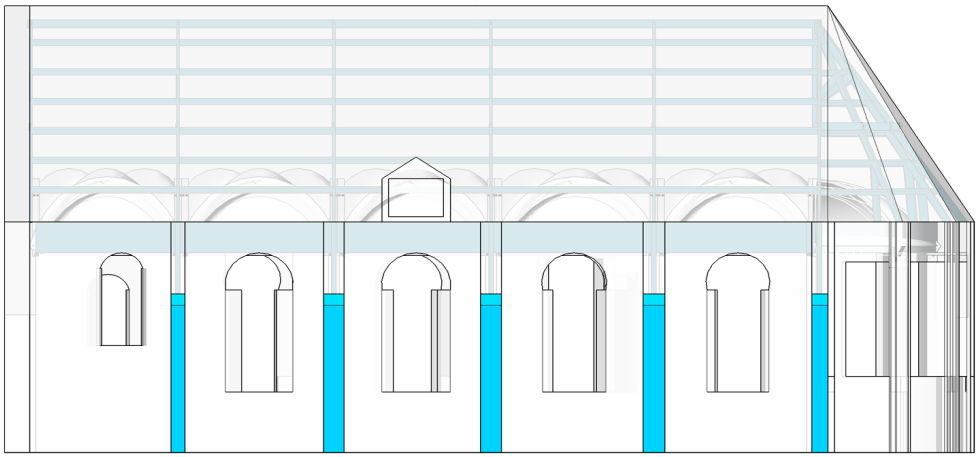

Figure 5.5: North facade

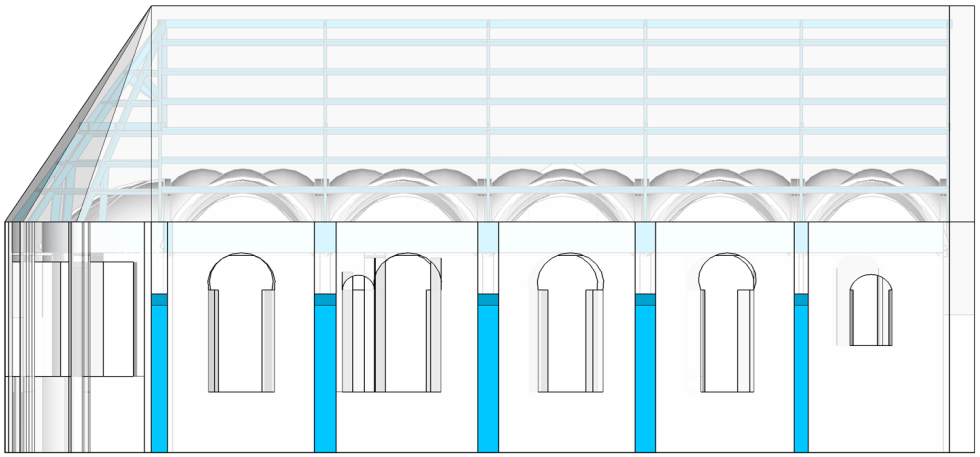

Figure 5.6: South facade

Walls

The structure is composed of 930-millimetre thick load bearing masonry walls and does not contain non-load bearing walls. On the West-side the church was extended with an extra bay in the year 1550. Sketches and building plans retrieved from the restoration works by the contractor in 1932 describe the composition of the walls near the curved East facade. As can be seen from Figure 5.8, the cross-section of a previous opening in the curved wall of the church are composed of 3 layers (Masonry-Rubble-Masonry). Unfortunately,the sketch

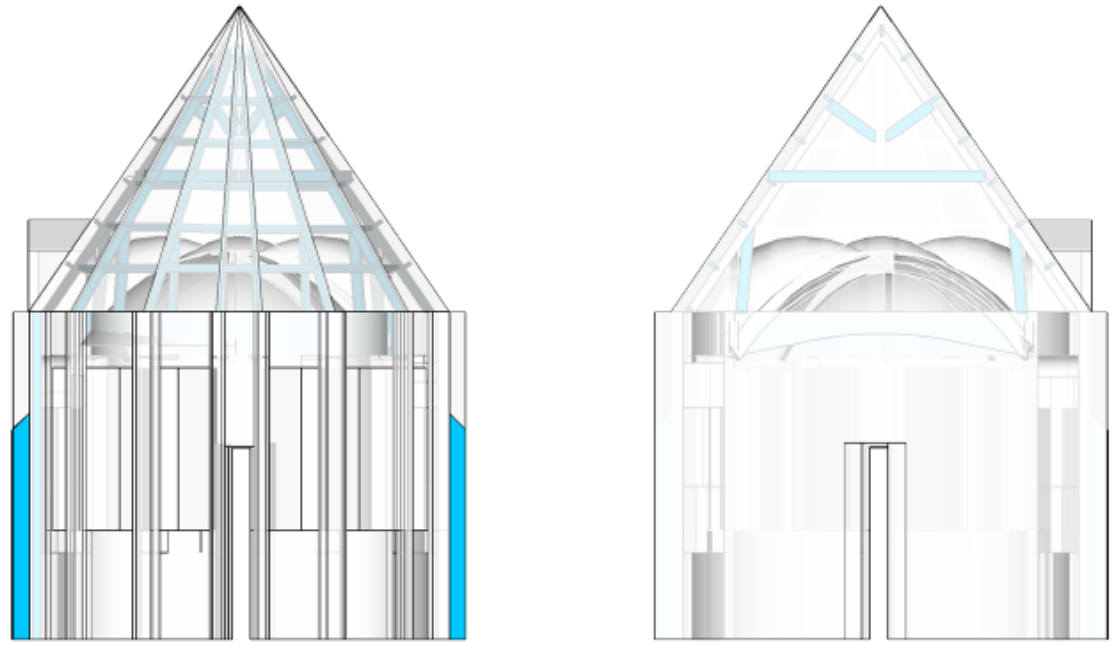

(a). East Facade (b). West Facade

Figure 5.7: East and west facade

and other technical drawings and documentation do not provide details about the composition of the main walls. However, they do indicate irregularity in the wall thickness. The wall thickness varies between 930 to 870mm. In 1929 all masonry is found in bad conditions. The walls could not resist the pressure of the arches. Cracks were found in the walls and the walls expanded due to movement of the roof. These cracks are restored in 1932.

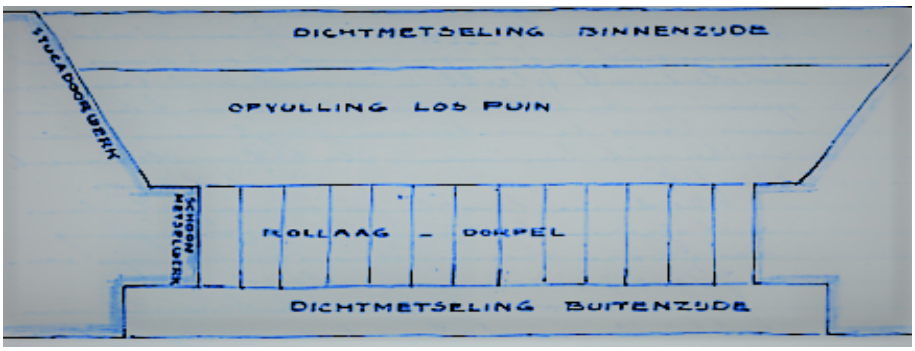

Figure 5.8: Building plan

Piers

Other vertical load bearing structural elements are the piers. Which are integrated in the main walls and carry the load of the masonry vaults. Figures 5.9, 5.10 and 5.11 depict the interior and exterior detail of the connection of the wall with the ribs of the vaults and the connection of the piers with the main load bearing walls. The connection between the main walls, piers and vaults are difficult to define based on the provided information. Therefore, assumptions are made regarding numerical model of the this connection. These assumptions are presented and discussed in the upcoming chapter, in which the numerical model of the structure is thoroughly discussed.

Figure 5.9: Photos the piers before (left) and after the modifications (middle and right)

Figure 5.10: Photos the piers after the modifications

Figure 5.11: Pier Details (left) and interior wall (right)

Vaults

Masonry cross-vault with diagonal ribs are integrated in the structural system and connected with the main walls. These vault are supported along their edges by masonry ribs. Consequently, these ribs are supported by point supports that rest on the piers and edge supports along the main walls. These edge supports are integrated in the main wall. From the provided information the properties of the connection can not be determined. Assumptions regarding the numerical modelling of this connection will be further discussed in the next chapter. During the construction works in 1932 parts of the vaults were severely damaged or lost. The vaults were then restored with reinforced concrete. Figure 5.12 depicts an example of a restored vault.

Figure 5.12: A concrete reinforced masonry Vault

Roof Structure

The roof structure is composed of timber rafters and timber cladding. Figure 5.13 depict the old and new state of the rafters and roof system. Figure 5.14 shows the blue prints of the rafters and a detail of the anchor point of the rafters on the walls. Before the restoration works in 1932 the roof structure was declared dangerous as it did not fulfill its structural function. The anchors of the wooden tensile beams under the arches were being pushed out due to the expansion of the walls.

(a). Old Rafters 1932

(b). New Rafters 1932

Figure 5.13: Old state of the rafters (a) pre- and (b) post constructions works 1932

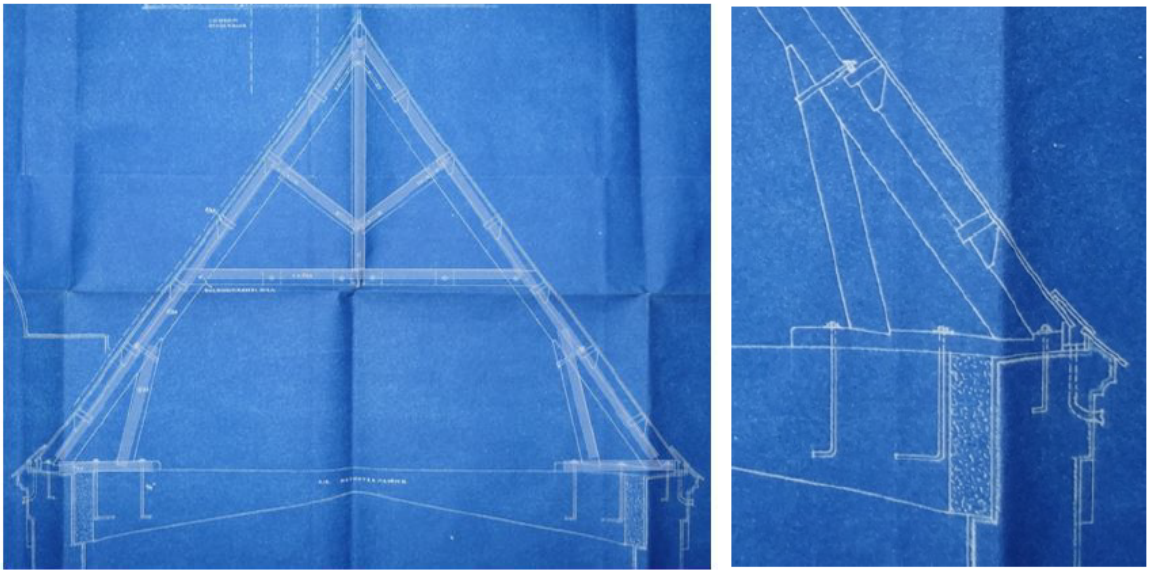

(a). Blueprint Rafters 1932 (b). Detail connection Rafter

Figure 5.14: Blueprint Rafter structure 1932

5.1.2. Characteristics church post structural modifications 1931

After the renovation in 1932 the following interventions were executed: The bearings on the outer part of North and East wall were reduced in thickness, steel columns were added in the bearings. Moreover, a reinforced concrete beam frame structure was added on the upper part and along the perimeter of the main masonry walls in order to keep the walls together while it is under pressure of the arches. Lastly, all masonry walls and vaults are repaired and some are reinforced with concrete and the timber roof structure was renewed. Material properties are further unknown and the adopted properties for the analysis of the church are discussed in more detail in the upcoming chapters. Peculiarities and details concerning the building plans and connections are presented in Appendix B.

Concrete Beams

The reinforced concrete beam system was added as measure against the walls being pushed away by the top pressure of the roof system. The concrete beams that are added along the perimeter of the walls have a rectangular shape. Whereas the concrete beams added perpendicular to the longitudinal direction have unique shape. If we were to divide these beams in three parts, the outer parts do have a non-prismatic rectangular shape and the inner part of the beams have a curve linear shape. An blueprint drawing of such beam is depicted in Figure 5.15. The beams rest on the main walls and are connected with steel columns at the North Facade side. The beams in the transverse direction connected monotonically with the beams in the longitudinal direction.

Figure 5.15: Concrete Beam in transverse direction

Steel Columns

The original bearing/piers were not able to resist the thrust caused by the top loading. Therefore, the masonry piers are reinforced with steel columns. The steel columns have a I-profile and are embedded in the masonry piers. The columns are clamped in a reinforced concrete beam at the base and connected with anchors at the top. Anchors are used only in the direction perpendicular to the main walls, in the parallel direction the columns are unsupported at the topside. Figure 5.16 depicts details regarding the added steel columns. Lastly, note that it is unclear why the columns are only added at the north facade and not at the South facade as well. Visual inspection of the piers should provide more information regarding the actual dimensions of the piers.

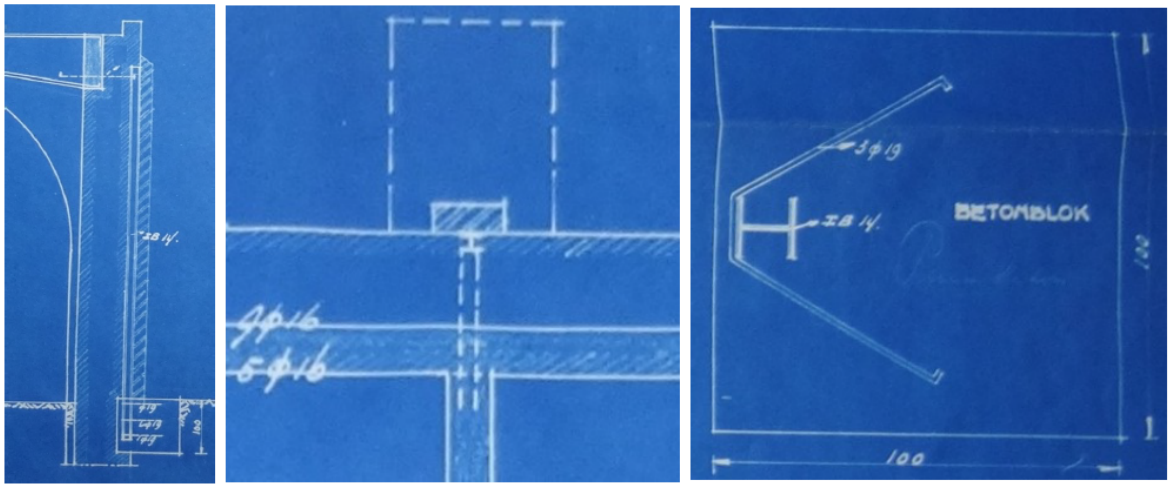

(a). Steel Column (b). Top constrained Column (c). Bottom constrained Column

Figure 5.16: Steel column embedded in masonry pier

5.2. The Simple Lateral Mechanism Analysis method (SLaMA)

In this section the Simplified Lateral Mechanism Analysis (SLaMA) method is used as a simple preliminary analysis, prior to the numerical pushover analysis, to predict the structural response of the church. The starting point for the SLaMA calculations is to determine the load-path, by dividing the structure in lateral and vertical load bearing elements. Figure 5.19 & figure 5.22 presents the chosen load-path for analysis in the load direction West-to-East and that of the East-to-West, respectively. For the analysis the vertical load bearing elements are divided into bearing and piers, in order to take into account the geometrical difference in thickness between the elements. The horizontal elements are considered as overburden and are divided in segments for the analysis. Moreover, as can be seen the overburden load caused by the roof structure and the lateral load are depicted in the figure 5.19 and 5.22.

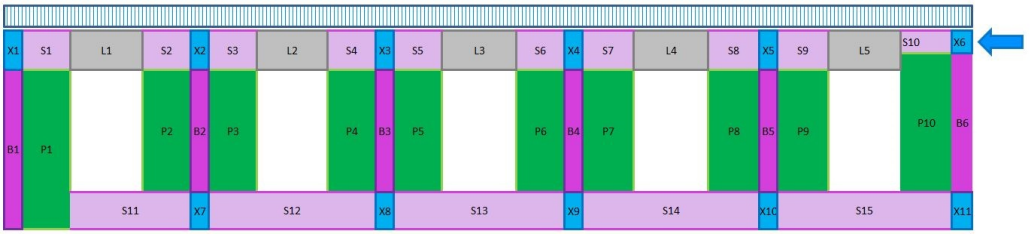

(a). For Structure prior to Modifications - as presented in chapter 6

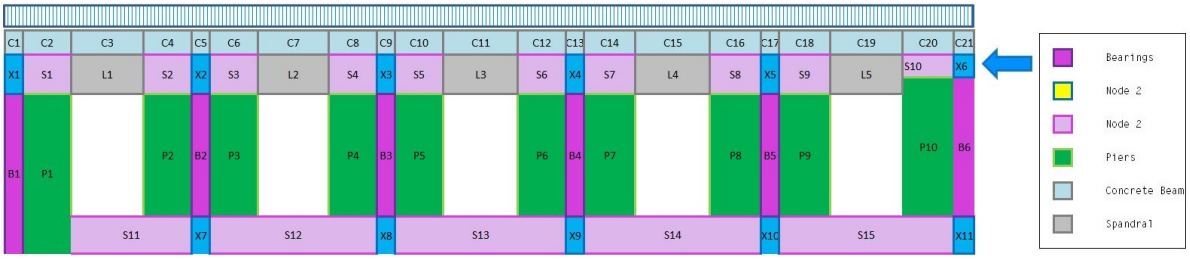

(b). For Structure post Modifications - as presented in chapter 9

Figure 5.19: SLaMA Schematization Load direction West-to-East

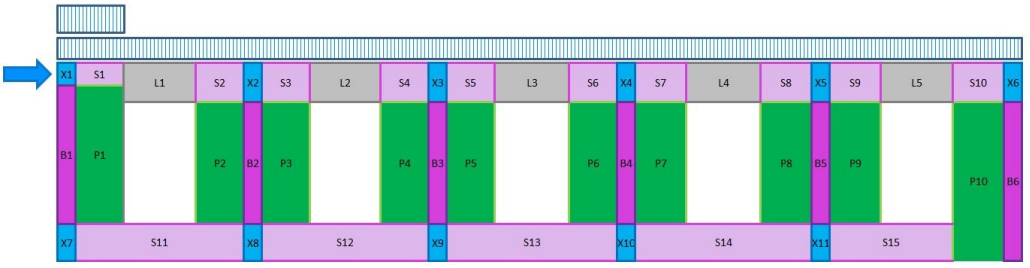

(a). For Structure prior to Modifications - as presented in chapter 6

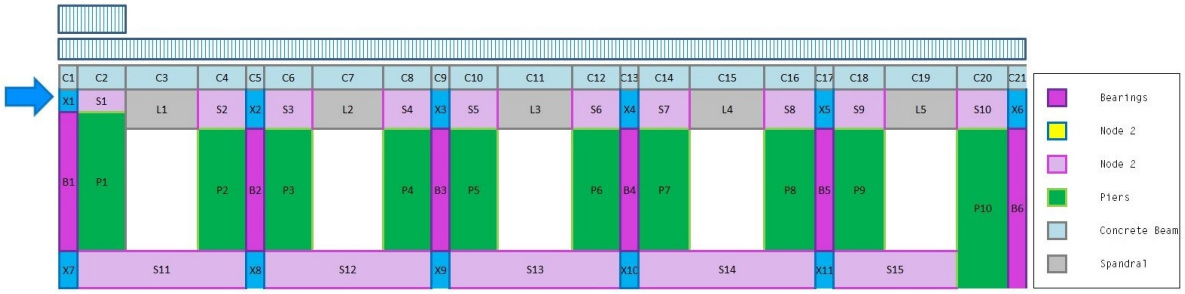

(b). For Structure post Modifications - as presented in chapter 9

Figure 5.22: SLaMA Schematization Load direction East-to-West

For the analysis in the load direction East-to-West the flange-effect caused by the presence of the gable can be and is considered in this case as an overburden load. As for the structure after the structural modification, the contribution from the steel columns are accounted for at the position of the bearings, the concrete ring beam frame is added as overburden and the West facade is considered without openings. As depicted in figure 5.26 (b).

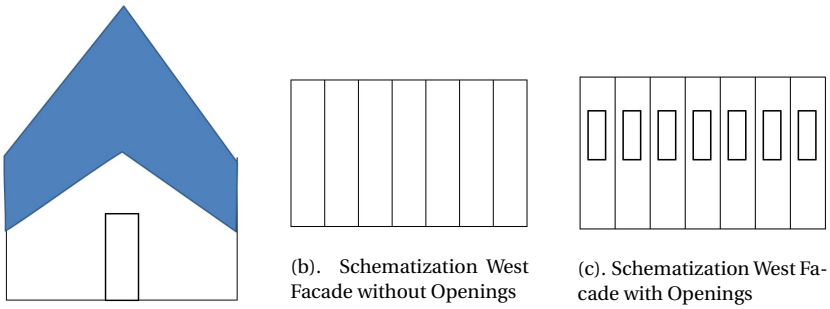

(a). Flange Effect due to presence Gable

(b). Schematization West Facade without Openings

(c). Schematization West Facade with Openings

Figure 5.26: SLaMA Schematization Load direction East-West

Results

Figure 5.27 present the capacity curves for the church prior and post structural modifications. The horizontal reaction force at ground floor level in the global positive X-direction is plotted against the displacement at the top elevation.

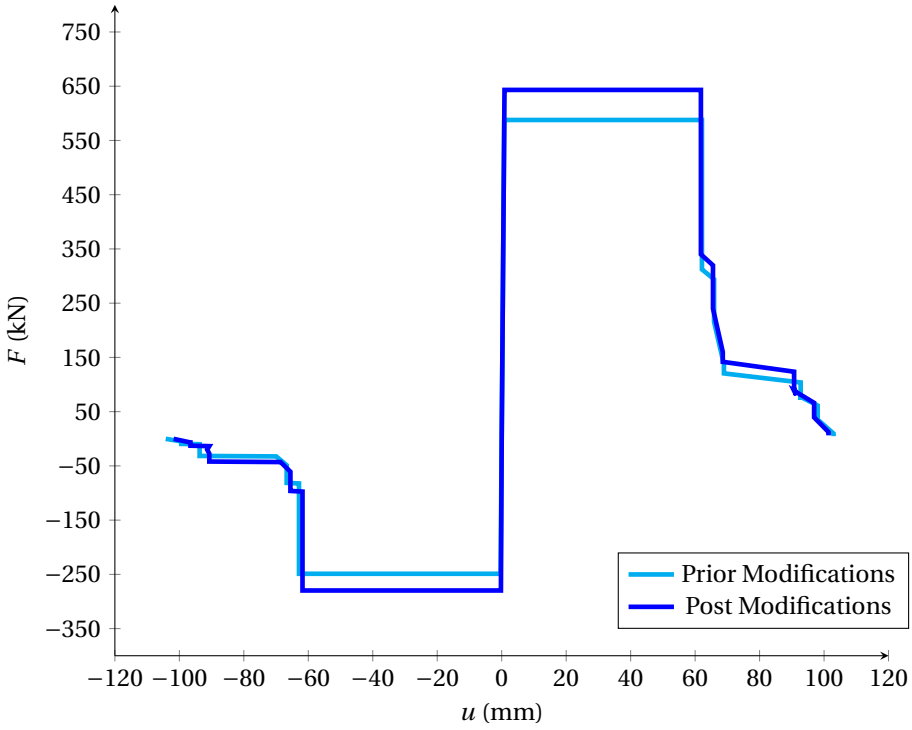

Figure 5.27: Capacity curve church obtain by SLAMA Analysis

As can be seen from the results a small difference is observed in the results of both models in the positive and negative longitudinal direction. The church post structural modifications has as expected a higher force capacity. The initial stiffness and softening behaviour of both models closely resemble one and other. For both models all load bearing elements fail due to rocking. No other failure mechanisms are detected. Table 5.1 compares these characteristics for the positive longitudinal direction.

Parameter	Unit	SLaMA+ Church 1230	SLaMA+ Church 1931
Initial global stiffness	kN/mm	734.7	739.7
Maximum force capacity	kN	587.7	643.2
Yield displacement	mm	0.80	0.87
Softening behaviour	%	0.8	1.0

Table 5.1: Comparison Capacity Curve Global X-Direction Parameters

The SLaMA analysis is conducted to determine the global inelastic mechanisms and to determine the global response of the structure. The small difference between the results of both models can be better understood if one understands the limitations of this simplified pushover method. Limitations for the SLaMA method are as follows: In these analysis a two-dimensional representation of the church models are considered. Therefore, torsional stiffness irregularities are not considered. Torsional amplification effects arise from the demand and resistance eccentricities for buildings with rigid diaphragms. However, for the representation of the church prior and post structural modifications the connection between the diaphragms (vaults) and the main walls are considered rigid. In a case for which the horizontal structural elements would be in the same plane and the connections are rigid a box behaviour can be observed. However, due to the curved shape of the vaults rigid diaphragm behaviour may not be present. Secondly, the sequence of inelastic failures is not possible to determine as SLaMA is a mechanism based analysis method. Additional checks are required to confirm if the prediction by SLaMA are close to what is expected.

5.3. Numerical model representation - Church 1230 vs. 1931

A 3D representation of the case study as presented in section 5.1 is set-up with the aid of the commercial software package DIANA FEA 10.3 [42]. This section presents the modeling choices for the nonlinear pushover analyses and elaborates on the characteristics of the numerical model relevant for all analyses. The goal of this study is to investigate the structural characteristics of the church up to failure. Note that all numerical models mentioned in this report are the work of the author.

5.3.1. Model geometry

The numerical model of the church prior and post structural modifications are presented in Figure 5.28. With the aim of reducing the computational time and effort, simplifications are made to the numerical model. Firstly, for the models a homogenized cross-section is considered for the walls. In contrast to the physical model, where the masonry walls are composed of three layers, two outer masonry brick layers and one inner rubble layer. Secondly, the timber roof-structure and the gable are not modelled but considered as overburden on the walls. Calculations for the overburden load are presented in annex B. Thirdly, the bays are considered at an equidistant distance in contrast to the physical model. An average bay width is chosen based on the size of the original bays. Lastly, the openings in the first bay in the numerical model are considered equal to the openings in the other bays, whereas in the original structure these openings are about half in width and height. These details are presented in Figure 5.28 (a) (see also Section 5.1. for technical details of the case study).

After the restoration works in 1931 several structural modifications were done. These modifications were discussed in detail in section 5.1.2. The structural modifications that are considered in the numerical model are: The shortening of the piers on the North facade, the addition of the steel columns in the piers in the North facade, the addition of the concrete beams on top of the main walls and the filling of the openings with masonry on the curved West facade. These changes are presented in Figure 5.28 (b).

Structural modifications that are not considered in the numerical model are: The filling of damaged parts of the vaults with concrete, the filling of damaged parts of the masonry parts with new masonry, change material properties of the timber roof system and a possible interface between the first two bays near the East facade.

Support & load conditions

The models are supported at ground level, the structures are supported using tyings. All rotational and transitional DOFs are fixed for the master node and the DOFs of the slave nodes are equalized accordingly. All elements in the numerical model share a mutual node. Therefore, all other connections can be considered fully fixed.

The structure has been subjected to a conventional monotonic pushover with a modal loading scheme and an overburden load around the perimeter of the walls. The modal loading has been applied with the shape of the governing modal shape. The governing modal shape will be discussed in chapter 6 and chapter 9. Additionally, an overburden load is added on the edge of the east facade, equivalent to the self-weight of the gable.

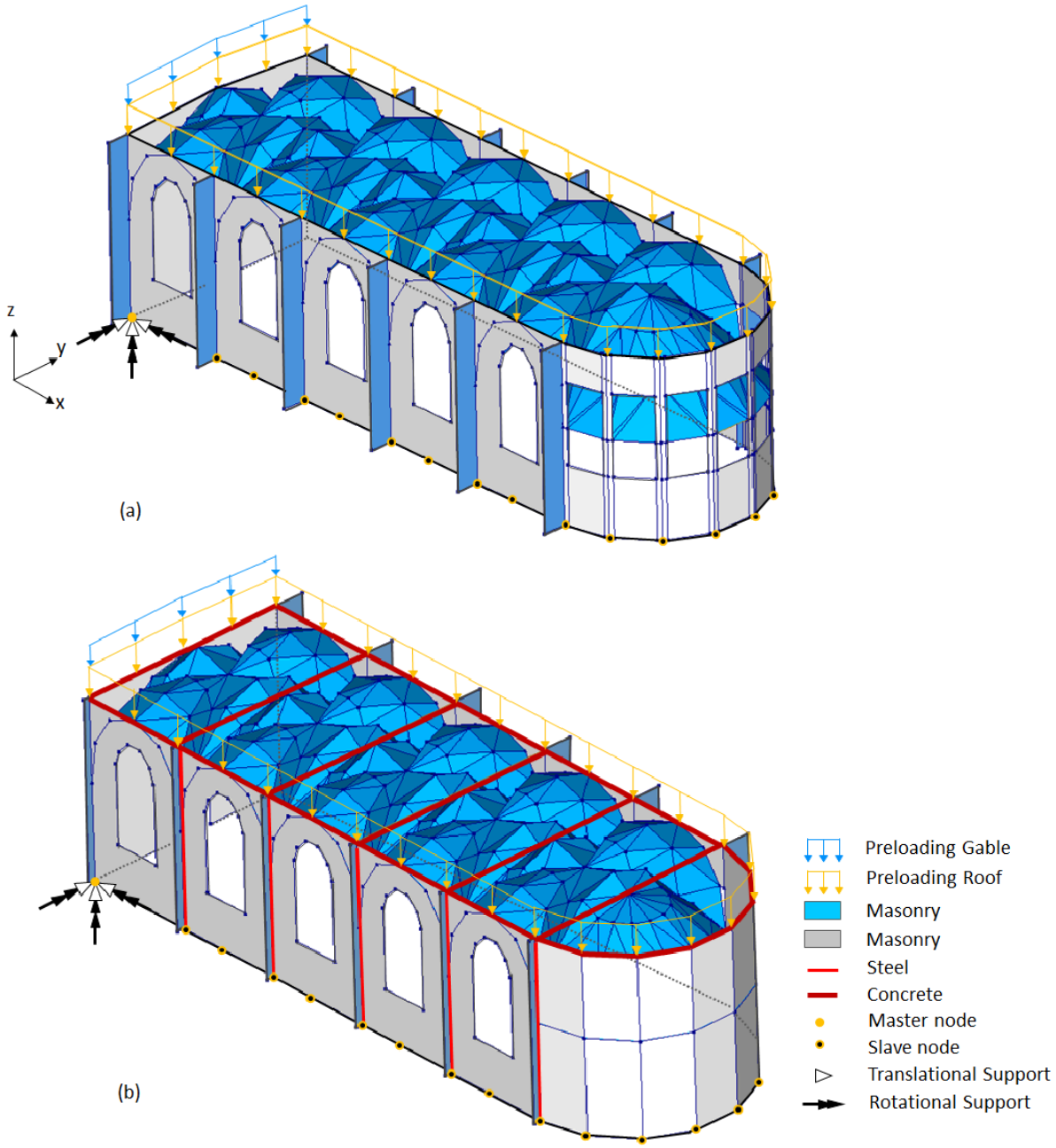

Figure 5.28: Numerical model set-up for (a) The church as built in 1230 and (b) The church post structural modifications in 1931

5.3.2. Discretization

The numerical models, that are composed of masonry walls, vaults & ribs and concrete and steel beam elements, are discretized by quadrilateral elements of about 300 mm × 300 mm and beam elements of about 300 mm. Regular curved shell elements and class-III beams are adopted to capture the in- and out-of-plane behaviour of these structural components. These higher order finite elements are based on the so-called Mindlin-Reissner theory for which transverse shear deformation is included. Nonlinear behaviour is included for the masonry only. An overview of the discretization of the structure is given in table 5.2 and the descretized models are depicted in Figure 5.31. Lastly, the orientation of the local axes of the masonry walls needs to be treated with extra care, due to the orthotropic material properties of masonry. The local x-axis of walls parallel to the global x-axis are aligned, whereas for the walls perpendicular to the global x-axis the local x-axis is considered inline with the global y-axis. The theoretical background regarding the use of the Engineering Masonry model was previously discussed in section 5.3.3.

	Masonry Walls	***Masonry Vaults***	***Masonry Ribs Vaults***	***Concrete Beams***	***Steel Columns***
Element type	Curved Shells [CQ40S]	Curved Shells [CQ40S]	Class-III beams [CL18B]	Class-III beams [CL18B]	Class-III beams[CL18B]
DOFs	$u_x, u_y, u_z, \phi_x, \phi_y$	$u_x, u_y, u_z, \phi_x, \phi_y$	$u_x, u_y, u_z, \phi_x, \phi_y, \phi_z$	$u_x, u_y, u_z, \phi_x, \phi_y, \phi_z$	$u_x, u_y, u_z, \phi_x, \phi_y, \phi_z$
Integrations scheme	3x3x7	3x3x7	3-point Gauss	3-point Gauss	3-point Gauss
Mesh size [mm]	300x300	300x300	300	300	300
Thickness [mm] / Cross-section [mm]	930	140	140x140	250x1000 - Transverse beams 250x1000 - Ring beam	140x140
Material Model	EMM	EMM	LE Isotropic	LE Isotropic	LE Isotropic

Table 5.2: Discretization properties the church models

5.3.3. Material models

Constitutive models of interest for practice are normally developed according to an approach in which the observed mechanisms are represented in such a manner that simulations are in reasonable agreement with experiments. These models should be able to simulate the desired nonlinear behaviour of structural elements or the entire structure. Two constitutive models where used in this research and are discussed in further detail hereafter.

Total Strain Crack Model

This model was first developed by Feenstra et al. [43] to simulate the crack behaviour in concrete. It was implemented in the FEM software DIANA FEA. This constitutive model requires the following input:

- *Elastic properties, such as: Young's modulus and Poission's Ration*
- *Material strength parameters, such as tensile, compressive and shear strength*

The tensile and compressive stress-strain relation in the model is characterized by a predefined tensile and compressive softening curve and corresponding tensile and compressive parameters. More details on these curves and predefined functions can be found in the DIANA FEA User's manual. The schematic stress-strain relationship used in this thesis is presented in Figure 5.29. Drawbacks of this model, however, are:

- *that it does not distinguish between mode I and Mode II crack failure patterns*
- *does not include the anisotropic material properties of masonry*
- *highly underestimates the energy dissipation under cyclic loading*

Therefore, using this model for the simulation of masonry may lead to inaccurate results. Especially, since it is not able to simulate the different failure modes.

Engineering Masonry Model

Based on the Total Strain formulation the Engineering Masonry Model was developed to overcome the shortcomings of the Total Strain Crack Model for the applications of Masonry [44]. The Engineering Masonry Model (EMM) is a continuum smeared failure model and can be applied in combination with regular plane stress (membrane) and curved shell elements for modelling failure of masonry walls (see Figure 5.30).

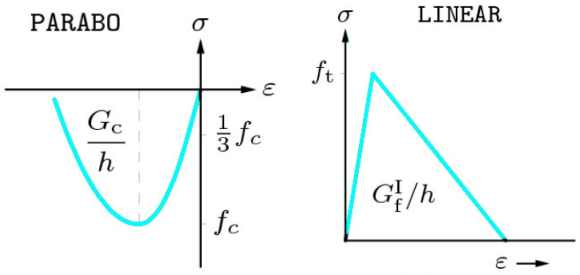

(a). Crushing behavior of Total Strain Crack model - parabolic

(b). Cracking behavior of Total Strain Crack model - linear fracture energy based

Figure 5.29: Material model:the Total Strain Crack model

In comparison with the Total Strain Crack model, the Engineering Masonry model is able to describe the unloading behaviour more realistically assuming a linear unloading for compressive stresses with initial elastic stiffness. In addition, a shear failure mechanism based on the standard Coulomb friction failure criterion is included in the model. The use of this model is especially recommended for static nonlinear cyclic or transient dynamic nonlinear analyses of components and full structure [45]. The following failure mechanisms are considered with the EMM Model:

- *tensile cracking of the bed-joint or head-joint*
- *compressive crushing in the direction normal to the bed-joint or head-joint*
- *cracking in the direction normal to the diagonal staircase cracks*
- *frictional shear sliding*
- *out-of-plane shear-failure*

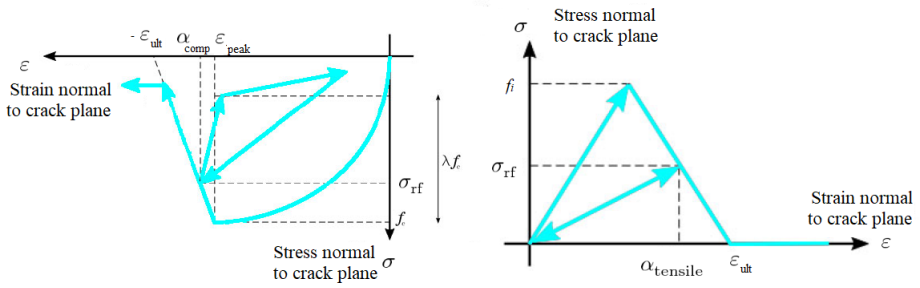

(a) Crushing behavior of Engineering Masonry Model

(b) Cracking behavior of Engineering Masonry model

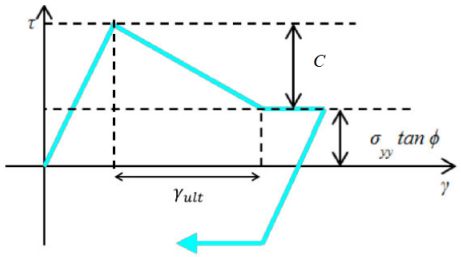

(c) Shear behavior of Engineering Masonry model

Figure 5.30: Material model: Engineering Masonry model

Furthermore, the orthotropic nature of masonry is included in the Engineering Masonry Model. Different properties for strength and elasticity can be assigned. A local axis is assigned to masonry structural components, in which the orientation of the local x-axis is parallel to the bed joint, whereas the local y-axis is orthogonal to the bed joint.

5.3.4. Material properties

All beam elements mentioned in table 5.2 are modelled with linear elastic isotropic behaviour. Their material properties can be found in table 5.3. For the masonry walls the Engineering Masonry model (EMM) with a diagonal crack orientation is adopted and for the masonry vaults the Total Strain crack model (TSCM) with a rotating crack orientation is adopted. For the wall the EMM model is adopted as it is relatively easy to assign the local axes, which is required for the model. For the vaults the TSCM is assigned as it is not feasible to assign the local axes due to the global orientation of each segment of the vaults. For the details regarding the crack orientation in these material models the reader is referred to section 5.3.3. An overview of adopted material properties for the walls and vaults can be found in table 5.4 and table 5.5. Note that the values for masonry are partially obtained from the NPR 9998 [14] and partially from experimental test correlations.

Property	*Parameter*	*Symbol*	*Unit*	*Masonry ribs*	*Concrete beams*	*Steel columns*
Elasticity	Young's Modulus	E	MPa	2900	33,500	210,000
	Poission's ratio	v	-	0.15	0.2	0.3
	Density	ρ	kg/m3	1600	2,500	7,800

Table 5.3: Material properties beam elements

Property	*Parameter*	*Symbol*	*Unit*	*Value*
Elasticity	Young's Modulus	E_{xx}	MPa	2900
		E_{yy}	MPa	4000
	Shear Modulus	G_{xy}	MPa	1800
	Density	ρ	kg/m3	1600
Cracking	Tensile strength	f_{tx}	MPa	0.30
		f_{ty}	MPa	0.10
	Tensile fracture energy	G_{ft}	N/mm	0.01
	Diagonal crack orientation	α	rad	0.5
Crushing	Compressive strength	f_c	MPa	8.0
	Compressive fracture energy	G_c	N/mm	20
Sliding	Cohesion	c	MPa	0.15
	Shear fracture energy	G_{fs}	N/mm	0.15
	Friction angle	ϕ	rad	0.5

Table 5.4: Material properties masonry walls with EMM model

Property	*Parameter*	*Symbol*	*Unit*	*Value*
Elasticity	Young's Modulus	E	MPa	2900
	Poission's ratio	G_{xy}	MPa	0.15
	Density	ρ	kg/m3	1600
Crack orientation	Rotating			
Cracking	Linear-crack energy based			
	Tensile strength	f_t	MPa	0.30
	Tensile fracture energy	G_t	N/mm	0.01
Crushing	Compressive strength	f_c	MPa	8.0
	Compressive fracture energy	G_c	N/mm	20

Table 5.5: Material properties masonry vaults with TSCM model

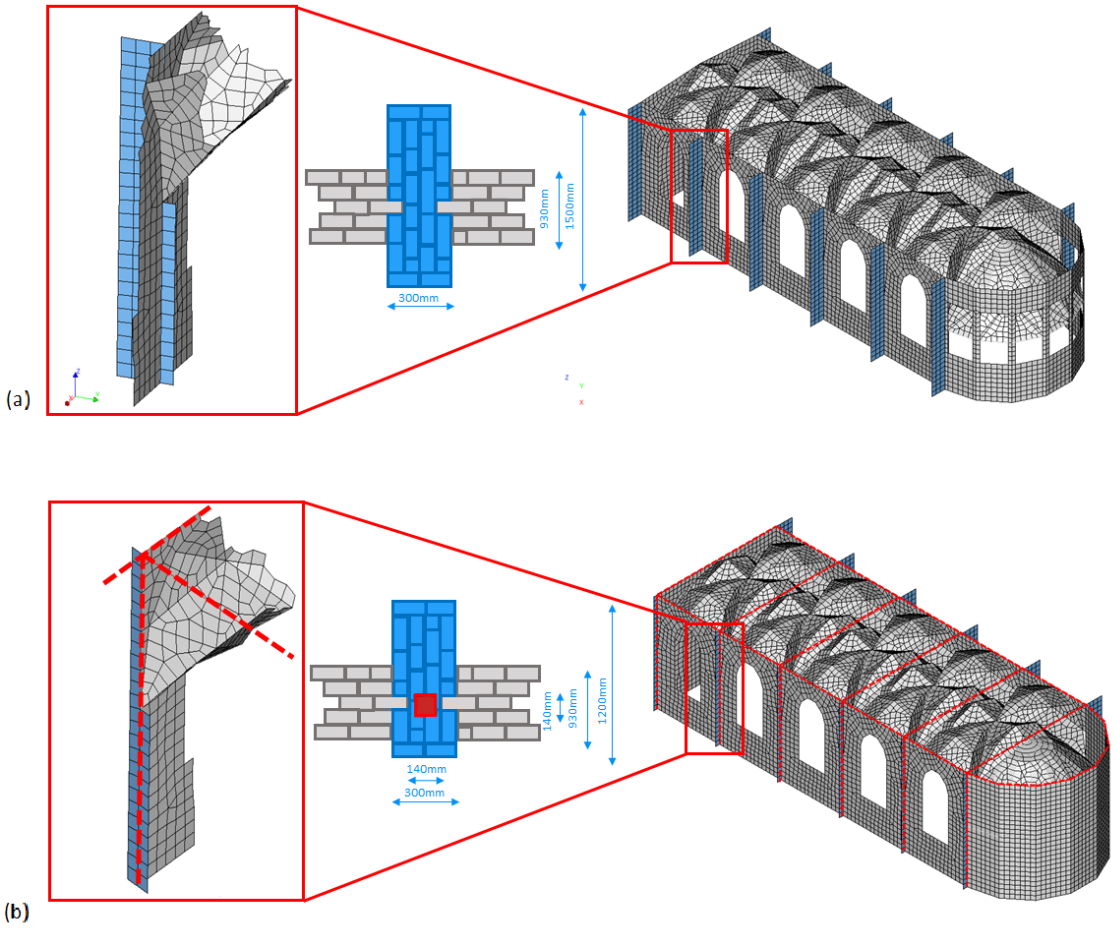

Figure 5.31: Meshed numerical model for (a) The church as built in 1230 & The church post structural modifications in 1931

5.3.5. Numerical analysis procedures

For the church model as built in 1230, a structural nonlinear analysis procedure is adopted for which both geometrical and physical non-linearity are included. For this procedure the self-weight is applied prior to the application of the modal pushover load, such that stresses resulting from the self-weight are calculated properly. An overview of the adopted analysis procedure is presented in table 5.6.

Masonry Structure	***Load step size***	Self-weight	0.2(5)
		Pushover loading	0.02(40) 0.005(50) 0.0005(5) 0.005(200)
	Iteratie procedure	Procedure	Regular Newton-Raphson + Quasi-Secant
		Max. iterations	50
		Line search	True
	Convergence criterium	Norm	Energy
		Tolerance	0.005
		No convergence	Continue
	Satisfy both norms	Norm	Displacement
		Tolerance	0.05
		No convergence	Continue

Table 5.6: Adopted analysis procedure for the church as built in 1230

For the church model post structural modifications in 1931, a structural nonlinear analysis procedure is adopted for which as well both geometrical and physical non-linearity are included. However, for this procedure a phased structural nonlinear analysis procedure is adopted to consider the different construction phases of the model and therefor stress changes in the structure. In phase 1: The construction of the masonry structure is considered. Whereas in phase 2: the addition of concrete and steel beams to the existing structure is accounted for. An overview of the adopted analysis procedure is presented in table 5.7. Note that in phase 1 only the self-weight of the structure is considered whereas in phase 2 the self-weight of the concrete and steel are added prior to the application of the pushover loading.

Phase 1: Masonry Structure	***Load step size***	Self-weight	0.2(5)
	Iteratie procedure	Procedure	Regular Newton-Raphson
		Max. iterations	50
		Line search	True
	Convergence criterium	Norm	Energy
		Tolerance	0.005
		No convergence	Continue
	Satisfy both norms	Norm	Force
		Tolerance	0.05
		No convergence	Continue
Phase 2: Masonry Structure + Concrete & Steel	***Start steps***	Use load of previous phase	
	Load steps size	Pushover loading	0.2(40) 0.005(50) 0.0005(5) 0.005(200)
	Iterative procedure	Procedure	Regular Newton-Raphson + Quasi-Secant
		Max. iterations	50
		Line search	True
	Convergence criterium	Norm	Energy
		Tolerance	0.005
		No convergence	Continue
	Satisfy both norms	Norm	Force
		Tolerance	0.05
		No convergence	Continue

Table 5.7: Adopted analysis procedure for the church post structural modifications in 1931

6

Results numerical analysis - Church as built 1230

Technical details regarding the church were discussed in chapter 5. This chapter starts with a presentation of the behaviour of the church as built in 1230 under static load conditions, presents the results of the modal eigenvalue analysis and ends with a presentation of the results of the NLPO analysis. Furthermore, a section is devoted to the presentation and discussion of the importance of the numerical modelling strategy for the piers. The numerical model of the church used for the analysis in this chapter is presented in Figure 6.1.

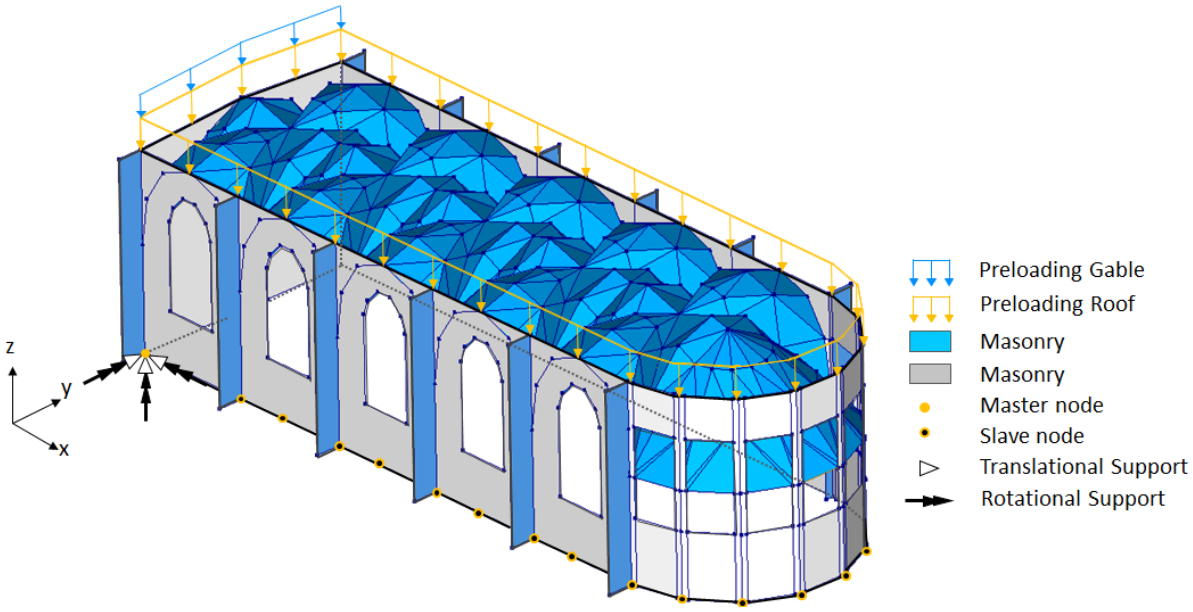

Figure 6.1: Numerical model representation of the church as built 1230

6.1. Eigenvalue analysis

As a starting point, a model eigenvalue analysis is conducted to find the eigenmodes of the structure. Important properties of the eigenmodes are the natural period, shape and the modal mass participation. The modal mass participation provides a method for judging the significance of each eigenmode. The modal shape indicates the direction in which the structure is most likely going to deform due to a dynamic loading. Additionally, in case the software is able to execute the analysis, a good indication of possible modelling mistakes in geometry or connections of the structure are provided. Figures 6.2 and 6.3 present the eigenperiodes and the mode mass participation factor for each mode in the global X- and Y-direction, respectively.

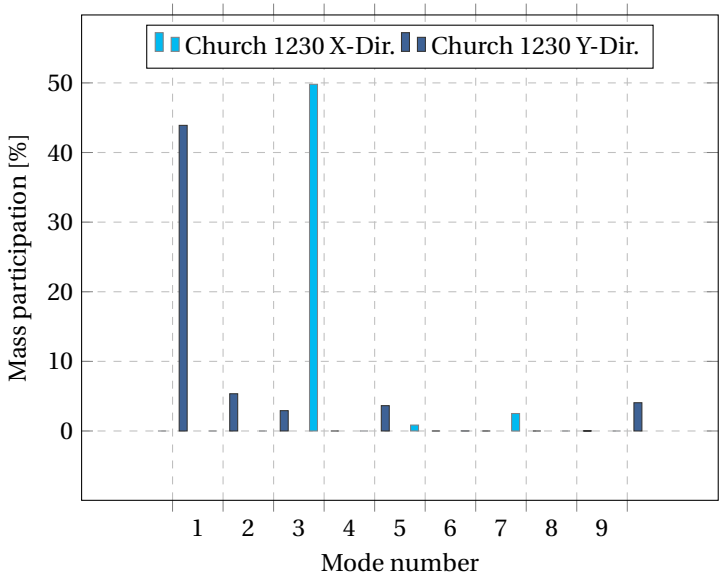

Figure 6.2: Results Modal Analysis for Church as built in 1230

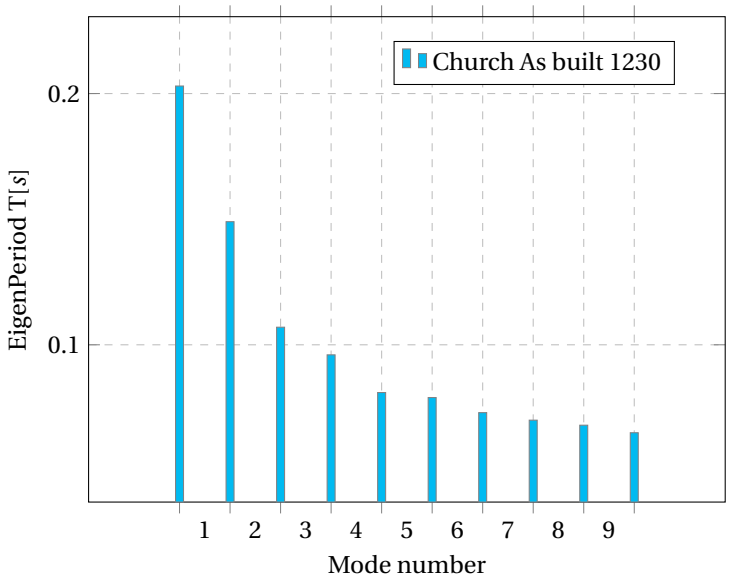

Figure 6.3: Main frequencies for the first 10 modes of the church as built in 1230

Governing Eigenmodes Global X-direction

The governing eigenmode and modal shape of the structure prior to the structural modifications for the global X-direction is presented in Figure 6.4. The governing mode shape is a typical out-of-plan mode. The natural period for this mode is 0.10s and the modal mass participation is equal to 49.8%. The governing modal shape is subsequently used as the input for the NLPO analysis.

As the modal mass participation factor is less than 60%, the NPR 9998 [14] states then that higher modes are likely to be significant for the structural response of the church. Using the conventional NLPO analysis method in this case results in results that are on the conservative side. To solve this issue, an adaptive NLPO in combination with an MRS analysis or an NLTH are recommended to use in which more modes can be combined to reach the 60% mass participation criteria. However, within the scope of this study it is chosen to limit the study by using the NLPO analysis method only.

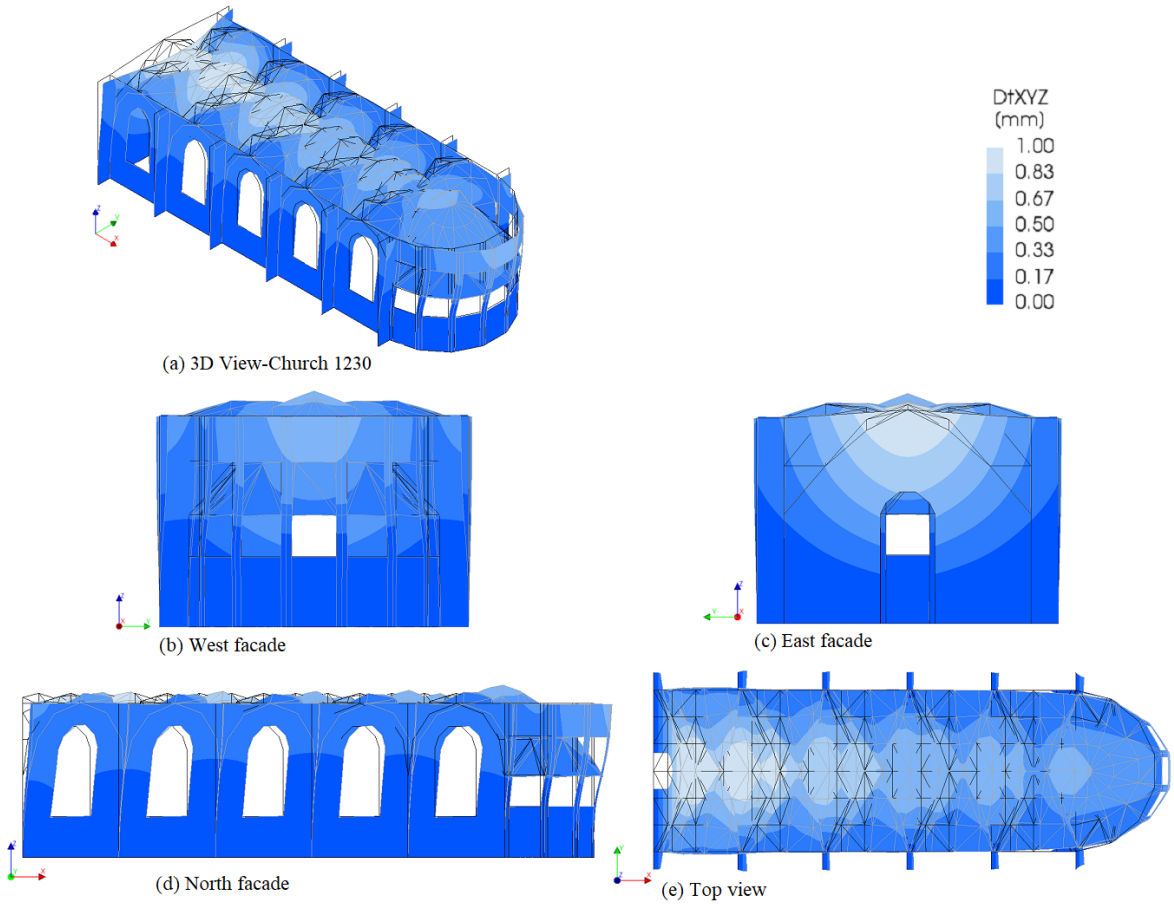

Figure 6.4: Governing Eigenmodes Global X-direction Church Prior to modifications, [scale factor=0.05]

Governing Eigenmodes Global Y-direction

The governing eigenmode and modal shape of the structure prior to the structural modifications for the global Y-direction is presented in Figure 6.5. The governing mode shape is a torsional mode, which is triggered by the difference in rigidity of the parts of the structure along this direction. As can be seen from the geometry of the structure, the more rigid part of the structure is located near the East facade and the less rigid part near the curved West facade. Due to the geometry of the curved West facade this part is more susceptible to motion and this part therefore moves more than the other parts. The natural period for this mode is 0.20s and the modal mass participation is equal to 43.9%. This again less than the required 60% according to the NPR 9998 [14] which indicates that by using the conventional NLPO analysis method results in results that are on the conservative side. Note that the difference in the mass participation factor in the global X versus the global Y-direction is about 6.1%, which is relatively small.

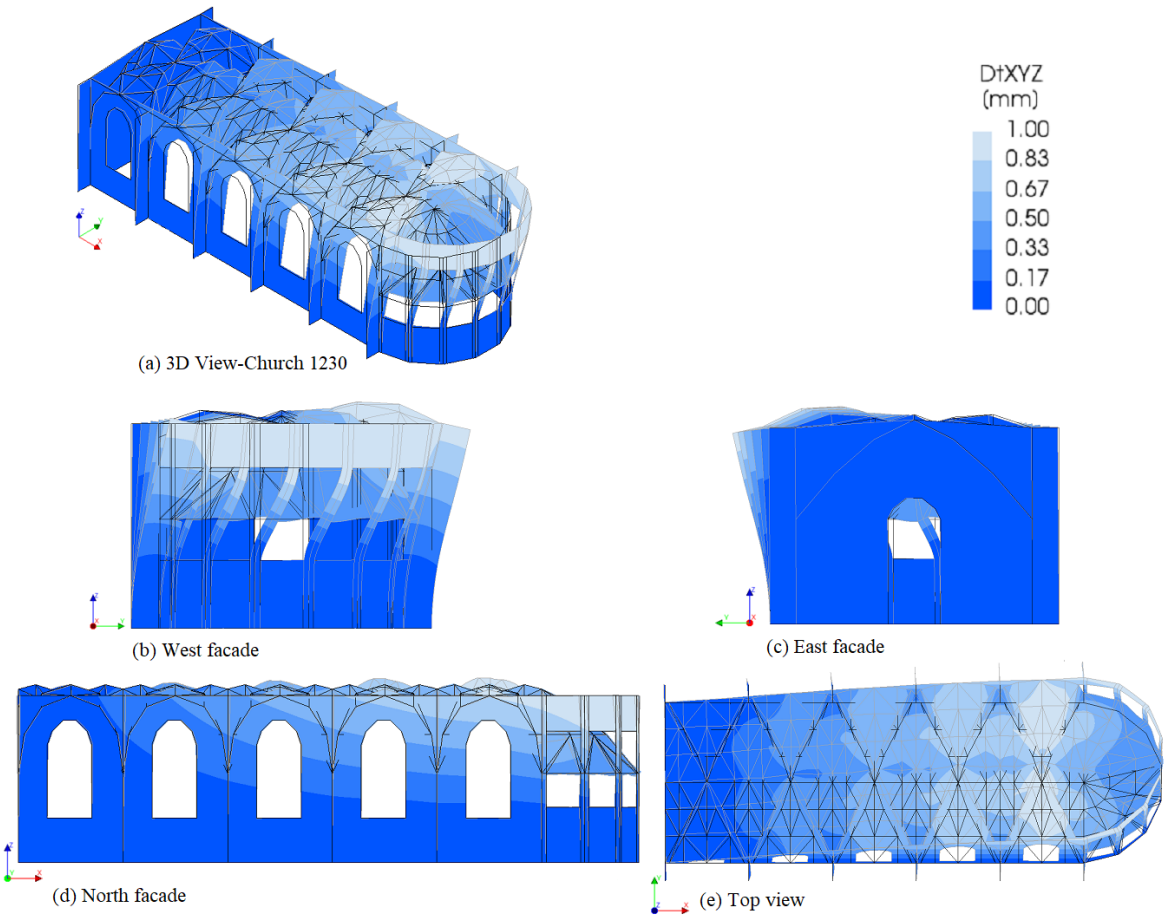

Figure 6.5: Governing Eigenmodes Global Y-direction Church Prior to modifications, [scale factor=0.05]

6.2. Overall behaviour under vertical loading

Analyses under static conditions are performed to validate the model. Output such as the deformations, internal forces, reaction forces are then studied to gain greater insight into the behaviour of the model under linear and nonlinear static load conditions. The analyses are performed by applying the dead weight and the pre-loading, as indicated in Figure 6.1, on the structure. Results are presented in Figure 6.6 (a) for the linear load conditions and Figure 6.6 (b) for the nonlinear load conditions.

Deformations

After the application of the loads a symmetric displacement pattern is observed for both the linear and non-linear load conditions. Maximum displacement are found in the centre of the vaults with a quantity of 0.91mm and 0.91mm, respectively for the linear and nonlinear load conditions. When examining the deformations in the vertical direction for the main walls, note that the deformations at the top of the wall are 0.16mm & 0.16mm respectively and are equal to zero at the location of the supports for both load conditions. Based on the pattern of the deformations in the vertical direction it can be concluded that all elements are properly connected and that the dead loads are applied in the correct manner. Displacements of the walls in horizontal plane, due to the application of loading only in the vertical direction, is in both global directions relatively small in comparison to the vertical direction. As there are no irregularities in the structural system in the vertical plan, horizontal displacements are then not caused or amplified. Thus the resultant the dead weight does not have a lever arm with respect to the centre of the structure. Note that, the quantities of the results for the nonlinear static analysis in comparison to the linear static analysis are significantly smaller. As nonlinear effects are accounted for in this case.

Internal stresses and reaction forces

Stress concentrations can be observed in parts of the main walls and piers. At the base and at mid-span height of structure parts of the walls and piers are in compression. Whereas at mid-span height of the piers tension is observed. As can be seen in the displacement pattern of the piers, an outward curvature towards the main walls can be observed, which results in tensile stresses in the other part of the piers and at the same height in compressive stresses at the main walls. Additionally, as can be seen, the compressive stresses increase gradually from top to bottom. Lastly, a comparison with the resultant force obtained from hand calculations is made. For the numerical model a reaction force of 904.5 kN is found where as for the hand calculations a value of 1011.21 kN.

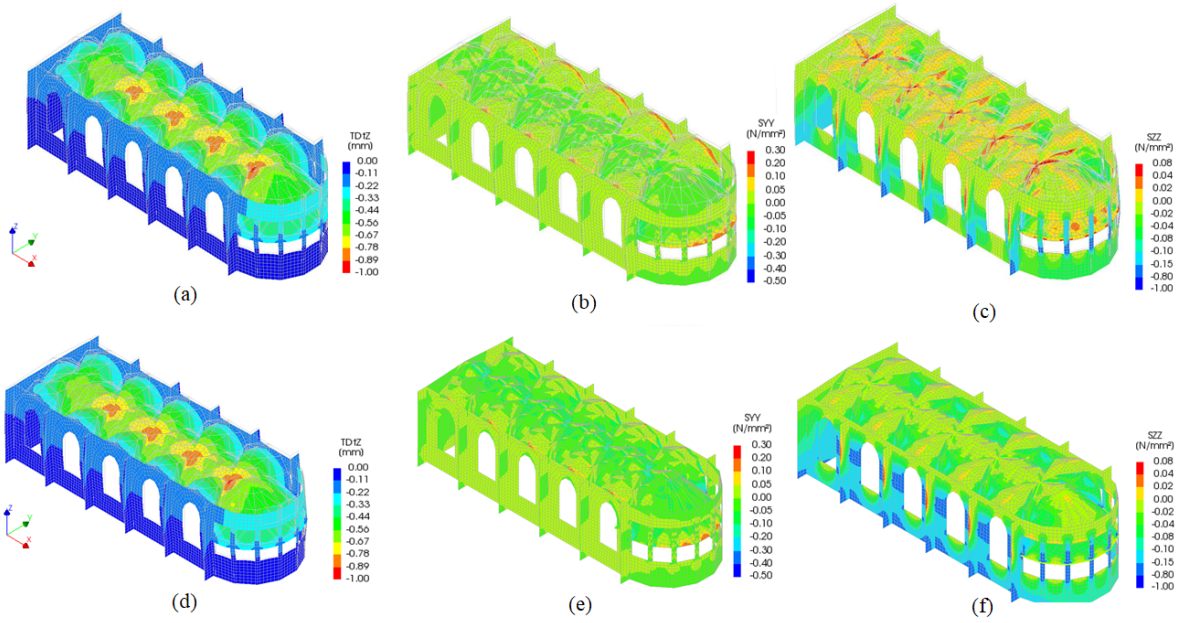

Figure 6.6: Displacement contour, stress contours (Y and Z-direction) church due to vertical precompression for the linear elastic model (a, b, c) and non-linear model (d,e,f), [scale factor=0.05]

6.3. Overall behaviour under pushover loading

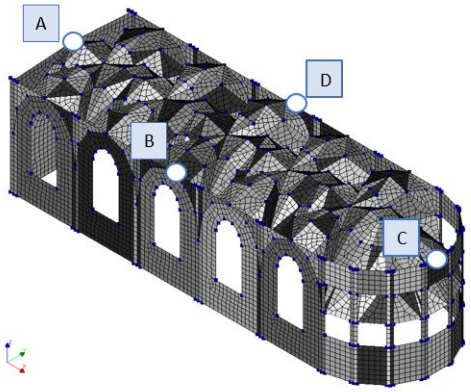

Figure 6.7: Selected control nodes for the capacity curves

For the NLPO analysis the pushover loading is applied in the positive global X-direction and results are presented for the chosen control nodes. Figure 6.7 presents the control nodes for which the capacity curves are plotted. The nodes are chosen along the perimeter of the main wall at top elevation level. Figure 6.8(a) shows the response of the church model in terms of base shear force with respect to the control nodes. The capacity curve for node A with characteristic points is illustrated in Figure 6.8(b). The base shear force is equal to the sum of the reaction forces at the base of the church model. From the capacity curves important characteristics, such as initial stiffness, maximum force capacity and the softening behaviour of the structure can be deducted. As can be observed from the results obtained for the control nodes, for all important characteristics a difference is found. When examining the values for the ultimate load capacity for node A, B, C and D a value of 2500 kN is found. For the initial stiffness, a higher stiffness if found for node B and D, followed by node C and then node A. The differences can be declared by the location of the nodes and the location of the application of the loading. As control node A is located at the location of the application of the pushover loading a much higher displacement is captured in this node in comparison to the other nodes. For node B and D on the other hand a lower displacement is captured in this direction as the nodes are located along main walls where the loading is transferred in the in-plane direction. Moreover, note that due to the symmetry of the church geometry in this direction the behaviour of node B and D are symmetric. Lastly, control node C shows a deviation in behaviour after its peak loading. Due to the geometry of the curved West facade, this part starts to becomes very unstable and shows higher displacement behaviour than the other points.

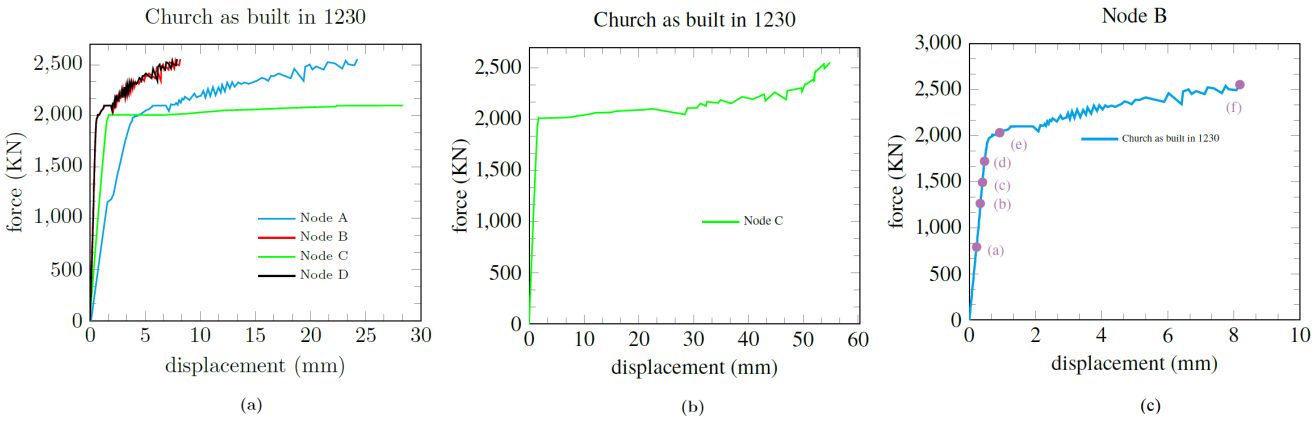

Figure 6.8: Capacity curves for (a) nodes A, B, C and D, (b) node C Zoom out and (c) Node B with characteristic points

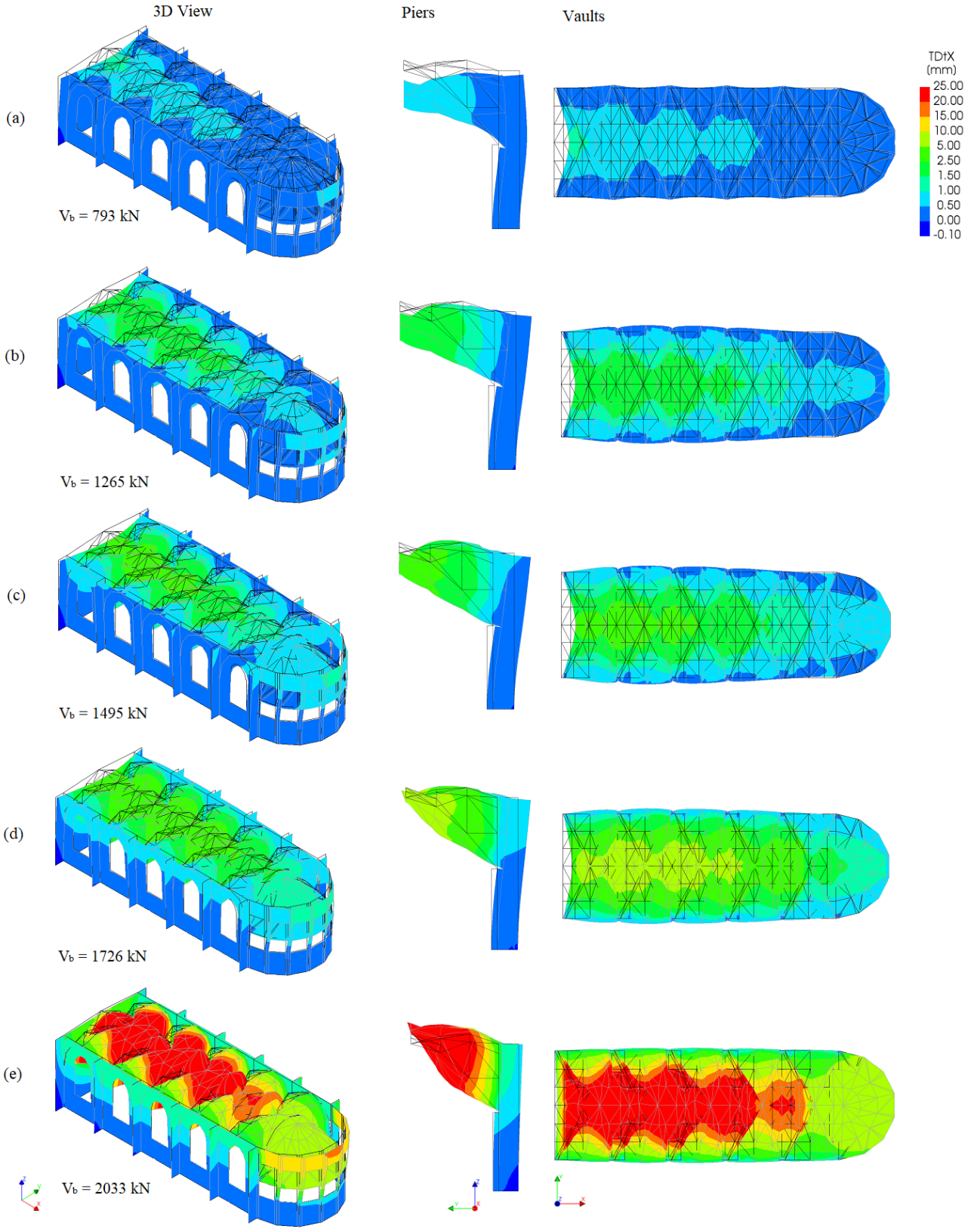

Figure 6.9: Displacement contour in the church as built 1230 due to pushover loading, [scale factor=0.05]

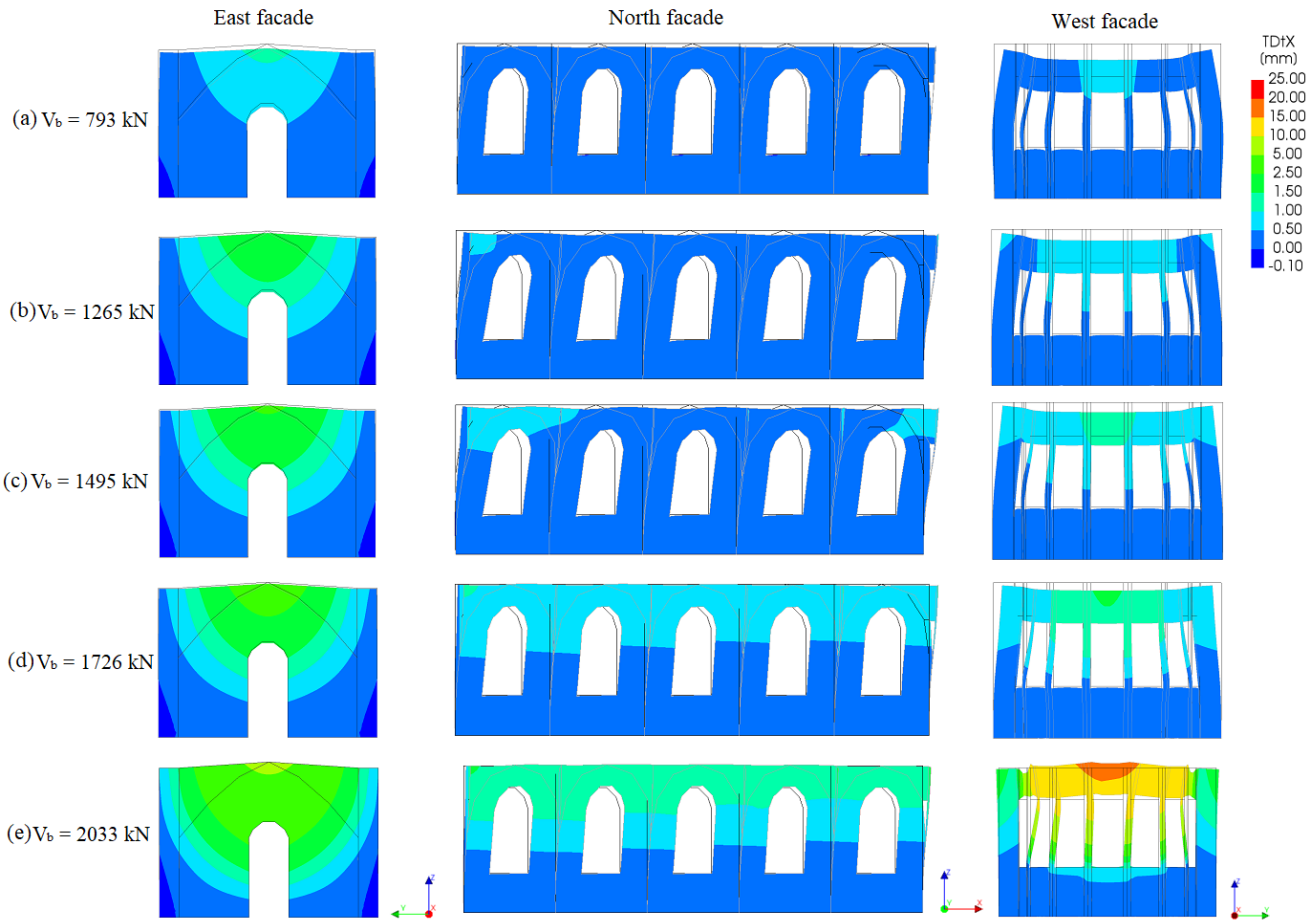

Figure 6.10: Displacement contour in the church as built 1230 due to pushover loading, [scale factor=0.05]

The results of all models show no softening behaviour and end early on due to divergence problems. More about the quality of the results will be reported in the next section which will address the convergence behaviour of the presented analysis results. In this section the overall behaviour of the church is further examined by observing the results at five points picked on the capacity curve of control node A. These points are chosen arbitrary at reaction force difference of about 500 kN. Figure 6.8-(b) presents the location of these points.

Point (a) on the graph is found to be in the linear elastic stage during the analysis. At this point a displacement of 1mm is found in control node A and the base shear force has reached a value of 670 kN. For the same force a displacement of 0.5, 0.2 and 0.2 mm are reached for node B, C and D respectively. From the contour plots of the deformations (see Figure 6.9 and 6.10), it can be observed that at point A the highest deformation takes place as it is the point where the modal pushover loading is applied. The base of the church does not displace and a symmetric displacement pattern is observed in the vaults. The displacement pattern in the vaults is symmetric due to the model of the geometry, however, the distribution of the displacement pattern in the longitudinal direction is not symmetric due to the shape of the vaults. Up to point (d) and (e) a gradual increase of the displacements observed during the initial push is observed. At the end of the analysis it can be seen that the East facade is fully pushed out-of-plane, the walls along the North and South facade are fully activated and a significant displacement at control node (C), which is located at the West facade can be observed. Lastly, the piers in located in the North and South facade which are initially as a consequence of the dead load curved inwards gradually bend outwards. The outward curvature has a negative effect on the equilibrium path of the vaults as it disturbs the trust forces. What the effect is on the main walls and on the global behaviour of the structure is interesting to study in detail. This will be done in section 6.6.

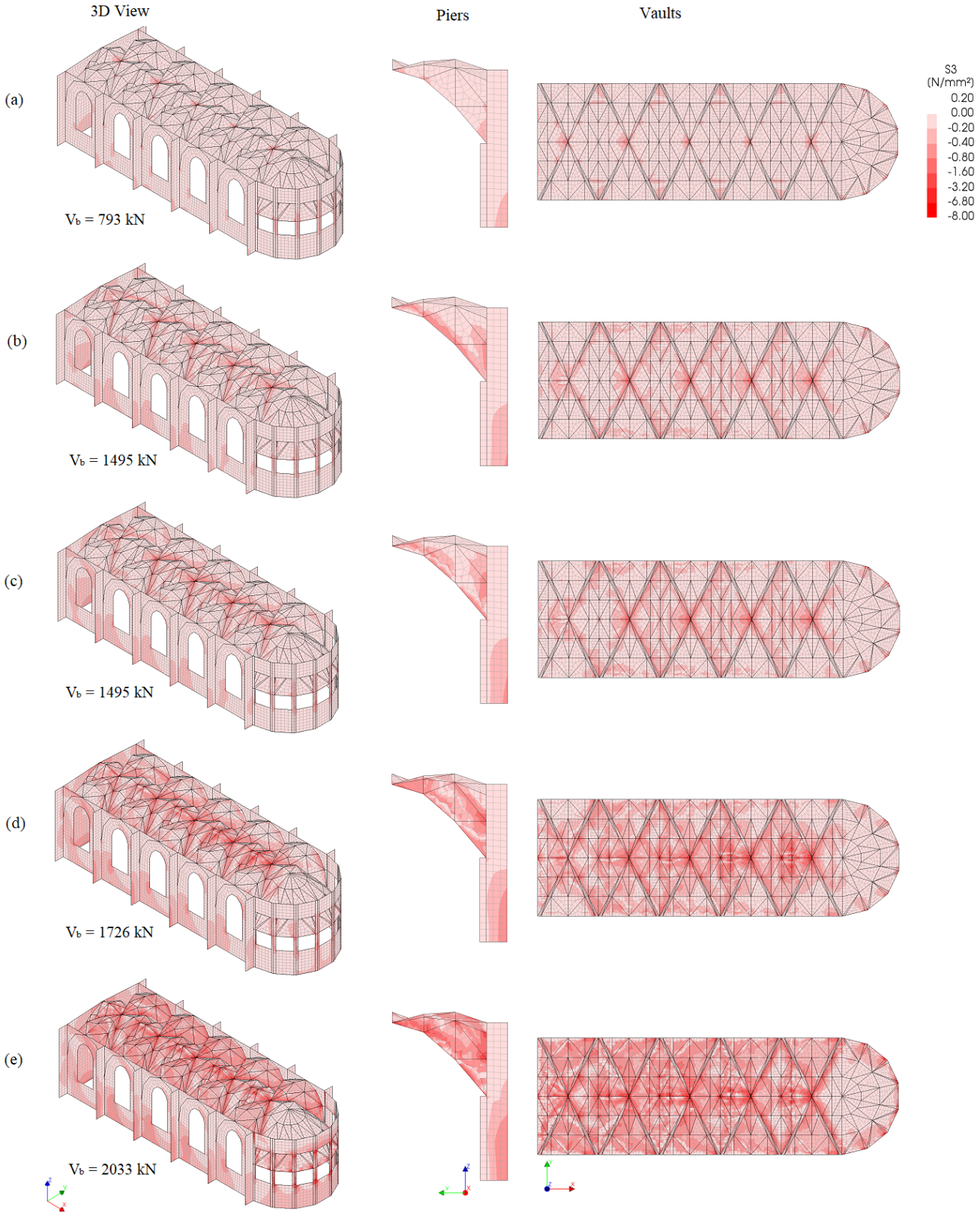

Figure 6.11: Compressive stresses in the church as built 1230 due to pushover loading, [scale factor=0.05]

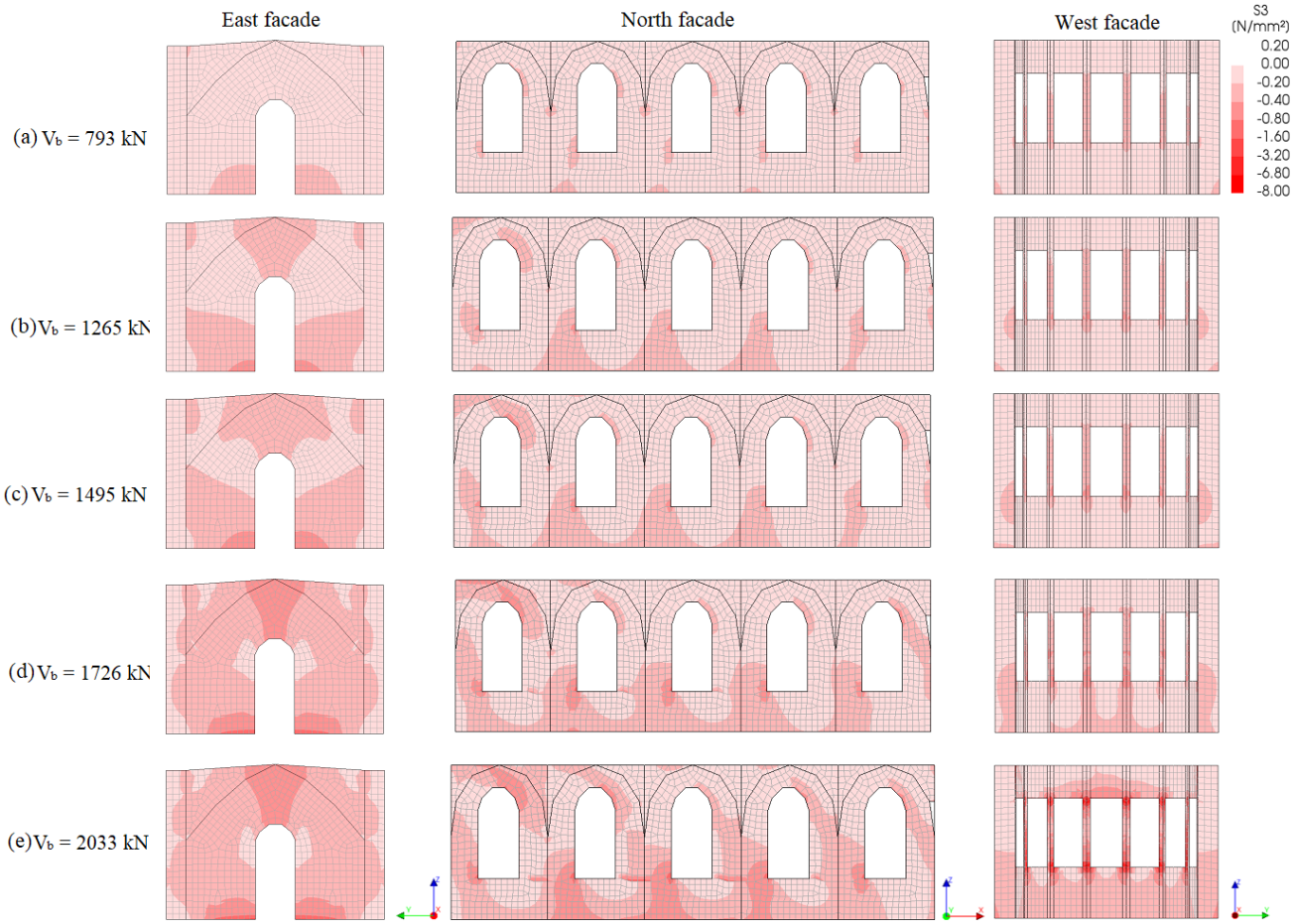

Figure 6.12: Compressive stresses in the church as built 1230 due to pushover loading, [scale factor=0.05]

Compressive stress concentrations are observed at the base of the walls, piers and in parts of the vaults (see Figures 6.11 and 6.12). A higher compressive stress concentration can be observed in the Eastern wall of the church as it is the wall where the pushover loading is applied. During the load application the stress concentrations grow further in the upwards direction in the walls and piers. The compressive stresses reach the limit stress of 8 MPa only in the vaults. Possible prone locations for crushing can be indicated at the base of the piers, corners window openings and at the corners of the door opening at the East facade. However, no crushing is observed during these analysis.

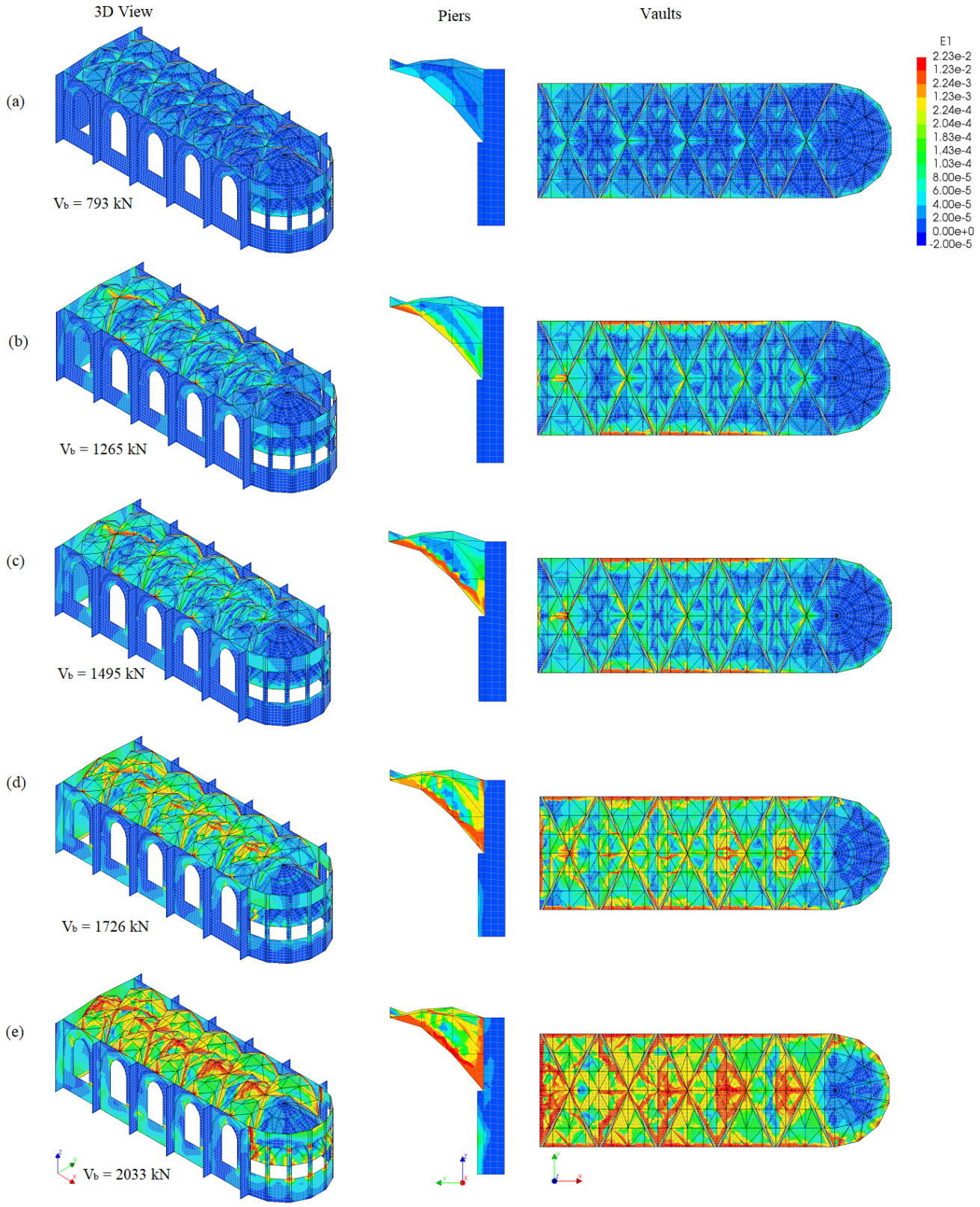

Figure 6.13: Tensile Strains in the church as built 1230 due to pushover loading, [scale factor=0.05]

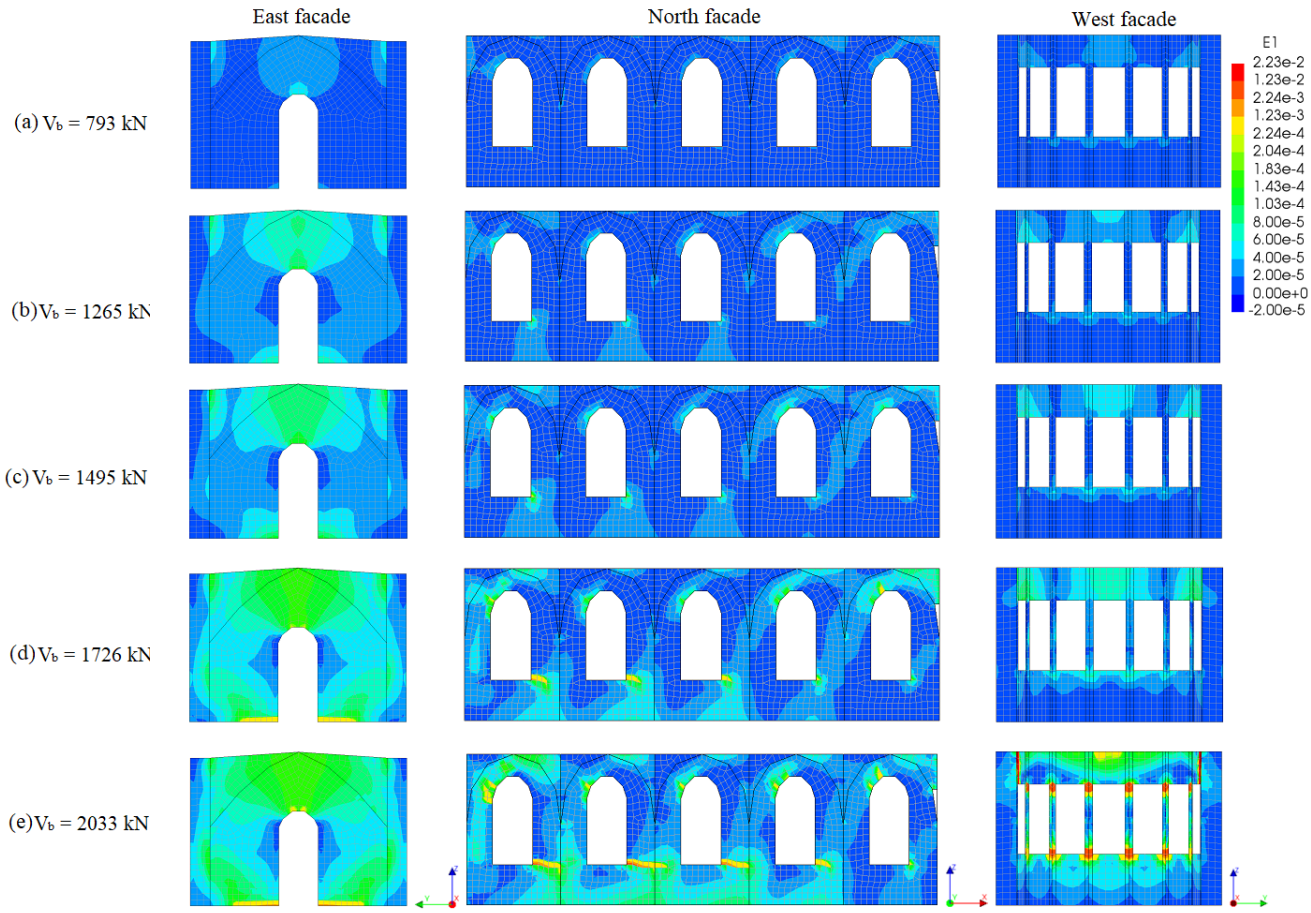

Figure 6.14: Tensile Strains in the church as built 1230 due to pushover loading, [scale factor=0.05]

Figure 6.13 and 6.14 present the results for the tensile strains in the church model. In the initial steps of the analysis, tensile strains start the develop in the vaults at the upper and lower corners of parts of window openings and door the opening. These strains develop the fastest in the East facade, where the pushover loading is applied. At the end of the analysis, high values of strains are found under the window openings and in corners of the openings.

6.4. Convergence behaviour

Figure 6.15 presents the number of iterations per load step. A limit of 50 iterations is set per load step during the analysis. As can be seen as the analysis is going towards the peak loading in the model the number of iterations per load step gradually increases, but does not exceed so often 50 iterations. Up to load step 151 the analysis is conducted with the aid of the Regular Newton-Raphson method. Up to that point the method works, however after that point the number of iterations exceeds for a longer period 50 iterations. Therefore, it is decided to proceed with the Quasi-Secant method after load step 151. As can be seen from the presented results, from the point 151 to 169 a drop is found in the number of iterations per load step. However, after load step 169 another period can be seen with steps that exceed 50 iterations. For all load steps and in particular for the load steps where 50 iterations are exceeded the balance of the energy norm is check. The deviation in the energy norm explodes towards the end of the analysis. Therefore, results are considered not valid after load step 168 in this analysis.

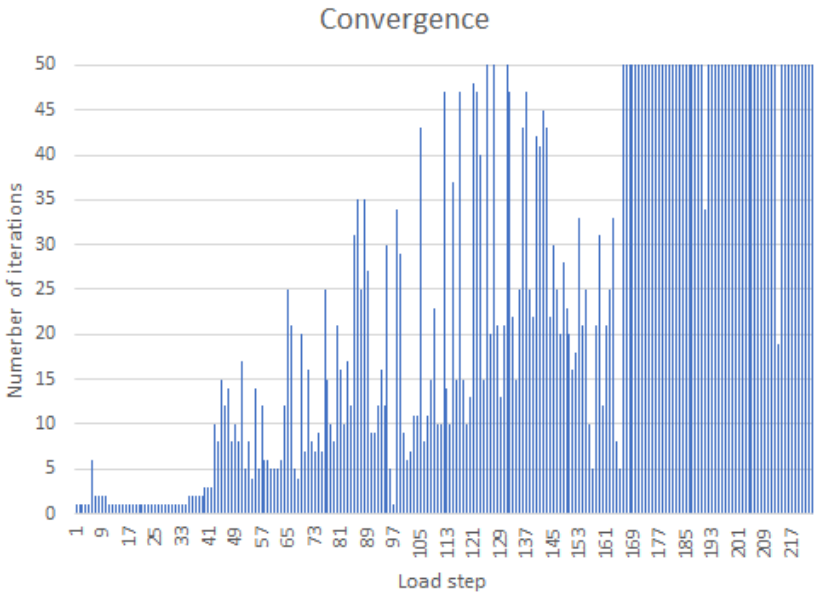

Figure 6.15: Convergence Behaviour in terms of number of iterations per load step

6.5. Crack pattern evolution

Figure 6.16 and 6.17 present the crack evolution of the structure during the application of pushover loading in the positive X-direction.

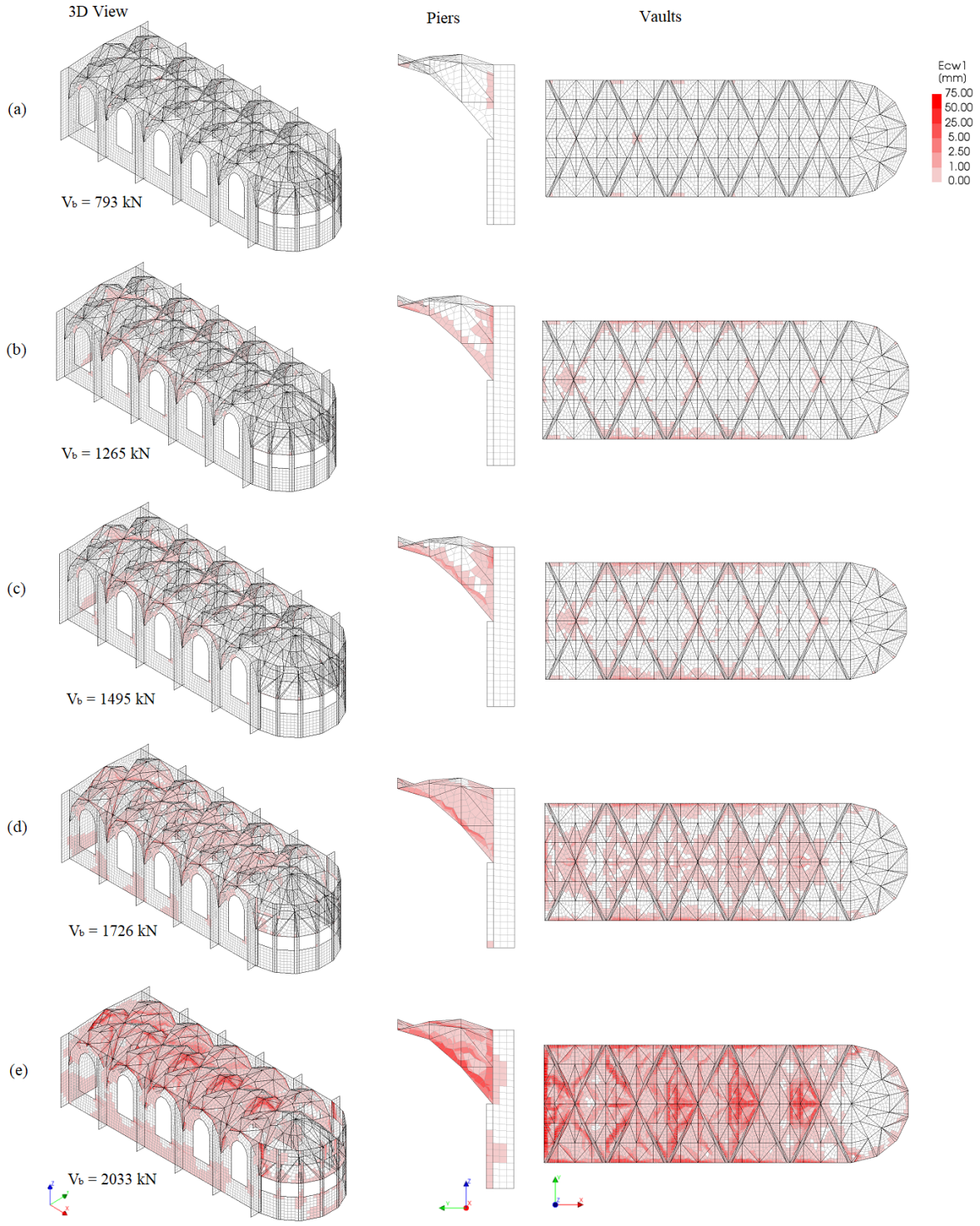

Figure 6.16: Crack patterns in the church as built 1230 due to pushover loading: 3D piers and vaults, [scale factor=0.05]

In the pseudo-linear stage of the analysis initial cracks are observed in the vaults and these have cracks widths of about 0.08mm. These cracks develop in the vaults along the boundary of the vaults with the main walls. The cracks in the vaults develop up to 25mm and show a very irregular pattern up until the end of the

Figure 6.17: Crack patterns in the church as built 1230 due to pushover loading: East, West and North walls, [scale factor=0.05]

analysis. Then as for the piers, there is no cracking observed up until the peak loading, where initial cracks start at the interface of the main walls with the piers. In the main walls, cracks develop in the corners of openings, which develop further in distributed cracks in the walls. Values of the cracks in the wall are found to be in the range of 1.0 to 3.0mm. With exception of the concentrated horizontal cracks in the corners of the openings, for which values of up to 5.0mm are found.

6.6. Local behaviour pier-wall connections

As indicated in section 6.4, it would be interesting to study the local behaviour of the piers on the global behaviour of the walls and the structure in more detail. As seen in section 6.6, right after the application of the pre-compression loading the piers bend inwards. But as the pushover loading is applied and grows the piers start to restore their original position and then start to bend outwards. As a consequence the support point of the vaults moves with values in the margin of 1mm. As the most sensitive structural elements in the structure are the vaults and therefore these have a governing influence on the global behaviour of the other structural elements during the application of the pushover loading. A small movement of the supports has a great influence on the rest of the vaults and subsequently on the entire structure. As the vaults are pushed, they start to push away the main walls and the piers are not able to resist the outward push and bend therefore outwards. Additionally, due to the horizontal movement of the main wall and the piers are pushed at their top away from their base. As for the crack up to the end of the analysis (peak stage) no cracking is observed in the piers, Figure 6.18.

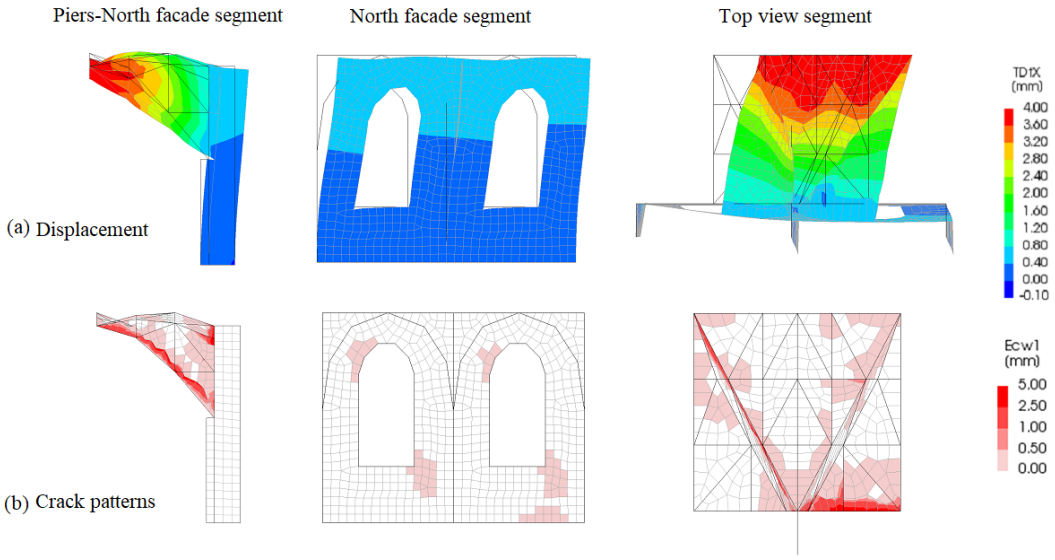

Figure 6.18: Crack patterns in the church as built 1230 due to pushover loading, [scale factor=0.05]

In Figure 6.19, at the location of the interface, at the base and at mid height, of the pier with the main wall a stress-stress relationship as presented in Figure 6.19 is observed. The results confirm that the pier is still in the linear elastic stage for both the compressive as tensile branch.

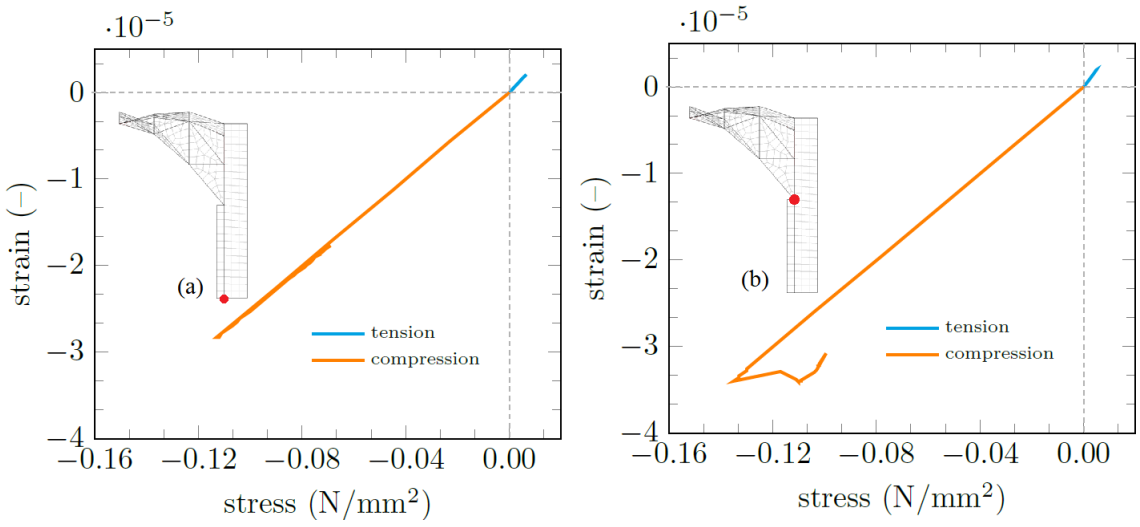

Figure 6.19: Stress-strain Relationship for (a) a base node and (b) a mid node at the interface of a pier and wall

6.7. Conclusions

The capacity curve for the church was presented for four control nodes along the perimeter of the main walls. A symmetric pattern was observed for all results along the global X-direction. Due to the complex shape of the vault structure the propagation of the displacements, crack patterns and stresses are not evenly distributed between control node A to node C. Moreover, cracking in the spandrels under the window openings are observed up to the peak displacement of the structure. The formation of hinges at the connection of the vaults with the walls and at the diagonal ribs are observed.

The results in the last load step of the pre-compression loading show the occurrence of an initial curvature in piers and as a results of this tensile and compressive stress concentrations were observed. As already indicated in the main modelling assumptions of the church, the pier-to-wall connections is an unknown due to the lack of technical information. In this chapter, for this particular pier-to-wall configuration, the global behaviour of the church was observed. It would be interesting to look at the local behaviour of this connection and its eventual effect on the global behaviour of the church. Moreover, the modelling choice of this connections with respect to the global behaviour of the church can be reviewed in more detail. This is done and presented in chapter 7.

For the analysis the behaviour up until the peak load have been captured. Several suggestions can be made to improve the numerical model. Firstly, the damage characteristics are mostly likely to improve by adopting a more detailed modelling approach, for example by a 3D solid elements or a micro-modelling approach for the masonry elements. Secondly, the capacity curve is likely to improve by replacing the assumed rigid connections between masonry walls and vaults by a more detailed description using interface elements. Thirdly, different numerical solving procedures can be employed to find the most suitable method that could help us to capture the post-peak behaviour of the church. In addition to the Newton-Raphson method, the application of the Quasi-Secant method and Arc-length method are studied and applied to the case study (Church as built in 1230) in chapter 8.

7

Sensitivity study pier-wall connections

As previously highlighted in chapter 5, technical details regarding the connections of the structure are not available. Three important connections that can be pointed out are the wall-to-wall, wall-to-vaults or wall-to-roof and the pier-to-wall connection. For the setup of the numerical model of the church various assumptions can be made regarding these connections. Within the scope of this study it is chosen to focus are the pier-to-wall connections and all other connections are considered by default fully fixed. This chapter kicks off with a description of the pier-to-wall configurations and the main assumptions on which these connections are based. Hereafter, the global behaviour of the church models under static loading is discussed. Followed by a discussion on the global and local behaviour after the application of the pushover loading. Lastly, the difference in damage observed in each model is presented and the findings of this chapter are presented.

7.1. Proposed pier-to-wall configurations

Figure 7.1, 7.2, 7.3 and 7.4 present the four proposed and studied pier-to-wall configurations (A1,A2,A3,A4) in this thesis. All configurations have the same geometric properties as the physical model, however as the interlocking of the masonry bricks in the global x- and y-directions is the main unknown parameter different modelling approaches can be adopted to account for the difference. A wide variety of configurations can be studied to assess the global structural behaviour of the church. However, within the scope of these thesis as only shell elements are used, the study is limited to four configurations as introduced in this chapter. Hereafter, the numerical modelling, analysis and results are presented. In this chapter, the church model as built in 1230 is referred to as model A2, the first, second and third variation are referred to as model A1, A3 and A4, respectively.

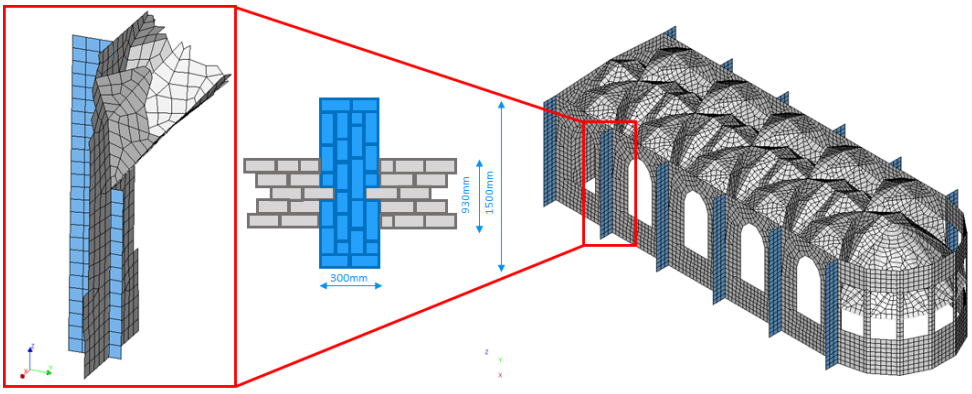

Figure 7.1: Pier-to-Wall Configuration A2

The church model as built in 1230, hereafter referred to as configuration A2 is presented in figure 7.1. For this configuration it is assumed that the piers are considered transverse to the main walls. This assumption is based on the possibility of an out-of-plane interlocking of masonry bricks of the walls with the bricks of the piers, as depicted in Figure 7.1.

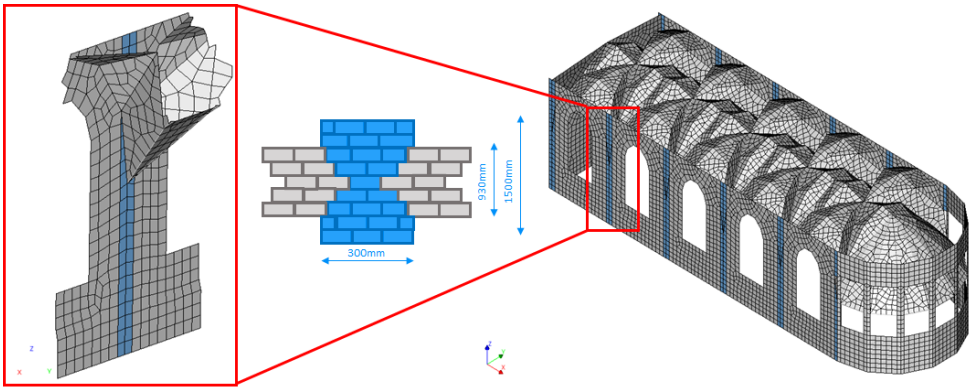

Figure 7.2: Pier-to-Wall Configurations A1

Pier-to-Wall Configurations A1, the first variation on the church model as built in 1230, is presented in Figure 7.2. For this configuration the piers are considered in-plane with the main walls. An in-plane interlocking of masonry bricks of main walls with bricks of piers is assumed in this case.

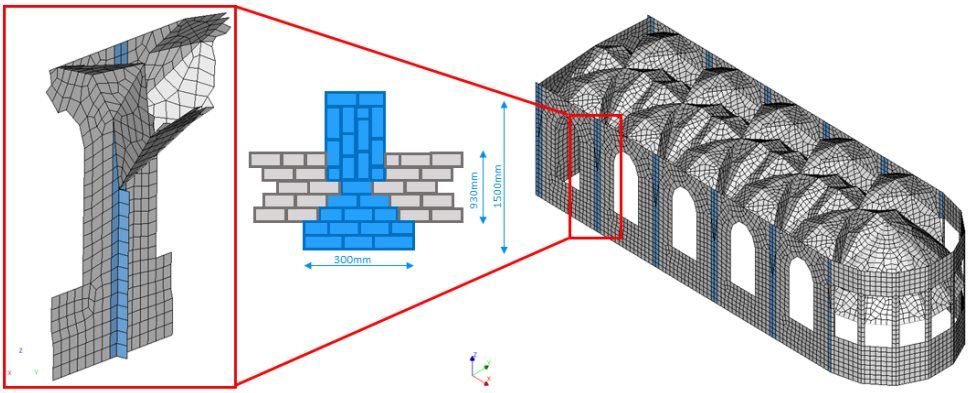

Figure 7.3: Pier-to-Wall Configuration A3

Pier-to-Wall Configurations A3, the second variation on the church model as built in 1230, is presented in Figure 7.3. For this configuration the piers are considered partially in-plane and partially out-of-plane with the main walls. An in-plane interlocking of masonry bricks of main walls with bricks of external piers and an out-of-plan interlocking of the external piers is assumed in this case.

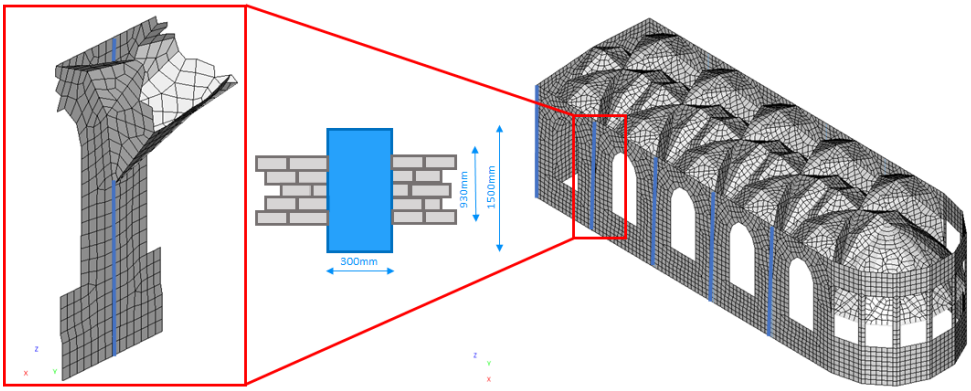

Figure 7.4: Pier-to-Wall Configuration A4

Pier-to-Wall Configurations A4, the second variation on the church model as built in 1230, is presented in Figure 7.4. For this configuration no interlocking of the piers with the main walls is considered. Additionally, the piers are considered with linear elastic properties.

7.2. Overall behaviour models under vertical loading

During this stage(a) the dead and live loads are applied to the structure. Results for all four models are presented in Figure 7.6, 7.5, 7.7 and 7.8. With respect to the displacements, after the application of the loads a symmetric displacement pattern is observed for all models. Maximum displacement are found in the centre of the vaults for all models with a quantity of 0.91mm, 1.00mm, 1.04mm, 1.08mm for model A2, A1, A3 and A4 respectively. Displacements of the walls in the global X and Y direction in this stage are negligible in all models. With regards to the stresses, as the pre-compression loading is applied on the main walls, stress concentrations in parts of the main walls and piers can be observed. At the base and at mid-span height of the walls we observe parts of the walls and piers to be in compression. Where as at mid-span height of the piers we observe that the piers are in tensions. As can be seen in the displacement pattern of the piers, a outward curvature towards the main walls can be observed, which results in tensile stresses in the other part of the piers and at the same height in compressive stresses at the main walls. As can be seen in the presented figures, model A4 has the highest stress concentrations in the walls as the piers are considered with linear elastic properties in this case. For model A1, A3 and A4 we see due to the outward bending of the piers higher stress concentrations in the vaults in comparison with model A2. Moreover, in this stage cracking is not yet observed again for all models.

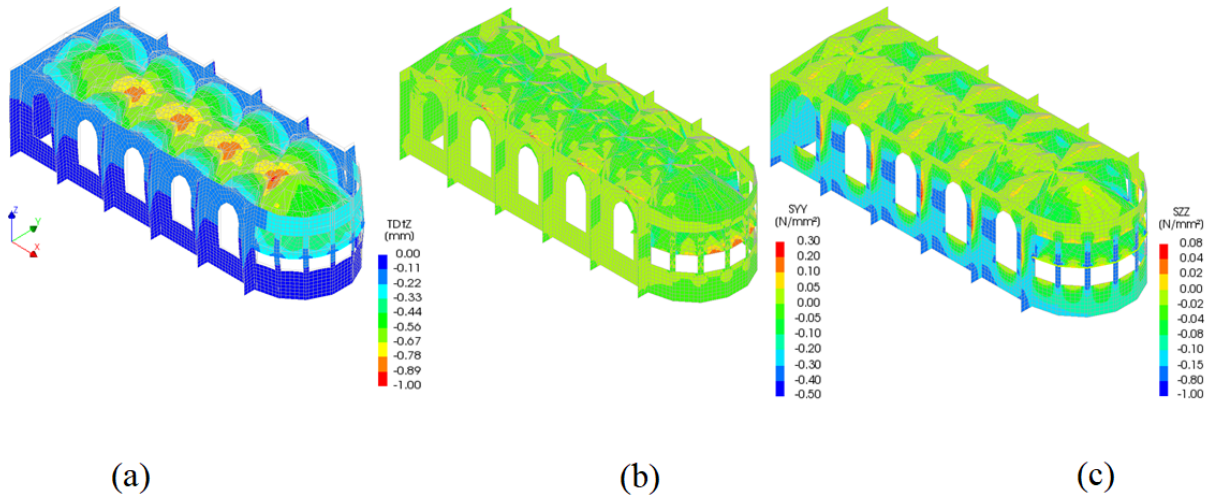

Figure 7.5: Church as built in 1230 (Model A2): (a) displacement contour due to vertical pre-compression, (b) stress in Y-direction, (c) stress in Z-direction, [scale factor=0.05]

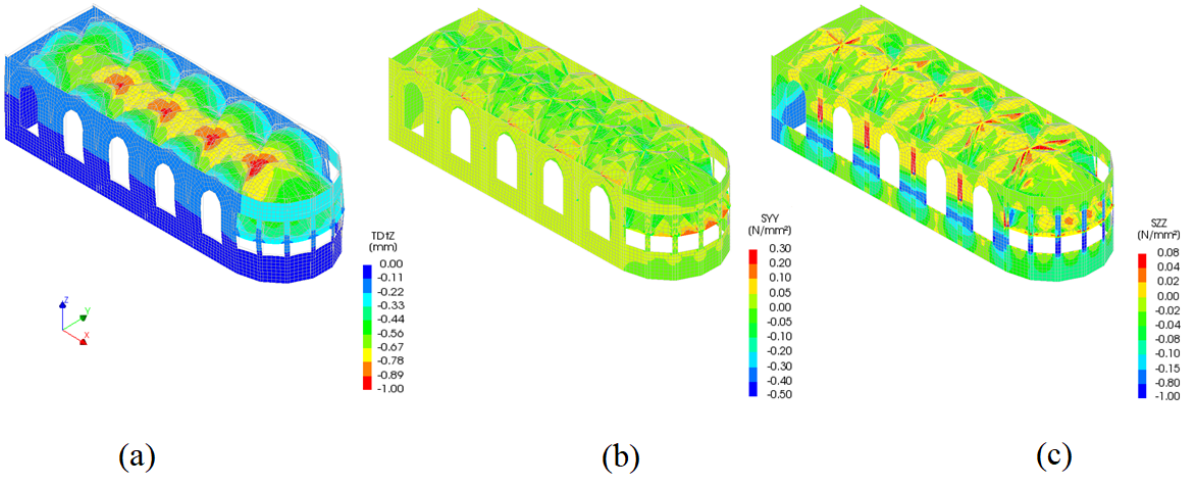

Figure 7.6: Church as built in 1230 (Model A1): (a) displacement contour due to vertical pre-compression, (b) stress in Y-direction, (c) stress in Z-direction, [scale factor=0.05]

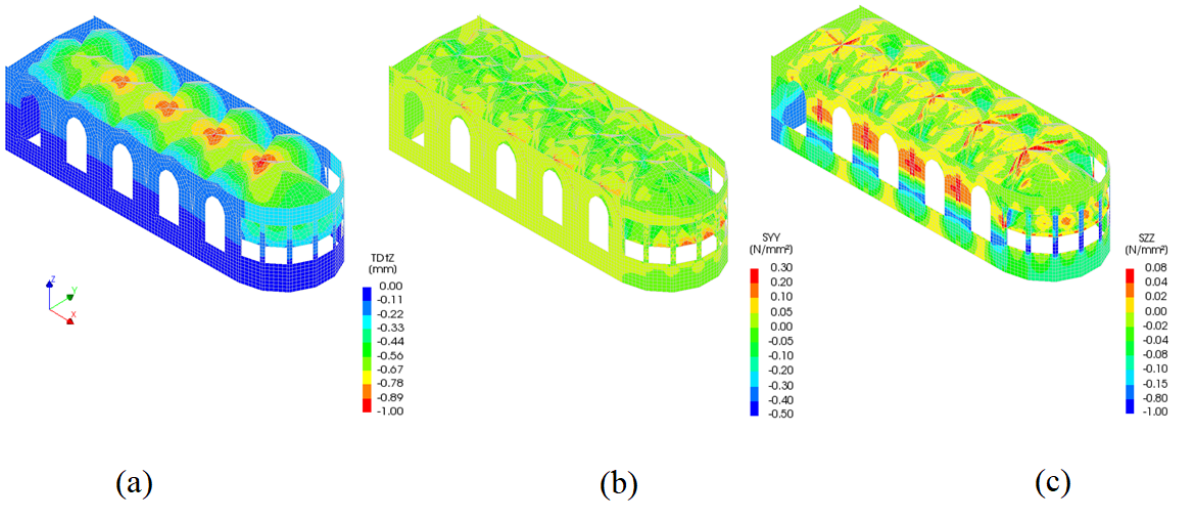

Figure 7.7: Church as built in 1230 (Model A3): (a) displacement contour due to vertical pre-compression, (b) stress in Y-direction, (c) stress in Z-direction, [scale factor=0.05]

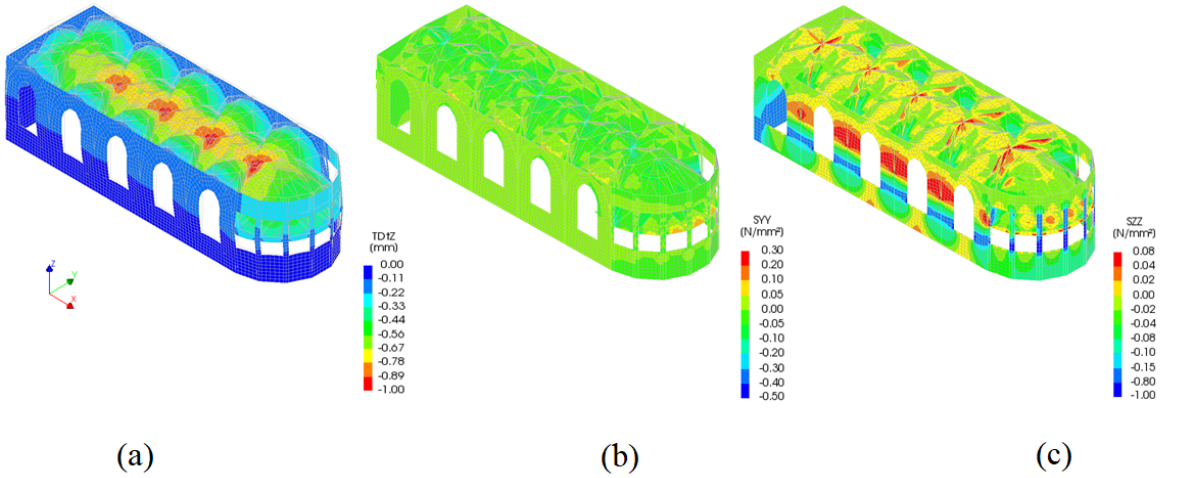

Figure 7.8: Church as built in 1230 (Model A4): (a) displacement contour due to vertical pre-compression, (b) stress in Y-direction, (c) stress in Z-direction, [scale factor=0.05]

7.3. Overall behaviour models under pushover loading

For the models A1 to A4 a structural nonlinear analysis procedure is adopted as previously introduced for model A2 in chapter 6, table 5.6. For these analyses both geometrical and physical non-linearity are included. For this procedure the self-weight is applied prior to the application of the modal pushover load, such that stressed resulting from the self-weight are calculated properly.

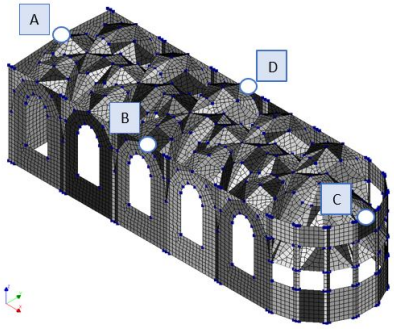

Figure 7.9: Selected control nodes for the capacity curves

Capacity Curves

Figure 7.9 presents the nodes for which the capacity curves are plotted. Figure 7.10 compares the capacity curves from the numerical models A1 to A4 for the selected nodes with respect to one and other. The horizontal reaction force at ground floor level is plotted against the displacement at top level of the walls.

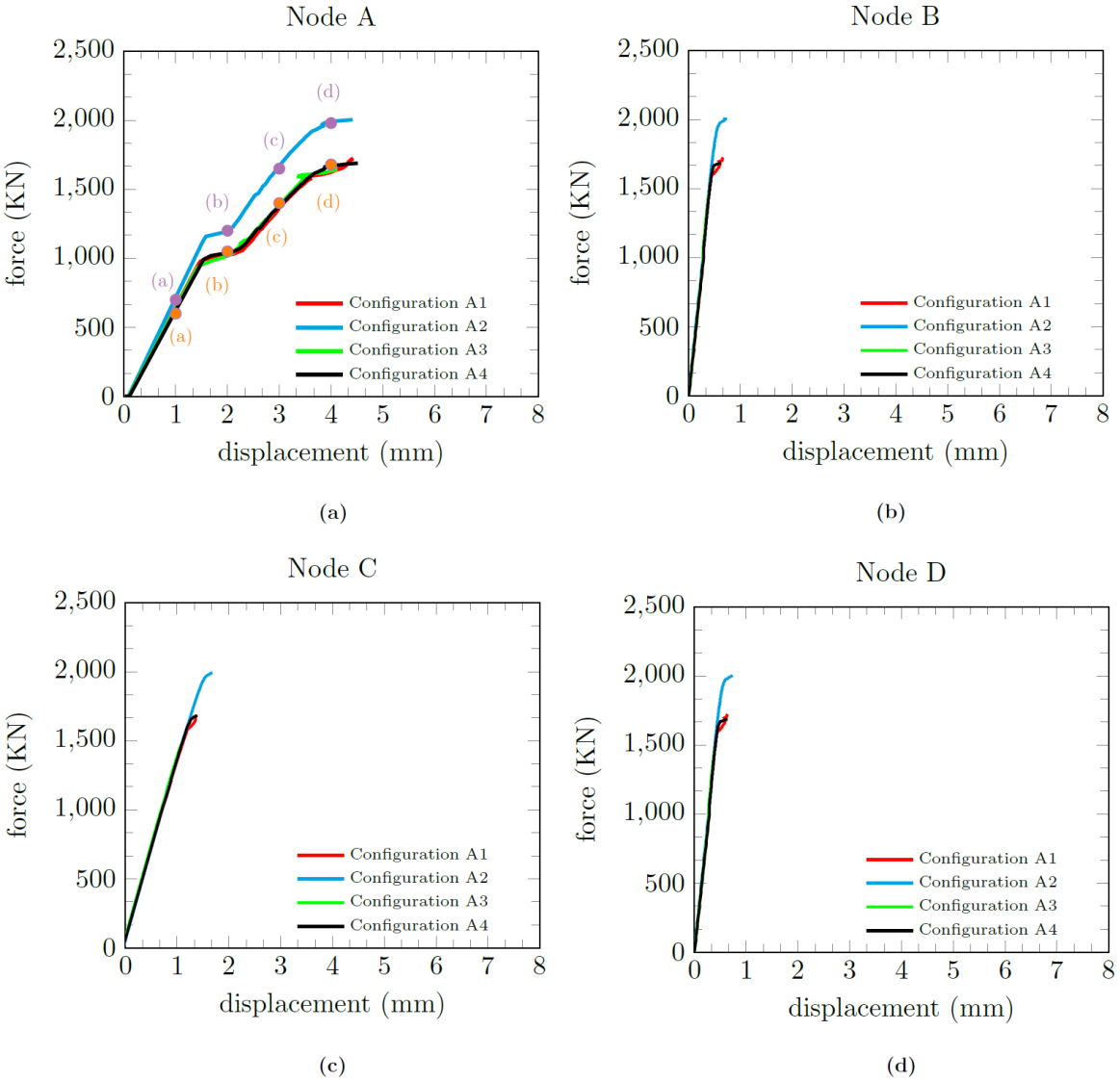

Figure 7.10: Capacity Curves for Nodes: (a) A, (b) B , (c) C and (d) D

An overview of all numerical simulations conducted and pre-
sented in this chapter is presented in table 7.1. Here F_{max} and d_e denotes the maximum force and displacement in the peak-point. For all analysis, with the current setting (see table 5.6) and figure 7.10 presents the capacity curves of the church model in terms of base shear force with respect to the Node A, B, C and D. The base shear force is equal to the sum of the reaction forces at the base of the church model. The numerical results show a good agreement with respect to the Node A, B, C and D for the initial stiffness phase (see point (a) in Figure 7.10-(a)) for all four models. The results up to the peak (point d in Figure 7.10) only are captured. As after the peak, all models show numerical instabilities caused by the damaged models and no softening behaviour is yet captured due to divergence problems. Hereafter, the results of above-mentioned four stages are explained.

Configuration type	F_{max} (KN)	d_e mm	Number of nodes	Simulation time (hr)
A1	1723.8	4.427	31194	21
A2	2004.2	4.416	31936	22
A3	1643.2	4.118	31604	18
A4	1688.8	4.515	30754	18

Table 7.1: Details Analyses for the church A1 to A4 Models

Model A2 shows a deviation in overall stiffness and maximum force capacity after the linear stage. Although, the piers in the presented models own similar physical properties, due to the modelling approach, model A2 has more surface for cracking due to the continuum cracking assumption and therefore it is able to allow redistribution of forces in nonlinear stage. Model A1 and Model A3 show similar results as expected, since the models closely resemble one and other. The addition of the internal pier seems to have minimal effect on the ultimate force and the displacement capacity of model A3 in comparison to model A1. Lastly, model A4 resembles model A2 when considering the connections of the main walls of the bays with one and other. However, as the piers in model A4 are considered linear isotropic its behaviour is not similar to model A2. In terms of capacity model A4 closely resembles the behaviour of model A1 and A3. Regardless of the shorter length of the main walls in model A1 and A3.

In Figure 7.11 presents the displacement contours for the church models. As all models are symmetric along the X-axis and show therefore a symmetric displacement pattern. However, note that the outward curvature of the piers in each model is different. And therefore the supports of the vaults do move slightly more. In general model A4 shows a higher outward displacement than the other models with a value of ...mm. As for the displacement of the vaults, it can be observed that the pattern in especially the dome part on the side of the curved facade most certainly differs.

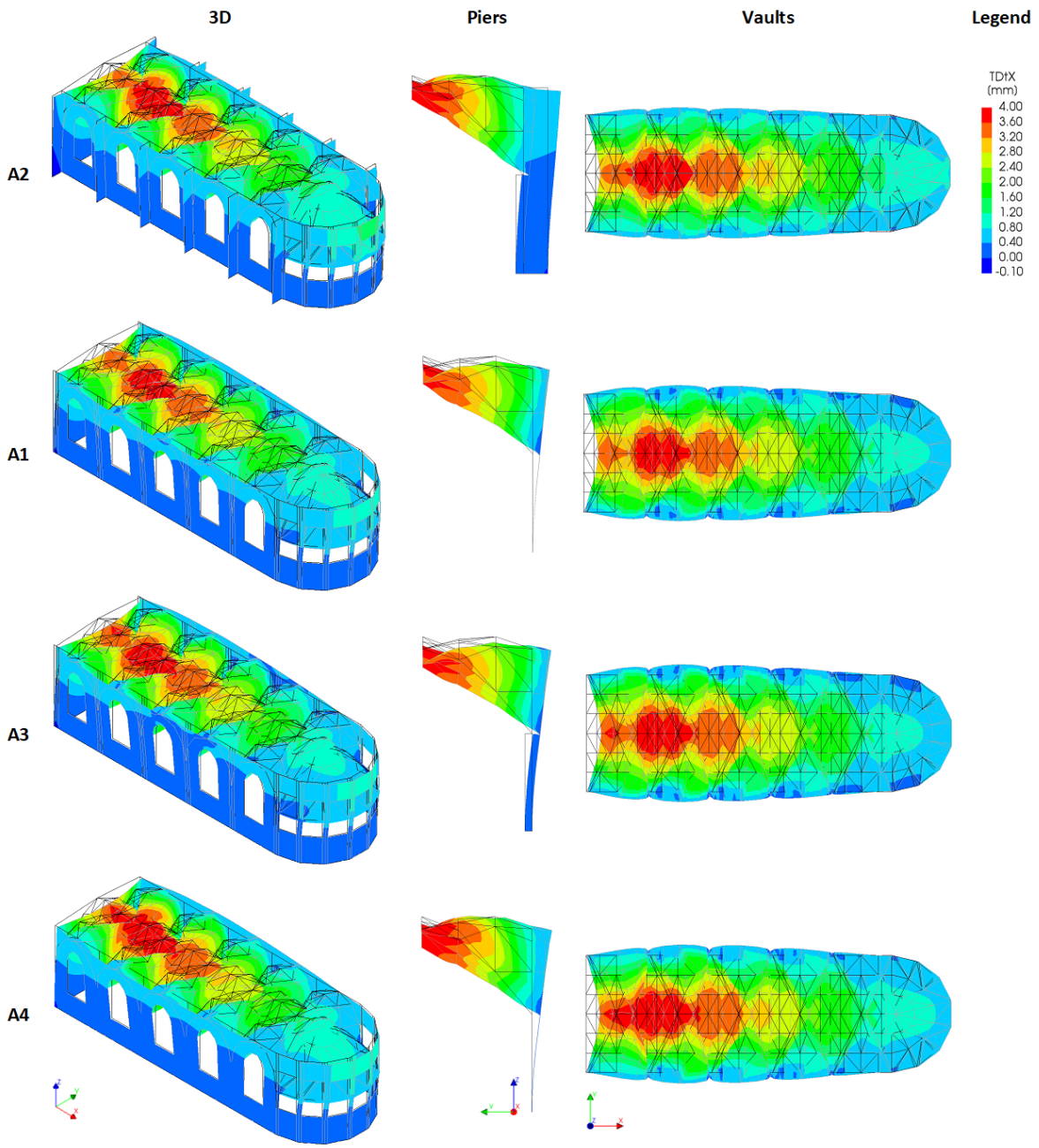

Figure 7.11: Displacement patterns for the church due to the pushover loading, [scale factor=0.05]

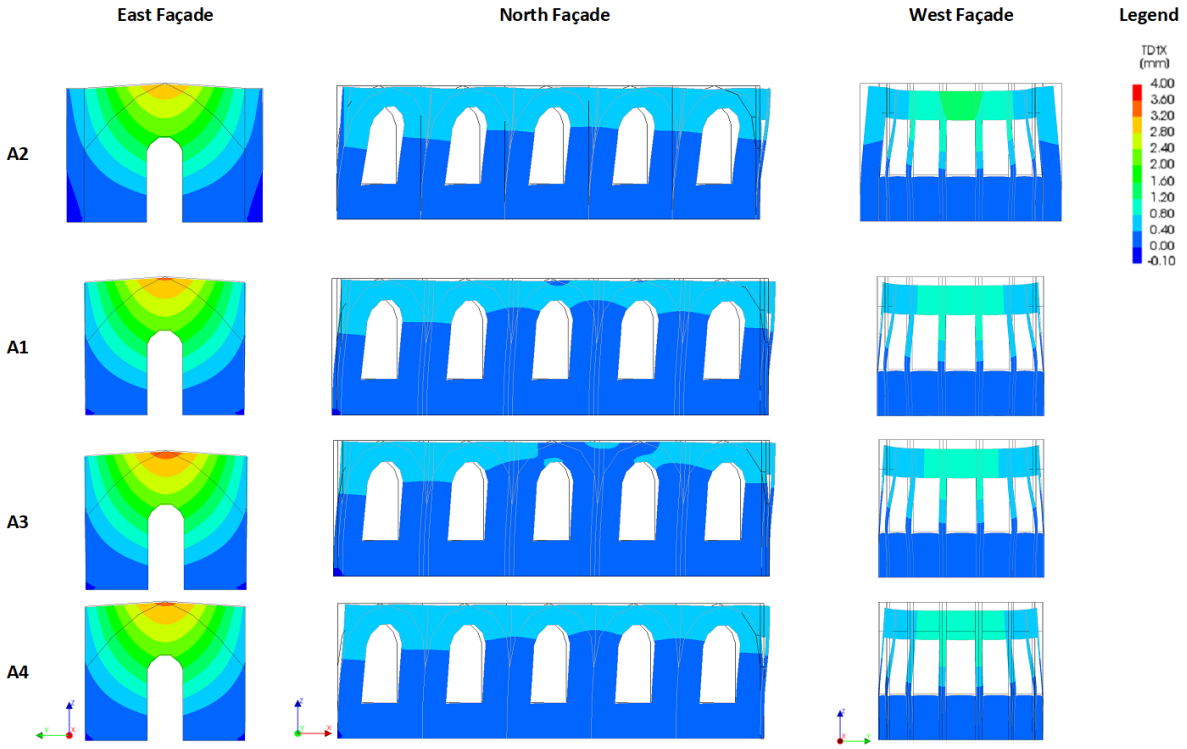

Figure 7.12: Displacement patterns for the church due to the pushover loading; for facades, [scale factor=0.05]

Figure 7.12 presents the contour plots for the displacements for the East, North and West facade. As can be observed here for the East facade, the displacements are almost identical. With exception some small deviations. As for the North facade, it can be seen that model A2 has the highest displacement in the global X-direction at its top boundary in comparison to the other models. The other models show a similiar displacement pattern with respect to one and other. Lastly, with exception of model A2, some small differences can be found for the West facade of all other models. Model A1 closely reflect the behaviour of model A4. As for both models the piers are assummed in-plane the displacements at the curved facade is relatively more than for model A3.

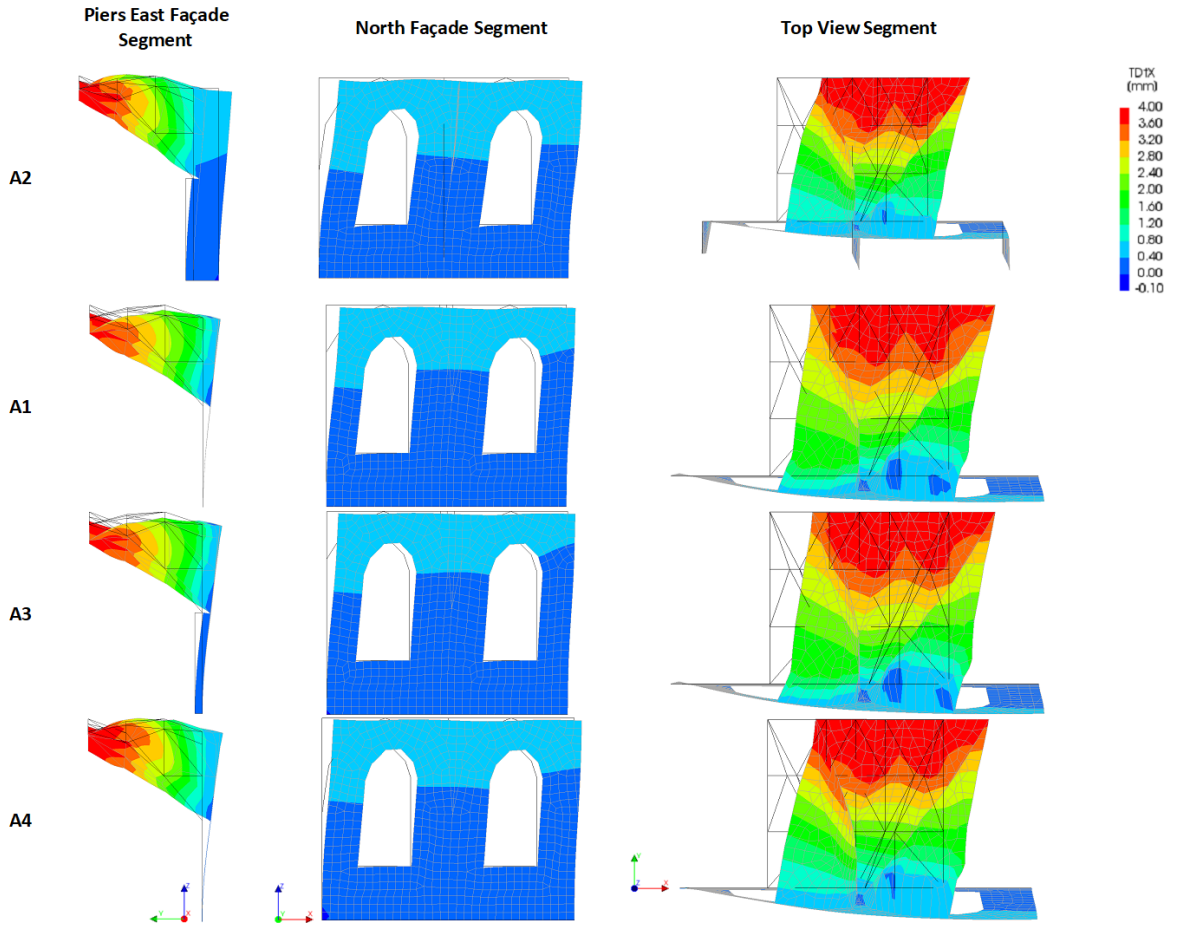

Figure 7.13: Displacement patterns for the church due to the pushover loading; for piers, [scale factor=0.05]

Figure 7.13 zooms into the piers. A segment of at the North facade is highlighted, where a side, front and top view is shown. In this figures it can be seen that the out-of-plane movement of the top of the piers differs for all models. However, there are no difference to be found in the in-plane direction. Lastly, in the top view a small difference is seen in the displacement of the vaults at the cross-section with the piers.

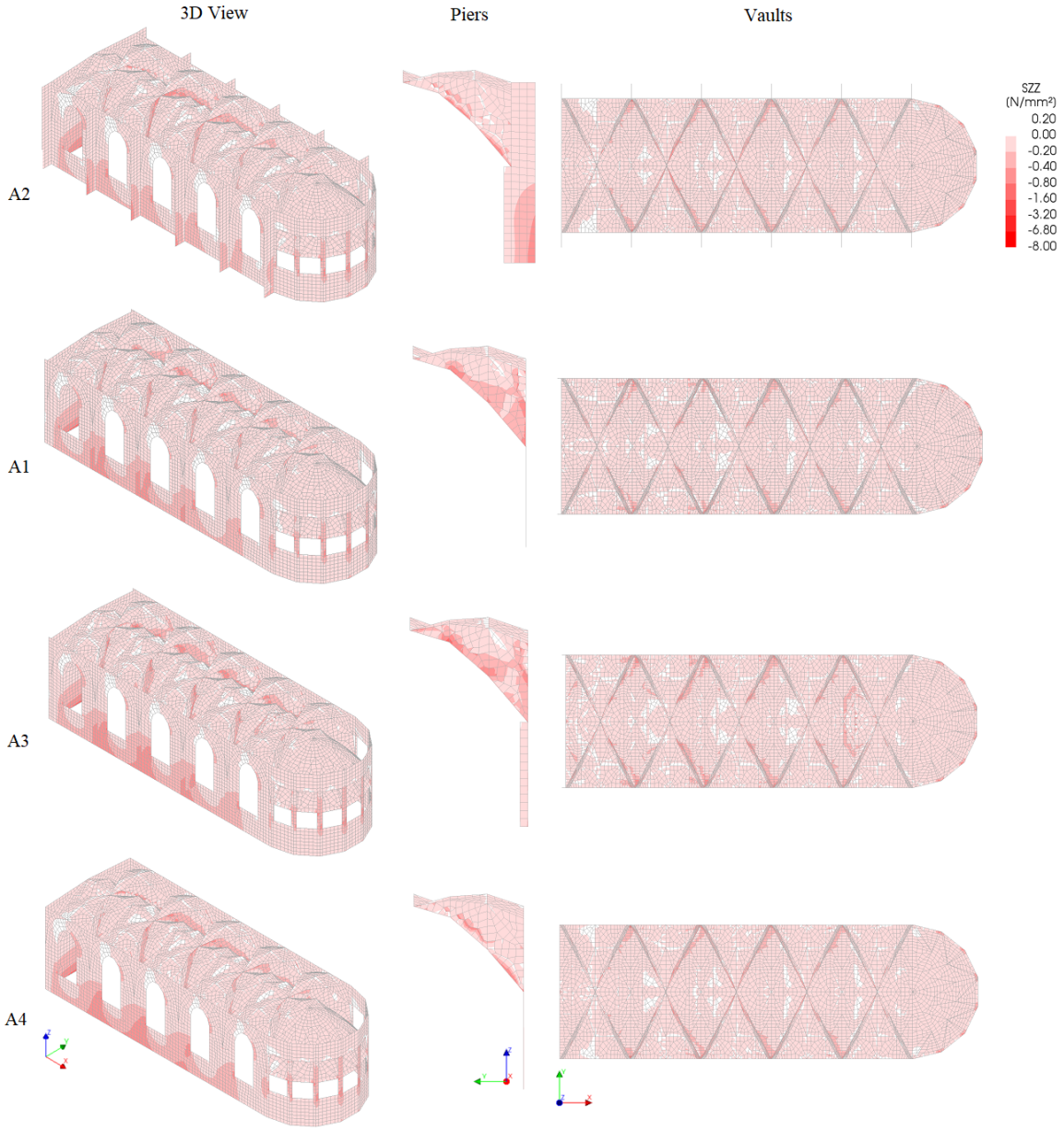

Figure 7.14: Compressive stresses for the church due to the pushover loading, [scale factor=0.05]

Figure 7.14 presents the stress concentrations on the church models. As can be seen the results are symmetric for all models. Model A2 shows a concentration of stresses at the outer corner of the piers which is not possible to see for the other models due to their modelling approach. For the vaults an almost identical pattern is observed.

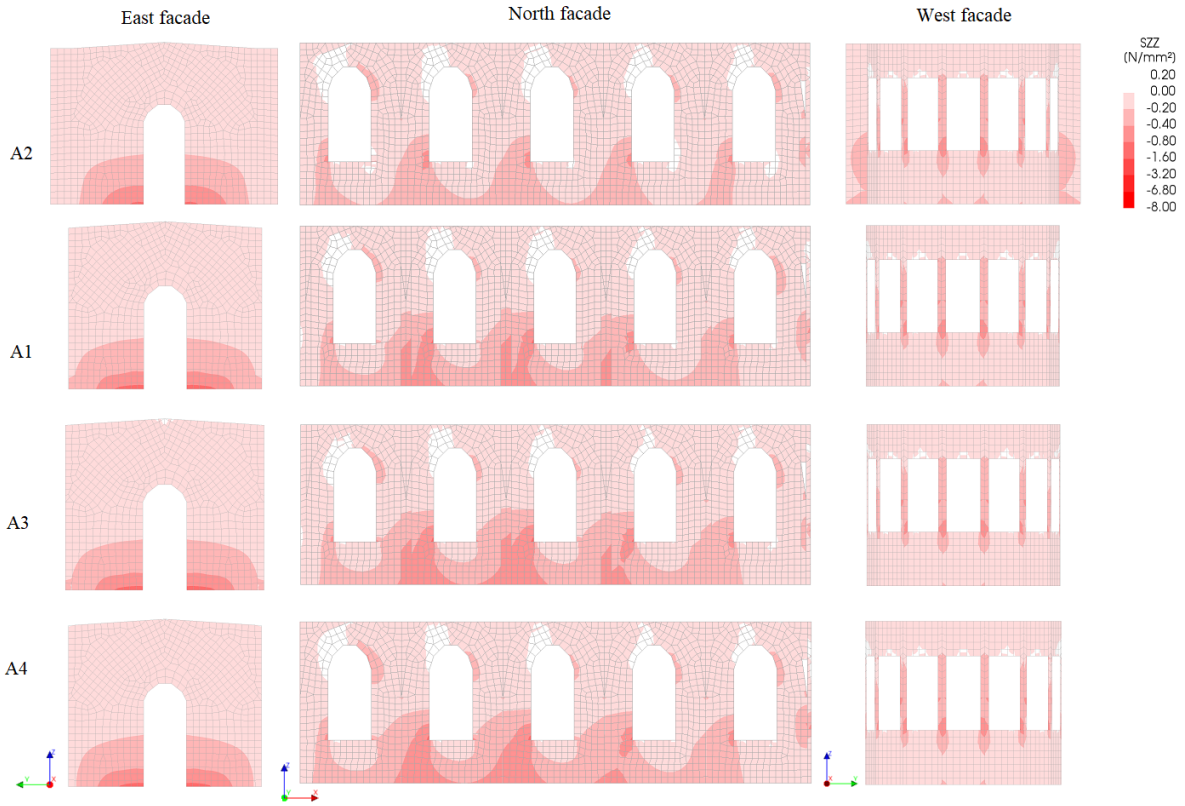

Figure 7.15: Compressive stresses for the church due to the pushover loading, [scale factor=0.05]

Figure 7.15 presents the stress concentrations for the East, North and West facade. For the East facade it can be observed that for Model A2 and A4 the stresses are not spread up to the interface of the pier-to-wall connection, whereas this is the case for model A1 and A4. When looking at the North facade note that model A1, A3 and A4 closely resemble one and other. As a higher stress concentration is observed near the base of the piers. As these models have less or no transverse pier elements, the stresses lump up in the in-plane direction. Lastly, for the curved facade no particular differences in stress concentrations are found.

7.4. Crack pattern evolution

Figure 7.16, 7.17 and 7.18 show the crack patterns for all four church models. As can be observed all four models show a symmetric crack pattern. However, when zooming into the piers the distribution of the crack patterns are different. cracks in the vaults appear for models A1, A3 and A4 in the outer edge of the vaults where as for model A2 cracks appear in the cross-edges of the vaults too. As for the North facade note that for model A4 the highest crack distribution is found and for model A2 the lowest amount of cracks are found. Most of the cracks in all models remain under 2.50mm. Whereas for the vaults cracks up to 5.00mm are found. As a consequence of a difference in movement of the piers out of the plane of the North facade, note when looking at the top view of the vaults that the crack patterns differ.

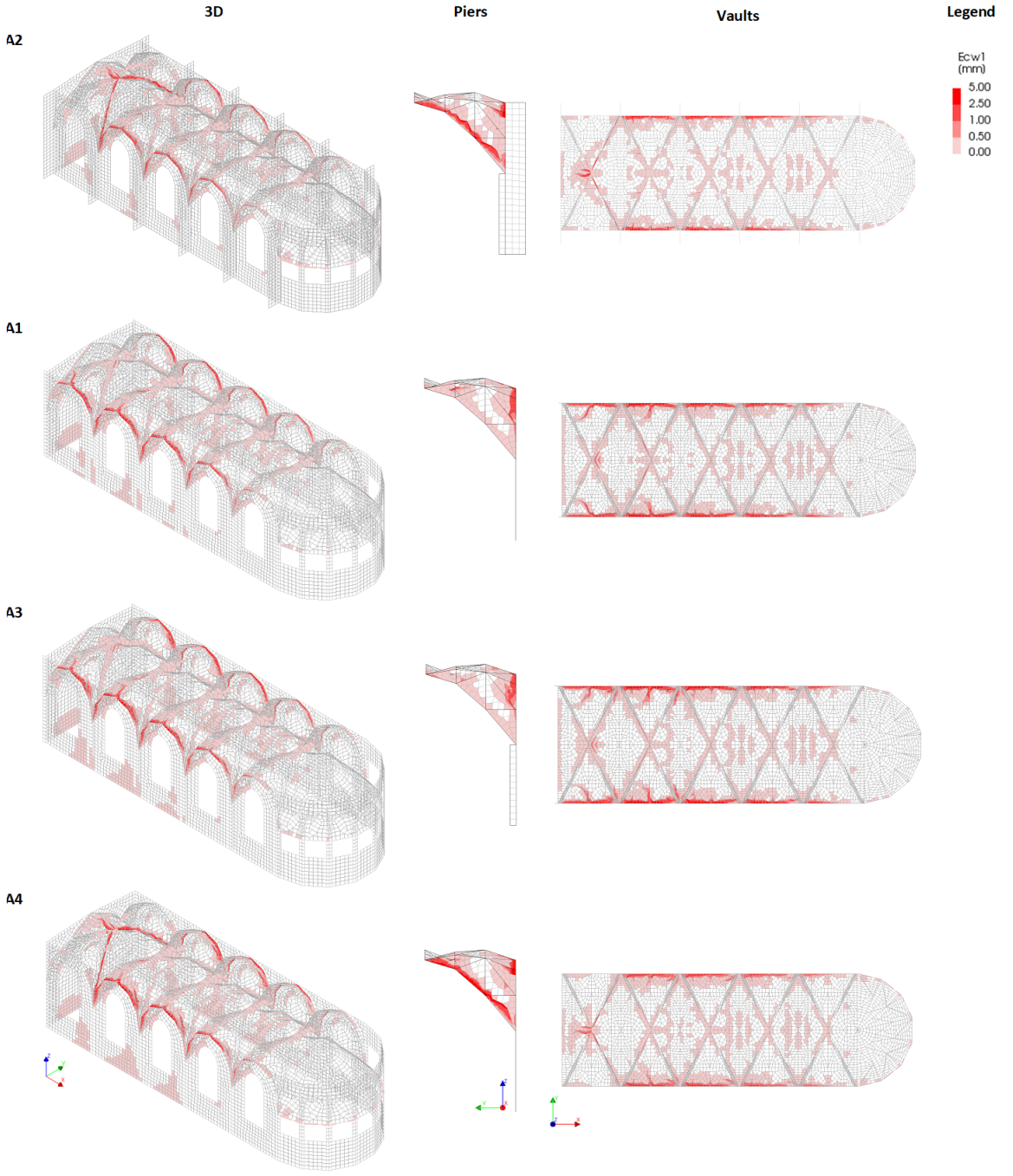

Figure 7.16: Crack Patterns church due to pushover loading the church models and details the piers, [scale factor=0.05]

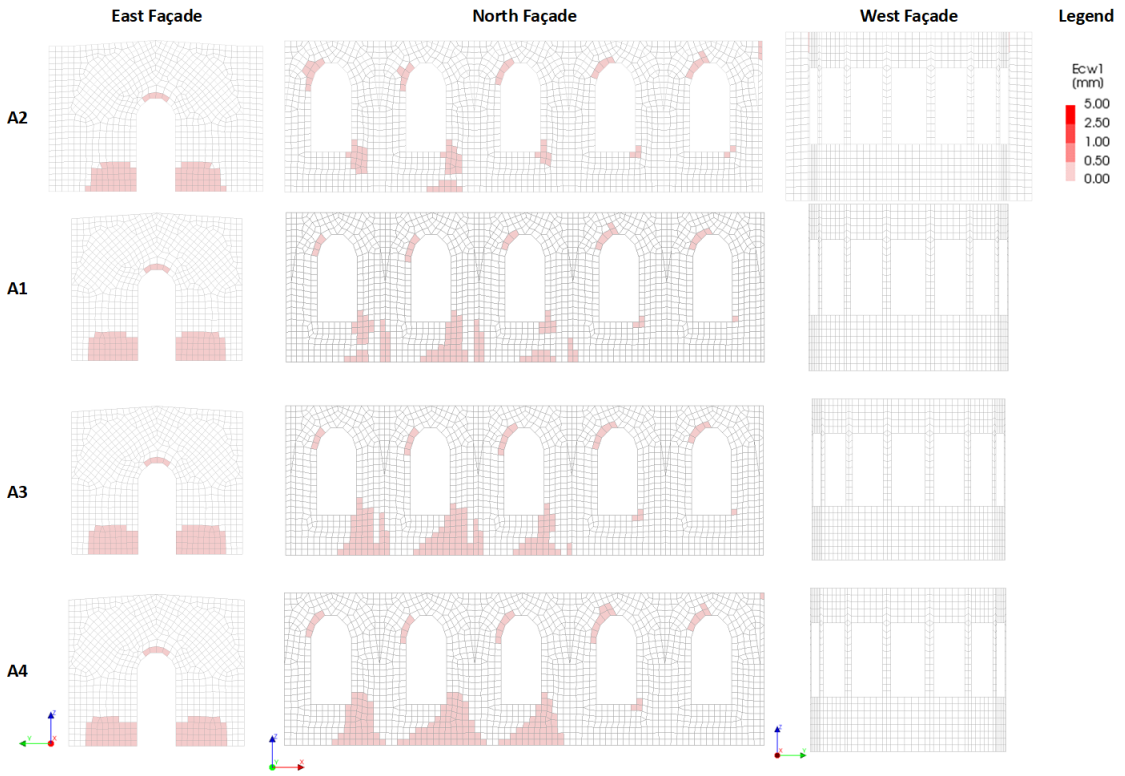

Figure 7.17: Crack Patterns church due to pushover loading the church models and details the piers, [scale factor=0.05]

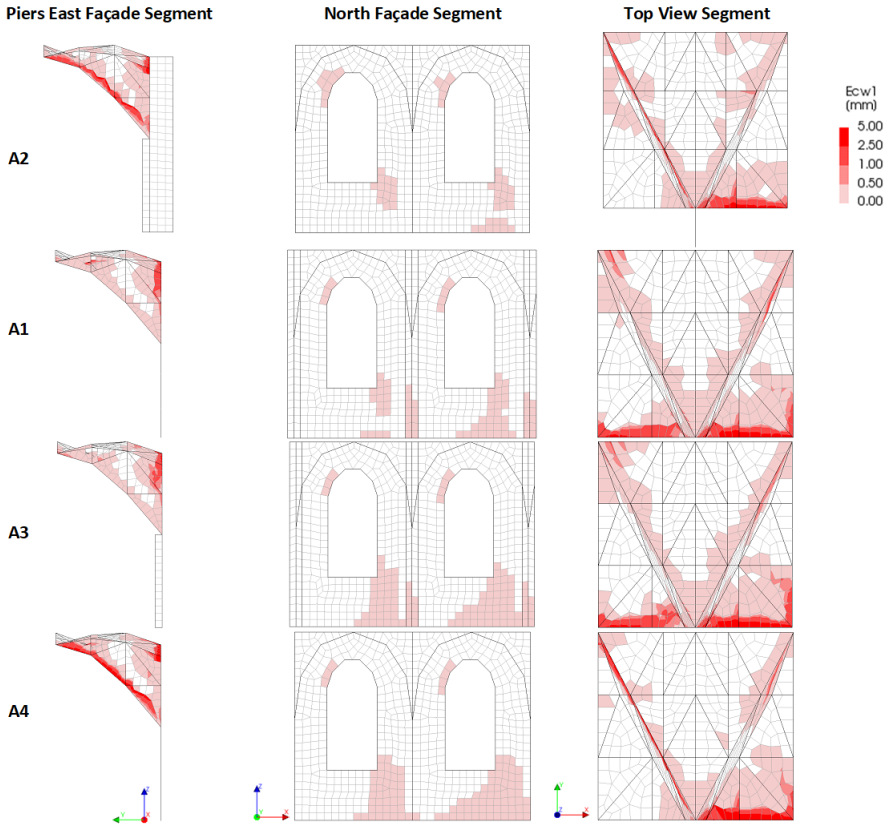

Figure 7.18: Crack Patterns church due to pushover loading the church models and details the piers, [scale factor=0.05]

7.5. Conclusions

In this chapter four models with different pier-to-wall configurations were presented. Among the various unknown connections it was chosen to study the modelling assumptions regarding the piers and their influence on the global behaviour. Within the scope of these thesis the study was limited to four configurations, however a wide variety of configurations can still be studied.

Prior to presentation of the results obtained for the four configurations, the local behaviour of model A2 was presented. This model was presented and studied in chapter 6. For the results of the local behaviour of the piers in model A2, it can be concluded that no limit stresses in compression and tension were not exceeded during the analysis. Therefore, no cracking or crushing was observed. The stress concentrations observed where in the compressive zone and it is assumed that if the church can be further pushed that possible cracks due to crushing can appear in the piers. Moreover, the stresses and strains in the compressive and tensile zone at the interface of the piers with the walls were plotted. These plots also confirm that the limit stresses are not yet exceeded in the interface of the pier-to-wall configuration.

This chapter starts with a presentation of the contour plots for the displacements of the four pier-to-wall configurations. For models that were introduced were the church model as built in 1230 referred to as A2 and its three variations mentioned as A1, A3 and A4, respectively. The results for the pre-compression stage show not a significant difference between the models. A symmetric displacement pattern was observed. Also, during the pushover loading a symmetric load pattern was observed. However, for all models at the final stage of the pushover analysis a different curvature of the North and South facade was observed. In particular, it can be seen how the displacement pattern of A1 resembles that of A3 and how the displacement pattern of A2 resembles that of A4. At the end of the pushover analysis all piers are curved outwards at the top, however, the values are different for all models. Model A2, in particular seems to have stiffening effect and does not move as much at the top main walls as the other models.

In the next section, the results of the NLPO Analyses of the four pier-to-wall configurations were presented. The results of the capacity curves show how model A2 in comparison to model A1, A3 and A4 has a higher force capacity than the other models. For all other important characteristics such as initial stiffness or ultimate displacement the model does not present differences. A possible reason for the observed deviation in the results of model A2, could be that as the piers are modelled with more surface (although the geometric properties of the piers in all models are similar), that a different continuum crack pattern can occur. That in combination with the use of integration points in the thickness direction of the elements could result in a higher force capacity. Furthermore, model A1 and model A3 showed similar results, as expected. Since the models closely resemble one and other. The addition the piers in model A3 seemed to have minimal effect on the results. Lastly, model A4 showed a close resemblance with model A2 in contour plots and crack patterns. However, as the piers in model A4 were model with linear elastic properties no redistribution of stresses was possible as in model A2.
As for the crack patterns. A higher crack distribution was observed for model A4, followed by model A3, A1 and then model A2. All models show the development of cracks in the same areas. Particular areas where cracks occur are in the spandrales under the window, in the vaults, front part of the dome and at the East facade at the base near the door opening. Type of cracks that are observed are diagonal cracks.

8

Sensitivity study on model uncertainties

In this chapter the focus is orientated on different numerical algorithms that could help to capture the post-peak behaviour of the structure. As it is explained in chapter 6, section 6.3, using the Newton-Raphson method alone we were not able to capture the post-peak behavior in the simulations. To solve the convergence problem it has been decided to perform the simulations with other algorithms. Herein we employed two different algorithms: Newton-Raphson method combining with arc length method and Quasi-secant method. Moreover, other uncertainties, such as the influence of poor material properties, the influence of linear elastic vaults and the influence of using the Total Strain Crack material model instead of the Engineering Masonry Model are discussed in this chapter.

8.1. Influence of numerical analyses procedures

The results for all these three methods to solve the nonlinear system of equations (Newton-Raphson, Newton-Raphson + Arc length method and Quasi-secant algorithm) for four reference points (point A, B, C and D in Figure 7.9) are presented in Figure 8.1.

As it is shown in Figure 8.1, the combination of Newton-Raphson and arc length methods were not able to capture the post peak curves. In fact the simulations using the Newton-Raphson and arc length method failed at about the same load step as that the previous simulations where only the Newton-Raphson method was used. On the other hand, with the Quasi- secant algorithm we are able to capture the post peak responses up to almost 10 times more than the value of the peak load displacement. The secant method can be interpreted as a method in which the derivative is replaced by an approximation and is thus a Quasi-Newton method.

Generally the Newton-Raphson method converges faster (with an order 2 against 1.6) in comparison with the secant method. However, the secant method may occasionally be faster in practice. As the Newton-Raphson algorithm requires the evaluation of both f (convergence function in the system of equations) and its derivative f' at every step, while the secant method only needs the calculation of f. If we assume that evaluating f takes as much time as evaluating its derivative and we neglect all other costs, we can do two steps of the secant method for the same cost as one step of Newton method, so the secant method is faster. If, however, we consider parallel processing for the evaluation of the derivative, Newton's method proves its worth, being faster in time, though still spending more steps. However in our simulation in this chapter we did not see a significant differences between the speed of these both algorithms. As it is mentioned above, the Quasi-secant algorithm were able to capture the structural behavior beyond the peak load and this means that the cracks and damage have more time to propagate and we can have a better understanding of the structural behaviour in larger displacements. The contour plots for the displacements and the crack propagation for the simulation with church model as built in 1230 using the Quasi-secant method are shown in Figure 8.2.

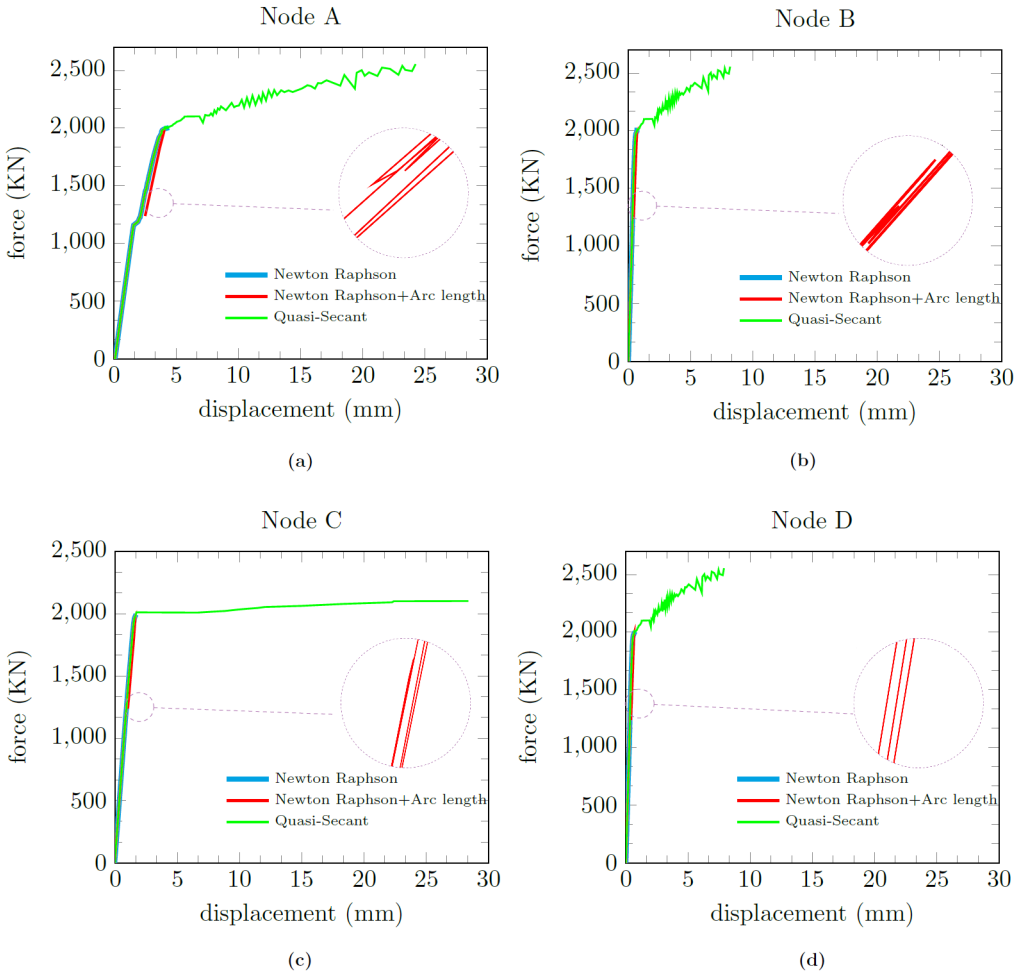

Figure 8.1: Influence of numerical analyses procedures; capacity Curves for Nodes: (a) A, (b) B, (c) C and (d) D

Comparing Figure 8.2 with Figures 6.9 and 6.16 in chapter 6, where church model as built in 1230 was presented and the Newton-Raphson method was used, by using the Quasi-Secant method we can have a better knowledge of the material response under the loading. As it is illustrated now the cracks have more time to propagate through the structure and also displacements can be transferred to the curved facade of the structure as it is shown in Figure 8.2. As can be seen, we can observe the formation of cracks in the curved facade and an increase of the existing cracks.

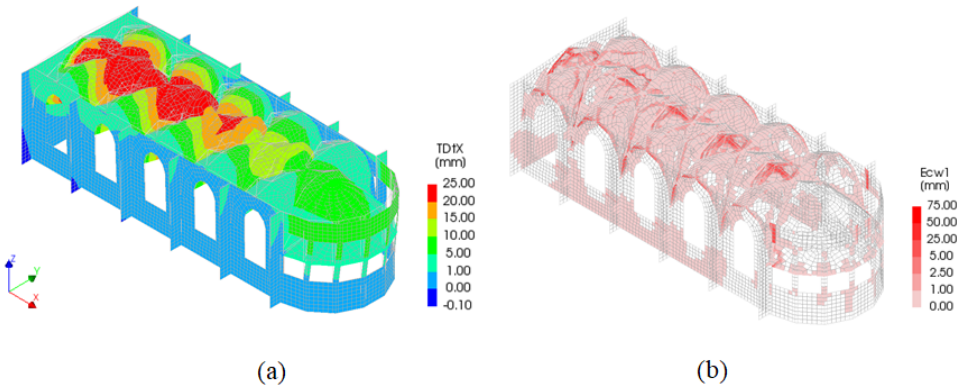

Figure 8.2: (a) Displacement contour and (b) crack pattern for the Quasi-Secant method. At a base shear force of 2503kN and a displacement of 6.6mm for the longitudinal facades [scale factor=0.05]

For all above mentioned reasons we decided to choose the Quasi-secant algorithm as the method to study the post-peak regime in FE simulation and investigate the effect of material properties on the overall structural behavior in the next section. In the following section a sensitivity study on the material properties and its effect on the structural response of the structure is studied. The use of poor material properties and the use of linear material properties for only the vaults for church model as built in 1230 is studied and the results are compared with the the existing church model as built in 1230 as presented in chapter 6.

8.2. Influence material properties

An important unknown in the presented models are the material properties. As the church is 800 years old, the current assumptions regarding the material properties may be not accurate. Therefore, in this section the influence of poor material properties are studied. However, please note, up to this point no research has been carried out on the real material properties of the church. The aim of this sensitivity study is then, to test the influence of the of poor material properties on the global behaviour of the church.

8.2.1. Poor material properties

Table 8.1 presents the properties of the standard material properties as has been used for all studies up to this point and the poor material properties as used in the sensitivity analysis in this section. Main difference between the so-called poor and standard material properties is a reduction in all parameters of the material properties. As can be seen in table 8.1 the poor material properties are half of the values of the standard material properties. Once, real material properties are available, it is advisable to carry out these analyses once more to review the results.

Property	***Parameter***	***Symbol***	***Unit***	***Value Standard***	***Value Poor***
	Young's Modulus X	E_{xx}	MPa	2900	1450
	Young's Modulus Y	E_{yy}	MPa	4000	2000
	Shear Modulus	G_{xy}	MPa	1800	900
	Density	ρ	kg/m3	1600	1600
Cracking	Tensile strength	f_{tx}	MPa	0.30	0.15
		f_{ty}	MPa	0.10	0.05
	Tensile fracture energy	G_{ft}	N/mm	0.01	0.0025
	Diagonal crack orientation	α	rad	0.5	0.5
Crushing	Compressive strength	f_c	MPa	8.0	4.0
	Compressive fracture energy	G_c	N/mm	20	10
Sliding	Cohesion	c	MPa	0.15	0.075
	Shear fracture energy	G_{fs}	N/mm	0.10	0.025
	Friction angle	ϕ	rad	0.61	0.5

Table 8.1: Material properties, standard versus poor

A comparison of the results of poor versus standard material properties for node A,B,C,D are presented in Figure 8.3. As can be seen from the results, due to the poor material properties a significant difference is found for all important characteristics of the capacity curves. Characteristics such as initial stiffness and maximum force capacity. Again as in the case for the results of the model with standard material properties no softening behaviour has been captured. The ultimate force reached for the poor material property model is $1002kN$. This is exactly half of the force capacity found for the model with standard material properties. And the initial stiffness of the poor material model is lower as expected.

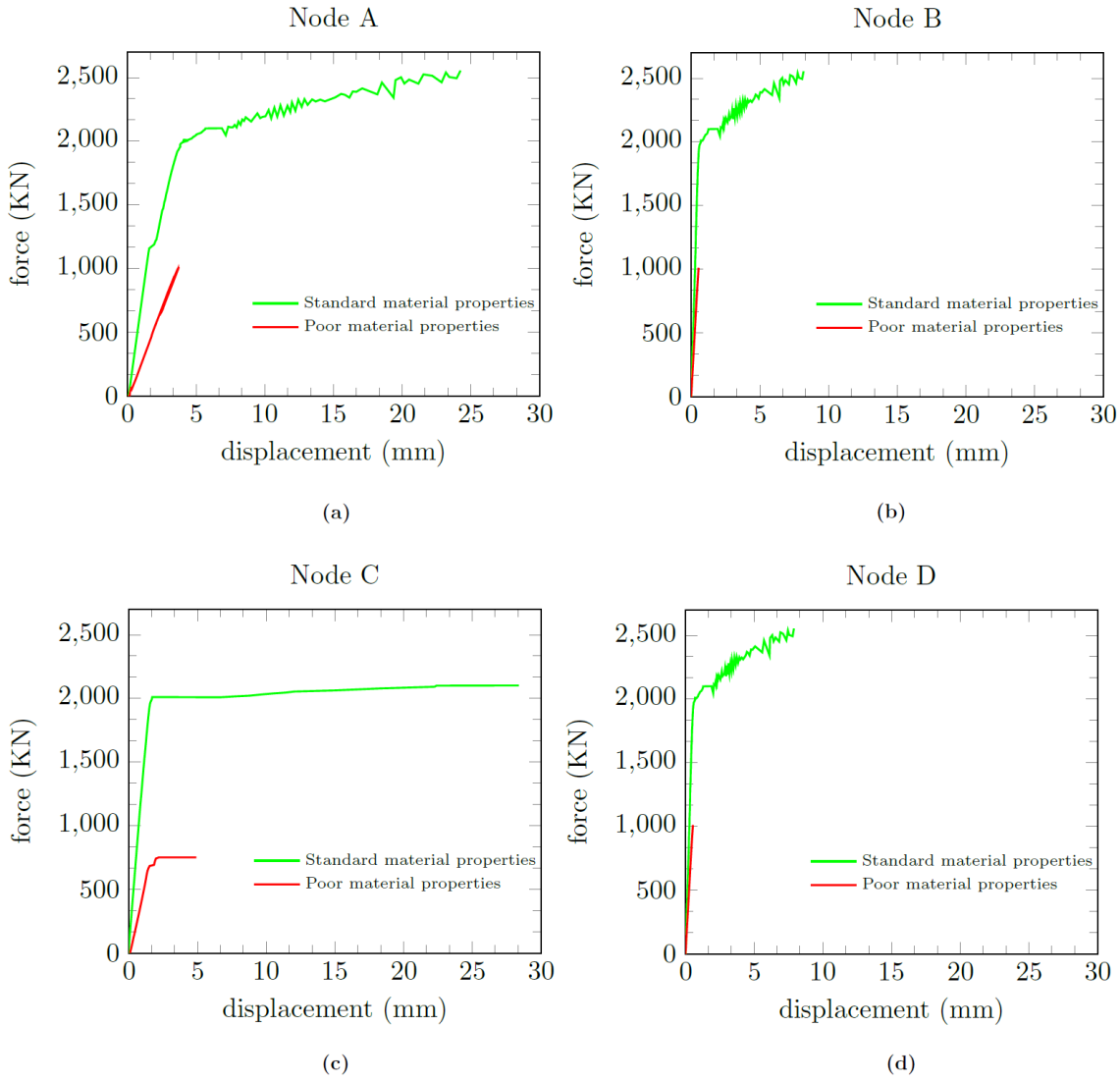

Figure 8.3: Comparison of poor versus standard material properties; capacity Curves for Nodes: (a) A, (b) B, (c) C and (d) D

The contour plots of the displacements and crack propagation for the simulation with church model as built in 1230 using the poor material model are shown in Figure 8.4 and 8.5. At a base shear force of 2503kN. For the results of the displacement at the same load step a slightly different displacement pattern is observed as for the model with standard material properties. An outward curvature of the top of the main walls is observed for the model with poor material properties in contrast with the model with standard material properties. As for the crack pattern more cracks are observed for the entire structure in general in comparison to the model with standard material properties. The cracks in the vaults propagated further to the in the direction of the curved West facade.

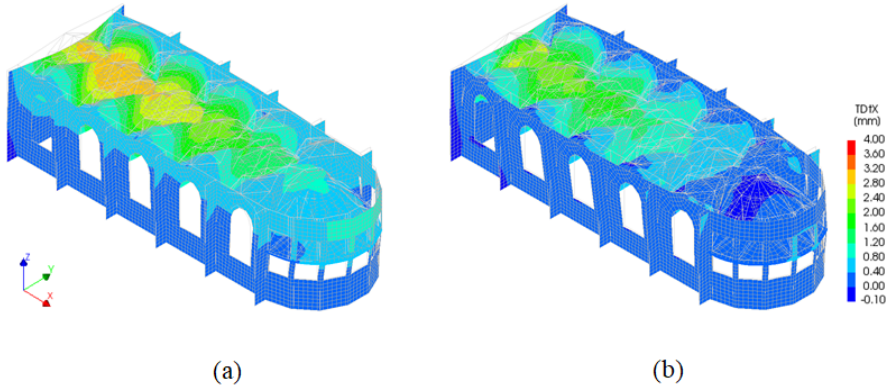

(a) (b)

Figure 8.4: Displacement Contour for the (a) Standard and (b) Poor Material Model at the same load step, [scale factor=0.05]

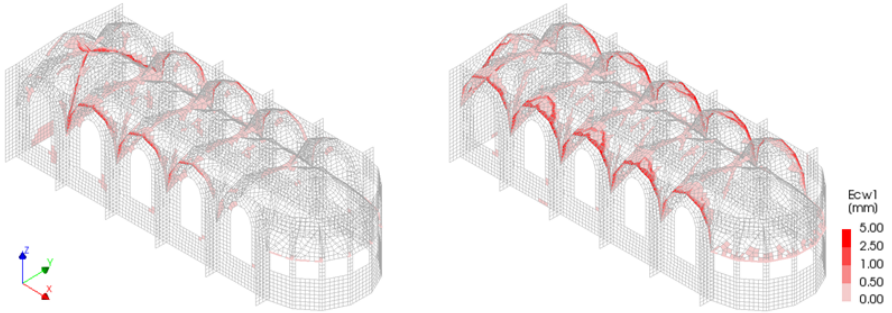

(a) (b)

Figure 8.5: Crack patterns for the (a) Standard and (b) Poor Material Model at the same load step, [scale factor=0.05]

8.2.2. Linear material properties for the vaults

So far from the observations of the results of all presented studies it can be concluded that the behaviour of the vault system, with its particular shape, has an significant influence on the global behaviour of the church structure. The aim of the sensitivity studies in this chapter is partly to capture the post-peak behaviour. It is therefore interesting to see how significant the influence of the vault system is for the global behaviour of the structure. It may be possible to capture the post-peak behaviour of the church in case the vault structure is not considered with nonlinear material properties. The results of the analysis are presented for node A,B,C and D again. A comparison of the results of partially linear elastic model versus the fully nonlinear model for node A,B,C,D are depicted in Figure 8.6.

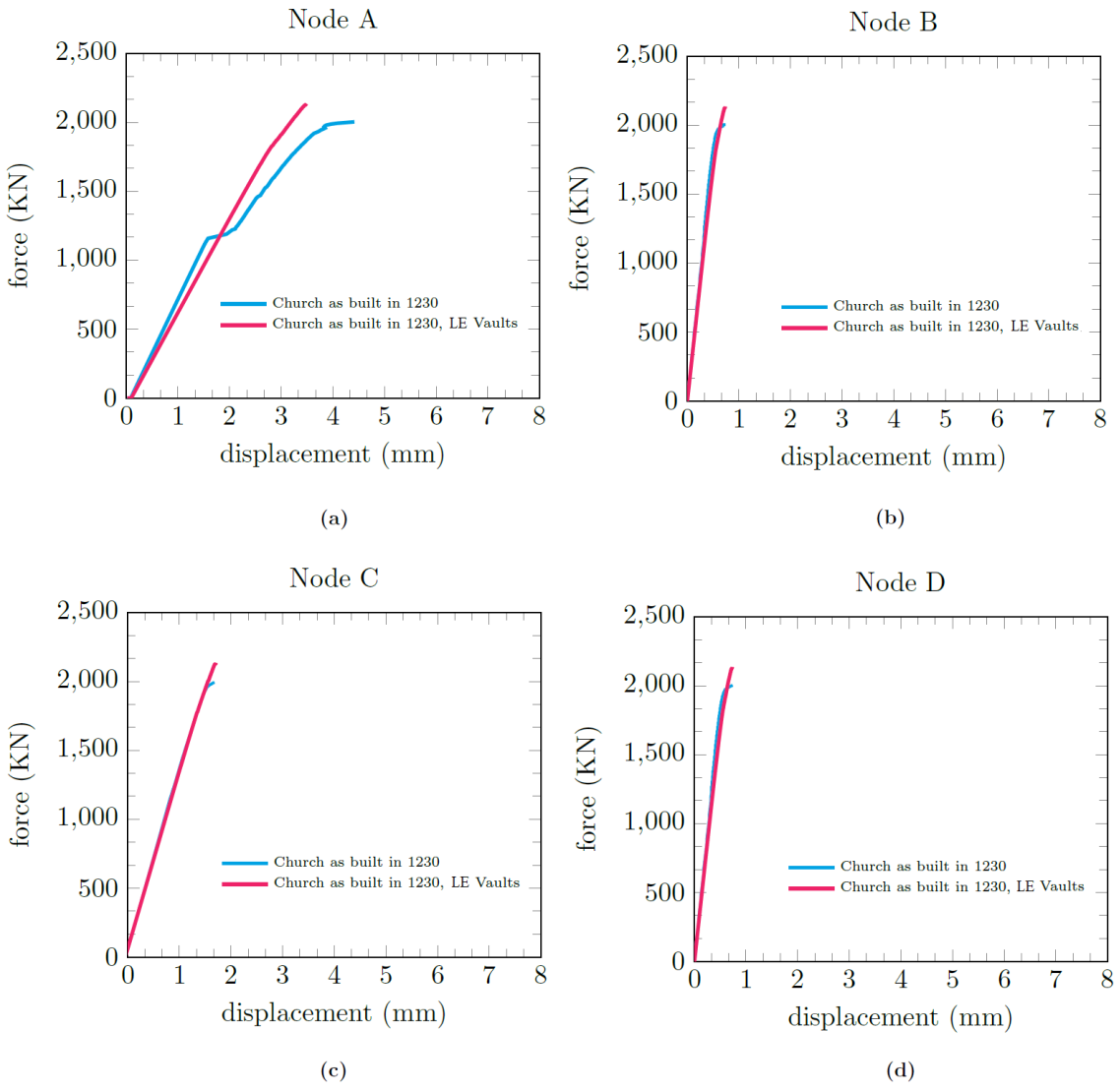

Figure 8.6: Partially linear elastic model versus the fully nonlinear model; capacity Curves for Nodes: (a) A, (b) B, (c) C and (d) D

As can be seen from the results, due to the linear elastic material properties for the vaults a significant difference is found for all important characteristics (such as initial stiffness and maximum force capacity) of the capacity curves. For the model with linear elastic vaults in comparison with the model with nonlinear vaults it can be observed that the peak load is much higher, the initial stiffness of the structure is significantly higher, and a higher displacement is reached. In addition, no softening is observed for the model as the post-peak is not captured. The contour plots of the displacements and crack propagation for both simulations (model with linear elastic vaults and the model with nonlinear vaults) are shown in Figure 8.7 and 8.8, at a base shear force of 1726kN.

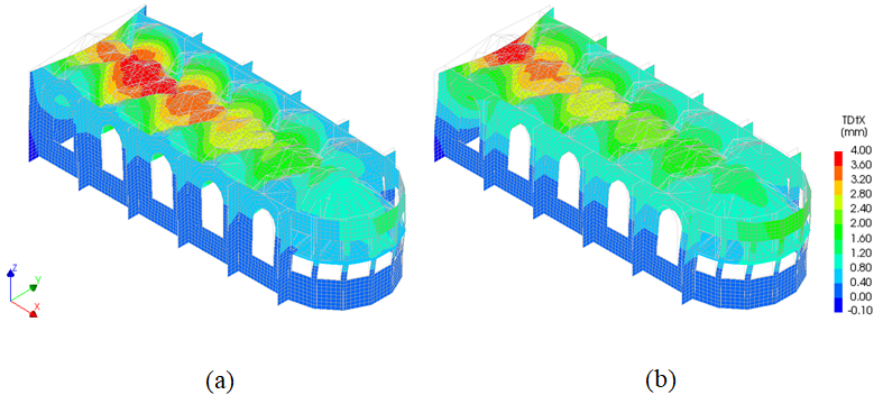

(a) (b)

Figure 8.7: Displacement contour for the (a) Nonlinear and (b) Linear material model for the vaults at the same load step, [scale factor=0.05]

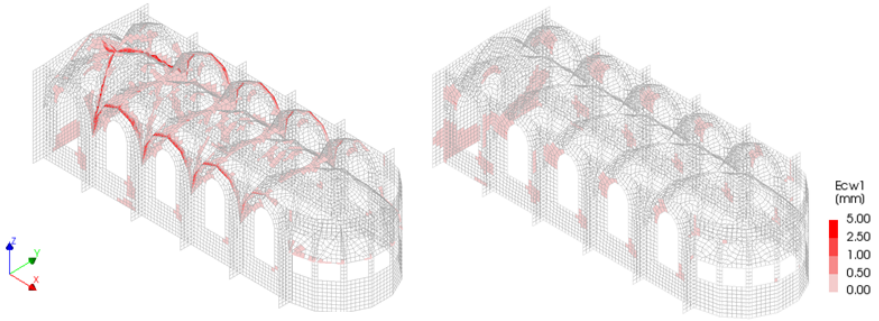

(a) (b)

Figure 8.8: Crack patterns for the (a) Nonlinear and (b) Linear material model for the vaults at the same load step, [scale factor=0.05]

As for displacement contour plots it can be seen that a similar symmetric pattern is found. But in the model with linear elastic vaults a greater inward curvature of the top of the main walls is observed. For the model with nonlinear vaults a inward displacement of 1.02mm is observed, whereas for the model with linear vaults a inward displacement of 1.40mm is observed. For the crack patterns of the walls a similar pattern is observed. However, due to the fact that no cracking occurs in the vaults and due to the higher displacement of parts of the vaults close to the main walls more cracks are observed in the walls for the model where the vault system is considered as linear elastic. Also, it should be noted that the cracks in the East facade near the door opening spread more compared to the model with nonlinear material properties.

8.3. Influence constitutive model

Various constitutive models can be used to simulate the behaviour of quasi-brittle material, such as masonry. DIANA 10.3 provides two constitutive models that can be used. Namely, the Engineering Masonry Model and the Total Strain Crack Model. The Engineering Masonry has been developed in 2016 by DIANA FEA BV in a joint project with professor J. G. Rots of Delft University of Technology. The Engineering Masonry model is a smeared failure model and can be applied in combination with regular plane stress (membrane) and curved shell elements for modelling failure of masonry walls. The engineering masonry in comparison to the Total Strain crack models has some advantages and benefits to the results. As the Total Strain crack models are based on secant unloading and reloading, they underestimate the energy absorption under cyclic loading in the masonry. The Engineering Masonry model, however, describes the unloading behaviour more realistically by strong stress decay with the original linear stiffness. In addition a shear failure mechanism based on the standard Coulomb friction failure criterion is included in the model. In this section a sensitivity analysis has been conducted on the use of the above mentioned constitutive models. Results obtained for both models are presented and compared for node A,B,C and D. A comparison of the results of Total Strain Crack Model versus the Engineering Masonry Model for node A,B,C,D are presented in Figure 8.9.

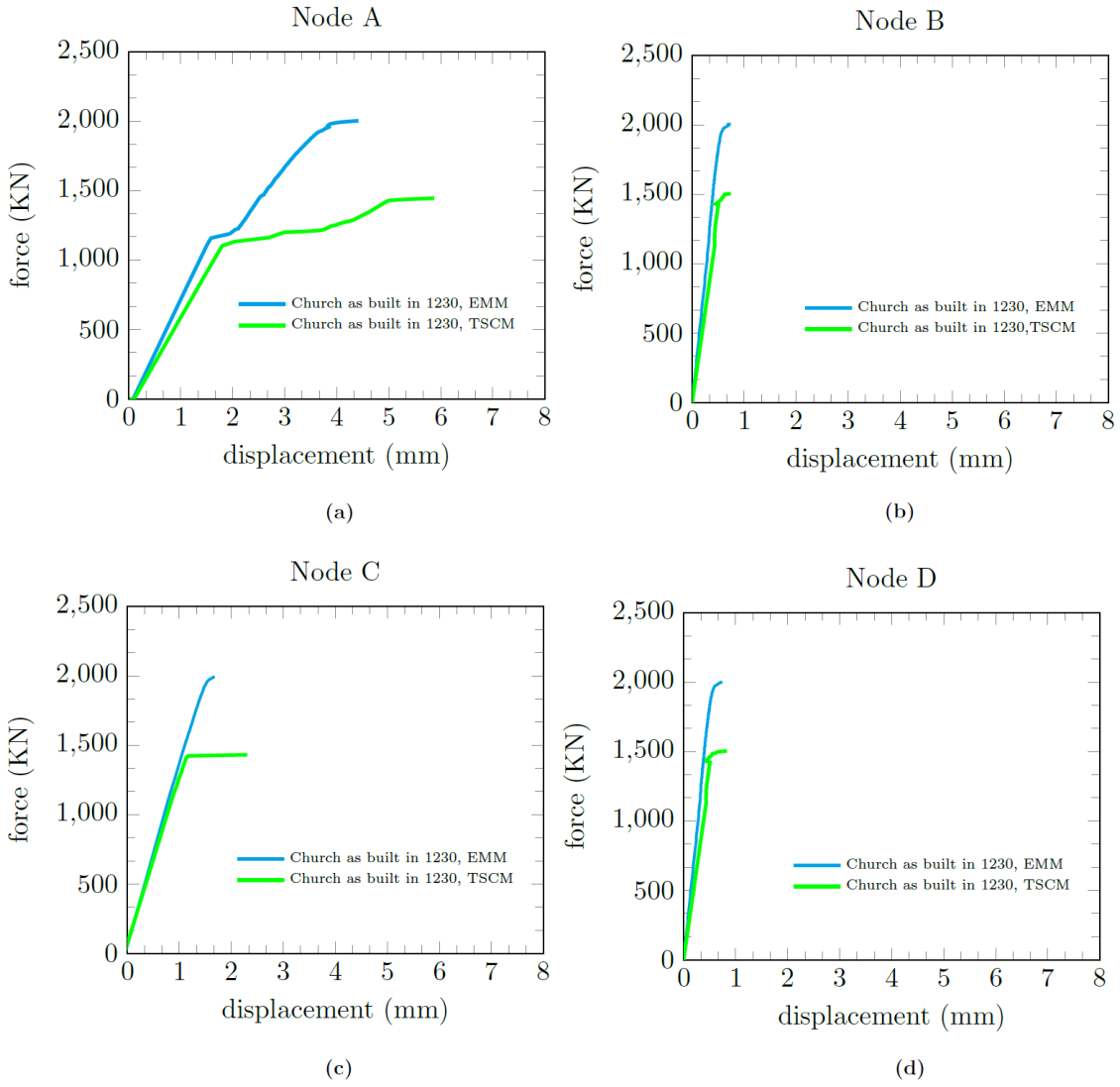

Figure 8.9: Total Strain Crack Model versus the Engineering Masonry Model; capacity curves for Nodes: (a) A, (b) B, (c) C and (d) D

As it is shown, a significant difference is found for all important characteristics like the initial stiffness

and maximum force capacity of the capacity curves. Results obtained for the Total Strain crack model show a maximum force capacity of 1500 kN in comparison to the Engineering Masonry model where 2004 kN was found. As for the initial stiffness it can be observed that the Total Strain Crack model has a lower initial stiffness. Furthermore, in this model no softening behaviour is observed. The contour plots of the displacements and crack propagation are presented in Figure 8.10 and 8.11. At a base shear force of 1726kN.

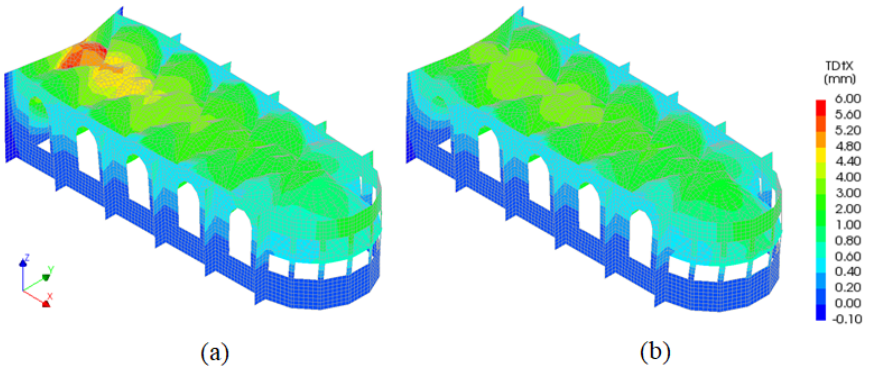

Figure 8.10: Displacement contour for the (a) Total Strain Crack Model and (b) the Engineering Masonry Model, [scale factor=0.05]

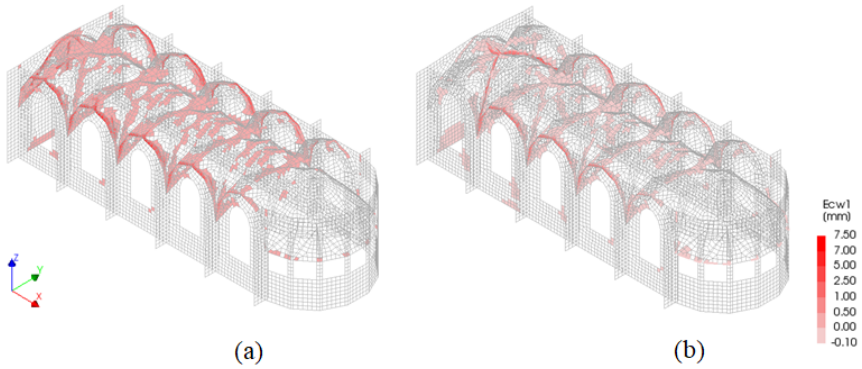

Figure 8.11: Crack pattern for the (a) Total Strain Crack Model and (b) the Engineering Masonry Model, [scale factor=0.05]

As for displacement contour plots it can be seen that a similar symmetric pattern and similar values are found. However, with the Total Strain Crack Model a higher maximum displacement is reached. For the model with the Total Strain Crack Model a maximum displacement at the east facade is reached with a value of 6mm. Where as for the model with the Engineering Masonry Model a maximum displacement of 4mm is reached. When reviewing the results for the crack patterns of both models, it can be concluded that a similar crack pattern is found. As the Total Strain Crack Model Reaches a higher displacement more cracks did develop up to this point.

8.4. Conclusions

In this chapter four sensitivity studies on church model as built in 1230 were presented. In the first section the effect of different numerical analysis procedures were discussed. Namely the Regular Newton-Raphson method in combination with the arc length method and the Regular Newton-Raphson method in combinations with the Quasi-Secant Method. The analysis procedures where tested in order to capture the post-peak behaviour of the church as this was not possible with the Regular Newton-Raphson method previously. The analysis conducted with the Arc-length method did not provide useful results, as the numerical solver could not find a proper equilibrium path in this particular case. The analysis kept on oscillating around its starting point. On the other hand the Quasi-Secant method did provide useful results for the post-peak stage. A ten times higher displacement was found. However, it should be highlighted that this method is significantly less accurate than the Regular Newton-Raphson method and that the results are merrily an approximation.

Other suggestions for trying to obtain the post-peak stage would be to use the Regular Newton-Raphson method with a much finer mesh than 300 mm as presented in the models of this treatise or to employ the Secant-Linear Analysis method. In the second section the influence of poor material properties for the masonry and the influence of the use of linear elastic properties for the vaults were studied. The first study was conducted to gain insight in the global behaviour of the church in a case degradation of the existing masonry was taken into account. Note that the real material properties of the church are not available and that the material properties used in this treatise are chosen based on the provided information in the NPR 9998 [14]. The second study in this section was conducted with the aim to study the influence of the vaults system on the global capacity in case its nonlinear properties were neglected. As the vaults have a very particular shape, its numerical behaviour may influence the results of the analysis significantly. In this study we could observe how the remaining structure behaves in case the vaults were not considered in the nonlinear regime. We have seen that the a higher force capacity was reached in comparison with the model were the vaults were considered with nonlinear material properties. Moreover, we have seen how the crack patterns of the walls changed. More cracks were observed in the walls as no cracking was possible in the vaults.

In the third and last section of this chapter the effect of the use of the Total Strain Crack model instead of the Engineering Masonry Model on the behaviour of the church was studied. The results for the Total Strain Crack model showed a lower force capacity and initial stiffness in comparison to the engineering masonry model. And again no softening behaviour was captured. As for the displacement pattern, for the Total Strain Crack model a higher displacement was captured around than for the Engineering masonry. Lastly, for the crack pattern no difference was observed in the location and type of cracks occurring in the structure.

9

Results numerical analysis - Church post structural modifications 1931

Technical details regarding the church were discussed in chapter 5. This chapter starts with a presentation of the behaviour of the church as built in 1230 versus the church post structural modifications in 1931, under static load conditions, presents the results of the modal eigenvalue analysis and ends with a presentation of the results of the NLPO analysis. Furthermore, a section is devoted to the presentation and discussion of the importance of the numerical modelling strategy for the piers. The numerical models of the church used for the analysis in this chapter is presented in Figure 9.1.

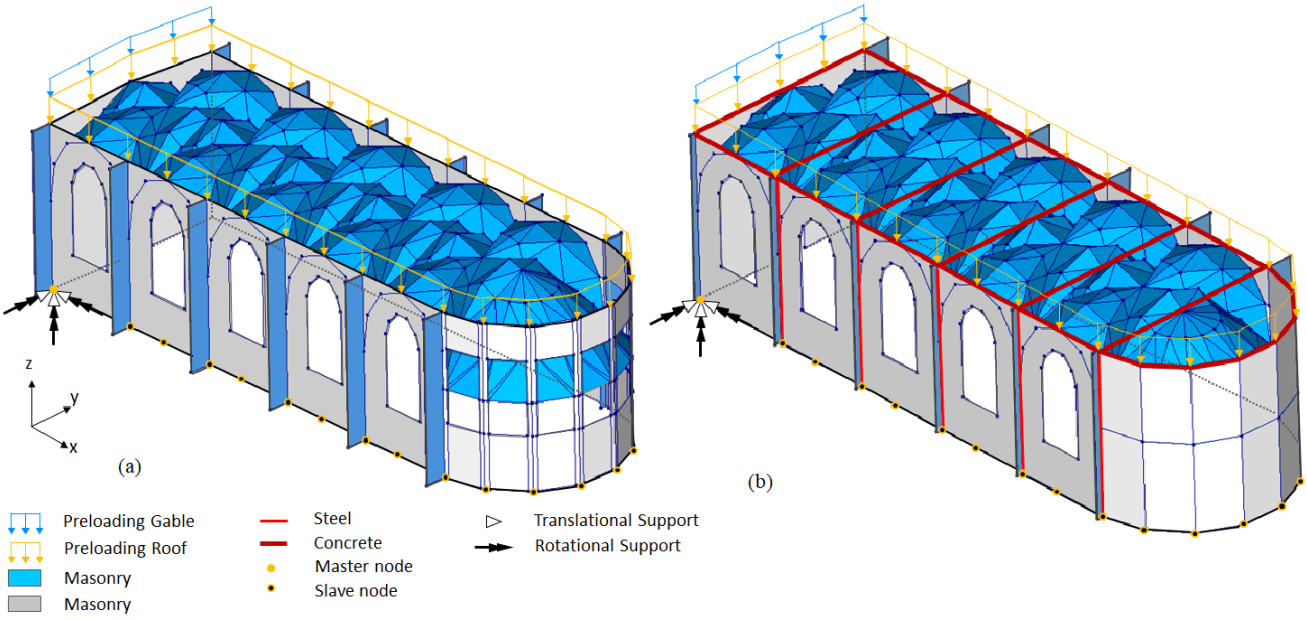

Figure 9.1: Numerical model representation of the church post structural modifications in 1931

9.1. Eigenvalue analysis

Prior to any analysis, a model eigenvalue analysis is conducted. The results of the church models are added to Figure 9.2 and 9.3. As can be observed in the global X-direction mode 7 is governing with a total mass participation of 61% for the church post structural modifications and mode 2 with a mass participation of 49.8% for the church as built in 1230. In the global Y-direction for the church post structural modifications, a mass participation of 65.8% is reached, where as for church as built in 1230 just 43.9% was reached.

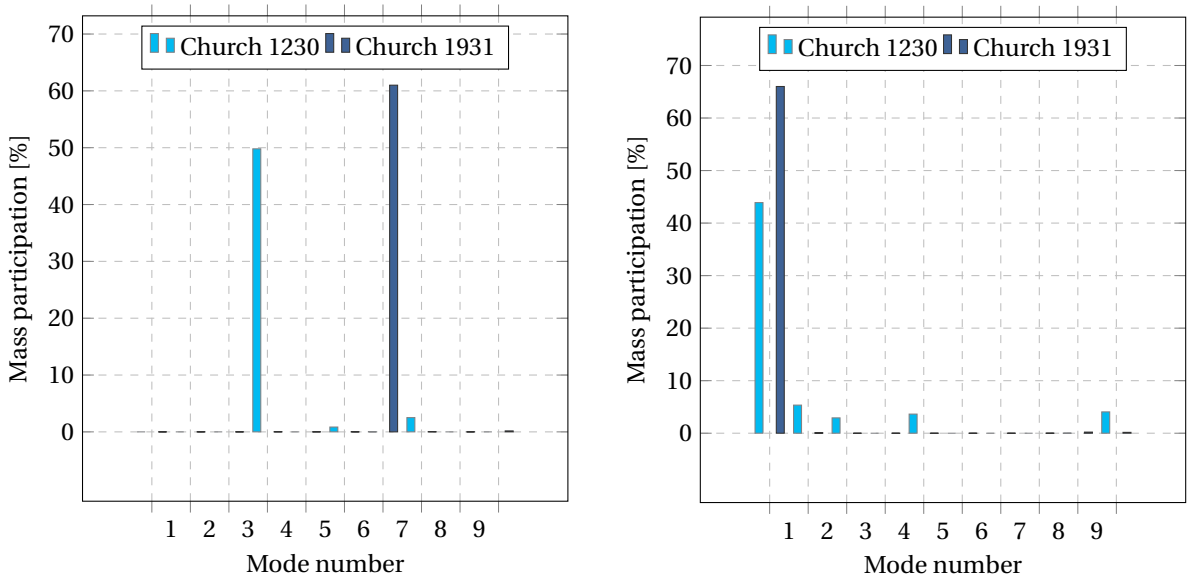

Figure 9.2: Results Modal Analysis for church as built in 1230 and the church post structural modifications in 1931

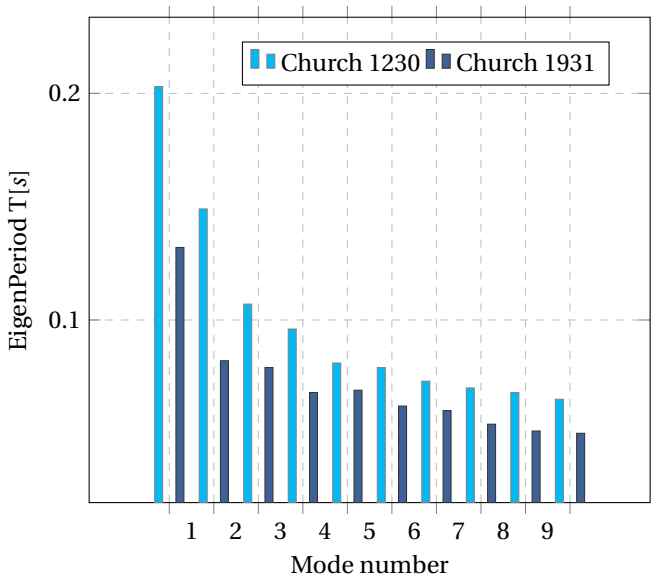

Figure 9.3: Main frequencies for the first 10 modes of the two church models.

Governing Eigenmodes Global X-direction

The governing eigenmodes and modal shapes of the structure prior and post modifications for the global X-direction are presented in Figure 9.4. As can be seen after the structural modifications the governing mode shape did certainly not change and is still a typical out-of-plane mode. The natural period is still equal to 0.10s, whereas the modal mass participation is shifted from a value of 49.8% to a value of 61%.

As in the modal mass participation factor for the church post structural modifications is above the required 60%, according to the NPR9998 [14] higher modes can neglected in this case and the behaviour of the structure can be simplified to that of a single degree of freedom system (SDOF). As can be seen in Figure 9.4, the church post structural modifications indeed shows a displacement pattern that can be simplified to a SDOF system.

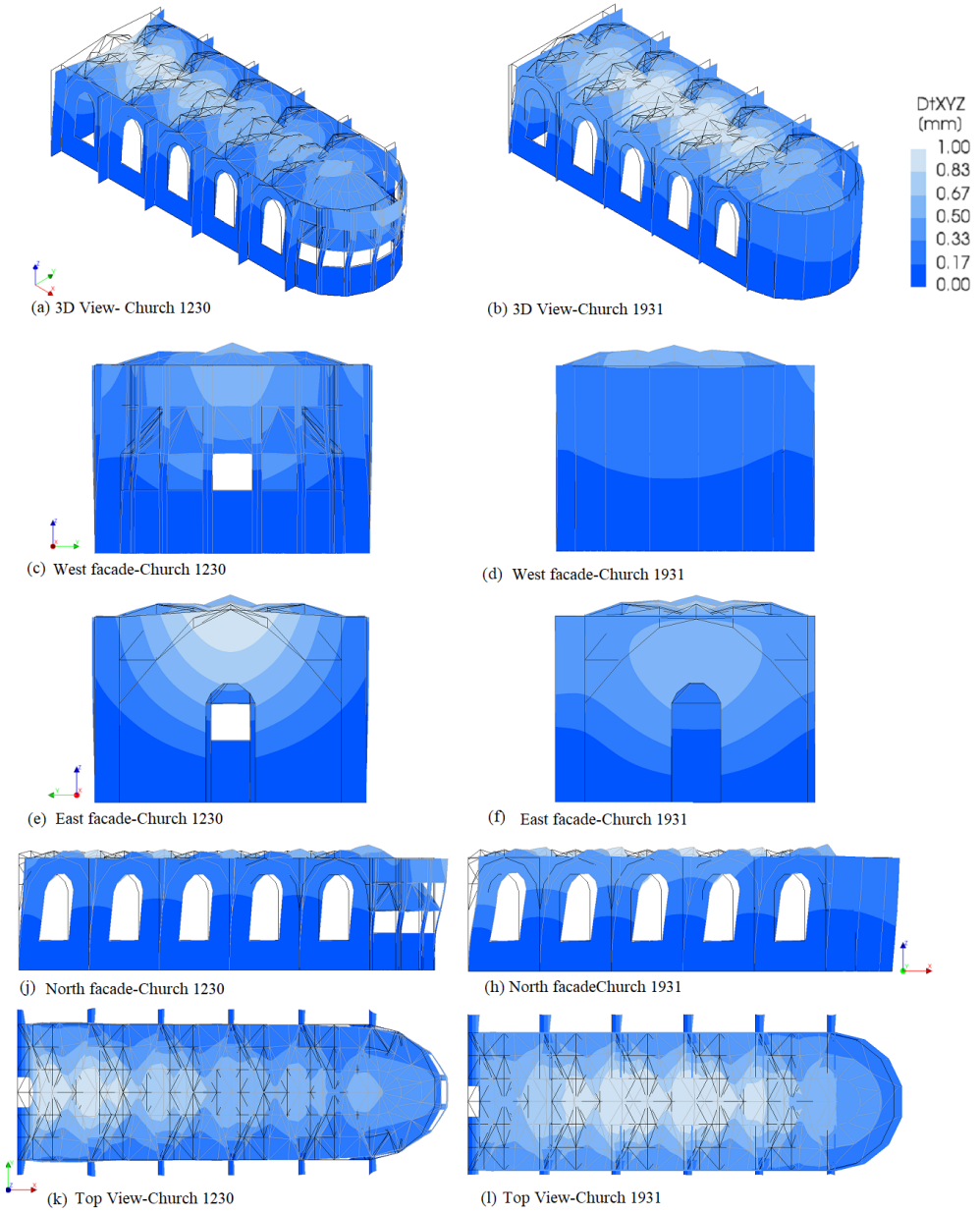

Figure 9.4: Governing eigenmodes in global X-direction for the Church prior (a, c, e, j, k) and post structural modifications (b, d, f, h, l), [scale factor=0.05]

Governing Eigenmodes Global Y-direction

The governing eigenmodes and modal shapes of the structure prior and post modifications for the global Y-direction are presented in Figure 9.5. The governing mode shape is a torsional mode for the church as built in 1230, whereas it is an out-of-plane mode for the church post structural modifications in 1931. Due to the addition of the concrete beams in combination of closing the opening on the West facade a higher rigidity is obtained in the curved facade in comparison to the church prior structural modifications changes from 43.9% to 65.8%, for the church prior and post structural modifications respectively. Similar to the results in the global X-direction due to this shift the behaviour of the structure can be estimated by a SDOF system and the use of the NLPO methods will not results in severe conservative results.

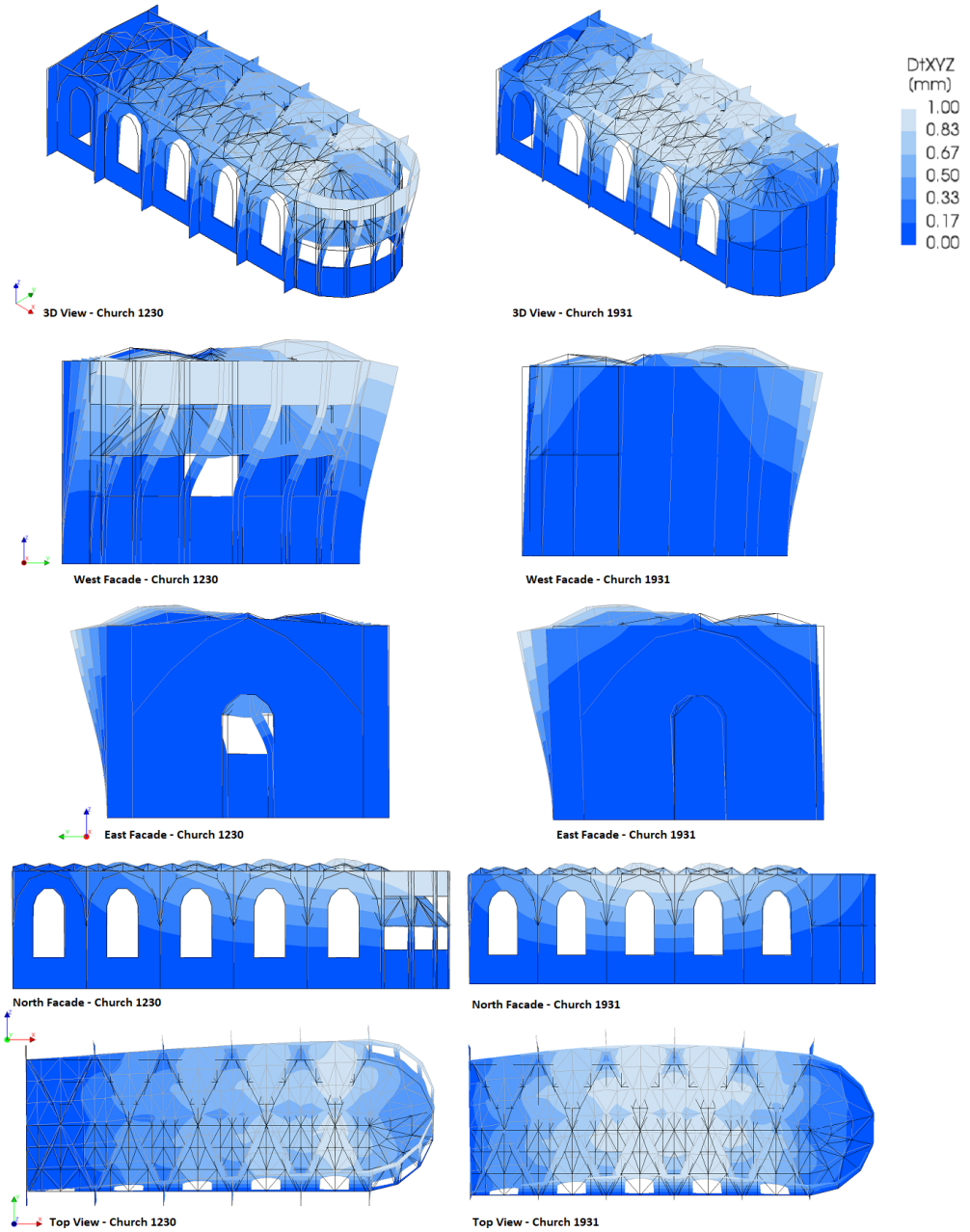

Figure 9.5: Governing eigenmodes in global Y-direction for the Church prior (a, c, e, j, k) and post structural modifications (b, d, f, h, l), [scale factor=0.05]

9.2. Overall behaviour under vertical loading

Analyses under static conditions are performed again to validate the model. The analyses are performed by applying the dead weight and the pre-loading, as indicated in Figure 9.1, on the structures. Output such as the deformations, internal forces, reaction forces are then compared to study the difference in the behaviour of the church model prior and post structural modifications under nonlinear static load conditions. Results are presented in Figure 9.6 for the church as built in 1230 and the church post structural modifications in 1931.

Deformations

After the application of the loads a symmetric displacement pattern is observed for both church models. Maximum displacement are found in the centre of the vaults with a quantity of 0.91 mm and 2.57 mm, respectively for the church prior and church post structural modifications (see Figure 9.6). When examining the deformations in the vertical direction for the main walls, note that the deformations at the top of the wall are 0.16 and 0.19 mm respectively and are equal to zero at the location of the supports for both models. The higher displacement in the church model after the structural modifications is the effect of the application of dead load due the concrete beams. Based on the pattern of the deformations in the vertical direction it can be concluded that all elements are properly connected and that the dead loads are applied in the correct manner. Displacements of the walls in horizontal plane for both models, due to the application of loading only in the vertical direction, is in both global directions relatively small in comparison to the vertical direction. Overall, higher displacements are observed in vaults of the church model after the structural modifications, but lower displacements are observed in the main walls.

Internal stresses and reaction forces

Both models show stress concentrations in the same areas for parts of the main walls and piers (see Figure 9.6). At the base and at mid-span height of structure parts of the walls and piers are in compression. Whereas at mid-span height of the piers tension is observed. As can be seen in the displacement pattern of the piers, an outward curvature towards the main walls can be observed for both models, which results in tensile stresses in the other part of the piers and at the same height in compressive stresses at the main walls. Additionally, as can be seen, the compressive stresses increase gradually from top to bottom. In the church model post structural modifications these stresses are concentrated in the main walls due to the shorter piers. Lastly, a comparison with the resultant force obtained from hand calculations is made. For the numerical model a reaction force of 1000.5 kN is found where as for the hand calculations a value of 1143.34 kN.

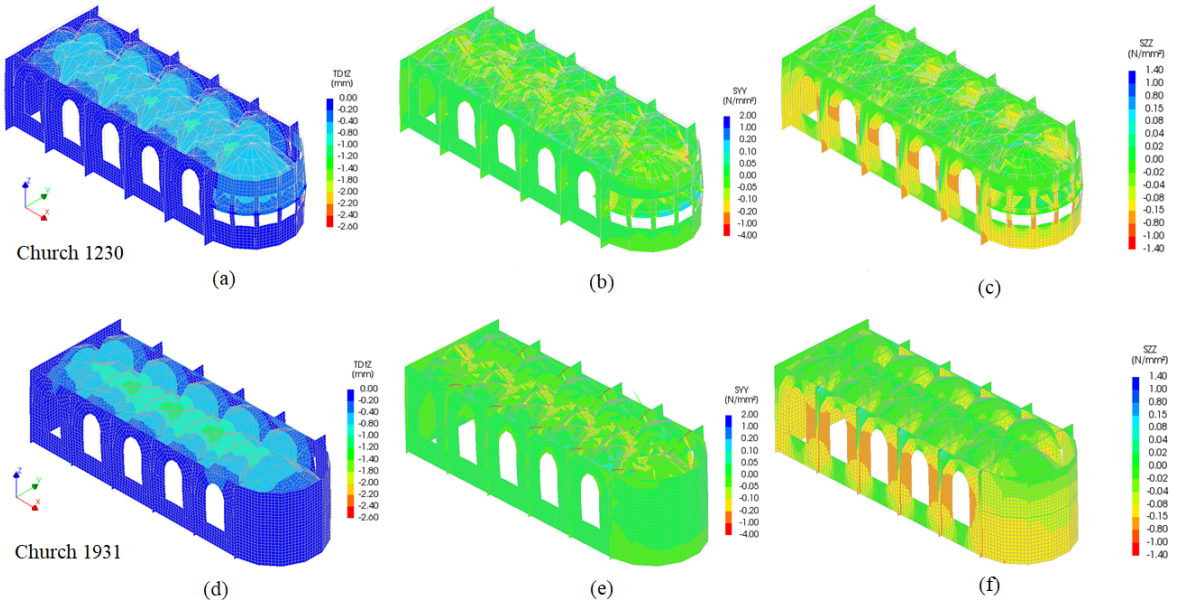

Figure 9.6: Displacements and stress concentrations (Y and Z-direction) for the church prior (a, b, c) and post structural modifications (d, e, f) due to vertical pre-compression, [scale factor=0.05]

9.3. Overall behaviour under pushover loading

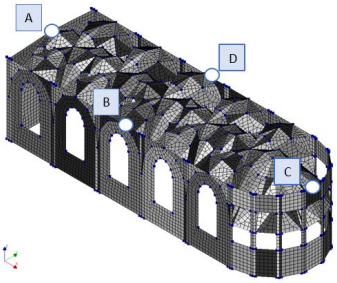

Figure 9.7: Selected control nodes for the capacity curves

In this section the result of the NLPO analysis for the pushover loading applied in the positive X-direction and results of the church post structural modifications is compared and reported for the chosen control nodes (see Figure 9.7 for the position of these nodes). As can be observed from the results, see Figure 9.8, for the control nodes and for all important characteristics a difference is found for the results of both church models. Note that, for the capacity curve of church model post structural modifications post-stage is observed as the analysis diverged after the peak. Regardless of that, point A,B,C,D are picked at comparable stages, which are located at the same base shear force and a comparison between the results is made. Results obtained for the church model post structural modifications shows a maximum capacity of 4200 kN in comparison with the model church model as built in 1230, where 2004 kN was found. As for the initial stiffness it can be observed that the church model post structural modifications has a higher initial stiffness. The addition of the concrete and steel members has a reinforcing effect on the overall stiffness of to the structure. Lastly, for both models no softening is observed.

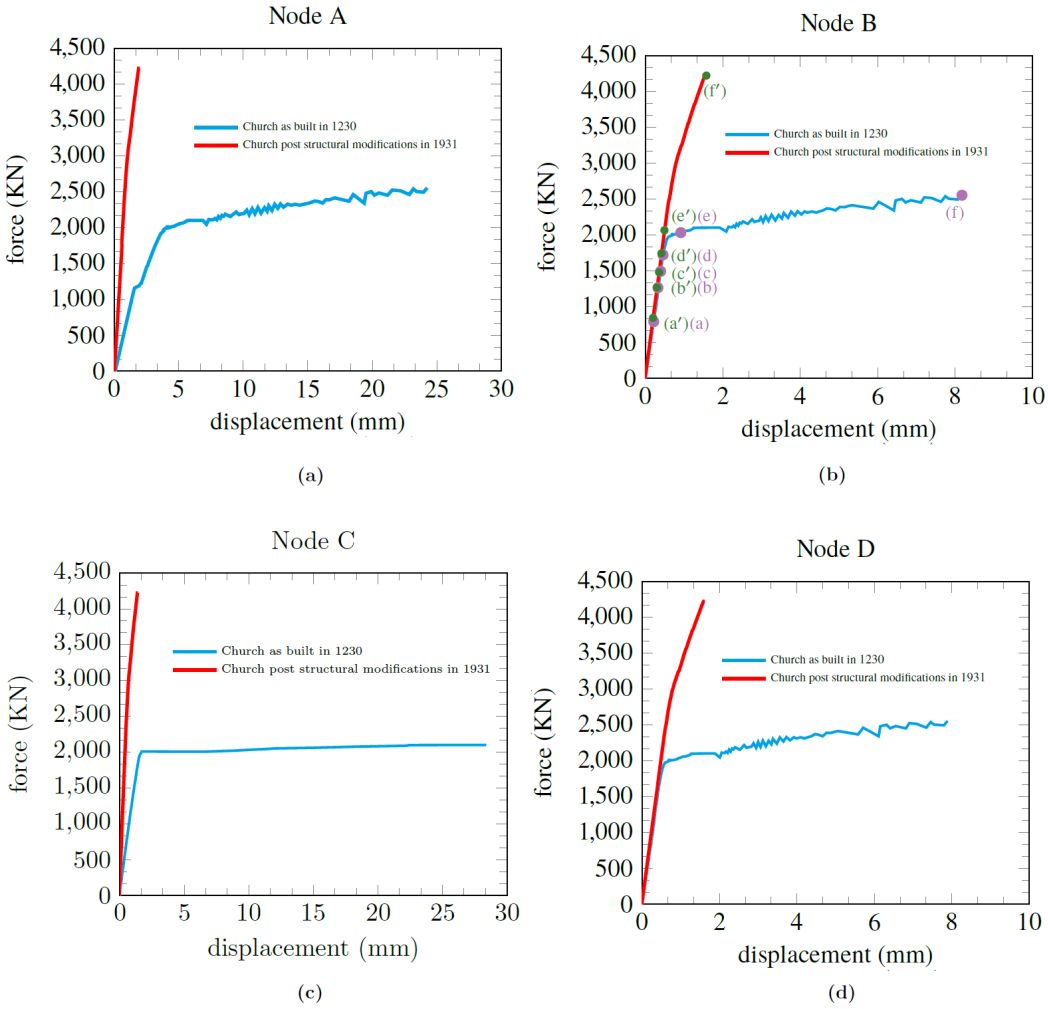

Figure 9.8: Church prior and post structural modifications; capacity curves for nodes: (a) A, (b) B, (c) C and (d) D

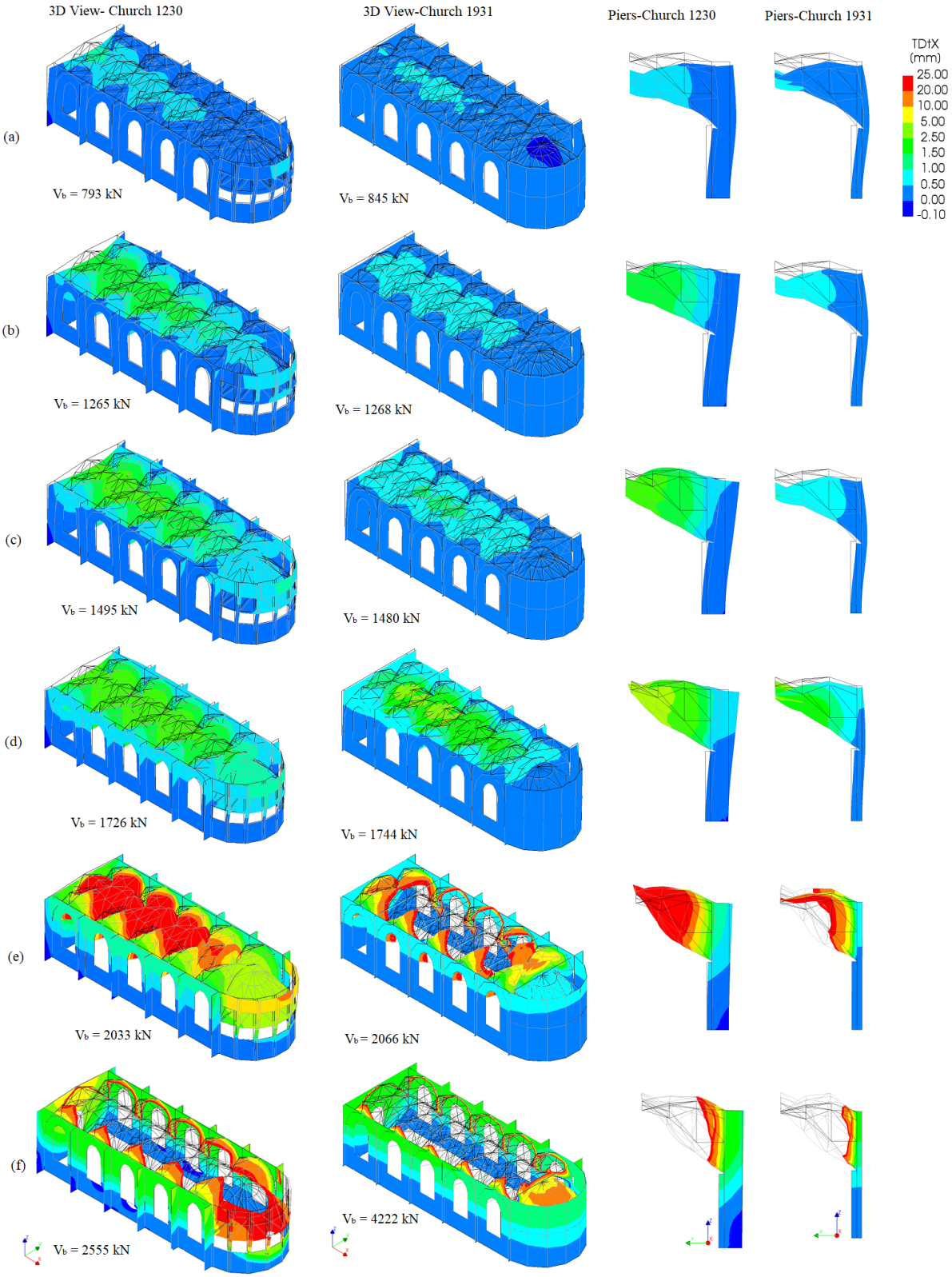

Figure 9.9: Displacement contour church due to pushover loading for the 3D models and piers, [scale factor=0.05]

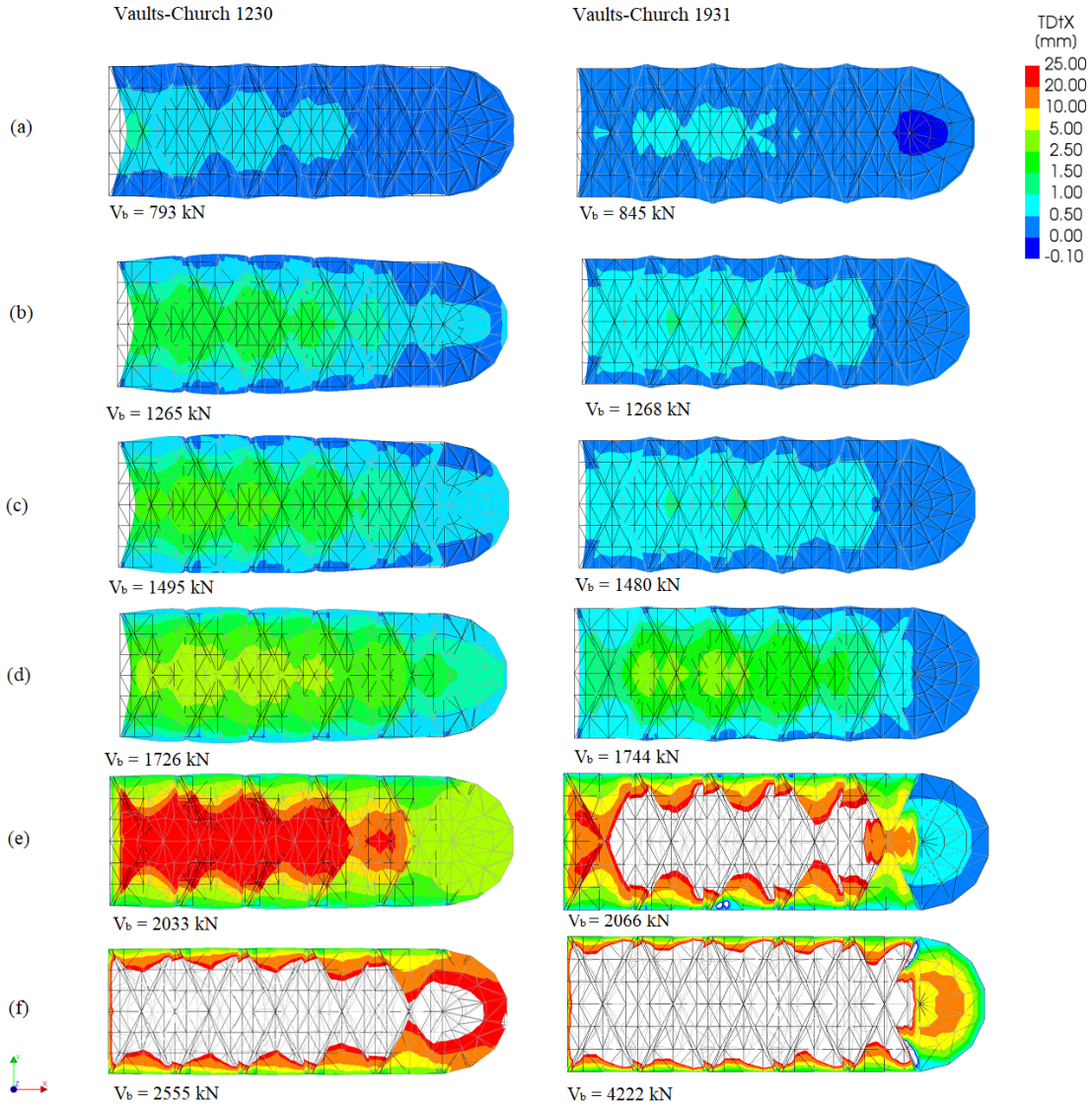

Figure 9.10: Displacement contour church due to pushover loading for the vaults, [scale factor=0.05]

In Figure 9.9 the displacement contours for the church model as built in 1230 versus the church model post structural modifications in 1931 are presented. The addition of the structural modifications, exists of the reduction of the geometry of the piers in the Northern facade, addition of the concrete beams on top of the walls and the addition of the steel beams in the piers of the Northern facade. Regardless of the asymmetry in the structural system of the church as built in 1230, for both models a symmetric displacement pattern can be observed. However, as can be seen at the same base shear force, for the church post structural modifications the overall displacements are much less in value. Although, in general the main walls bend less along their top constrained. At mid height the walls and subsequently the piers, see Figure 9.9, bend relatively more on the North Facade for the Church model post structural modifications. This happens as a consequence of the reduced cross-section of the piers. Then as for the behaviour of the vaults, in contrast to the church model prior to structural modifications for the church post structural modifications the displacement pattern spreads uniformly over the vaults and shows a propagation of the displacement in a gradual manner. The displacement contour plots for the vaults are depicted in Figure 9.10. Whereas, for the church prior modifications the displacement pattern seems to have a head and a wider tail. At the peak loading the vaults in the model prior to modification shows displacements of up to 25mm in its middle part. For the church post structural modifications the vaults moving beyond 25mm and reach values up to 100mm. For the purpose of a clear presentation of the results its chosen to only depict values up to 25mm.

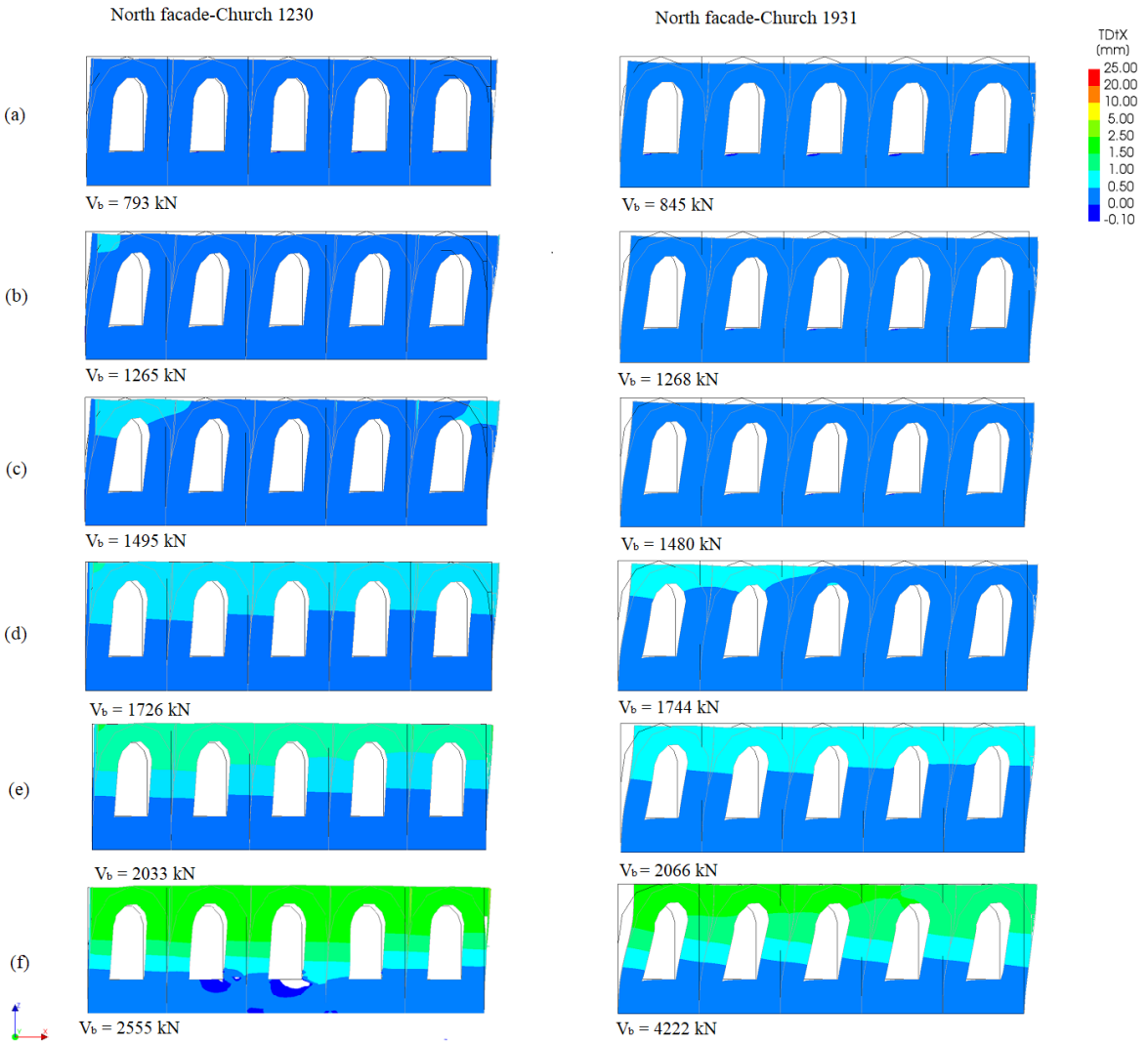

Figure 9.11: Displacement contour church due to pushover loading for the Northern facade, [scale factor=0.05]

In Figure 9.11 and 9.12 the displacement contours for walls of the church model as built in 1230 versus the walls the church model post structural modifications are presented. As can be seen all walls in the church model post structural modifications have an initial downward curvature due to the added self weight of the concrete beams. The results for North facade in figure 9.11 show additionally show how the wall in the church model post structural modifications move in a rather gradual manner side-ways in contrast to the model prior to structural modifications.

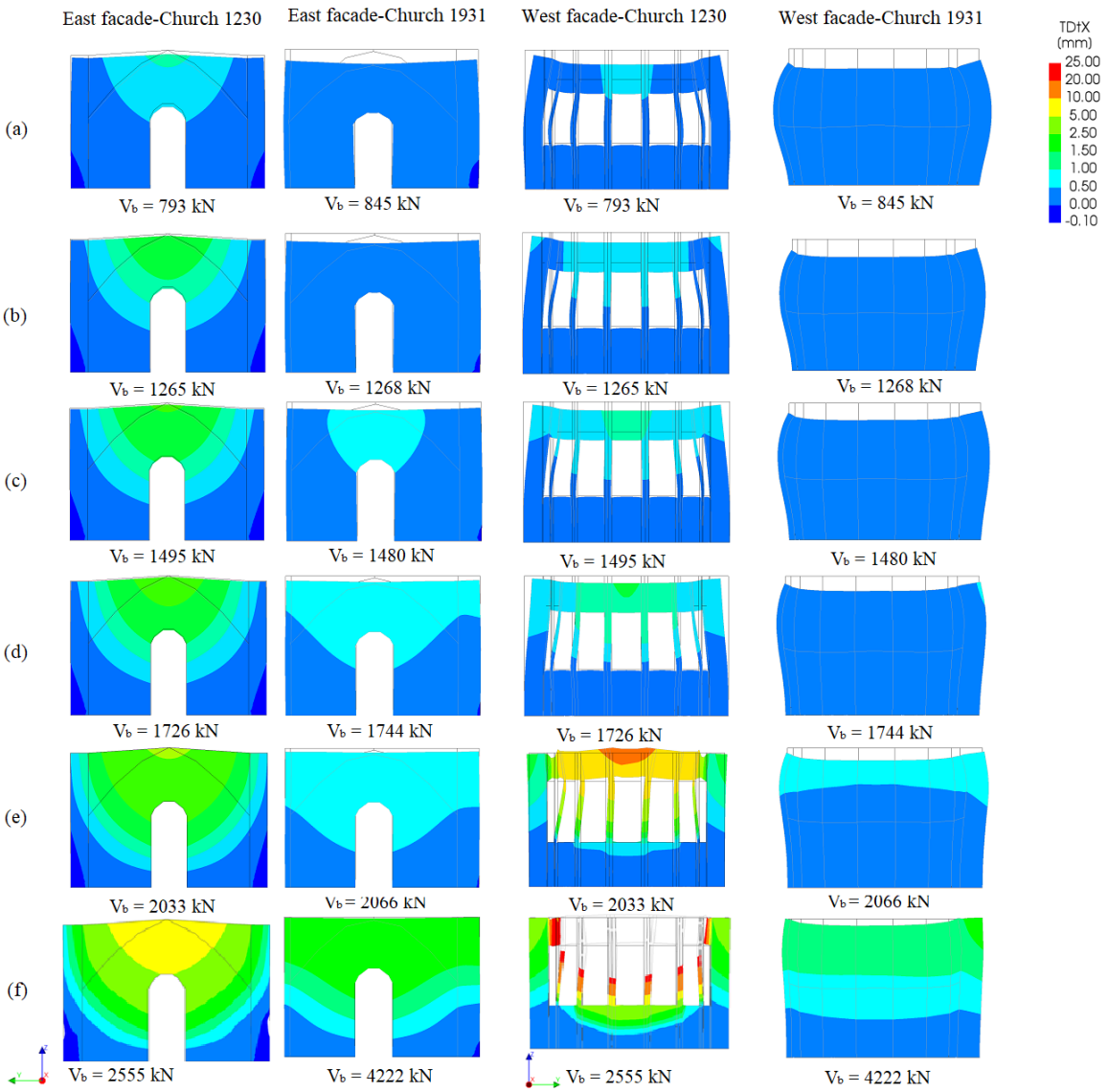

Figure 9.12: Displacement contour church due to pushover loading for the East and West facades, [scale factor=0.05]

As for the East facade (at the location of the application of the pushover loading), from the results presented in the 3D View in Figure 9.9, due to the addition of the concrete beams on top of the main walls that the top part of the Eastern wall is restrained from bending inwards unlike the Eastern wall in the church prior modifications. Due to this restrain, an out-of-plane motion of the main walls are observed much later in the church model post structural modifications. Lastly, it is interesting to look at the behaviour of the curved West facade. In the model prior to structural modifications the wall contains window openings, which are filled up after the structural modifications. In the case with window openings, the vertical structural members which hold the upper part of the curved wall are very slender in shape, as a consequence very early on in the analysis the upper part of the curved facade moves out of its plane. In the model after the modifications an out of plane displacement is only observed when the North and South facade move in the positive X-direction.

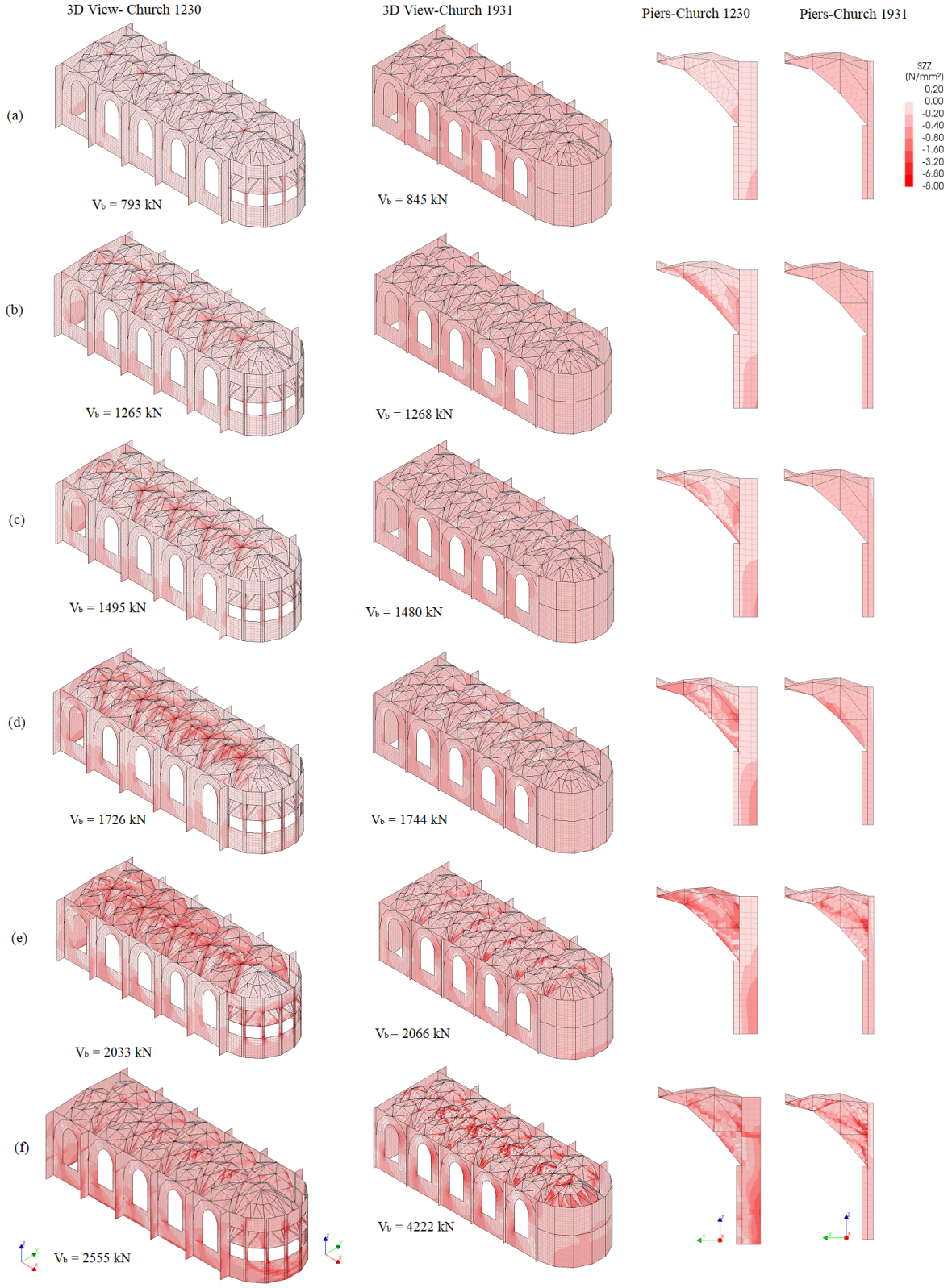

Figure 9.13: Compressive stresses for the church due to pushover loading for the 3D models and piers, [scale factor=0.05]

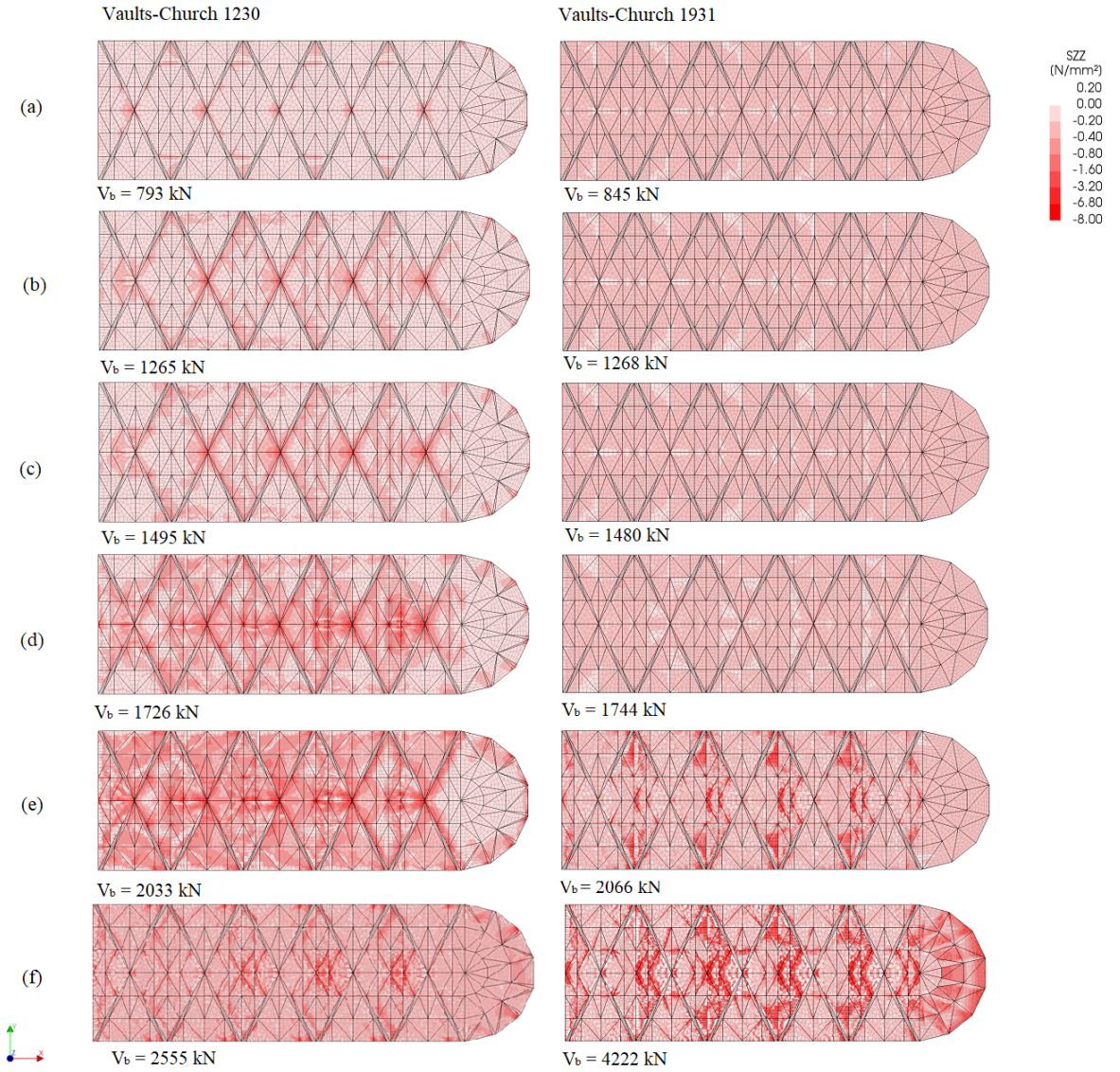

Figure 9.14: Compressive stresses for the church due to pushover loading for the vaults, [scale factor=0.05]

In figure 9.13 the compressive stress concentrations for the church model as built in 1230 versus the church model post structural modifications in 1931 are presented. For the church model post structural modifications a slightly higher stress concentration, of about 0.20 N/mm_2, is observed in comparison to the church prior modifications. Nevertheless, both models have during the initial phase of the analysis a rather symmetric stress concentration pattern. The church model prior modifications remains to show a symmetric pattern until the end of the analysis. However, this is behaviour is not observed in the church model post structural modifications. In this case due to the asymmetric shape of the church an asymmetric pattern is observed here. This can be seen in the East and West facade especially. As the top and bottom of the piers are fully constrained no stress constrains are observed at the base of the piers of the church model post structural modifications. Unlike the piers in the church prior structural modifications, for which due to the top movement of the piers the compressive stress concentration are found at the base of the piers. As for the vaults, see figure 9.14, note that here no asymmetric stress pattern are observed. As can be seen the compressive stresses in the vaults show a rather symmetric pattern for both church models till the end of the analysis.

Figure 9.15: Compressive stresses for the due to pushover loading for the Northern facades, [scale factor=0.05]

Figure 9.15 presents the compressive stress concentrations in the Northern facade for the church model prior and post structural modifications. Note that, due to the presence of the self weight of the concrete beams on top of the walls show much higher stress concentrations for the church model post structural modifications in comparison to the church model prior to the modifications. Then as for the compressive stress patterns in these facades; For the church prior modifications higher stress concentrations are observed near the window corners which develop downwards to the base of the church. For the church post structural modifications these stress concentrations are located mainly at the base and at mid height of the walls. Towards the end of the analysis the shape of the stresses do not change, they grow in magnitude. At the end of the analysis the highest stress concentrations are found at the corners of the window openings, which flow downward under the window opening.

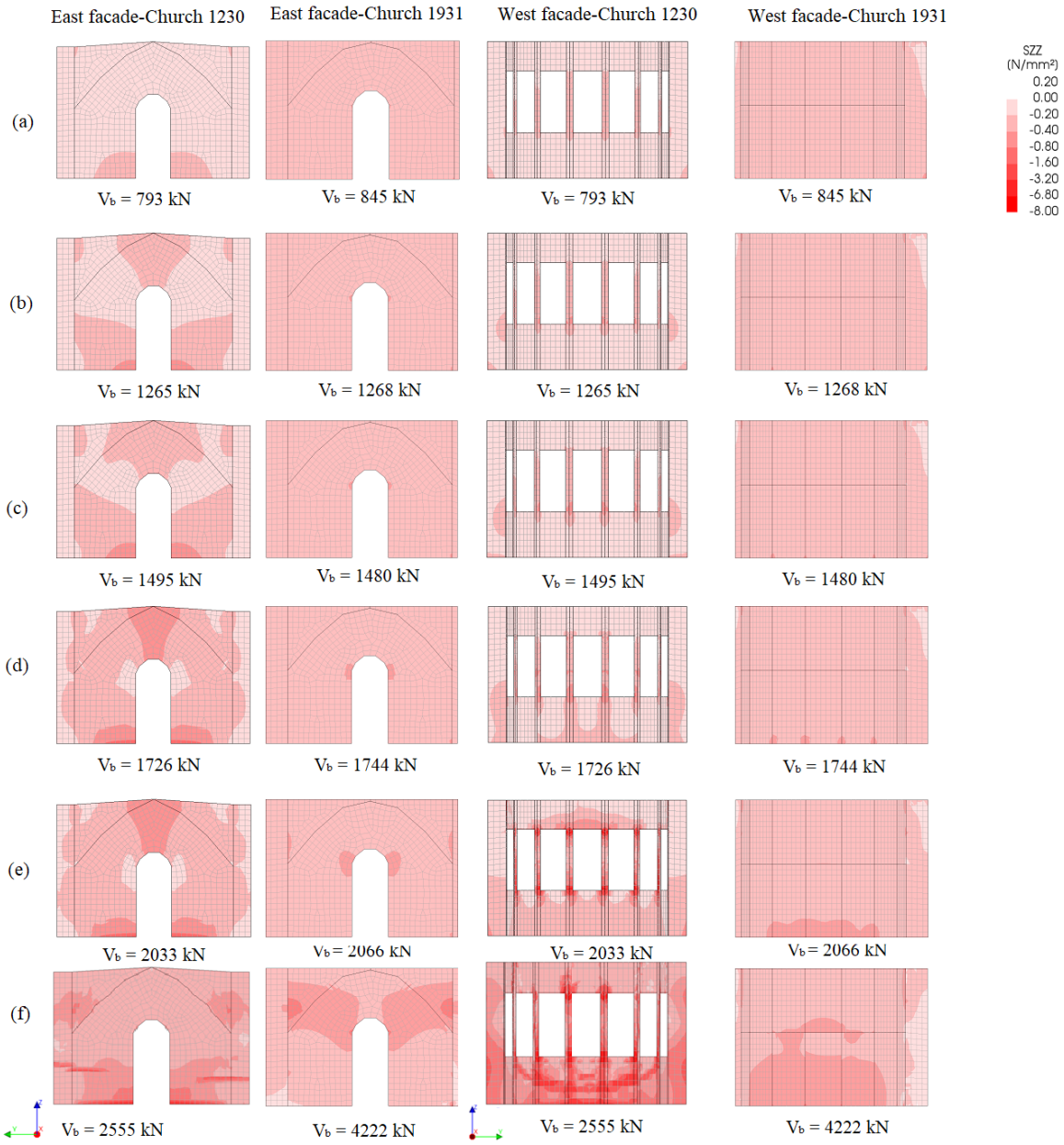

Figure 9.16: Compressive stresses for the due to pushover loading for the East and West facades, [scale factor=0.05]

As for the stress concentrations in the East and West facade a symmetric pattern is observed for the church models prior to the modifications in the East and West facade, see figure 9.16. Whereas, for the church post structural modification a deviation is observed. As can be seen the stronger North facade side, due to the presence of the steel columns in the walls unloads parts of the South facade side, when only looking at the East and West facade.

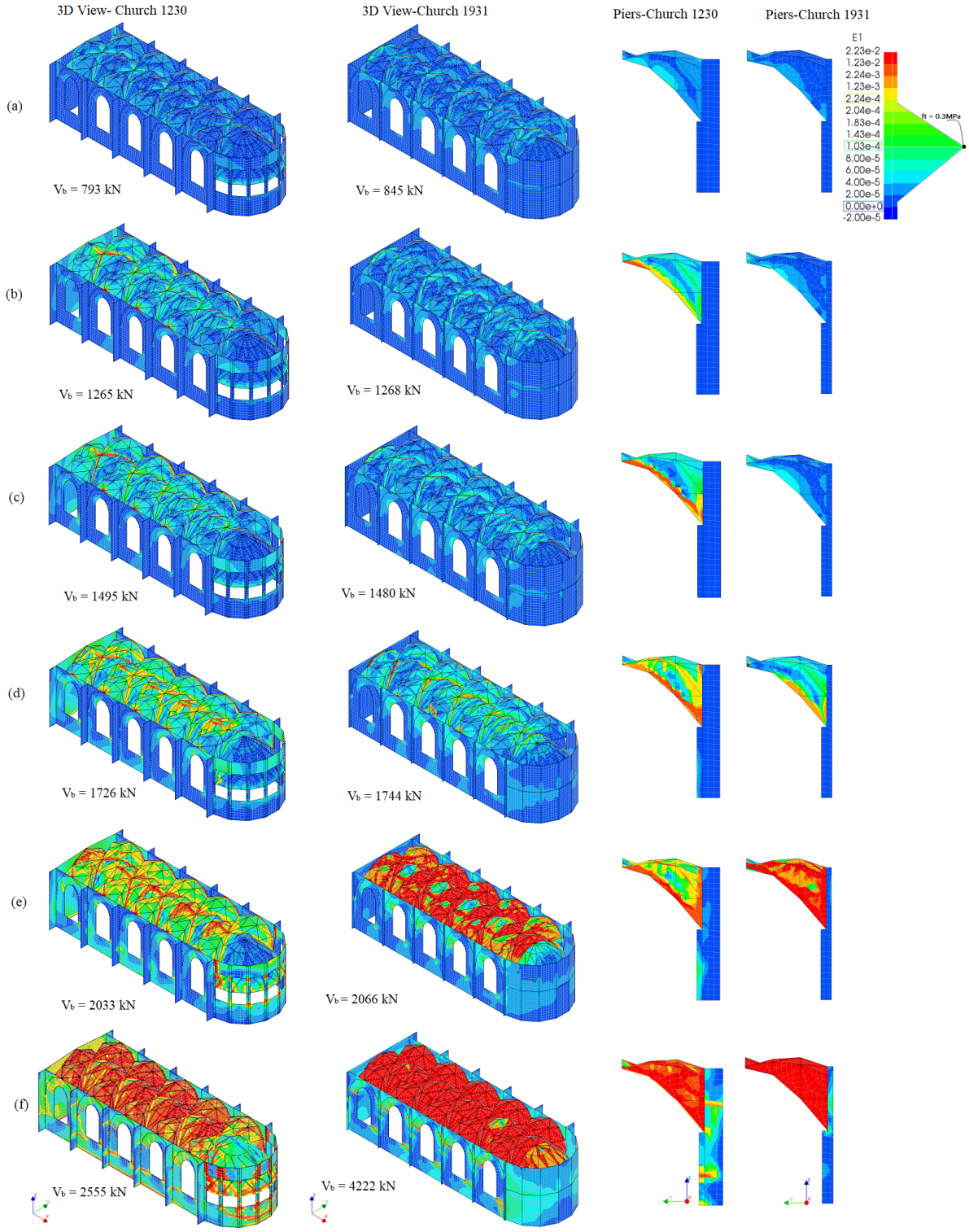

Figure 9.17: Tensile Strain distribution for the church due to pushover loading for the 3D models and piers, [scale factor=0.05]

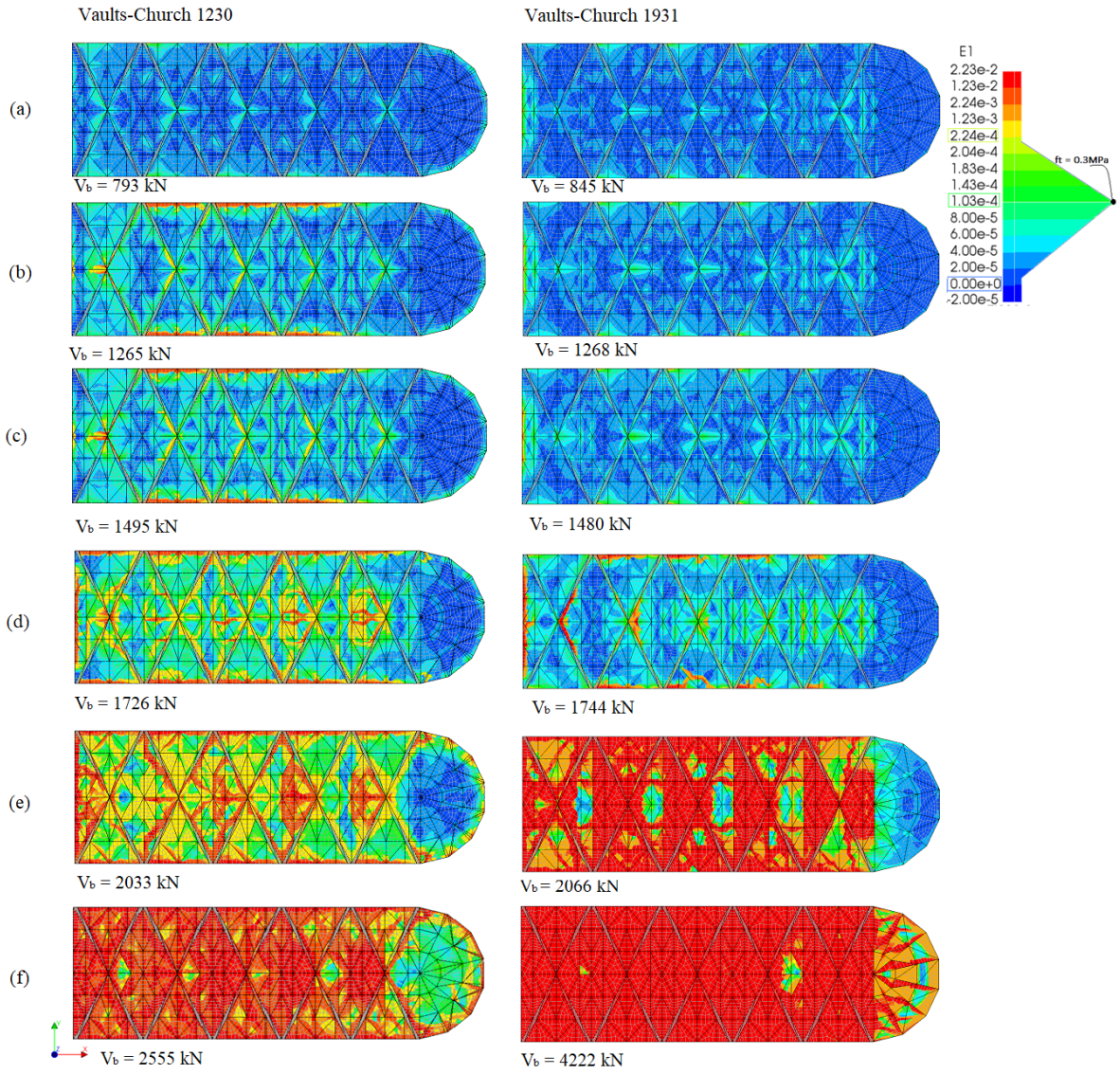

Figure 9.18: Tensile Strain distribution for the church due to pushover loading for the Vaults, [scale factor=0.05]

In figure 9.17 the tensile strains for the church model as built in 1230 versus the church model post structural modifications in 1931 are presented. Both models show a rather symmetric strain pattern along the global X-axis. The highest tensile strain concentrations are found in the vaults near the East facade, where the pushover loading is applied. Towards the peak loading, a great part the vaults show a tensile strain concentration that exceeds the ultimate value of 2.235E-4. At the base of the piers for the church prior to the structural modifications tensile strain concentrations are observed. Figure 9.18 presents the tensile strains for the vaults of both models. For both models a symmetric tensile strain pattern is observed. However the models do differ from each other. For the vaults of the structure prior to structural modifications the tensile strains built up gradually. Whereas, due to that the vaults in the structure post-structural modifications, are constrained at their supports as a consequence of the application of the concrete beam high tensile strains build up in the vaults.

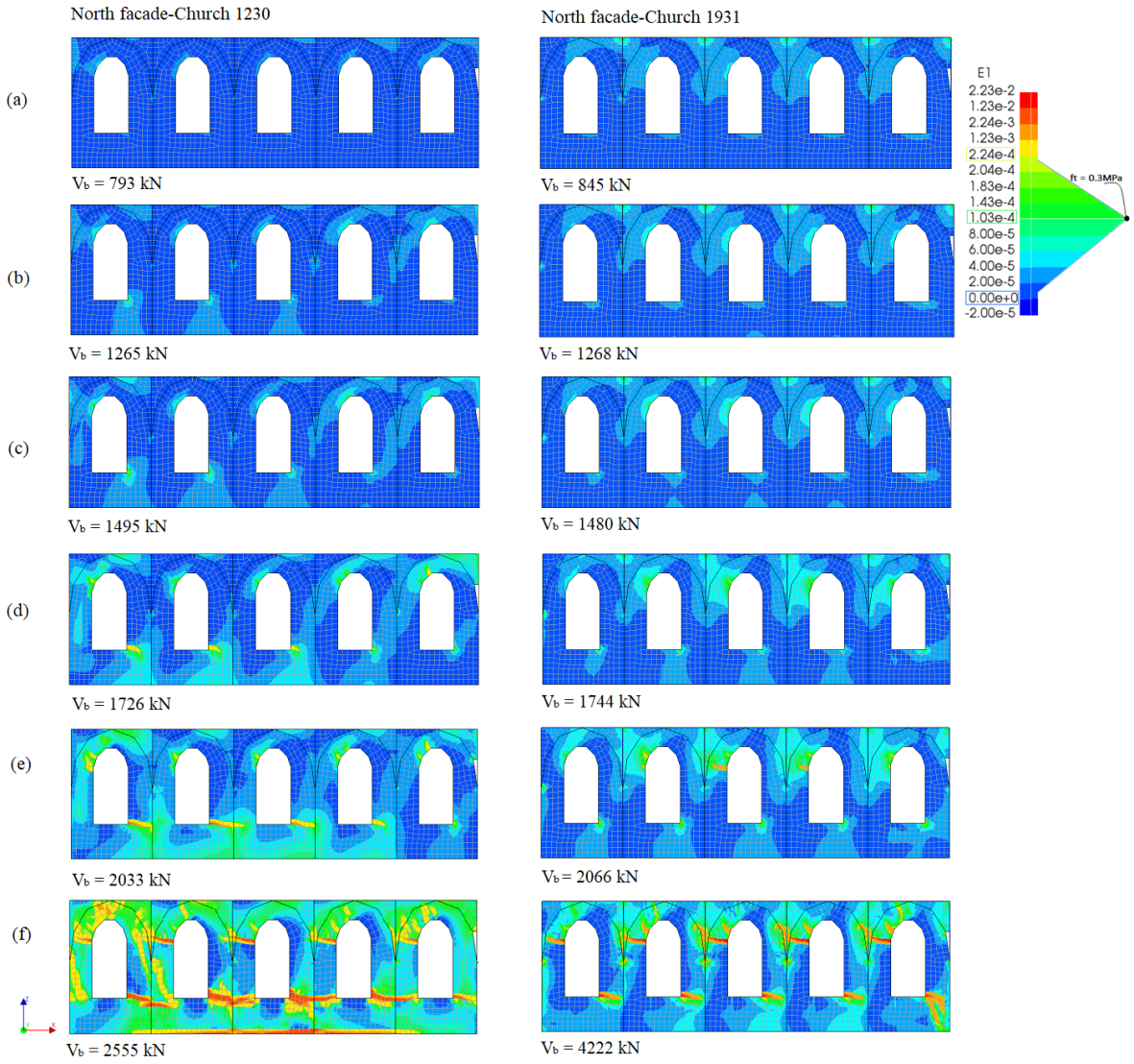

Figure 9.19: Tensile Strain distribution for the church due to pushover loading for the Norther facades, [scale factor=0.05]

Figure 9.19 present the tensile strain concentrations for the North facades. As can be observed, due to the presence of the concrete beams high strains are found at the top edge of the facade for the church post structural modifications. These concentrations can be explained due to that the top edge of the facades are constrained, while the vaults are trying to push the facades out-of-plane. As the pushover loading is applied, tensile strain concentrations are observed in the lower right corners of the window openings and upper left part of the window openings. At these locations the limit for the ultimate tensile strains are exceeded and cracks form as a consequence. For the church model post structural modifications at the same locations the strains develop further in the horizontal direction. And in the last bay the tensile strain concentrations develop in a diagonal fashion downwards.

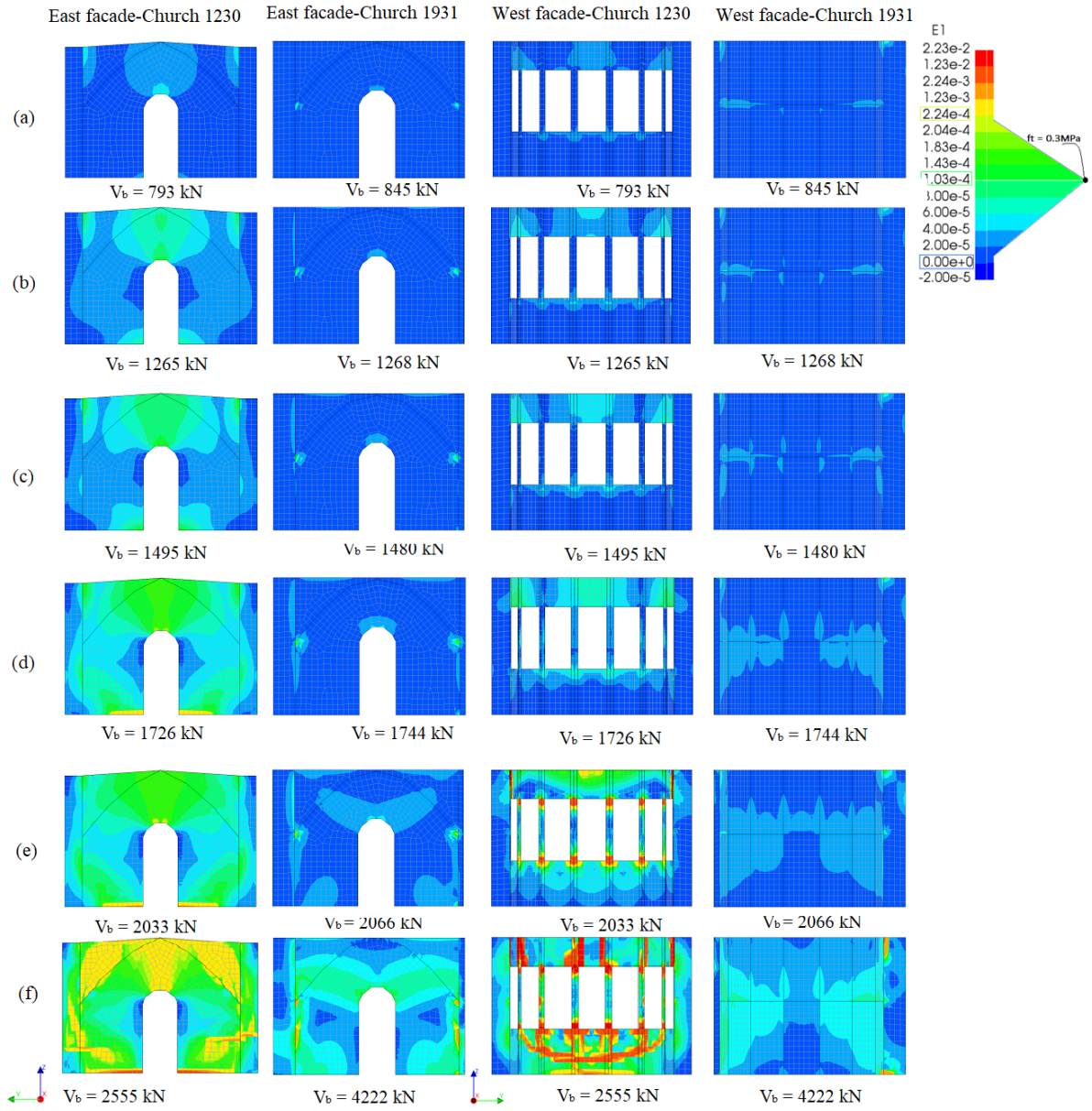

Figure 9.20: Tensile Strain distribution for the church due to pushover loading for the East and West facades, [scale factor=0.05]

Figure 9.20 present the tensile strain concentrations for the East and West facades of the church models. As can be seen in the figures, for both facades a symmetric tensile strain pattern is observed throughout the analysis. However, for the church post structural modifications the tensile strains are much lower for the same base shear force. Moreover, at the end of the analysis a concentration of tensile strains are observed in a different location for each church model. In the church model prior to modifications the ultimate strains are exceeded at the base near the door opening. Whereas for the church model post structural modifications the strains are exceeded at the interface of the main wall with the piers. The same behaviour is observed for the curved West facade. Where, for the church prior to modifications the strains are exceeded at the corners of the window openings, in the church post structural modifications the strains are exceeded at the interface of the main wall with the pier.

9.4. Convergence behaviour

Figure 9.21 presents the number of iterations per load step for the church model post structural modifications. A limit of 50 iterations is set per load step during the analysis. As can be seen as the analysis is going towards the peak loading in the model the number of iterations per load step gradually increases, but does not exceed so often 50 iterations. Up to load step 228 the analysis is conducted with the aid of the Regular Newton-Raphson method. Up to that point the method works, however after that point the number of iterations exceeds for a longer period 50 iterations. Therefore, it is decided to proceed with the Quasi-Secant method after load step 228. As can be seen from the presented results, a few steps do not exceed the limit of 50 iterations per step, however very soon a period can be seen which exceeds this limit. All load steps in this analysis were check on extreme exceeded of the balance of energy norm. The deviation in the norm were out of control towards the end of the analysis. Therefore, results are considered not valid after load step 228 in this analysis.

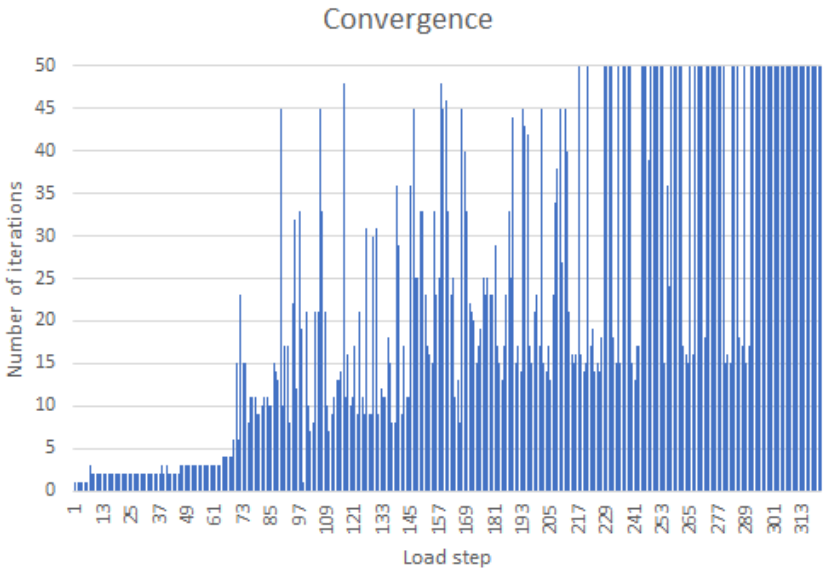

Figure 9.21: Convergence Behaviour in terms of number of iterations per load step

9.5. Crack pattern evolution

In figure 9.22 the crack evolution for the church model as built in 1230 versus the church model post structural modifications in 1931 are presented.

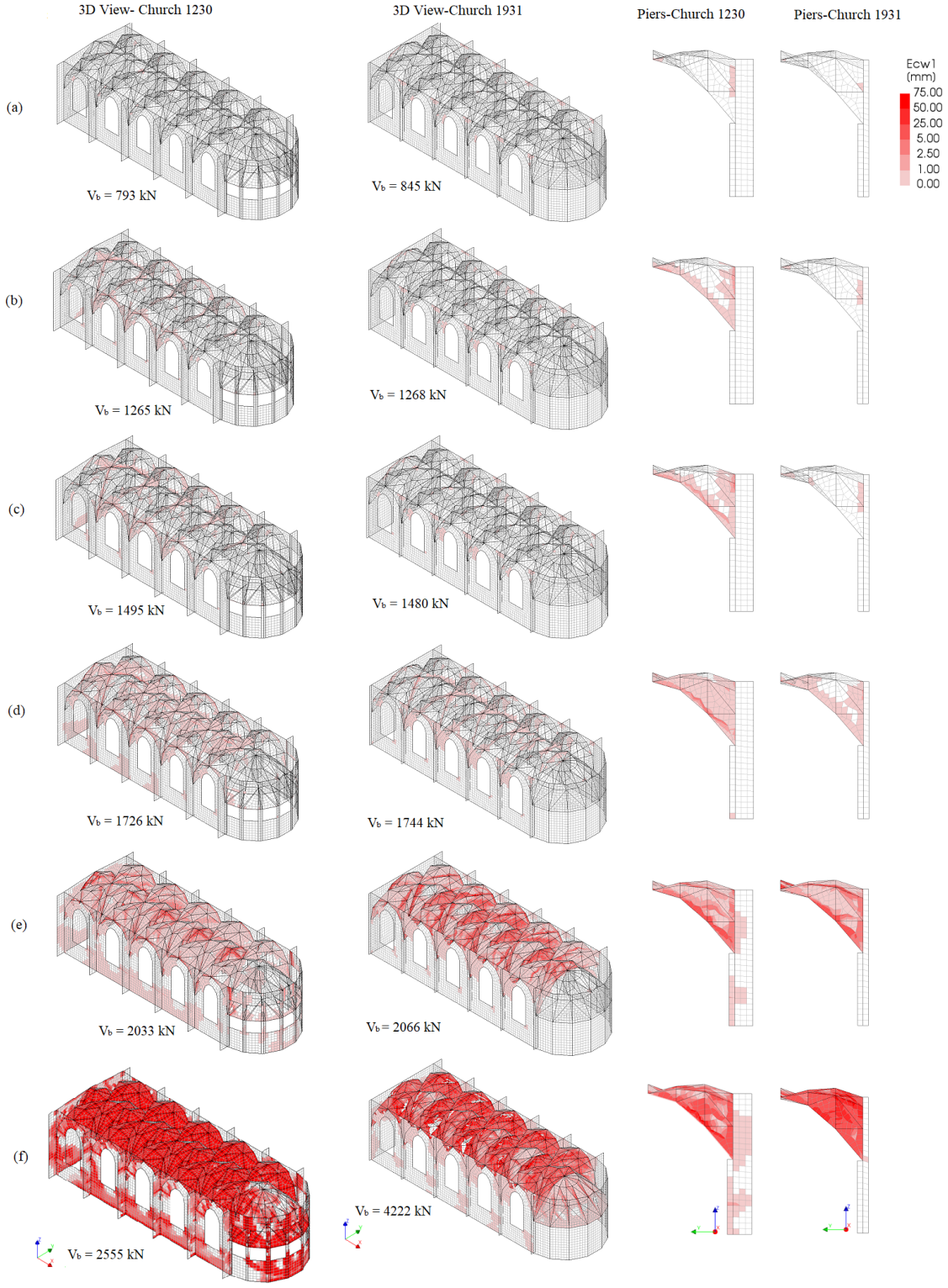

Figure 9.22: Crack patterns for the church due to pushover loading for the 3D models and piers, [scale factor=0.05]

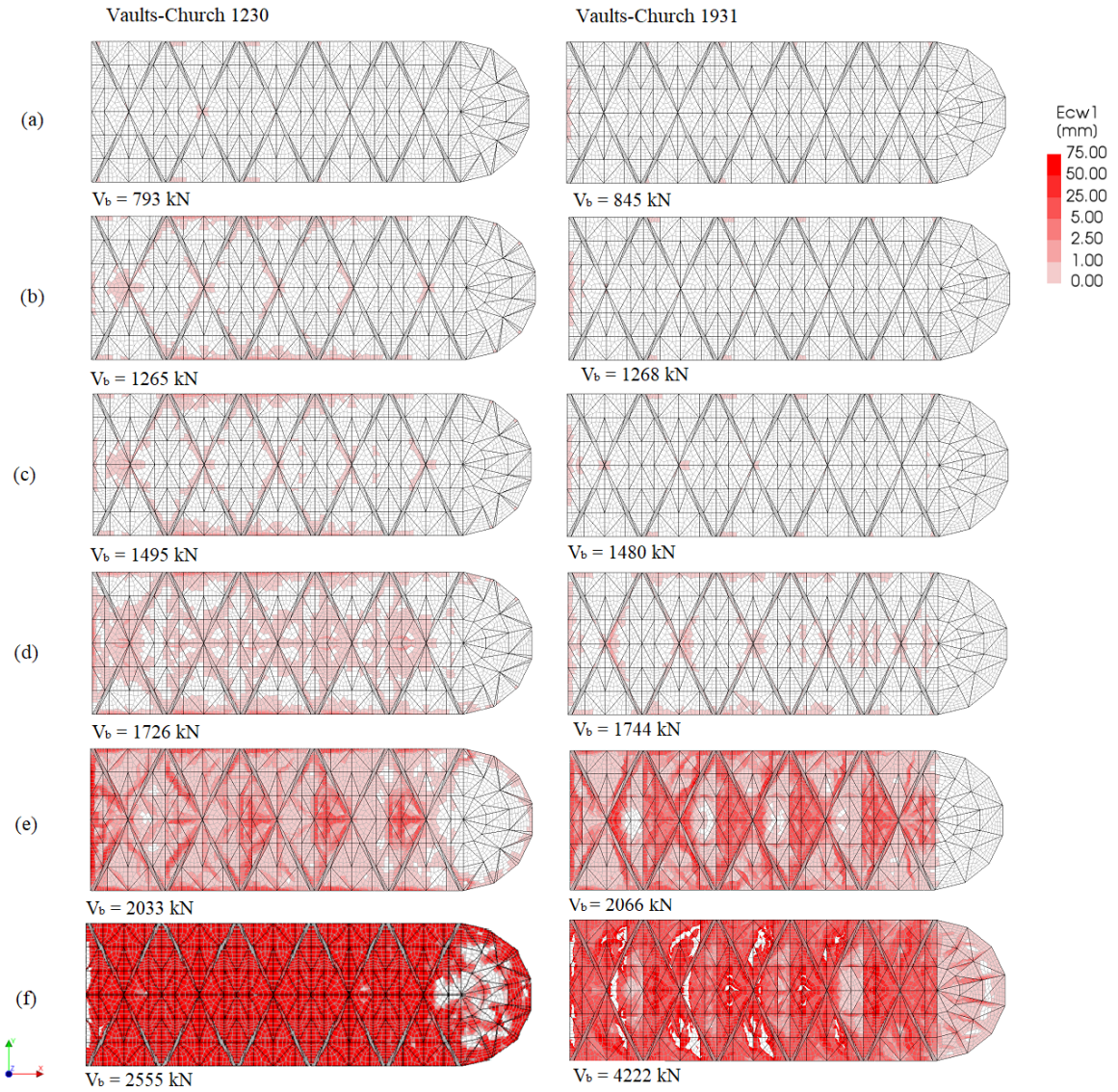

Figure 9.23: Crack patterns for church due to pushover loading for the vaults, [scale factor=0.05]

For both church models a symmetric crack pattern is found throughout the entire analysis with an a small exceptions for the church model post structural modifications. In general for the church post structural modifications initial cracks are observed for a higher base shear force, however quantity wise more cracks are observed for this model than the church model prior to the structural modifications. As for the piers, minor cracks are observed for both models. For the church prior to the structural modifications the cracks are observed at the base of the piers and at mid height, whereas for the church post structural modifications the minor cracks appear at mid height of the piers. As earlier observed, due to the addition of the concrete beams the top boundary of the piers are constrained, therefore compressive stresses and tensile strains at the base of the wall and piers are reduced for the church model post structural modifications. Which means that less cracking is to be observed in the model post modifications, especially at the base of the structure. Then, in Figure 9.23 the crack patterns of the vaults are presented. Here, again initially a symmetric pattern can be observed for both models. However, when comparing plot (c) with (d) for the church models, a small difference is found in this pattern for the church post structural modifications. Note, that on the side of the North Facade where the steel columns are added and the piers are shorter slightly more cracks are found than on the other side. The addition of the steel columns does have its influence here. Towards the end of the analysis for the church model post structural modifications the vaults are severely cracked and beyond repair. With maximum crack widths of around 75mm. This is not the case for the church prior modifications where the cracks remain moderate and have maximum values of around 25mm.

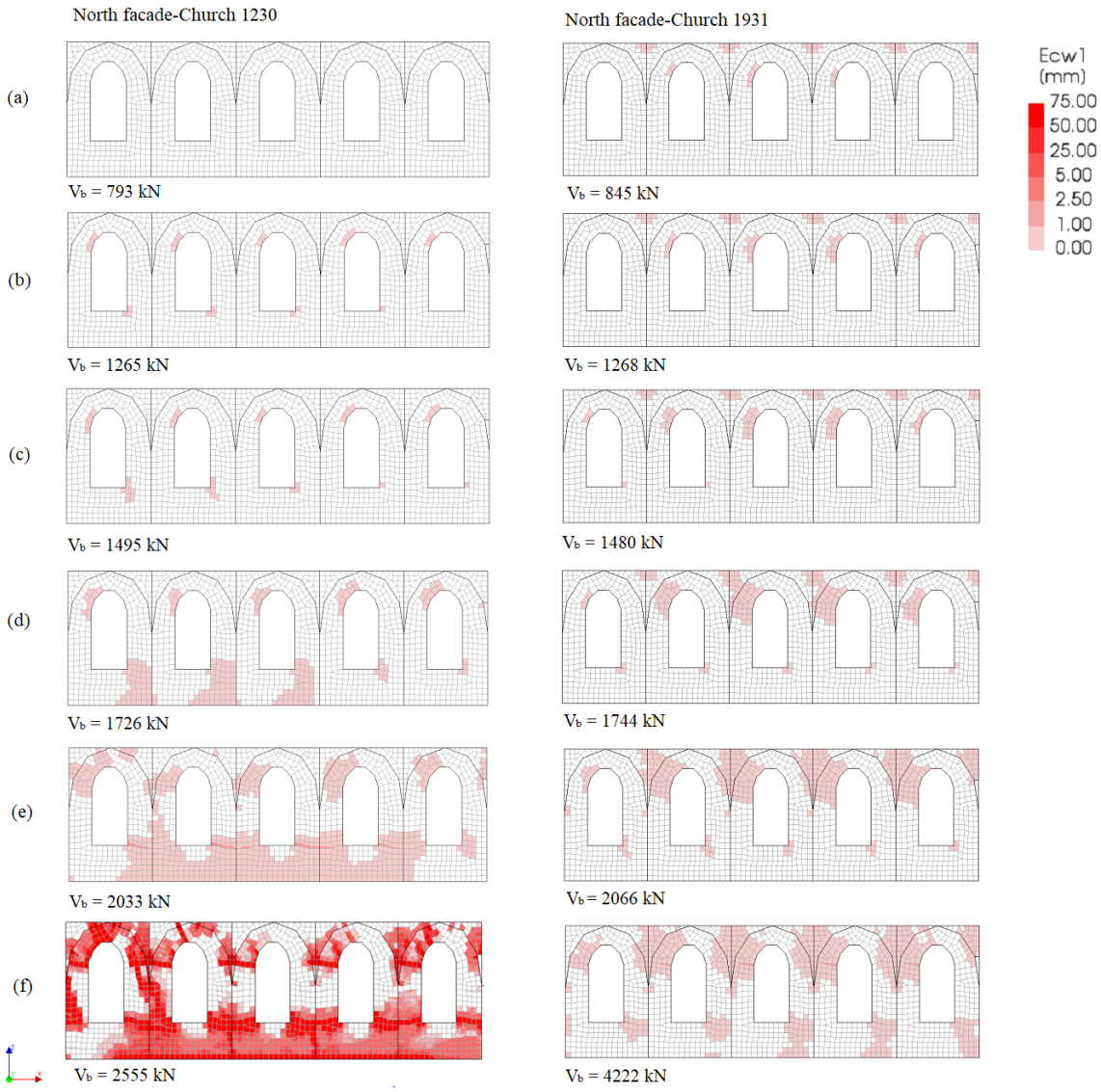

Figure 9.24: Crack patterns for church due to pushover loading for the Norther facades, [scale factor=0.05]

Figure 9.24 presents the crack patterns for the North facades in both church models. The difference in crack pattern is evident here. As can be observed, the church model post structural modifications shows initial cracks at a lower force capacity and at a different location than the church prior to structural modifications. As the top boundary of the main walls are constrained for the church post structural modifications, note that initial cracks appear near that boundary first. In the church model prior to the modifications the cracks appear near the corners of the window openings and as these develop further at the same location, the same cracks appear for the church model post structural modifications. Towards the end of the analyses, the same crack for both models which were located near the window opening did develop much further for the church model prior to the modifications and not for the church model post modifications. For the church model prior to the modifications maximum crack widths of maximum 5mm are observed in the window corners that grew in the horizontal direction, whereas for the church model post structural modifications the crack widths remain under 2.50mm.

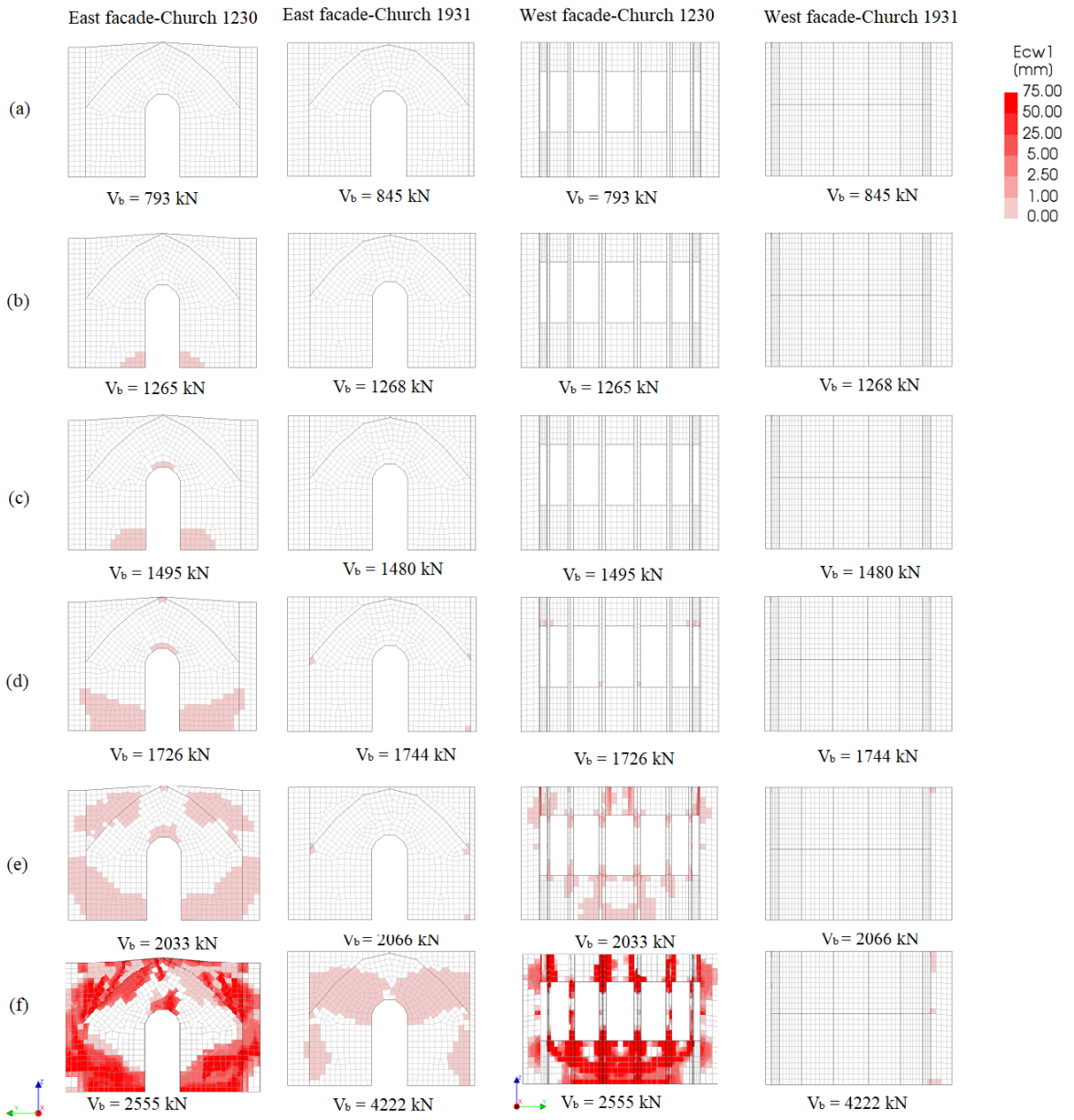

Figure 9.25: Crack patterns for church due to pushover loading for the East and West facades, [scale factor=0.05]

Figure 9.25 present the crack evolution for the East and West facades of the church models. For the East facades of both models show almost a symmetric crack pattern. Due tot he constrained of the upper boundary of the main walls in the church post structural modifications, and due to a higher concentration of stresses in the vaults for this model much less and at a higher base shear force cracking is observed. As for the North facades, these facades also show higher crack concentrations near the top boundary of the facades. Whereas, for the church model prior to the modifications the crack concentrations are higher near the base boundary of the walls. For the church prior to the modifications maximum crack widths of 5mm are observed at the base of the East facade near the door opening and at the corners of the window openings at the West facade. For the East and West facade of the church model post structural modifications the cracks widths do not exceed values beyond 2.50mm.

9.6. Conclusions

In this chapter a comparison of the results of the Modal and NLPO analyses for the church model as built in 1230 and the church model post structural modifications in 1931 were presented. The eigenvalue analysis suggested a change in the overall behaviour of the church in the positive global X-direction after the structural modifications. Before the structural modifications for the church just 43% of the modal mass is activated, whereas after the structural modifications around 60% of the mass is activated during the eigenvalue analysis. The NPR 9998 [14] recommends to use the NLPO analysis only for structures for which 60% of the mass is participating for the governing mode. As this is the case for the church post structural modifications, it can be concluded that considering the structure as a single degree of freedom is sufficient in this case. For the case of the church prior modifications as the modal mass participation factor is less than the recommended 60%, a different analysis method should be used. For future studies analysis methods in which multi-modes are considered are recommended to use. Suggestions for such analysis methods are the Modal Response Spectrum method (MRS) in combination with the NLPO analysis or the Nonlinear Time History Analysis (NLTH).

Results as the deformation contour, stress and strain concentrations and crack evolution were presented for the NLPO analyses. In the deformation contour plots it observed that due to the application of the concrete beam on top of the main walls the outward bending of the top edge of the walls is constrained now. As a consequence the edge of the Eastern wall did not bend as much as for the church prior to the structural modifications. This explains the reduced deformation capacity of the church in general. On the other hand due to the self-weight of the added concrete beam, higher compressive stresses are observed in the walls and a concentration of tensile strains were observed around the top boundary of the walls. As a consequence the first cracks appear around the top boundary of the main walls instead of the window corners which was the case for the church model prior to the structural modifications. At the end of the analyses, for the church prior to the modifications maximum crack widths of 5mm were observed at the window opening that developed further in the horizontal direction over a length of about 1m. The same cracks also appeared in the corners of the door openings in this model. In the church model post structural modifications the crack patterns are maximum 2.50mm and the cracks are smeared out over a region. Here the cracks remain in the crack formation stage rather than in the stage that the cracks widen as seen for the church model prior to the modifications. However, as the top boundary of the main walls are restrained subsequently, the edge supports of the vaults are also constrained. Due to the shape of the vaults and the nonlinear properties considered much higher stress concentrations are observed with the consequence of extreem cracking. The vaults in the church after the modifications have crack widths beyond 100mm. In contrast to the vaults in the church prior to the modifications were the vaults do not exceed values beyond 25mm. The effect on the results due to addition of the steel columns and reduction of the piers on the North facade are slightly less visible than it was for the concrete beams. Due to the addition of the steel columns the church model behaviour slightly stiffer on the North facade. Higher stress concentrations and cracking are observed in the walls and at the edge of the vaults than in the case for the church prior to this modification. Additionally, higher stress concentrations were observed in the walls at the location of the piers. Where originally the stresses were distributed within the piers, now part was distributed in the piers. Then lastly, closing off the window openings on the curved West facade showed that the stability of the curved wall increased drastically and therefore the out-of-plane displacement reduced significantly.

10

Seismic performance

10.1. Response Spectra for Zandeweer, Groningen

NEN provides the response spectra for different locations in the province of Groningen via an online webtool. This webtool provides the user a prediction of the response spectrum caused by earthquakes with different return periods at the chosen location . Figure 10.1 shows the ADRS for a ”weak” and ”strong” earthquake at the location of the case study, Zandeweer in Groningen. These weak and strong earthquake have a return period of respectively 95 years and 2475 years. This corresponds to the DL and NC limit state. The strong earthquake in Zandeweer results a maximum acceleration demand of 0.39g and a maximum deformation demand of 51.7mm. The weak earthquake in Zandeweer results a maximum acceleration demand of 0.12g and a maximum deformation demand of 6.4mm

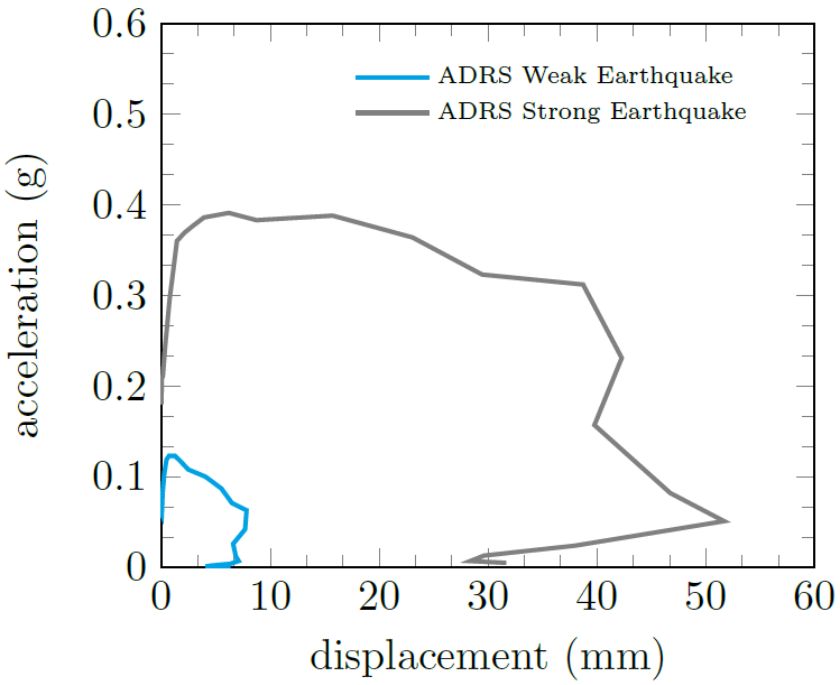

Figure 10.1: Acceleration-displacement response spectra for a strong(Tr=2475y) & weak(Tr=95y) earthquake at the location of the case study, Zandeweer in Groningen. Data obtained via Webtool NPR 9998

10.2. Church as built 1230 versus 1931

10.2.1. Seismic Performance

The seismic performance of the church prior and post structural modifications can be evaluated based on their effective mass. Figure 10.2 presents a comparison of the results of the church prior and post structural modifications. Additionally, a posterior check is conducted to take into account the gable, that is not considered in the models analysed in this thesis. The seismic performance is evaluated for a weak earthquake of the location of the church in Zandeweer, Groningen in the Netherlands.

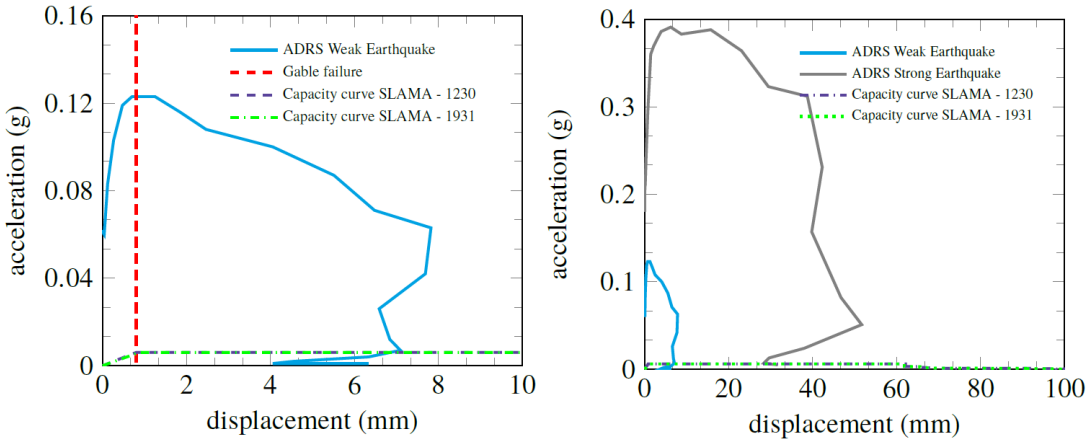

Figure 10.2: Capacity Check Church prior and post modifications for a weak Earthquake in Zandeweer, Groningen

Prior to the Nonlinear Pushover Analysis (NLPO) method, the church was analysed with the Simplified Lateral Mechanism Analysis (SLaMA) method. The SLaMA calculations predicted a capacity of 0.006g and a displacement capacity of 100mm up until all elements in both church models would fail. The NLPO analysis on the other hand, predict a capacity of 0.026g and a displacement capacity of 8.2mm for the church prior modifications and a capacity of 0.040g and a displacement capacity of 2.0mm for the church post structural modifications.

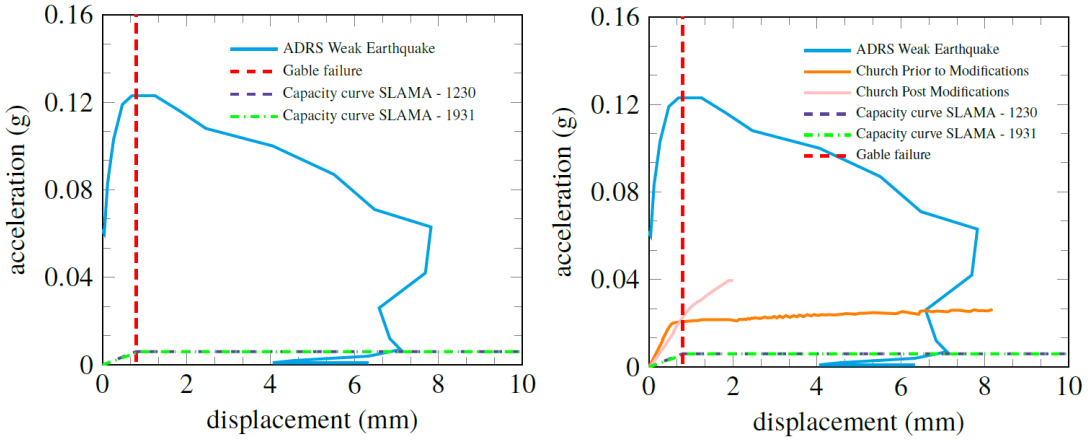

Figure 10.3: Capacity Check Church prior and post modifications for a weak Earthquake in Zandeweer, Groningen

As can be seen, the SLaMA calculation does not reflect the behaviour as observed during the NLPO method. This significant difference in results can be explained by a few reasons. First of all the SLaMA method is a method that determines the global capacity of a structure by means of summation of simple representations of the capacity of individual structural components. This method is a mechanism-based method. In which first modes response is dominant and higher modes amplifications are negligible. The governing mechanism at local level is extrapolated to global building behaviour by assuming either that load redistribution is possible (ductile response) or is not (brittle response). In the results of the NLPO it was observed that in particular for the church prior to the structural modifications higher modes should not be neglected.

Additionally, it was observed that load distribution takes place in the models. In that sense, SLaMA's main weakness is that the sequence of development of inelastic action between different members of the structure may not be identified. For structures with low member ductility capacity there may be a tendency to overestimate the load distribution and thus also the global strength and displacement capacity. Additionally, with the assumption of rigid diaphragms in the SLaMA analysis, the results are overestimated, as the curved shapes of the vaults do not behave as a rigid diaphragm. Furthermore, as the gable fails very early on wards, the SLaMA results which included the flange effect in the church models results in an additional overestimation of the global response of the structure. Lastly, SLaMA does not take into account walls with high thicknesses such for this church. In this regard, the formulations in SLaMA neglects load distributions and inelastic behaviour. With the consequence that it higly underestimates the force capacity of the structure.

The failure of the gable is predicted by means of a Nonlinear Kinematic Analysis (NLKA), as a posterior check for the analysis conducted in this thesis. A displacement capacity of 0.8mm is found for the gable with the NLKA. It should be noted that the values found from the NLKA calculation appears to be on a conservative side. As the collapse mechanise of the gable is solely based on a one-dimensional representation, which account for the out-of-plane constraints by the roof rafters. In case a two-dimensional representation is considered a shift in the collapse of the gable will be found. The gable may collapse at later moment than presented here. The NLKA can be found in appendix B. The early failure of the gable means that the results after the gable failure point can not be considered for the seismic performance of the church. However, in case by retrofitting measure the gable is prevented from failure the results can be considered for the seismic performance of the church.

In that case, when looking at the seismic performance of the church, SLaMA predicts to meet the demand of a weak earthquake at 6.8mm and 0.006g for both church models. The NLPO analysis predicts that the church model prior modifications will meet the demand at 6.6mm and 0.025g and the church model post modifications will not meet the demand due to early failure of the vaults. In the previous chapters it has been discussed that due to divergence problems for the church model post-structural modifications the post-peak stage is not found. Additionally, one should beware that during the eigenvalue analysis as presented in chapter 6 the modal mass participation factor remains under 60% for the church model prior modifications. Therefore, the response of the church is governed by multi-modes and the results of the NLPO method are on the conservative side. When the capacity of the church models is check for against a strong earthquake the church models prior and post structural modifications meet the demand at 31.8mm and 0.006g, according to the SLaMA method.

At the location of 6.6mm and 0.025g the demand is met for the church as built in 1230 according to the NLPO method. For this point the displacement contour plot and crack patterns of the church are depicted in figure 10.4 and 10.5, respectively. As can be seen in figure 10.4 at this stage a symmetric displacement pattern is observed for the church along the X-direction. The highest displacements are found in the vaults and at the edge of the curved West facade. with values that exceed 25mm. At the East facade an out-of-plane displacement pattern is observed in the shape of the governing mode.

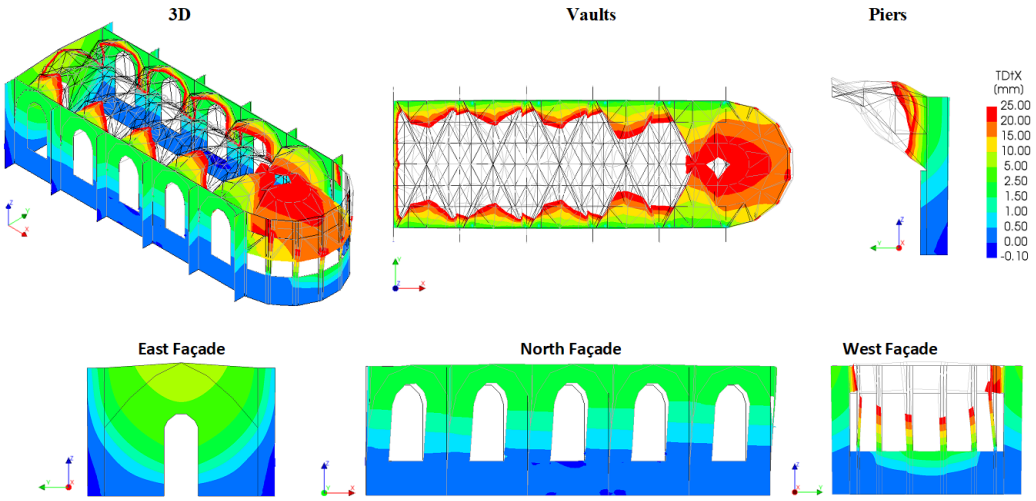

Figure 10.4: Displacement contour church as built in 1230 for intersection point with ADRS. At a base shear force of 2503kN and a displacement of 6.6mm for the longitudinal facades.

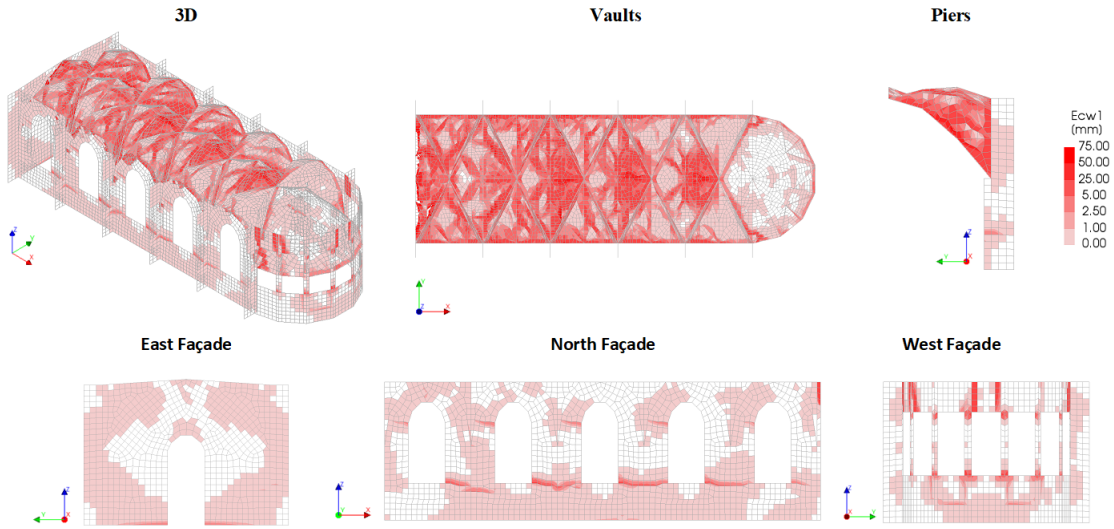

Figure 10.5: Crack Patterns church as built in 1230 for intersection point with ADRS

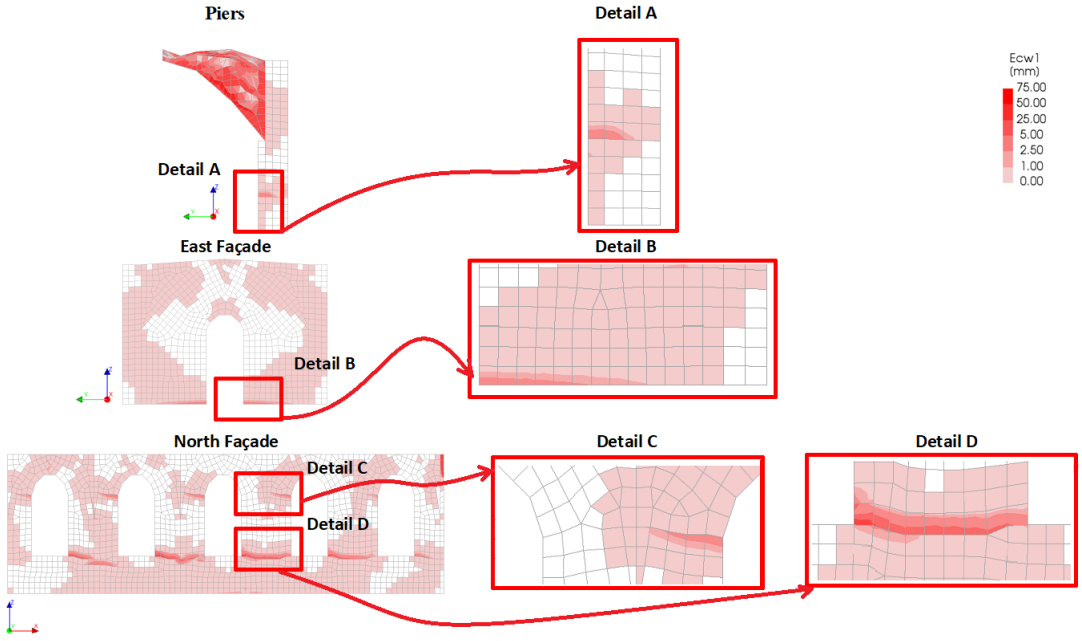

Figure 10.6: Crack Pattern Details

In figure 10.5 the crack patterns for the church are presented. When looking at the 3D of the church and the vaults, a symmetric crack pattern is observed. The highest cracks appear in the vaults with values of about 75mm. In the piers, the North, East and West facade the highest cracks that are observed are in the about 3.0mm. Figure 10.6 zooms into these cracks. As can be seen, initially diagonal cracking around the opening resulted in horizontal cracks that grew further in this direction. In chapter 3 the damage classification for this thesis was presented in table 3.2. Accordingly, the cracks in the vaults at this stage can be classified as severe to very severe. Whereas the cracking in the walls can be classified as slight to moderate in the details highlighted here.

10.2.2. Drift limits

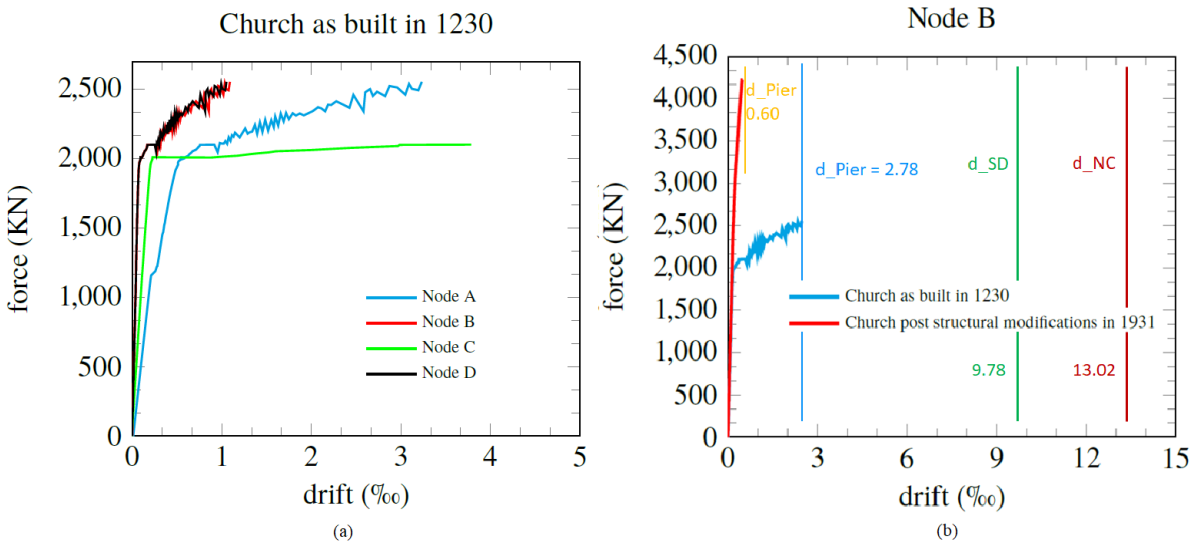

Figure 10.7: Drift limits church prior and post structural modifications

In performance-based design interstory drift limits are considered as a principal design consideration. The system performance level is evaluated with the aid of this parameter. The interstory drifts provides information about the ductility in different floors. For masonry structures the Eurocode refers to element storey drifts. The formula is associated to a specific limit state and the type of failure. where H_0 is the height and D_w is the width of the segment, respectively. In this case study the governing failure is rocking in the longitudinal walls of the church. For which the drift will be evaluated for a wall segment with the geometry of H_{eff} = 3.3m and D = 2.7m. Where d_{SD} is the failure modes in rocking for the severe damage ($d_{R,SD}$) and near collapse ($d_{R,NC}$) limit state are given in formula 10.1 and 10.2 respectively.

$$d_{R,SD} = 0.008(H_{eff}/D_w) \tag{10.1}$$

$$d_{R,NC} = 4/3 * 0.008(H_{eff}/D_w) \tag{10.2}$$

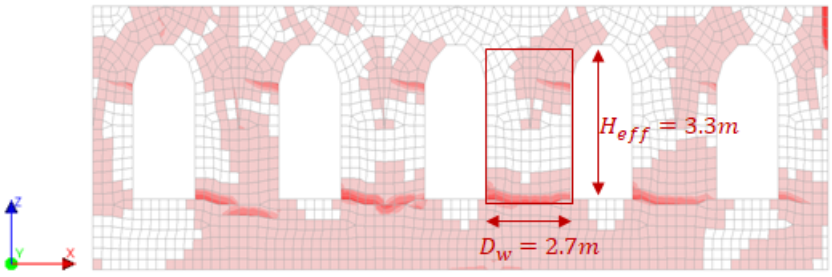

Figure 10.8: Selected wall element for the drift limit state checks

The drift limits for the severe damage state and near collapse result in values of 9.78 ‰and 13.03 ‰, respectively. With a maximum drift of 2.78 ‰and 0.60 ‰for the church as built in 1230 and post structural modifications respectively, the limits are not exceeded. As these limit state only consider the behaviour of the walls and consider a diaphragm effect, the checks are on a very conservative side. As for this this case study the structural behaviour of the vaults are governing over that of the walls.

10.3. Church as built 1230 including uncertainties

The seismic performance of the church prior to the modifications is additionally check for uncertainties. Uncertainties that are considered in this thesis are the church with linear elastic vaults, the church with the a different material model, the church with poor masonry properties. Figure 10.9 presents a comparison of the results of the church prior structural modifications with its variations where the above mentioned uncertainties are included. The seismic performance is evaluated for a weak earthquake of the location of the church in Zandeweer, Groningen in the Netherlands.

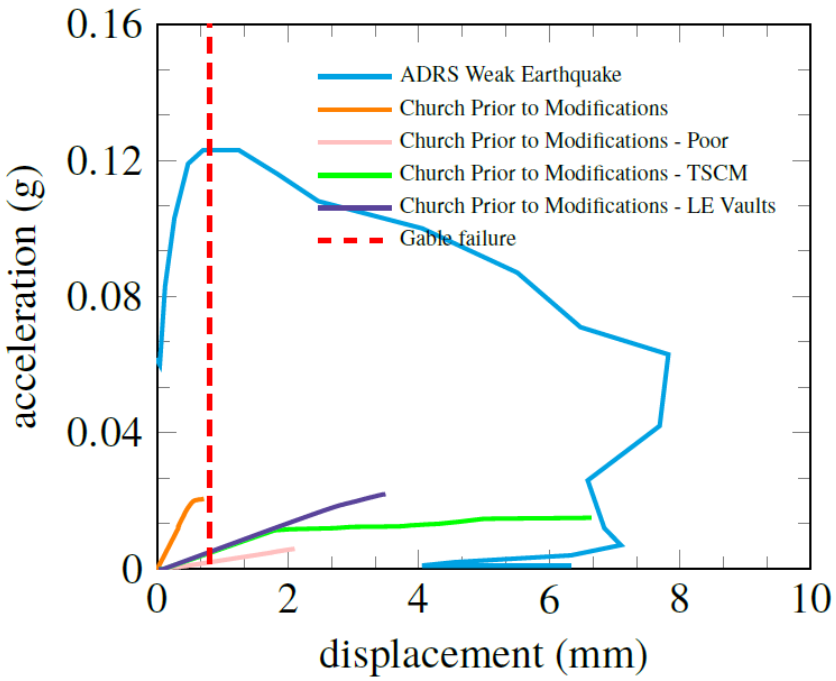

Figure 10.9: Capacity Check Church prior modifications + Church models including uncertainties for a weak Earthquake in Zandeweer, Groningen

As can be seen the response of the church models including uncertainties do differ to some extend. The models including uncertainties present a much lower stiffness in comparison to the church model prior modifications. Please, not that the results for all church models are presented up to peak loading, which were captured by the Regular Newton-Raphson method. The remaining tale that was captured by the Quasi-Secant method, for the church model as built in 1230, is not presented in Figure 10.9, as the analysis for the models including uncertainties are also not executed beyond the peak with the Quasi-Secant method.

11

Conclusions and recommendations

In this thesis the seismic performance of the historical unreinforced masonry Dutch church Zandeweer, prior and post structural modifications, in the earthquake prone area Groningen was studied. The church, built by the Moncks of Abdij van Aduard in the year 1230, underwent major renovation works in 1931. Its seismic performance was investigating in the positive longitudinal direction by studying its global nonlinear response and structural elemental behaviour and by indicating uncertainties and damage. The first objective of this thesis was, to evaluate the global seismic behaviour of the church prior and post structural modifications by means of a Simplified Lateral Mechanism Analysis (SLaMA) and a Nonlinear Pushover Analysis (NLPO) method . With limited research and no experimental results available to support the applicability of these analyses methods for this building typology, the second objective was to investigate to which extend these analyses methods can provide insight in the global behaviour.

11.1. Conclusions

Prior to the SLaMA and NLPO analyses, eigenvalue analyses were conducted. These analyses indicated that the structural modifications indeed have an influence on the global response of the church.

- *An increase in global stiffness, an increase in base shear, a reduction in deformations, a change in the mass participation factor from* 43.9% *to* 61% *in the longitudinal direction (X-direction in Figure 1) and from* 49.8% *to* 65.8% *in the transverse direction (Y-direction in Figure 1) was observed.*
- *In longitudinal direction the out-of-plane mode for the transverse facade was governing prior and post structural modifications.*
- *In the transverse direction a torsional mode was governing prior to the structural modifications and an out-of-plane mode for the longitudinal facades was governing post structural modifications as a consequence of change in the global stiffness introduced by closing the window openings in the curved façade.*

The Simplified Lateral Mechanism Analysis (SLaMA) and the Nonlinear Pushover Analysis (NLPO) method, were used as to predict the seismic response of the church models in the positive longitudinal direction. The results obtained show:

- *A displacement capacity of 100mm, a base shear capacity of about 588kN and 643kN for the church model prior and post structural modifications, respectively by the SLaMA. Furthermore, an increase in softening behaviour of about 25% and failure as a consequence of rocking in the piers of the main walls was found for the church models prior and post structural modifications.*
- *A displacement capacity of 25mm & 2.0mm and a force capacity of 2555kN & 4222kN were captured for the church model prior and post structural modifications, respectively by the NLPO analyses. Moreover, no softening was captured as the post-peak was not captured for church models.*
- *For observed results of the church model as built in 1230, a 5 times higher base shear capacity and a 1.25 higher global stiffness is observed by NLPO in comparison to SLaMA.*
- *For the results for the church model post structural modifications, a 6.5 times higher base shear capacity and a 1.25 higher global stiffness in comparison is found in the NLPO in comparison to SLaMA.*

The difference was explained by the modelling and loading approach in the two analysis methods. For the NLPO analyses a three-dimensional representation of the church is considered, whereas for the SLaMA a two-dimensional representation is used. Consequently, the influence of the vaults to the global behaviour is not considered in the response. Additionally, SLaMA is a mechanism based method for which the sequence of inelastic failure, the redistribution of the forces and torsional effect are neither considered. Lastly, limitations introduced by not modelling the gable in the SLaMA and NLPO analysis are accounted for with an Nonlinear Kinematic Analysis (NLKA) as a posterior check in the assessment of the church.

In general the structural modifications had a positive influence on the deformation behaviour of the main walls, yet a counteractive effect on the behaviour of the vault structure.

- *Damage in the vaults were found up to a severe state, whereas damage in the main walls remained slight to moderate.*
- *For both church models similar damage at similar locations were observed, but with a difference in value and spread.*
- *Cracks in the walls as a consequence of rocking were found in both church models. For the church post structural modifications additional cracks were initiated at the top edge of the main walls as a consequence of the addition of the concrete beams that restrained their lateral motion.*
- *Damage induced in the vaults as a consequence of an uneven distribution of the lateral pushover loading due to the particular shape of the vaults showed parts of the vaults to be compressed while other parts were less compressed or elongated.*
- *Collapse of the vault system occurred in the post structural modification church much earlier than prior to the modifications.*
- *As a consequence of the more stable response of the curved facade in the post structural modification church, due to closing the window openings, the dome part in the vaults could participate also in the response.*

The reliability of the numerical model results were checked by means of the accuracy and convergence behaviour of the models. Consequently, it was found that:

- *Poor convergence and an early divergence were observed towards the end of the numerical analyses, which were most probably caused by instability in either the physical models or the numerical models.*
- *Numerical instabilities are caused by a highly distorted mesh found in the vaults, consequently introduced zero pivots in the global stiffness matrix*
- *Instabilities in the physical model are most likely caused by extreme deformations in the curved façade and in the vaults of the church models.*
- *As the instability problems mainly found in the vaults were addressed by a sensitivity study with linear elastic vaults for the church as built in 1230 was conducted. A higher convergence for a higher load level was reached, however the improvement was not significant. It was concluded that geometric nonlinear effects do play an important role on the behaviour of the vaults and the convergence of the analyses.*
- *Additionally, several attempts were made by changing the numerical solvers in the analyses to find the root cause of the early divergence problems. Only with the aid of the Quasi-Secant method, it was possible to capture a higher displacement capacity, yet no post-peak behaviour. The use of the arc-length method was not successful either and resulted in a poor convergence.*

The capacity curves for the SLaMA and NLPO analysis, as obtained for the positive longitudinal direction, were subsequently compared against the seismic demand of a “weak” (return period=95 years) and a “strong” (return period=2475 years) earthquake at the location of the case study in Zandeweer, Groningen. As the gable is presumed to fail very early on wards, only if, retrofitting measures are considered to ensure that the gable failure and the roof structure failure, then in that case:

- *The capacity curve for the SLaMA analysis reach values up to 0.006g, a displacement of 100mm and the demand of the weak earthquake will be met at 6.18 and 0.006g for both the church model prior and post structural modifications.*
- *The capacity curve for the SLaMA analysis could meet the demand of the strong earthquake at 31.8 and 0.006g for both the church model prior and post structural modifications.*
- *The capacity curves obtained with the NLPO analyses for the church prior modifications reaches values up to 0.026g, a displacement of 8.18mm and could possibly meet the demand of a weak earthquake at 6.63mm and 0.029g.*

- *For the church models post structural modifications values up to 0.039g, a displacement of 1.98mm are reached and the demand curve is not met.*
- *The drift limits for the main walls of both church models for both the severe damage stage and the near collapse stage the limits were not exceeded.*

Moreover, additional sensitivity studies were done to understand the influence of the modelling approach of the pier-to-wall connections and to understand the influence of the use of the Engineering Masonry Model (EMM) instead of the Total Strain Rotating Crack Model (TSCM):

- *The connection of the models were chosen based on the assumptions of the interlocking of masonry units of the piers with the ones of the main walls. In this study it was not possible to observe the influence of the local behaviour of the piers with the walls on the global behaviour of the church models.*
- *The results for the TSCM showed a lower force capacity and initial stiffness in comparison to the EMM. Also in this case no post-peak was captured. As for the displacement pattern, for the TSCM a higher displacement was captured than with the EMM. For the crack pattern no difference was observed in the location and type of cracks occurring in the structure.*

11.2. Discussion

Based on the results acquired by the Eigenvalue Analysis, the Simplified Lateral Mechanism Analysis (SLaMA) and and the Modal Proportional Nonlinear Pushover Analysis (NLPO) method for the unreinforced historical Zandeweer church in this thesis, it can be concluded that both the SLaMA as the NLPO method are not suitable analysis methods to capture the influence on the seismic response of the presented church. The cyclic nature of the earthquake is not possible to simulate by these analysis methods. Although, the presented results for the church models show an insight in the influence of the structural modifications for this particular case study to a certain extend, it can be concluded that the adopted single-mode analysis methods will provide the user conservative results. In particular for the behaviour of the church prior to the structural modifications as it is governed by multi-modes. For the church post structural modifications a higher mass participation was observed during the eigenvalue analysis, above the recommended 60% by NPR 9998 [14], therefore the NLPO method can be a solution. However, the presented results for both cases do not provide an insight in the ductility behaviour of the structure and with respect to the base shear capacity it can be assumed that it is merely an estimation based on the simplifications and assumptions made in the presented models. Moreover, with SLaMA one is not able to capture the inelastic behaviour between structural elements, the influence of the cross-vaults on the global capacity, torsional effects and the sequence of failure. One should be aware that the base shear force capacity is mostly likely overestimated as the flange effect is considered which is not accurate as the gable collapses very early onwards based on the NLKA. Therefore, both single-mode methods provide to a limited extend insight in the global seismic performance of the church. Additionally, due to the observed non-convergence and divergence problems and with the highly unpredictable behaviour of the vaults in the structure the presented results are greatly influence by physical and numerical instabilities. Therefore, additional studies need to be conducted with regards to the vaults and subsequently changes need to be made in the modelling and analysis procedure of the church in order to capture a better insight in the influence of the structural modifications on the seismic performance of the church models. Lastly, it should be noted that within the scope of this thesis a full assessment of the church models were not done. Additional analyses are required to complete the assessment, especially focusing on the local failure mechanisms. In this thesis an assessment in one direction was conducted without considering torsional effect, eccentricities and one load condition for the pushover was considered.

11.3. Recommendations

For future studies it is recommended:

- *To collect samples from the real structure or more detailed information by observations in order to eliminate assumptions regarding the boundary & interface connections and material properties.*

- *To dedicate a detailed study to the numerical modelling and analysis of masonry ribbed cross vault structures. In which either a single and a group of cross-vaults are studied. With research motivations to explored, for examples, the influence modelling of the shape, choice of finite element discretization, mesh discretization, influence of ribs, boundary conditions and dynamic or static load conditions.*

- *To conduct a detailed study on the church walls, with flat lateral structural elements for which subsequently various analysis methods can be employed, and the influence of orthotropy on the global response, local failure for the walls and degradation of material properties can be studied.*

- *To consider a modelling approach with solid finite elements for the walls in combination with curved shell elements for the vaults. Compatibility of the finite elements can be ensured by appropriate use of tying and interfaces.*

- *To study the orthotropy of multi-leaf walls on component level as for historical structures in particular the physical model is reflected better. Layered curved shell elements can be used with appropriate material properties for the layers to study the effect of orthotropic walls for a three-dimensional case. In addition the influence of the integration scheme can be studied.*

- *To use the Nonlinear Pushover Analysis (NLPO) method in combination with the Modal Response Spectrum Analysis (MRS) method or the Nonlinear Time History Analysis (NLTH) method. The methods provide a solution for considering multi-modes simultaneously and the use of dynamic analysis methods is known for its less numerical instability problems than for static analysis methods.*

- *To conduct a cyclic nonlinear analysis for the study of the church structure and the study of the vaults in order to observe the degradation and propagation of the damage.*

- *To use the Sequential Linear analysis method with the aim to capture the post-peak behaviour or other solution methods, in combination with a mesh refinement study.*

- *To study global behaviour of the church in both global direction, in order to gain a better insight in the global seismic response of the church when using single-mode analysis methods such as in this thesis. The assessment should be done for both global directions considering the weakest direction including eccentricities and accounting for two seismic load conditions.*

- *To conduct analysis for other church typologies, such that a conclusion can be extrapolate for several cases on the influence of structural modification to the seismic response of historical church structures in Groningen.*

Bibliography

[1] B. D. J. Spetzler, Probabilistic seismic hazard analysis for induced earthquakes in groningen, update june 2017 (2017).
URL https://cdn.knmi.nl/system/readmore_links/files/000/000/408/original/20170615_Technisch_rapport_hazardkaart_Groningen_2017.pdf?1497511525.

[2] S. Gerrits, Minder gas oppompen gaat de aardbevingen in groningen niet stoppen, update february 2018 @ONLINE (2018).
URL https://www.ftm.nl/artikelen/minder-gas-oppompen-aardbevingen-groningen?share=1

[3] Swing, Heritage database @ONLINE (2019).
URL https://erfgoed.databank.nl/jive

[4] C. V. W. (CVW), Aardbevingen groningen - schademeldingen 2012-2017 @ONLINE (2018).
URL https://erfgoedmonitor.nl/indicatoren/aardbevingen-groningen-schademeldingen-2012-2017

[5] G. Augusti, M. Ciampoli, P. Giovenale, Seismic vulnerability of monumental buildings, Structural Safety 23 (3) (2001) 253–274 (2001).

[6] T. Goded, J. Irizarry, E. Buforn, Vulnerability and risk analysis of monuments in málaga city's historical centre (southern spain), Bulletin of Earthquake Engineering 10 (3) (2012) 839–861 (2012).

[7] P. Roca, M. Cervera, G. Gariup, et al., Structural analysis of masonry historical constructions. classical and advanced approaches, Archives of Computational Methods in Engineering 17 (3) (2010) 299–325 (2010).

[8] S. Lagomarsino, S. Podesta, Seismic vulnerability of ancient churches: Ii. statistical analysis of surveyed data and methods for risk analysis, Earthquake Spectra 20 (2) (2004) 395–412 (2004).

[9] S. Lagomarsino, S. Cattari, Seismic performance of historical masonry structures through pushover and nonlinear dynamic analyses, in: Perspectives on European Earthquake Engineering and Seismology, Springer, Cham, 2015, pp. 265–292 (2015).

[10] D. F. D'Ayala, S. Paganoni, Assessment and analysis of damage in l'aquila historic city centre after 6th april 2009, Bulletin of Earthquake Engineering 9 (1) (2011) 81–104 (2011).

[11] C. S. Oliveira, Seismic vulnerability of historical constructions: a contribution, Bulletin of Earthquake Engineering 1 (1) (2003) 37–82 (2003).

[12] B. Pantò, F. Cannizzaro, S. Caddemi, I. Caliò, 3d macro-element modelling approach for seismic assessment of historical masonry churches, Advances in Engineering Software 97 (2016) 40–59 (2016).

[13] L. F. Ramos, L. Marques, P. B. Lourenço, G. De Roeck, A. Campos-Costa, J. Roque, Monitoring historical masonry structures with operational modal analysis: two case studies, Mechanical systems and signal processing 24 (5) (2010) 1291–1305 (2010).

[14] NEN, Assessment of structural safety of buildings in case of erection, reconstruction and disapproval - Basic rules for seismic actions: induced earthquakes, Tech. rep., Koninklijk Nederlands Normalisatie-instituut, 2017 (2017).

[15] POLIMI, Inventory of earthquake-induced failure mechanisms related to construction type, structural elements, and materials 2010 @ONLINE (September 2010).
URL http://www.niker.eu/assets/Files/Download

[16] S. Lagomarsino, A new methodology for the post-earthquake investigation of ancient churches, in: 11th European Conference on Earthquake Engineering, 1998, pp. 1–12 (1998).

[17] A. K. Chopra, Dynamics of structures: theory and applications to earthquake engineering, Prentice Hall, 2013 (2013).

[18] B. Gupta, S. K. Kunnath, Adaptive spectra-based pushover procedure for seismic evaluation of structures, Earthquake spectra 16 (2) (2000) 367–392 (2000).

[19] K. Shakeri, M. Shayanfar, M. M. Asbmarz, A spectra-based multi modal adaptive pushover procedure for seismic assessment of buildings, in: Proceedings of the 14th World Conference on Earthquake Engineering, Beijing, 12-17 October, 2008 (2008).

[20] U. of Buffalo, Review of seismic design philosophies and analysis methods @ONLINE (Fall 2009).
URL http://sharif.edu/~ahmadizadeh/courses/strcontrol/

[21] S. Freeman, Evaluations of existing buildings for seismic risk-a case study of puget sound naval shipyard, in: Proc. 1st US Nat. Conf. on Earthquake Engrg., Bremerton, Washington, 1975, 1975, pp. 113–122 (1975).

[22] P. Fajfar, Capacity spectrum method based on inelastic demand spectra, Earthquake Engineering & Structural Dynamics 28 (9) (1999) 979–993 (1999).

[23] E. C. for Standardization, Eurocode 8: Design of structures for earthquake resistance – Part 3: Assessment and retrofitting of buildings, European Commission, 2016 (2016).

[24] S. Lagomarsino, S. Cattari, Perpetuate guidelines for seismic performance-based assessment of cultural heritage masonry structures, Bulletin of Earthquake Engineering 13 (1) (2015) 13–47 (2015).

[25] P. A. Korswagen, M. Longo, E. Meulman, J. G. Rots, Crack initiation and propagation in unreinforced masonry specimens subjected to repeated in-plane loading during light damage, Bulletin of Earthquake Engineering (2018) 1–37 (2018).

[26] G. Giardina, A. Marini, M. A. Hendriks, J. G. Rots, F. Rizzardini, E. Giuriani, Experimental analysis of a masonry façade subject to tunnelling-induced settlement, Engineering Structures 45 (2012) 421–434 (2012).

[27] R. Springenschmid, G. Adam, Mechanical properties of set concrete at early ages. test methods, Matériaux et Construction 13 (5) (1980) 391 (1980).

[28] M. Dhanasekar, A. Page, P. Kleeman, The failure of brick masonry under biaxial stresses., Proceedings of the Institution of Civil Engineers 79 (2) (1985) 295–313 (1985).

[29] C. Calderini, S. Cattari, S. Lagomarsino, In-plane strength of unreinforced masonry piers, Earthquake Engineering & Structural Dynamics 38 (2) (2009) 243–267 (2009).

[30] M. C. Griffith, J. Vaculik, N. Lam, J. Wilson, E. Lumantarna, Cyclic testing of unreinforced masonry walls in two-way bending, Earthquake Engineering & Structural Dynamics 36 (6) (2007) 801–821 (2007).

[31] K. Doherty, M. C. Griffith, N. Lam, J. Wilson, Displacement-based seismic analysis for out-of-plane bending of unreinforced masonry walls, Earthquake engineering & structural dynamics 31 (4) (2002) 833–850 (2002).

[32] J. Dawe, C. Seah, Out-of-plane resistance of concrete masonry infilled panels, Canadian Journal of Civil Engineering 16 (6) (1989) 854–864 (1989).

[33] A. Dazio, et al., The effect of the boundary conditions on the out-of-plane behaviour of unreinforced masonry walls, in: 14th World Conference on Earthquake Engineering, 2008, pp. 12–17 (2008).

[34] M. C. Griffith, G. Magenes, G. Melis, L. Picchi, Evaluation of out-of-plane stability of unreinforced masonry walls subjected to seismic excitation, Journal of Earthquake Engineering 7 (spec01) (2003) 141–169 (2003).

[35] L. Sorrentino, D. D'Ayala, G. de Felice, M. C. Griffith, S. Lagomarsino, G. Magenes, Review of out-of-plane seismic assessment techniques applied to existing masonry buildings, International Journal of Architectural Heritage 11 (1) (2017) 2–21 (2017).

[36] M. Tondelli, K. Beyer, M. DeJong, Influence of boundary conditions on the out-of-plane response of brick masonry walls in buildings with rc slabs, Earthquake Engineering & Structural Dynamics 45 (8) (2016) 1337–1356 (2016).

[37] R. Brincker, Yield-line theory and material properties of laterally loaded masonry walls, MASONRY INT. Masonry Int. (1) (1984) 8 (1984).

[38] D. D'Ayala, E. Speranza, Definition of collapse mechanisms and seismic vulnerability of historic masonry buildings, Earthquake Spectra 19 (3) (2003) 479–509 (2003).

[39] C. Meisl, K. Elwood, C. Ventura, Shake table tests on the out-of-plane response of unreinforced masonry walls, Canadian Journal of Civil Engineering 34 (11) (2007) 1381–1392 (2007).

[40] J. Rots, F. Messali, R. Esposito, S. Jafari, V. Mariani, Thematic keynote computational modelling of masonry with a view to groningen induced seismicity, in: Structural Analysis of Historical Constructions: Anamnesis, Diagnosis, Therapy, Controls: Proceedings of the 10th International Conference on Structural Analysis of Historical Constructions (SAHC, Leuven, Belgium, 13-15 September 2016), CRC Press, 2016, p. 227 (2016).

[41] P. Lourenco, Computational strategies for masonry structures [ph. d. thesis], Delft University, The Netherlands (1996).

[42] D. F. b.v., User's manual – release 10.3 @ONLINE (2019).
URL `https://dianafea.com/manuals/d103/Diana.html`

[43] P. Feenstra, J. Rots, A. Arnesen, J. Teigen, K. Hoiseth, A 3d constitutive model for concrete based on a co-rotational concept, in: Borst, R. deBicanic, N. Mang, H. Meschke, G., Computational Modelling of Concrete Structures. Proceedings of the Euro-C 1998 Conference on Computational Modelling of Concrete Structures, Badgastein, Austria, 31 March-3 April, 13-22, Brookfield, 1998 (1998).

[44] J. G. Rots, F. Messali, R. Esposito, V. Mariani, S. Jafari, Multi-scale approach towards groningen masonry and induced seismicity, in: Key Engineering Materials, Vol. 747, Trans Tech Publ, 2017, pp. 653–661 (2017).

[45] F. M. J. R. G.M.A. Schreppers, A. Garofano, Diana validation report for masonry modelling, DIANA FEA BV and TU Delft 1 (1) (2017) 143 (2017).

List of Figures

List of Tables

A

Annex A - Technical Drawings Case Study

Herein, the original drawing of the church as provided by the Rijksmonumentendienst are presented.

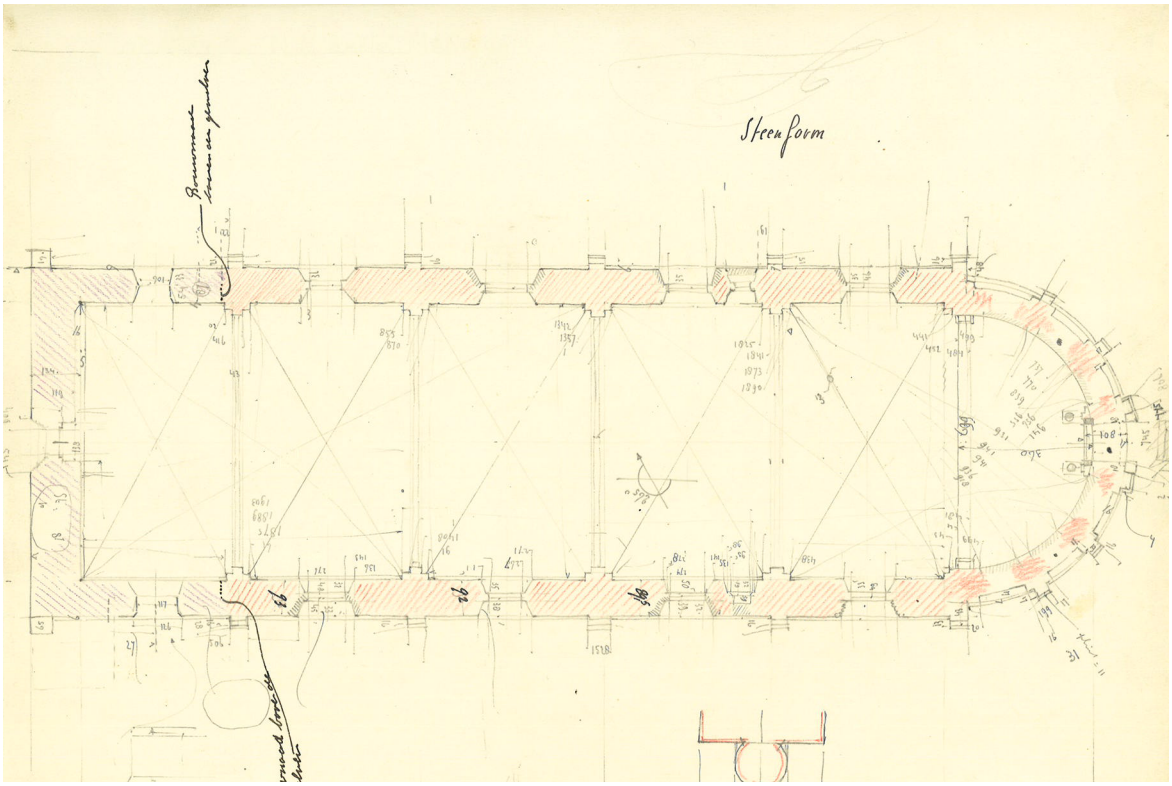

Figure A.1: Sketch dimensions church walls - 1931

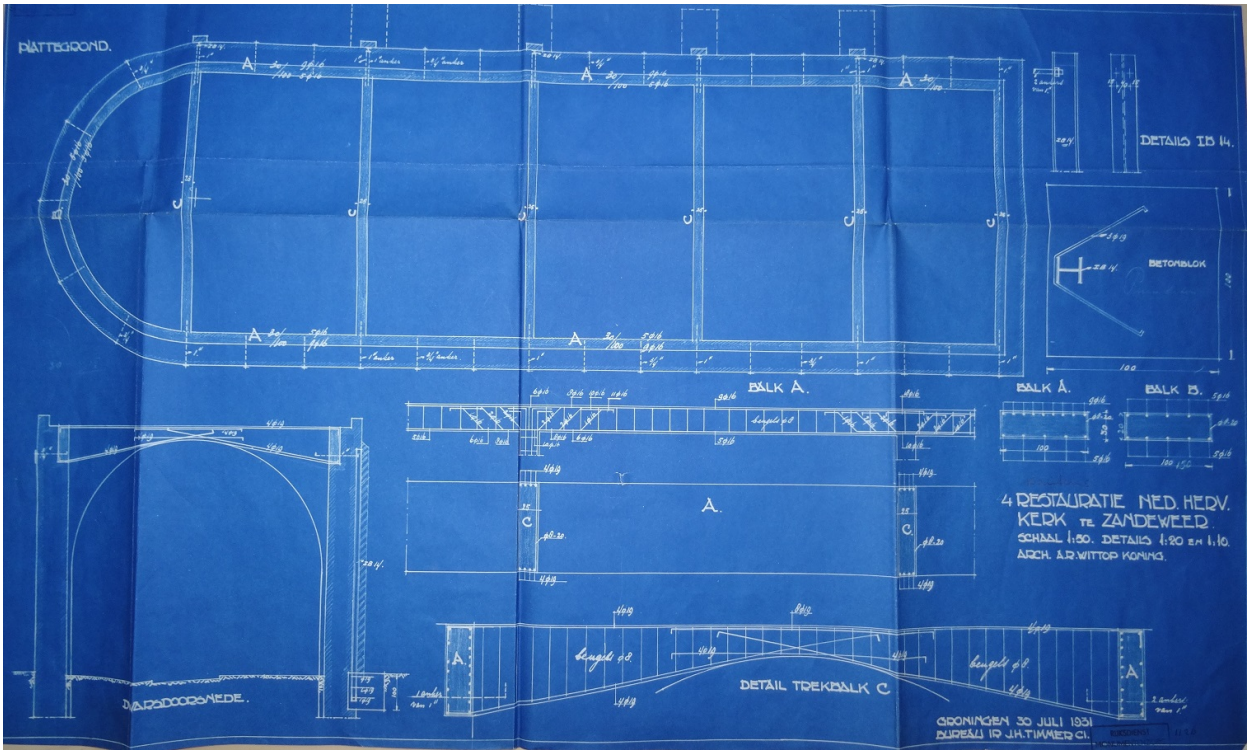

Figure A.2: Blueprints cross-section, plan of the church including concrete beams and detail of the concrete beams

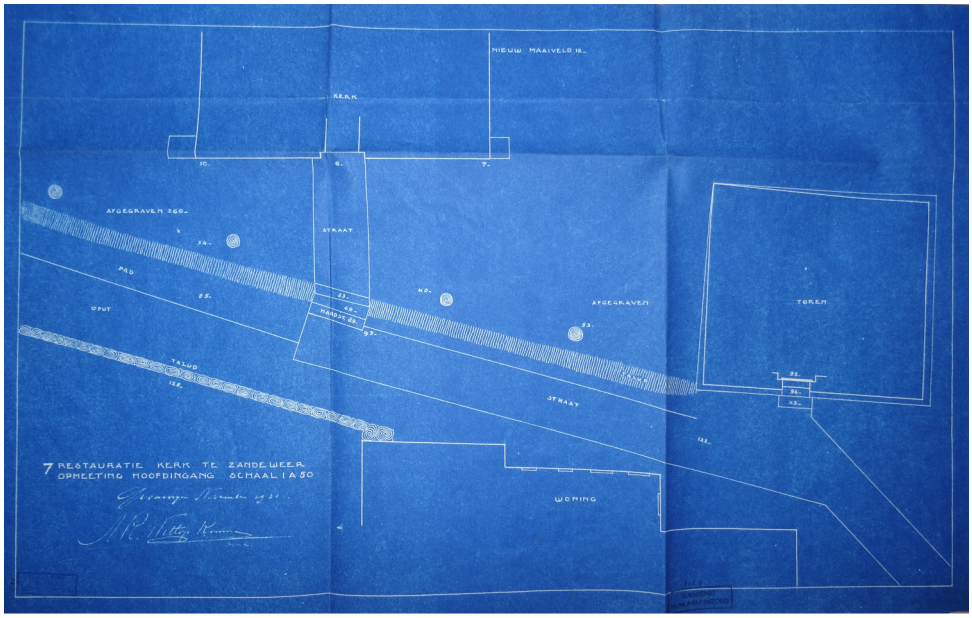

(a)

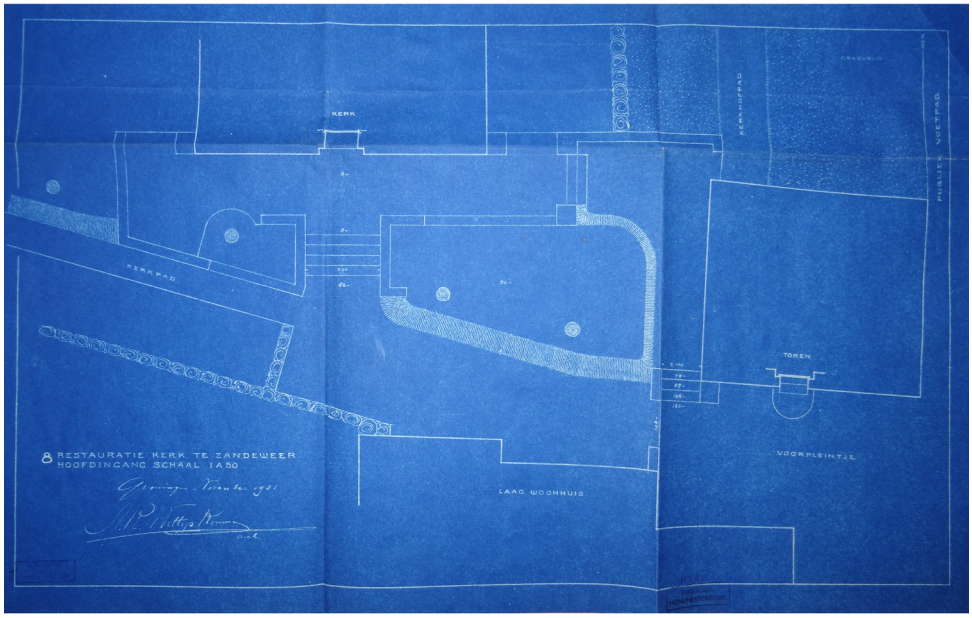

(b)

Figure A.3: (a) Blueprints entrance church before 1931 (b) entrance church after 1931

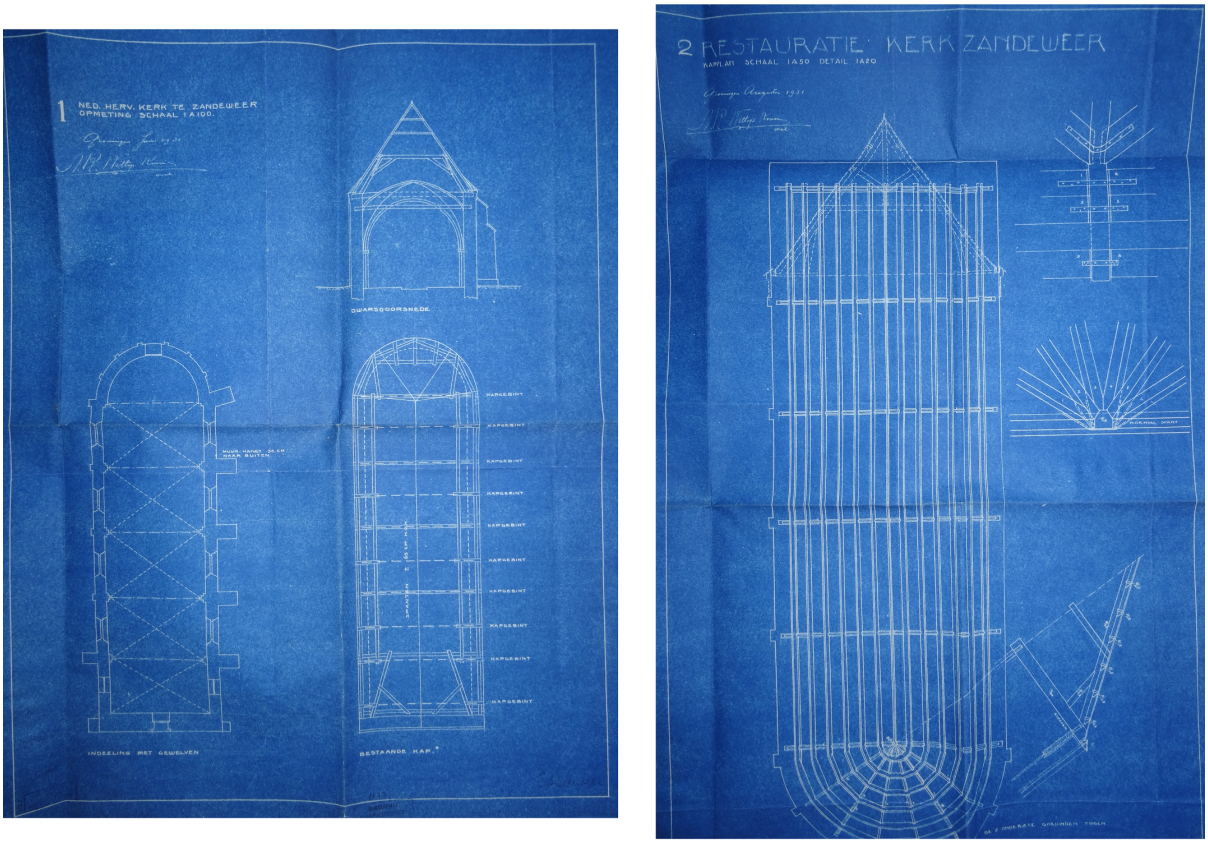

(a) (b)

Figure A.4: Blue prints cross-section and plan church with new rafters-1931

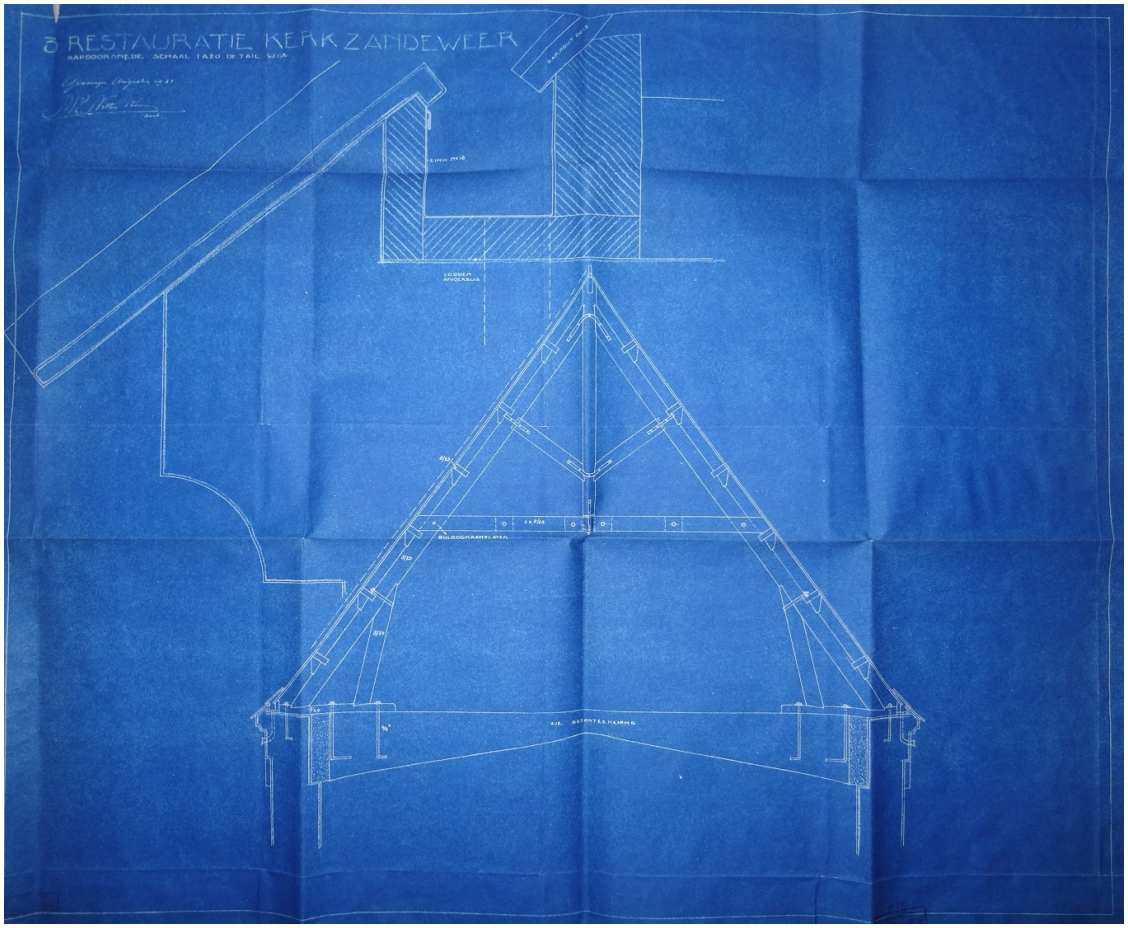

Figure A.5: Blueprint timber rafters roof including detail-1931

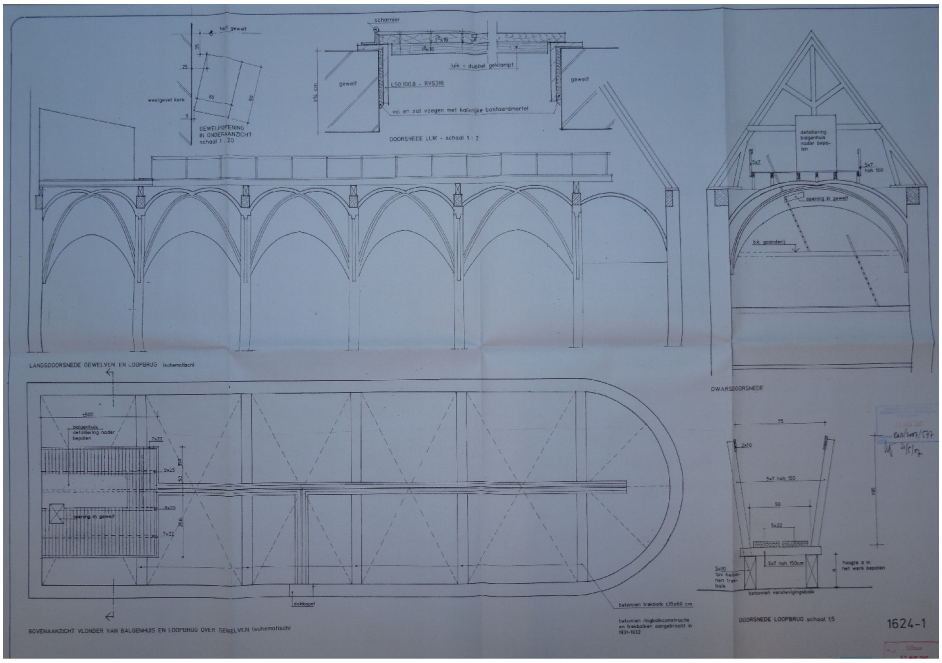

(a)

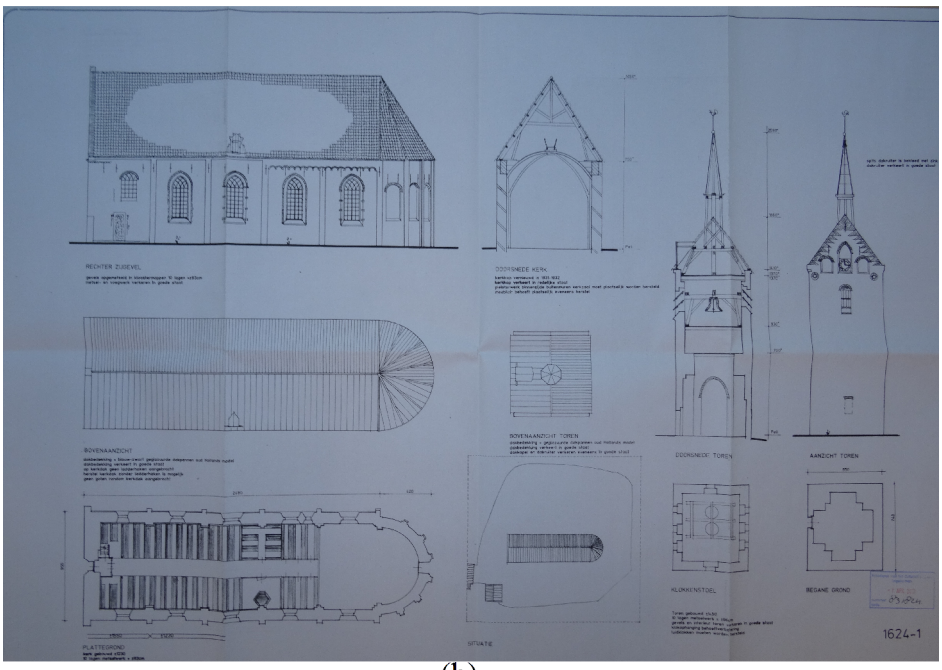

(b)

Figure A.6: (a) Cross-section in the longitudinal and transverse direction, plan church (b)facade views, top view, interior of church and facade and cross-section plan tower-2007

B

Annex B - Dead load calculations

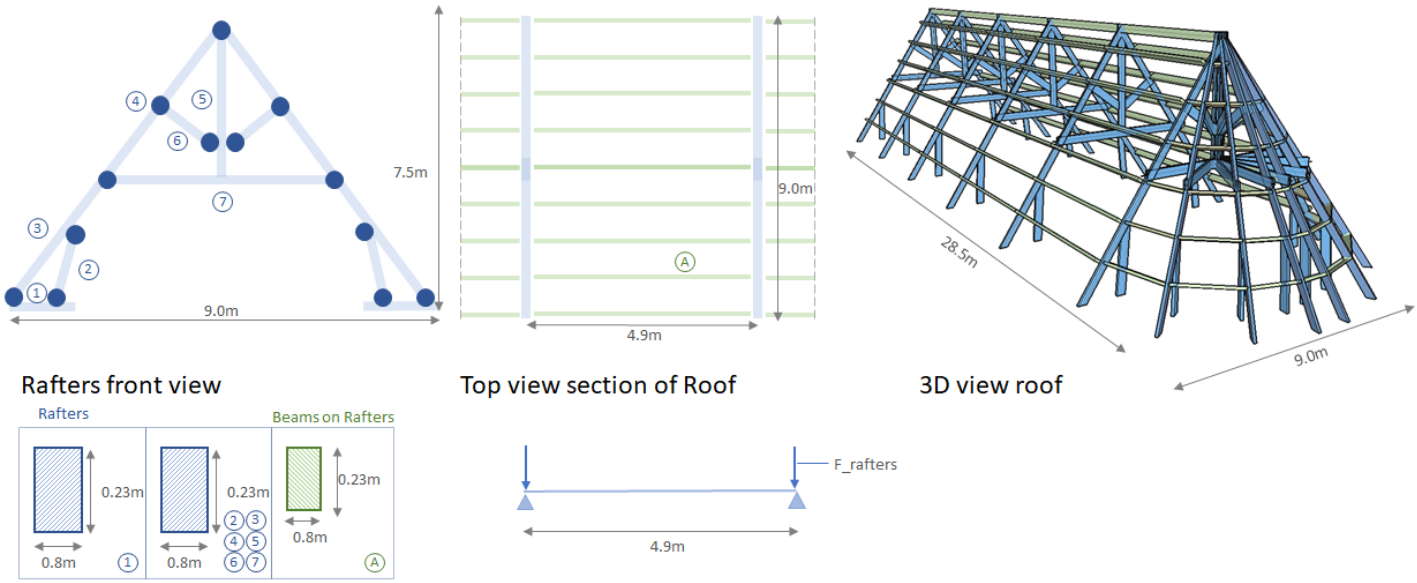

Figure B.1: Roof Structure

Beam	Length [m1]	Cross sectional Area [m2]	Quantity
1	2.500	0.184	1
2	2.500	0.200	1
3	4.374	0.200	1
4	4.374	0.200	1
5	3.750	0.200	1
6	1.500	0.200	1
7	4.000	0.200	1
A	4.900	0.184	8
Total Volume [m3]			11.77
Mass Density [kg/m3]			800
g [m/s2]			9.81
Weight [N]			92390
Cladding	**Length [m1]**	**Width[m1]**	**Thickness[m]**
	9.0	4.9	0.025
Total Volume [m3]			6.17
Mass Density [kg/m3]			600
g [m/s2]			9.81
Weight [N]			6490

Figure B.2: Roof Structure - dead load

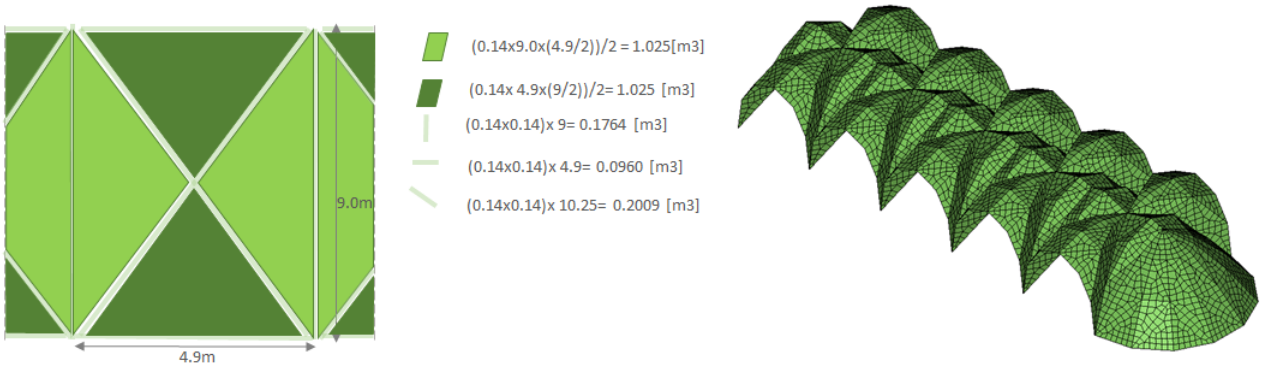

Figure B.3: Vaults

Vaults	Length [m1]	Width[m1]	Thickness[m]
	9.0	4.9	0.14
Total Volume [m3]			6.17
Mass Density [kg/m3]			1600
g [m/s2]			9.81
Weight [N]			96907

Figure B.4: Vaults - dead load

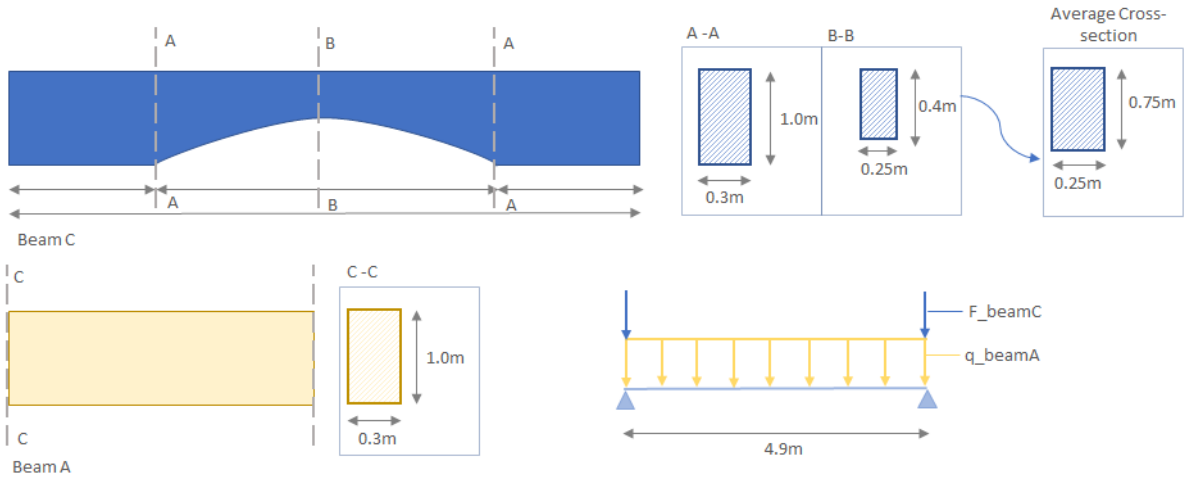

Figure B.5: Concrete Beams

Concrete Beams	Length [m1]	Width[m1]	Height[m]
Beam C	8.4/2	0.25	0.75
Total Volume [m3]			0.79
Mass Density [kg/m3]			2500
g [m/s2]			9.81
Weight [N]			19314
		Width[m1]	Height[m]
Beam A		0.3	1.0
Total Volume [m3]/m1			0.3
Mass Density [kg/m3]			2500
g [m/s2]			9.81
Weight [N/m1]			7360

Figure B.6: Concrete Beams - dead load

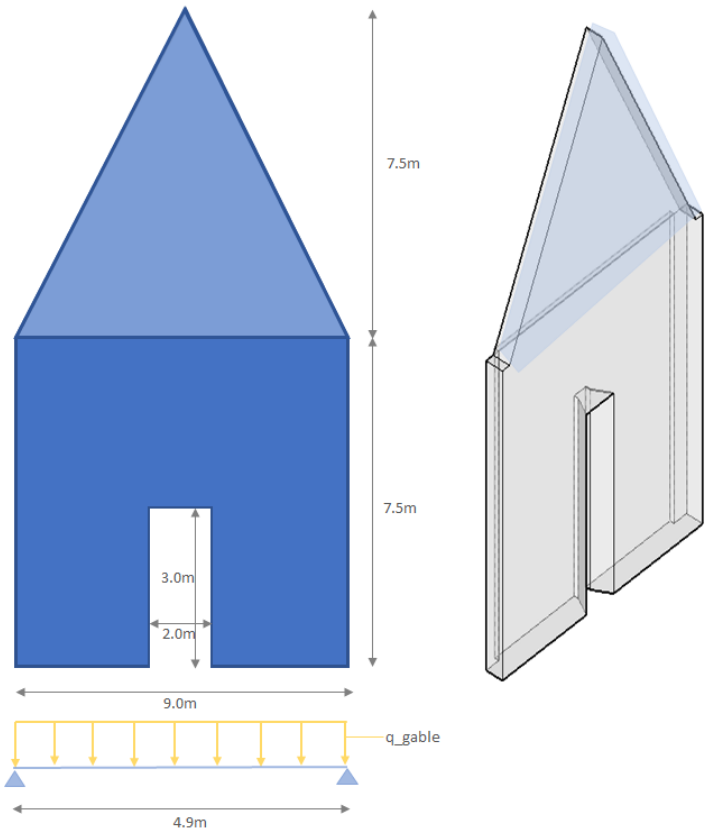

Figure B.7: Gable

Gable-Façade	Height[m1]	Thickness[m]
Gable	7.50	0.93
Total Volume [m3]/m1		3.50
Mass Density [kg/m3]		1600
g [m/s2]		9.81
Weight [N/m1]		54936
Remainder facade	7.50	0.93
Door opening	3.0	0.93
Total Volume [m3]/m1		6.85
Mass Density [kg/m3]		2500
g [m/s2]		9.81
Weight [N/m1]		107518

Figure B.8: Gable - dead load

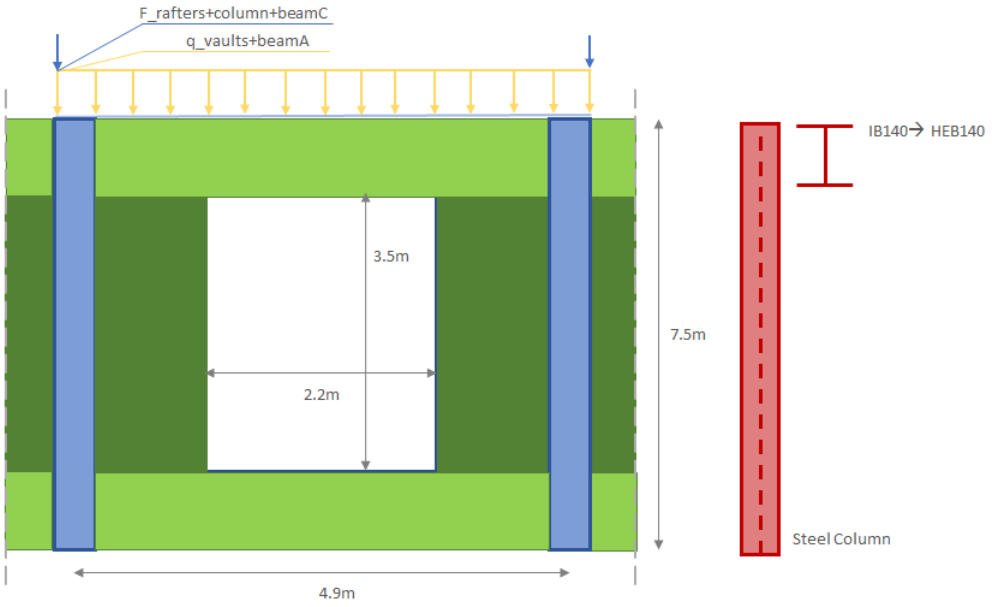

Figure B.9: In-Plane facade

In-Plane Facade	Height[m1]	Width[m1]	Thickness[m]
Façade	7.50	4.9	0.93
Opening	3.5	2.2	0.93
Total Volume [m3]/m1			5.52
Mass Density [kg/m3]			1600
g [m/s2]			9.81
Weight[N/m1]			86541
Steel Columns	7.5		
Mass Density [kg/m1]			34.4
g [m/s2]			9.81
Weight [N]			2531

Figure B.10: In-Plane facade - dead load

C

Annex C - Results NLKA Gable

The geometry of the gable is depicted in Figure C.1.

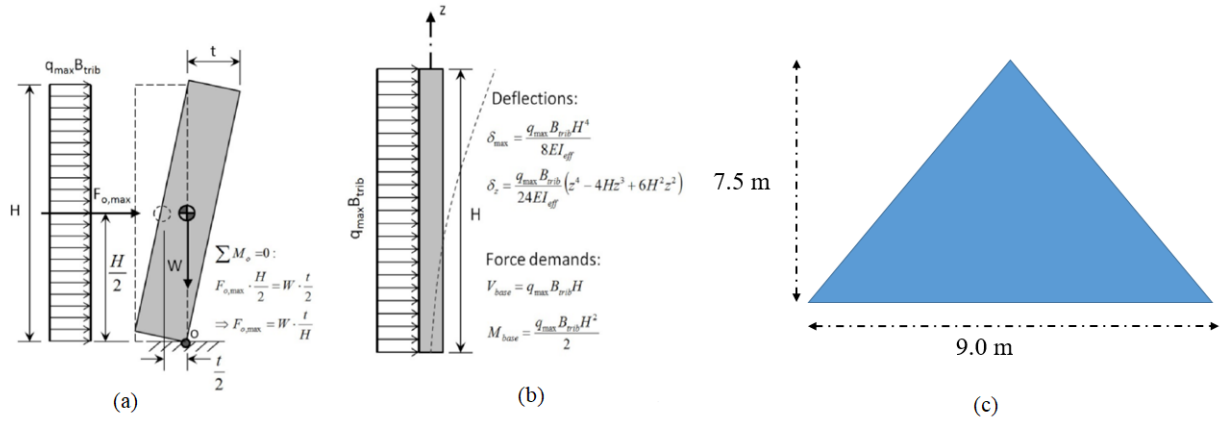

Figure C.1: The geometry of the gable

The parameters using for NLKA calculation are presented in Table C.1. In this table, t, B_{trib} and H denote the width, tributary area of the gable and height, respectively. The density of masonry, Elastic modulus masonry, moment of inertia and weight of the gable in kg are presented with ρ, E, I_{eff} and W, respectively. The self-weight of the gable in kN, overturning force and top displacement of the gable are shown as W_f, F_{0max} and δ_{max}, respectively.

t (m)	B_{trib} (m^2)	H (m)	ρ (Kg/m^3)	E (Kg/m^2)	I_{eff} m^4	W (Kg)	W_f (kN)	F_{0max} (kN)	δ_{max} (mm)
0.93	33.75	7.50	1600	2900000	10.90	50220.00	492.66	61.09	0.8

Table C.1: Parameters NLKA calculations